Dissertation zur Erlangung des Doktorgrades

der Fakultät für Chemie und Pharmazie

der Ludwig-Maximilians-Universität München

Energetic Polymers and Plasticizers Based on Organic Azides, Nitro Groups and Tetrazoles

– Synthesis and Characterization

Vera Anna Hartdegen

aus

München

2016

Erklärung

Diese Dissertation wurde im Sinne von § 7 der Promotionsordnung vom 28. November 2011 von Herrn Professor Dr. Thomas M. Klapötke betreut.

Eidesstattliche Versicherung

Diese Dissertation wurde eigenständig und ohne unerlaubte Hilfe erarbeitet.

München, ……..

.....

(Vera Anna Hartdegen)

Dissertation eingereicht am: 06. Mai 2016

1. Gutachter: Prof. Dr. Thomas M. Klapötke

2. Gutachter: Prof. Dr. Konstantin Karaghiosoff

Mündliche Prüfung am: 02. Juni 2016

„*Es riecht nicht alles gut, was kracht!*“

(Karl Valentin)

Danksagung

Mein Dank gilt zu allererst und ganz besonders, Herrn Professor Dr. **Thomas M. Klapötke** für die freundliche Aufnahme in den Arbeitskreis und die interessante Themenstellung dieser Dissertation. Des Weiteren danke ich ihm, dass ich mich mit Fragen jederzeit an ihn wenden konnte und diese dann sofort erörtert und gelöst wurden. Sein unermüdliches Engagement, auch außerhalb des universitären Alltags ist nicht selbstverständlich. Darüber hinaus danke ich ihm für das Einstellen weiterer „Büromitarbeiter“, die mir den normalen Arbeitsalltag immer wunderbar „versüßt“ haben.

Herrn Professor Dr. **Konstantin Karaghiosoff** danke ich für zahlreiche X-ray und NMR-Messungen und die Hilfe bei besonders schweren Fällen, sowie für die Übernahme des Zweitgutachtens. Anregende Diskussionen und lustige Abende sorgten für Ablenkung abseits des regulären Laboralltags.

Herrn Akad. Oberrat Dr. **Burkhard Krumm** und Herrn Akad. Rat Dr. **Jörg Stierstorfer** danke ich dafür, dass ich mich jederzeit mit chemischen und anderen Fragen an sie wenden konnte und für viele Anregungen und Hilfestellungen.

Frau **Irene Scheckenbach** möchte ich besonders herzlich für ihre Freundlichkeit, ihre riesengroße Hilfsbereitschaft (auch und vor allem jene, außerhalb des Universitätsbetriebs), die kompetente und unkomplizierte organisatorische Betreuung, sowie für zahlreiche schöne Unterhaltungen danken.

Stefan Huber danke ich für das Messen von Schlag- und Reibeempfindlichkeiten, Chemikalienbestellungen und die unterhaltsamen Wochen während der IT-Sanierung.

Für diverse Messungen bezüglich Molmassen, Viskositäten, DSCs, TGAs etc. und die nette Zusammenarbeit danke ich **Sven Hafner** (Fraunhofer Institut für Chemische Technologie, Karlsruhe) ganz herzlich.

Für ihre Hilfsbereitschaft bei der Lösung von Kristallstruktur- und anderen Problemen danke ich **Carolin Pflüger** und Dr. **Christina Hettstedt** ganz herzlich.

Dr. **Camilla Evangelisti** und **Johann Glück** danke ich für das sorgfältige Ausführen der Bombenkalorimetriemessungen.

Dem gesamten Arbeitskreis möchte ich für die schöne Zeit, auch (oder vor allem) außerhalb der „Kernarbeitszeiten“ und die gute Arbeitsatmosphäre danken. Ein besonderer Dank gilt hierbei meinen Laborkollegen aus D3.107: Dr. **Franz Martin** (weil er mich davon überzeugt hat, dass Golf auch eine Sportart ist), Dr. **Anian** „Erklärbär“ **Nieder** (für viele Antworten auf gestellte und nicht gestellte Fragen), Dr. **Marcos Kettner** (für die Erweiterung meines musikalischen Horizonts in die Bereiche der elektronischen Musik), Dr. **Magdalena Rusan** (für die Verbreitung von gutem Teeduft im Labor), **Michael** „Tiescha“ **Feller** (für gute und angenehme Sitznachbarschaft), **Thomas Müller**, **Martin Härtel**, **Benedikt Stiasny**, **Johann Glück**, **Stefanie Heimsch** und **Ivan Gospodinov**. Danke für die freundliche und angenehme Zusammenarbeit, für lustige Momente, anregende Gespräche und viel Kurzweil über die Jahre!

Für das (wohl mitunter mühevolle) Korrekturlesen meiner Arbeit möchte ganz besonders Dr. **Christina Hettstedt**, **Tiana Hanelt** und Dr. **Anian Nieder** danken.

Bei meiner „Polymerschwester“ Dr. **Franziska Naredi-Rainer**, sowie Dr. **Camilla** „Feinkost“ **Evangelisti**, Dr. **Christina** „Crit-Christl“ **Hettstedt** und **Tiana** „Oh NEIIIN!“ **Hanelt** bedanke ich mich, neben den veredelten Stunden innerhalb der Unimauern, auch und vielleicht noch mehr für unzählige, ernste, lustige, entspannte und tanzbare Abende, abseits der chemischen Welt.

Ein sehr großer Dank gilt auch meinen Praktikanten **Andreas Bellan**, **Michael Willmann**, **Maximilian Lang**, **Jutta Tumpach**, **Sinah Krönauer**, **Henning Lumpe**, **Maximilian Hofmayer**, **Nicolas Hilgert** und **Tiana Hanelt**, die einen großen Beitrag zu dieser Arbeit geleistet haben.

Auch den namentlich nicht ausdrücklich erwähnten Doktoranden, Masteranden und allen anderen Begleitern über all die Jahre gilt mein Dank für die schöne gemeinsame Zeit.

Ein ganz, ganz, ganz besonderer Dank gilt meinen Eltern, **Paul** und **Anneliese Hartdegen** und meiner übrigen Familie, für die bedingungslose Unterstützung, den Rückhalt über all die Jahre und einfach alles. Ohne deren Hilfe wäre ich wohl nie so weit gekommen…Ganz speziell sei in diesem Zusammenhang auch **Moritz** „Herr Gempel“ **Gemke** gedankt, der mich immer wieder zurück auf die Füße gebracht, motiviert und vom Alltagstrott abgelenkt hat. Außerdem danke ich ihm, dass er mir uneingeschränkt, auch in den garstigsten Lebenlagen, stets zur Seite stand und aus mir einen positiveren Menschen gemacht hat. Danke für alles und noch viel mehr!

Mein letzter Dank geht an unseren „Montagshund“ **Bali** („Frau Schleppel“, „das Bompf“, „Wampelmuse“), ohne deren „Schnorcheln“, „Knöttern“ und „Roafln“ das Leben nur halb so schön wäre. Frei nach Loriot: „Ein Leben ohne Mops ist möglich, aber sinnlos“.

ABSTRACT

Abstract

The aim of this thesis was the development and investigation of new energetic polymers and plasticizers, on the basis of different polymer backbones or organic compounds with varying energetic or nitrogen-rich functional groups, along with the syntheses of suitable precursors for further (polymeric) processing.

One of the main requirements of the newly developed compounds was their suitability as energetic binder or plasticizer, respectively, which includes high thermal and physical stabilities (to stabilize the energetic filler) and moderate to good energetic properties. In order to guarantee a good and save handling as well as a long storage time of the bound formulation, it is also mandatory that the developed compounds possess a high chemical stability, thus reactions with the energetic filler can be avoided.

This thesis is divided into four sections. The first part is a continuation of my master thesis.[1] It describes the synthesis and characterization of a glycidyl polymer containing nitramino groups. Known energetic polymers based on the glycidyl backbone possess energetic functional groups like azides (glycidyl azide polymer, GAP), or nitrate esters (poly(glycidyl nitrate), polyGLYN). As a new energetic compound based on the glycidyl backbone, a nitramine based polymer was developed, which was obtained in a four-step synthesis, using GAP as starting material. Analytical data as well as the results of the sensitivity testing and detonation parameter calculations have been accepted for publication in the *Central European Journal of Energetic Materials*.

The second part attempted the syntheses and investigation of energetic polyurethanes, polyureas and related polymers, using hexamethylene diisocyanate, diisocyanato ethane and diisocyanato methane with several energetic and nitrogen-rich diols, diamines, dicarbamates and dihydrazides. It turned out that only the polyaddition reactions with diols towards polyurethanes were successful and resulted in satisfying analytical and energetic data. Parts of the results of the polyurethane investigations have been accepted for publication in the *Journal of Applied Polymer Science*.

The third topic focuses on the investigation of polymers on the basis of mono- and difunctionalized tetrazolyl epoxides. For the syntheses towards the mono- and difunctionalized epoxy precursors several starting materials were prepared. Amongst others, two different constitutional isomers of divinyl and bisallyl derivatives of 1,2-bis(tetrazole-5-

yl)ethane were successfully synthesized and characterized. The attempted syntheses following different reaction paths towards the desired epoxides only revealed traces of the desired compounds in the reaction medium or yielded monoepoxy compounds instead of the difunctional molecules. Results of analytical and physical data concerning the divinyl and bisallyl derivatives of 1,2-bis(tetrazole-5-yl)ethane were submitted for publication in *Zeitschrift für Naturforschung B − A Journal for Chemical Science*.

Subject of the fourth part of this thesis is the synthesis of energetic plasticizers on the basis of 2,2-bis(azidomethyl)propane-1,3-diol, 2,2-dinitropropane-1,3-diol and 1,2-bis(hydroxyethyl tetrazole-5-yl)ethane. The syntheses were carried out in a one-step synthesis with three different acyl chlorides, varying in carbon chain length. The synthesized compounds were investigated regarding their high and low temperature behavior, as well as their plasticizing effects by analyzing certain properties of mixtures of them with two different energetic polymers. Parts of these results have been submitted for publication in *Propellants, Explosives, Pyrotechnics*.

TABLE OF CONTENTS

Table of Contents

INTRODUCTION

1. Introduction

1.1 Classification of Energetic Materials

With respect to its altering reaction behaviors and therefore varying application fields, the group of energetic materials can roughly be divided into four subgroups: 1. Primary explosives 2. Secondary explosives 3. Pyrotechnics and 4. Propellants (**Figure 1.1**).
Secondary explosives can additionally be divided into compounds for military and civil purposes, as well as propellants into rocket propellants and propelling charges for ammunition.[2]

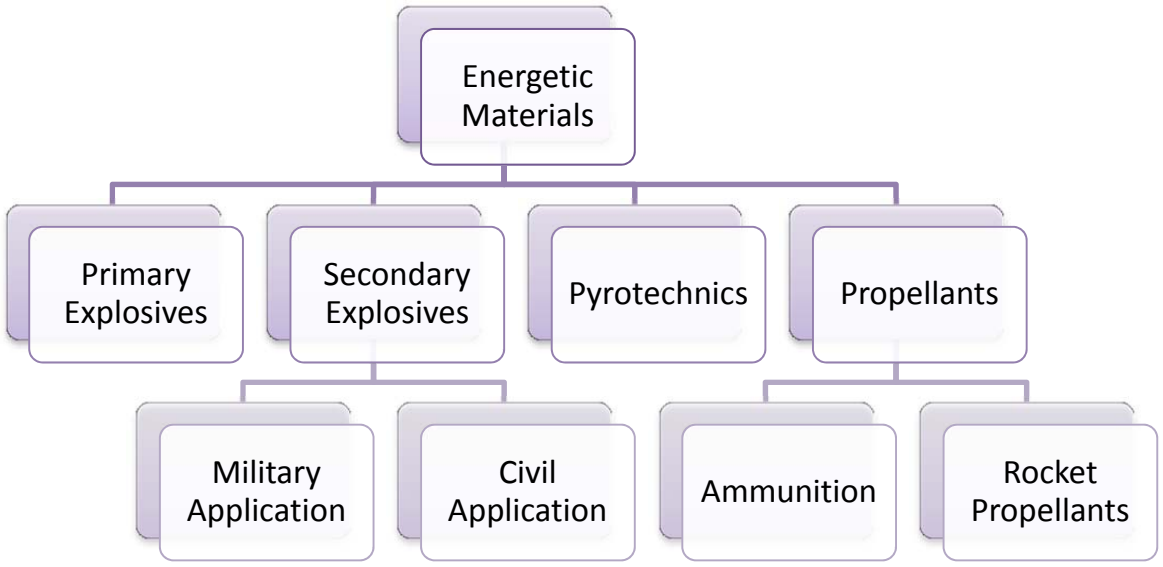

Figure 1.1 Classification of energetic materials.

1.2 Primary Explosives

Primary explosives are mainly used as initiators for explosive systems, taking advantage of the large heat quantity or shock wave, resulting from their rapid transition from combustion (or deflagration) to detonation. Therefore, as one of its main characteristics, a primary explosive presents high sensitivities towards external stimuli like heat, impact, friction or

electrical discharges.[2 3] After thus effected initiation, the released energy triggers the exothermic reaction of the less sensitive but energetically much more powerful secondary explosive within the respective explosive system. The usual detonation velocities (V_{det}) of primary explosives range between 3500 to 5500 m s^{-1} and hence are much slower than those of secondary explosives.[2]

Currently, due to their power and high sensitivities, lead azide and lead styphnate, as well as cadmium azide represent some of the most common primary explosives (**Figure 1.2**). [2]

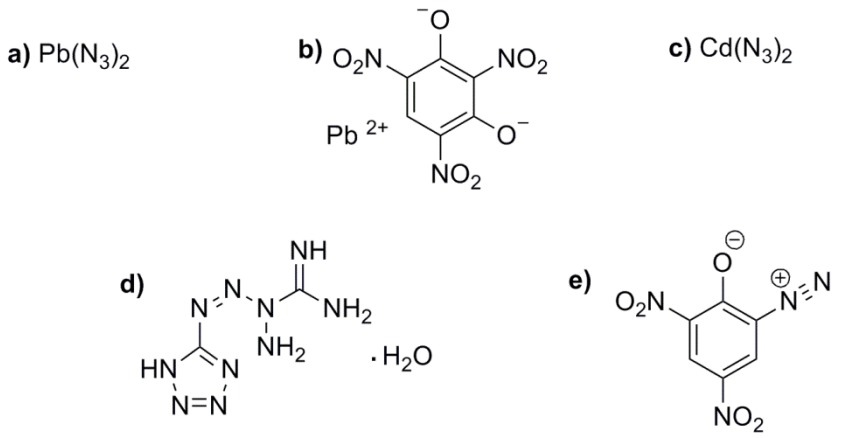

Figure 1.2 Examples of primary explosives **a)** lead azide, **b)** lead styphnate, **c)** cadmium azide, **d)** tetracene, **e)** diazodinitrophenole.

However, a severe disadvantage of these compounds represents their content of toxic heavy metal cations.[4] Therefore, some metal-free organic primary explosives, like tetracene or diazodinitrophenole have been developed (**Figure 1.2**). Besides these metal-free compounds, two other very promising replacements for lead azide containing the non- or less-toxic metals potassium (potassium 1,1'-dinitramino-5,5'-bistetrazolate, K_2DNABT)[5] and copper (copper(I) 5-nitrotetrazolate, DBX-1)[6] were developed in the last few years (**Figure 1.3**).

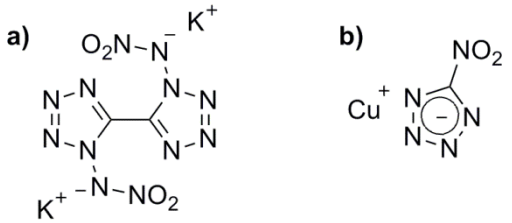

Figure 1.3 Promising, less toxic primary explosives **a)** K_2DNABT, **b)** DBX-1.

1.3 Secondary Explosives

Secondary explosives represent relatively stable and abundant components of explosive materials. Since their behavior towards external stimuli appears to be rather insensitive, its initiation needs to be triggered by an external detonator (usually containing a primary explosive). However, the resulting energy output of the secondary explosive is remarkably higher compared to primary explosives. Just like the corresponding detonation velocity (V_{det} = 5500 to 9000 m s^{-1}), pressure (p_{CJ}) and heat ($\Delta_E U°$), which represent important parameters of the energetic performance.

Widely known secondary explosives are TNT (2,4,6-trinitrotoluene), HMX (high melting explosive / her majesty's explosive, octogen, octahydro-1,3,5,7-tetranitro-1,3,5,7-tetrazine) or RDX (research department explosive / royal demolition explosive, hexogen, hexahydro-1,3,5-trinitro-1,3,5-triazine) (**Figure 1.4**).[2]

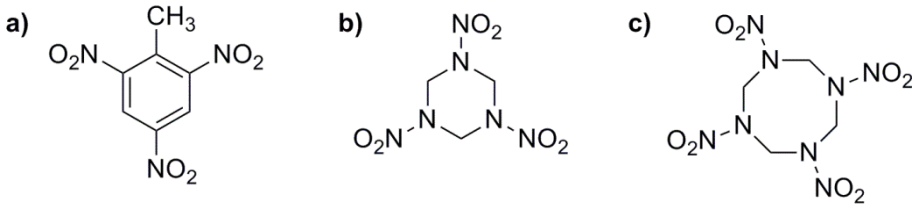

Figure 1.4 Examples of secondary explosives **a)** TNT, **b)** RDX **c)** HMX.

A quite promising new replacement for the broadly militarily used RDX seems to be the bistetrazole compound TKX-50 (dihydroxylammonium 5,5'-bistetrazole-1,1'-diolate) (**Figure 1.5**).[7] It shows a better energetic performance than RDX, but at the same time has proven to be less toxic towards micro bacterial organisms than RDX.

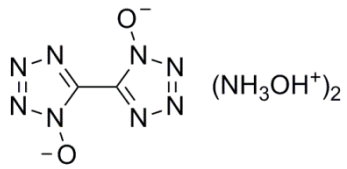

Figure 1.5 A promising RDX replacement, TKX-50.

Besides the military aspect, secondary explosives also find application within the civil sector.

They find application as explosives in the fields of tunneling, mining or oil drilling. Here, explosives with lower energetic performances are used due to aspects of safety and a cheaper synthesis (compared to RDX or HMX), like ANFO (ammonium nitrate fuel oil) or HNS (hexanitrostilbene) (**Figure 1.6**).[8]

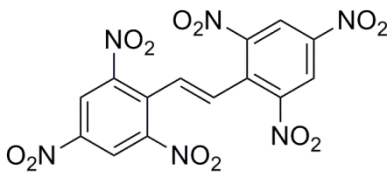

Figure 1.6 Structure of HNS.

1.4 Propellants

Unlike the previously described energetic materials, propellants are meant to deflagrate instead of detonate, generating a possibly high specific impulse I_s, which represents an essential parameter of propellants, describing their efficiency regarding propulsion.[9]

Propellants can be divided into two subgroups: ammunition and rocket propellants. The oldest known propellant charge is black powder, which can be assigned to the ammunition group. It is composed of 75 % KNO_3, 10 % sulfur and 15 % charcoal dust. However, due to its low performance and massive generation of corrosive gases (NO_x and SO_x), it is barely used today. Instead, the *via* nitration of cellulose generated nitrocellulose (NC, single-base propellant) represents a suitable replacement for black powder in e.g. pistols, burning almost without residues, due to its high oxygen balance. In order to improve the specific impulse double- and even triple-base propellants (nitrocellulose + nitroglycerine / + nitroguanidine) were developed (**Figure 1.7**). Those find application according to the respective type of artillery.

However, since the released high temperatures caused noticeable erosion problems in the gun barrel due to increased iron carbide formation, current research focuses on propellants that burn with possibly low temperature, but still result in good values for I_s.[10] Additionally by increasing the N_2/CO ratio, it is aimed to reduce the CO emission which contributes to the observed erosion. Since 1970, so called low-vulnerability ammunition (LOVA) propellants,

which do not deflagrate or detonate after external stimuli, became more and more prominent.[2]

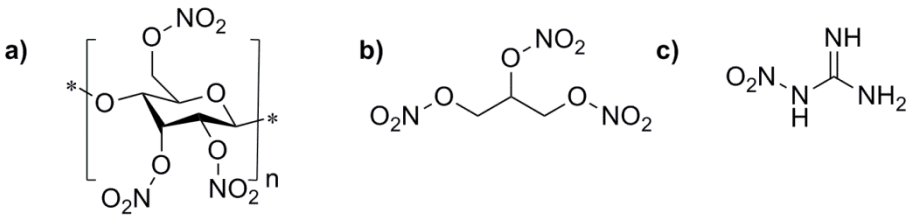

Figure 1.7 Structures of the propellants **a)** nitrocellulose, **b)** nitroglycerine, **c)** nitroguanidine.

Since rockets are usually fired only once, the requirements for rocket propellants differ from those of ammunition propellants. Here, the specific impulse plays an even more important role and should be as high as possible. The subgroup of rocket propellants can further be divided into solid and liquid propellants. Solid propellants are for example composed of double-base propellants or ammonium perchlorate in combination with aluminum. Liquid propellants are for example mixtures of HNO_3 or NO_2/N_2O_4 with hydrazine derivatives like MMH (Monomethylhydrazine).[2]

1.5 Pyrotechnics

Representing the average group within energetic materials regarding their exothermic reaction speed, pyrotechnics are compositions designed for a variety of applications, exploiting the generation of heat, light, smoke and noise. However, not only its composition, but also homogeneity of the pyrotechnic's mixture, as well as the particle size, represent crucial factors for the resulting reaction behavior.[2 11] Heat generating pyrotechnics find application as initiators, quickly triggering the release of a flame after impact of external stimulations, setting up e.g. a detonation. The generation of smoke is used for the purpose of camouflage, releasing a cloud of aerosol. Light emitting pyrotechnics particularly represent useful tools for the purpose of localization of either castaways or landing places for e.g. aircrafts in signal ammunition. But of course, they are also used for civil purposes in fireworks. The illumination intensities and the emitted wavelengths are directly linked to the used component mixture.[2]

1.6 Energetic Polymers

Over the decades, the use of energetic materials increased and the demand for more safety and better handling properties of those materials grew even more. This involved a reduction of the sensitivity towards outer stimuli like heat, impact, shock, etc., without decreasing the energetic performance of the system. Consequently, insensitive munitions[12], composite propellants[13] and polymer-bonded explosives (PBX)[14] were developed amongst others. Here, the crystalline or liquid energetic components are embedded in a matrix of cross-linked polymers. Thus, a better and easier handling of the mixtures is achieved, also by reducing the formulations sensitivity towards external stimuli.[15 16]

Proper mixing of the binder and its energetic filler can be achieved by melting a (homogenous) mixture of the components and a subsequent slow hardening by controlled cooling, or (in case of liquid binders) by the addition of a curing agent to a well mixed composite of the ingredients for cross-linking the polymer chains (hardening process).

In order to guarantee a high long-term safety standard of the energetic formulation, adhesion properties and interaction behavior between binder and the energetic filler are, besides the thermal and physical stability of the binder, of great importance. An insufficient adhesion or interaction can lead to severe problems, regarding safety in handling and use. Examples of resulting failures, due to lacks of adhesion or interaction, are crack-formations in the explosive composition[17], detachment of the polymeric matrix or exudation of the bound ingredients[18 19].

Specific problems concerning insufficient binder-filler interactions cause nitramine containing explosives, like the broadly used RDX and HMX. With most binders the nitramine groups only show poor interaction behaviors, which leads to dewetting of the energetic filler. Therefore, certain adhesion promoters were developed. One example of such promoters are substituted amides, which are able to interact with nitro groups.[19]

Today's state-of-the-art binder, which fulfills many of the demanded properties as binder for propellant and explosive formulations is hydroxyl-terminated polybutadiene (HTPB) (**Figure 1.8**).

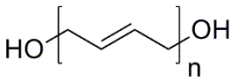

Figure 1.8 Hydroxyl-terminated polybutadiene (HTPB).

All in all, this compound shows very good properties, especially regarding its mechanical properties, ageing stability and chemical stability, together with desirable viscosity and solids loading.[15] When used as a binder the polymer provides a void-free matrix by wetting the solid filler and improving the mechanical and safety properties of the energetic formulation, which even guarantees a safe handling also in large casting amounts. However, the non-energetic character of HTPB leads to a loss of the energetic performance, unless the formulation harbours a high solids loading. But the increased amount of energetic solids leads in turn to safety issues and processing problems, which limits the possibilities of application fields. This dilemma can be avoided by the replacement of the inert binder by, or the addition of energetic polymers. This can also improve the composition's efficiency and even contribute to its energy output, simultaneously providing enhanced thermal and physical stability. This basic concept led to the development of various classes of energetic polymers over the last few decades.[15 16 14] Many known energetic polymers contain azido or nitrato moieties as energetic functional groups. In **Figure 1.9** different developed energetic polymers are depicted.

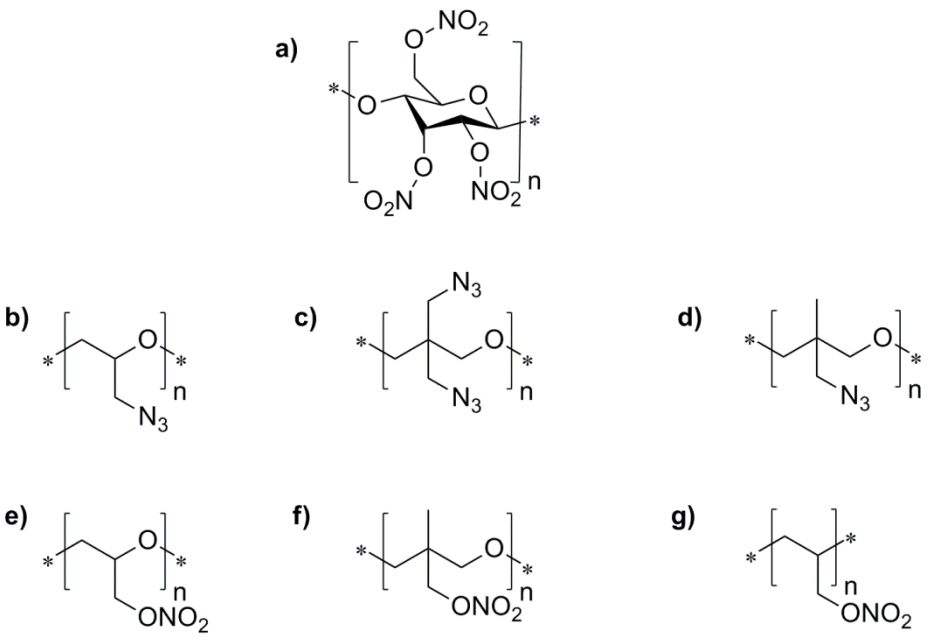

Figure 1.9 Selected energetic polymers **a)** nitrocellulose (NC) **b)** glycidyl azide polymer (GAP), **c)** poly[3,3-(bisazidomethyl)oxetane] (polyBAMO), **d)** poly(3-azidomethyl-3-methyl oxetane) (poly(AMMO), **e)** poly(glycidyl nitrate) (polyGLYN), **f)** poly(3-nitratomethyl-3-methyl oxetane) (polyNIMMO), **g)** polyvinyl nitrate (PVN).

The presence of the energetic functional groups, provided by the energetic polymer, allows a decrease in the amount of used energetic filler. This directly enhances the safety of the energetic formulation.

1.6.1 Energetic Polymers Based on Cellulose

The first encounter with nitrocellulose (NC) was accidentally made by SCHÖNBEIN in 1846.[20] Its high oxygen content and residue-free combustion represented good features. Together with other desirable properties, this aspect rendered NC a versatile material for different kinds of application. It was used as celluloid for former movies, in table tennis balls, membranes or varnishes. In the field of energetic materials, it is used in pyrotechnical compositions, as propellant or as binder. Despite its numerous negative properties, like its poor long term stability, as well as low thermal (T_{dec}~160 °C) and physical stability (IS > 3 J, FS >353 N, depending on the degree of nitration)[18], NC is still in use today, because of its

extremely low costs and easy application.

Further examples of cellulose based energetic compounds are azidocellulose and azidocellulose nitrate[21] which find application as propellants[22]. Azidocellulose can be obtained by substitution reactions of sodium azide with either iodocellulose or the respective tosylated compound.[23]

1.6.2 Energetic Polymers Based on Nitrate Esters

The best known polymers based on nitrate esters (aside from NC) PVN, polyGLYN and polyNIMMO, are derived from three different monomer types: vinyl compounds, epoxides and oxetanes.

Whereas PVN is mostly obtained from the nitration of polyvinyl alcohol[24], which means the energetic group is introduced after the polymerization step. The polymerization step of the other two compounds is performed after the synthesis of the respective nitrated monomer (**Scheme 1.1**).[15]

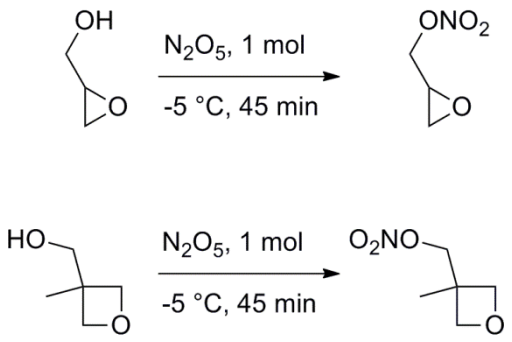

Scheme 1.1 Nitritaion of the monomers of polyGLYN and polyNIMMO

The synthesis has to be carried out in this order. Otherwise the nitration would lead to nitrated terminal hydroxyl groups, which are necessary for the subsequent cross-linking reactions, if the compounds are applied as binder. Special attention has to be payed to the exact adherence of the stoichiometry of the monomer to N_2O_5. If the nitrating agent is used in an excess (> 2 equivalents), this will result in a ring opening reaction and the formation of threefold nitrated nitroglycerin derivatives.

Despite their good energetic properties and moderate to good sensitivities (IS 10 J (PVN, polyGLYN)[18 25] to insensitive (polyNIMMO)[16], FS 112 N (polyGLYN)[25], 196 N (PVN)[18] to insensitive (polyNIMMO)[16]) the polymers based on nitrate esters lack in terms of thermal stability. With 170-175 °C their decomposition temperatures are relatively low. [18 26]

1.6.3 Energetic Polymers Based on Azides

When discussing energetic polymers based on azides GAP, polyAMMO and polyBAMO have to be named. Amongst these three compounds, GAP represents the best known one.
Just like the previously mentioned polyGLYN, GAP possesses a glycidyl backbone and is therefore based on an oxirane monomer. Contrary to polyGLYN, the introduction of the energetic group is carried out after the polymerization step (**Scheme 1.2**). The polymerization of the used monomer epichlorohydrin (ECH) is cationically initiated, usually by a Lewis acid and a (difunctional) alcohol. After the formation of polyepichlorohydrin the halogen-azide-exchange is carried out with sodium azide.

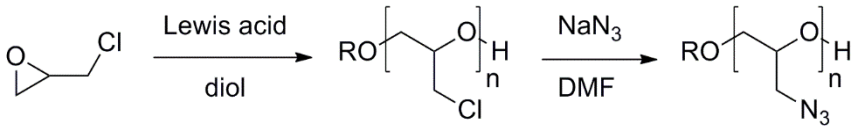

Scheme 1.2 Synthesis of GAP.

GAP is the most promising candidate for truly finding application in energetic formulations so far. It stands out due to its relatively high density (1.3 g cm^{-3})[27] and good thermal (216 °C)[18], as well as its physical stability (IS 7 J, FS >360 N)[18] (values are given for the hydroxyl terminated form with standard molecular weight of M_n = 2000 g mol^{-1}). Furthermore, GAP possesses a positive heat of formation ($\Delta_f H_m$), with literature given values up to +490.7 kJ mol^{-1} [15]. All these properties classify GAP as an interesting compound for application as binder in propellant formulations.[16] Due to its honey-like consistency GAP needs to be cured, if applied as binder, which is usually achieved by the formation of cross-linking carbamate groups *via* the addition of isocyanate compounds.[28] Unfortunately, GAP does not show the best mechanical properties, in that context.[29] Therefore, the search for an adequate energetic

binder, which can be applied in energetic formulations is not yet completed.

Like polyNIMMO, polyAMMO and polyBAMO are based on oxetane monomers. Unlike in the case of the previously described syntheses, the order of the carried out reaction steps is not of that importance in those cases. Both compounds can be synthesized over both routes, the previous introduction of the energetic group or first the polymerization step (**Scheme 1.3**).[30 31 32]

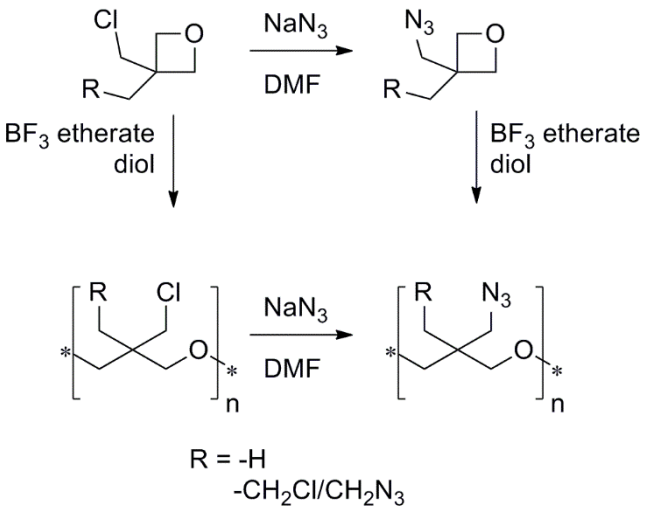

Scheme 1.3 Synthetic routes for polyAMMO and polyBAMO.

Contrary to GAP, polyAMMO and polyBAMO are solids at room temperature. In terms of the energetic output of the overall binder system this can be seen as an advantage, since no (usually non-energetic) curing agents are needed.[33] The solid character of these compounds also explain the higher sensitivities towards friction and impact with IS >5 J and FS >288 N (values for polyBAMO)[18], compared to the viscous GAP. The thermal stabilities of the oxetane based polymers are in the approximate range of GAP or above (203 °C (polyBAMO)[34] and 244 °C (polyAMMO)[35] vs 216 °C (GAP)).

1.6.4 Energetic Polymers Based on Other Energetic Functional Groups

Besides the already mentioned polymers based on nitrate esters or azido groups, several other energetic polymer classes are described in literature. Beneath those, two particular compounds (classes) should be mentioned:

On the one hand, a polymer based on nitro groups, polynitropolyphenylene (PNP) (**Figure 1.10**), which is obtained in an ULLMANN reaction using 1,3-dichloro-2,4,6-trinitrobenzene in nitrobenzene with copper powder.[18]

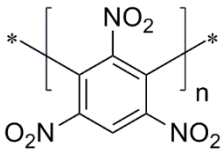

Figure 1.10 Polynitropolyphenylene (PNP).

PNP stands out because of its high thermal stability (280-304 °C)[18], which, together with the relatively good oxygen balance for energetic binders (−49 %) and insensitivity towards friction predestines this compound for LOVA high ignition temperature propellants. Its downside is a high impact sensitivity (3-5 J).[18]

The second compound class, which turned out to be of interest for newly developed energetic polymers nowadays, are tetrazoles. They offer interesting properties for the demands of new energetic polymers.[36] They bring along a high nitrogen content (up to 79 % for 1*H*-tetrazole) and hence an environmentally friendliness (due to their solely gasous decomposition products N_2 and CO/CO_2 and, in general, a lesser toxicity towards biota). Additionally, they possess overall good thermal stabilities and considerable energetic properties. They also offer high heats of formation, but are more stable than compounds harboring azide groups. [15] Consequently, polymers based on tetrazoles are considered to be promising new binders for energetic formulations.

One example of a tetrazole based polymer is poly(vinyl tetrazole) (PVT) (**Figure 1.11**).[37]

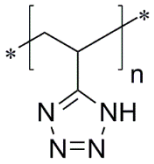

Figure 1.11 Polyvinyl tetrazole (PVT).

1.7 Energetic Plasticizers

Not only polymers (binders), but also plasticizers, play a certain role in energetic formulations, concerning their safety characteristics and processability. By adding plasticizers, the chain dynamics of (amorphous) polymers are modified in a positive way. This is acchieved by increasing its flexibility and softening point, resulting in a decreased glass transition temperature T_g.[38] The used binders often show poor low temperature behavior by becoming brittle and friable at certain temperatures. This leads to an increased failure rate (e.g. crack formation) and therefore bad safety characteristics. The addition of a plasticizer influences the consistency of the binder and hence leads to an earlier transition from a brittle like state ($T<T_g$) into the desired flexible, rubber-like material ($T>T_g$).

The average number of molecular weight of a typical plasticizer ranges from 200 to 2000 g mol^{-1}. While plasticizers with lower molecular weights tend to be more effective in reducing the glass transition temperature, they also are highly volatile and show some exudation behavior over time. This migration of plasticizers out of a formulation (exudation), represents a common problem which is related to the low molecular weight of the applied molecules, negatively affecting the quality of the explosive composition over time. Hence, in order to enable a better incorporation of the additives, molecular weights between 400 and 1000 g mol^{-1} proved to possess the best plasticizing characteristics.[16] Besides, an approach targeting an increased structural similarity between the energetic polymers and the plasticizer has resulted in more stable formulations with reduced exudation.[16]

As for the above mentioned binders, there are two classes of common plasticizers: the energetic and the non-energetic ones.

The non-energetic plasticizers are predominantly used for their excellent properties in modifying T_g, strength and elongation toughness of a binder. The obvious disadvantage of this type of plasticizer is the lack of energetic qualities. Typical representatives of utilized non-

energetic plasticizers in energetic compositions are triacetin, organic phthalates, like dioctyl phthalate (DOP) or esters of adipic acid, like dioctyl adipate (DOA) (**Figure 1.12**).[13 39]

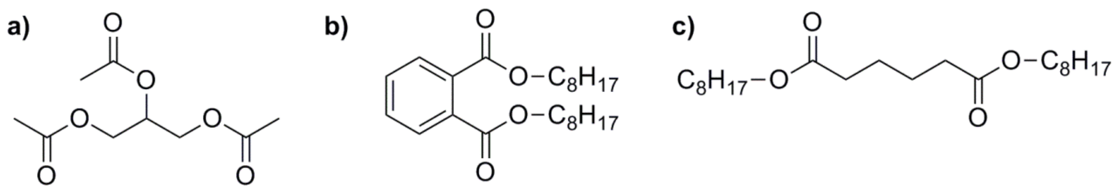

Figure 1.12 Examples of non-energetic plasticizers **a)** triacetin, **b)** dioctyl phthalate (DOP), **c)** dioctyl adipate (DOA).

The energetic representatives should preferably show a similar plasticizing effect, like their non-energetic counterparts, but also contribute to the oxygen balance and energetic performance of an energetic system. Because of their advantageous oxygen balance, most of the used energetic plasticizers are based on nitrate esters or nitramines (**Figure 1.13**)

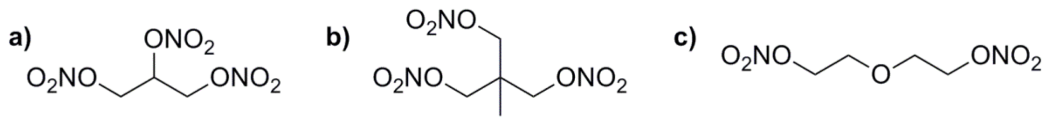

Figure 1.13 Examples of broadly used plasticizers based on nitrate esters **a)** nitroglycerine (NG), **b)** trimethylol ethane trinitrate (TMETN), **c)** diethylene glycol dinitrate (DEGDN).

Nonetheless, there are also examples of azido based plasticizers, which are often used in combination with GAP to improve its poor mechanical properties.[16] Selected examples of azido based plasticizers are depicted in **Figure 1.14**.

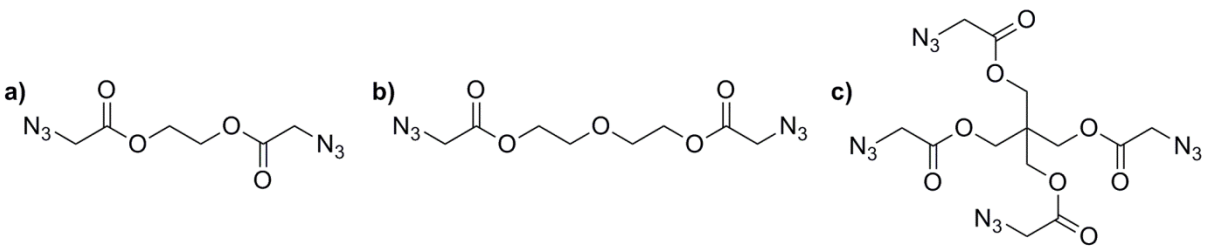

Figure 1.14 Examples of azido based plasticizers **a)** ethylene glycol bis(azidoacetate) (EGBAA), **b)** diethylene glycol bis(azidoacetate) (DEGBAA), **c)** pentaerythritol tetrakis (acidoacetate) (PETKAA).

Oligomers or dimers of GAP, polyNIMMO and polyGLYN were also developed as energetic plasticizer. Due to the structural similarity to their corresponding polymers, they represent useful plasticizers in terms of compatibility.[16]

1.8 References

1 V. A. Hartdegen, *Master Thesis*, Ludwig-Maximilians-Universität München, **2011**.

2 T. M. Klapötke, *Chemistry of High-Energy Materials*, 3. Edition, De Gruyter, Berlin, **2015**.

3 R. M. H. Wyatt, P. W. J. Moore, G. K. Adams and J. F. Sumner, *Proceedings of the Royal Society of London. Series A, Mathematical and Physical Sciences*, **1958**, *246*, 189-196.

4 a) S. H. DeMent, J. J. Chisolm, M. A. Eckhaus, J. D. Strandberg, *Journal of wildlife diseases* **1987**, *23*, 273-278; b) S. J. Kopp, J. T. Barron, J. P. Tow, *Environmental health perspectives* **1988**, *78*, 91-99; c) N. A. Ankrah, Y. Kamiya, R. Appiah-Opong, Y. A. Akyeampon, M. M. Addae, *East African medical journal* **1996**, *73*, 375-379; d) G. G. Yannarelli, A. J. Fernandez-Alvarez, D. M. Santa-Cruz, M. L. Tomaro, *Phytochemistry* **2007**, *68*, 505-512; e) D. K. Gupta, U. N. Rai, A. Singh, M. Inouhe, *Pollution Research* **2003**, *22*, 457-463.

[5] D. Fischer, T. M. Klapötke, J. Stierstorfer, *Angew. Chem. Int. Ed.* **2014**, *53*, 8172-8175.

[6] J. W. Fronabarger, M. D. Williams, W. B. Sanborn, J. G. Bragg, D. A. Parrish, M. Bichay, *Propellants, Explos., Pyrotech.* **2011**, *36*, 541-550.

[7] N. Fischer, D. Fischer, T. M. Klapötke, D. G. Piercey, J. Stierstorfer, *J. Mater. Chem.* **2012**, *22*, 20418-20422.

[8] a) C. P. Achuthan, S. S. Samudre, J. S. Gharia, *J. Sci. Ind. Res.* **1984**, *43*, 197-199; b) B. Singh, R. K. Malhotra, *Def. Sci. J.* **1983**, *33*, 165-176.

[9] T. L. Davis, *Chemistry of Powder and Explosives*, John Wiley, New York, **1943**.

[10] a) R. L. Simmons, H. L. Young, *US 4450110A*, **1984**; b) W. Kloehn, H. Schubert, *DE 2329558A1*, **1975**; c) B. K. Bertram, G. L. Mackenzie, F. J. Pisacane, *US 3734789A*, **1973**.

[11] J. A. Conkling, C. Mocella, *Chemistry of Pyrotechnics: Basic Principles and Theory*, 2. Edition, CRC Press, Boca Raton, **2011**.

[12] B. H. Bonner *Propellants, Explos., Pyrotech.* **1991**, *16*.

[13] J. P. Agrawal, *High Energy Materials*, WILEY-VCH, Weinheim **2010**.

[14] M. A. Daniel, Report *DSTO-GD-0492*, Defence Science and Technology Organisation, Edinburgh South Australia,, Australia **2006**.

[15] H. G. Ang, S. Pisharath, *Energetic Polymers − Binders and Plasticisers for Enhancing Performance*; 1. Edition, Wiley-VCH, Weinheim, **2012**.

[16] A. Provatas, Report *DSTO-TR-0966*, Defence Science and Technology Organisation, Melbourne Victoria, Australia **2000**.

[17] C. Hübner, E. Geißler, P. Elsner, P. Eyerer, *Propellants, Explos., Pyrotech.* **1999**, *24*, 119-125.

[18] R. Meyer, J. Köhler, A. Homburg, *Explosives*, 6. Edition, Wiley-VCH, Weinheim, **2007**.

[19] J. M. Bellerby, C. Kiriratnikom, *Propellants, Explos., Pyrotech.* **1989**, *14*, 82-85.

[20] T. Urbanski, *Chemie und Technologie der Explosivstoffe*, VEB Deutscher Verlag für Grundstoffindustrie, 2. Edition, Leipzig, **1963**.

[21] a) E. E. Gilbert, *Journal of Energetic Materials* **1985**, *3*, 319; b) Y. P. Garignan; E. E. Gilbert, *US 87247091*, **1988**.

[22] R. D. Guthrie, D. Murphy, *J. Chem. Soc.* **1965**, 6956-6960.

[23] a) E. E. Gilbert, *US 4849514*, **1989**; b) Azow et al. *Chem. Abstracts* **1973**, *79*, 93618.

[24] L. A. Burrows, W. F. Filbert, *US 2118487A*, **1938**.

[25] values determined **2003** by the *Fraunhofer-Institut für Chemische Technologie*, Pfinztal, Germany.

[26] M. E. Colclough, H. Desai, R. W. Millar, N. C. Paul, M. J. Stewart, P. Golding, *Polym. Adv. Technol.* **2003**, *5*, 554-560.

[27] M. B. Frankel, *J. of Propul. Power* **1992**, *8*, 560-563.

[28] H. R. Blomquist, *US 6802533*, **2004**.

[29] B. S. Min, *Propellants, Explos., Pyrotech.* **2008**, *33*, 131-138.

[30] R. A. Earl; J. S. Elmslie, *US 4405762*, **1983**.

[31] H. Desai, *Telechelic polyoxetanes. The polymeric materials encyclopedia: Synthesis, Properties and Applications*, 11. Edition, CRC Press, **1996**.

[32] Y. M. Mohan, Y. Mani, K. M. Raju, *Des. Monomers Polym.* **2006**, *9*, 201–236.

[33] a) R. B. Wardle, P. C. Braithwaite, A. C. Haaland, J. A. Hatwell, R. R. Hendrickson, V. Lot, I. A. Wallace, C. B. Zisette, High Energy Oxetane/HNIW Gun Propellants, *27th Int. Annual Conference of ICT*, Karlsruhe, Germany, June 25 - 28, **1996**; b) Y. Oyumi, T. B. Brill, *Combust. Flame* **1986**, *65*, 127.

[34] J. K. Nair, R. S. Satpute, B. G. Polke, T. Mukundan, S. N. Asthana, H. Singh, *Def. Sci. J.*, **2002**, *52*, 147-156.

[35] U. Barbieri, G. Polacco, E. Paesano, R. Massimi, *Propellants, Explos., Pyrotech.* **2006,** *31*, 369-375.

[36] a) S. M. Sproll, *Ph.D. Thesis*, Ludwig-Maximilians-Universität München, **2009**; b) F. M Betzler, *Ph.D. Thesis*, Ludwig-Maximilians-Universität München, **2013**.

[37] a) W. G. Finnegan; R. A. Henry; S. Skolnik, *US 3,004,959*, **1961**; b) P. A. Aleshunin; U. N. Dmitrieva; V. A. Ostrovskii *Russ.J. Org. Chem.* **2011**, *47*, 1882.

[38] S. Koltzenburg, M. Maskos, O. Nuyken, *Polymere: Synthese, Eigenschaften und Anwendungen*, 1. Edition, Springer Spektrum, Berlin-Heidelberg, **2014**.

[39] R. S. Damse, A. Singh, *Def. Sci. J.* **2008**, *58*, 86-93.

CONCEPTS AND AIMS

2. Concepts and Aims

Despite the broad variety of already established energetic polymers and plasticizers, the development of new energetic polymers is still of interest. Since previously developed compounds are not suited to fully replace the well-established non-energetic binders and plasticizers in insensitive and high performance propellants, explosives or pyrotechnic formulations. Most of these compounds show considerable disadvantages, like low thermal or physical stability, low adhesive properties, poor low temperature behavior or, in general bad mechanical properties.

Therefore, the aim of this dissertation was the development of new polymers and plasticizers with different energetic functional groups and the investigation of their physical and energetic properties. The main focus was put on three different energetic functional groups:

1. Organic azides, due to their high heats of formation and good thermal stability
2. Nitro groups, due to their low physical sensitivities and high oxygen balance
3. Triazoles and tetrazoles, due to their high nitrogen content, their environmental friendliness and good thermal and physical stability.

The main demands for the suitability as binder of the newly developed compounds were high thermal (decomposition temperature >200 °C) and physical (impact sensitivity > 15 J, friction sensitivity >100 N) stability and, in case of liquid products, possibly low glass transition temperatures to stabilize the energetic filler. Moreover, a high chemical stability is required to avoid reactions between the binder and the filler and therefore guarantee a long-term stability. The energetic properties of the new compounds should exceed or at least be equal with those of established energetic polymers or plasticizers.

ENERGETIC NITRAMINE POLYMER WITH GLYCIDYL BACKBONE

3. Energetic Nitramine Polymer with Glycidyl Backbone

Abstract: A new energetic glycidyl based polymer containing nitramine groups (glycidyl nitramine polymer, GNAP) was synthesized using glycidyl azide polymer (GAP) as starting material. The synthesis involved STAUDINGER azide-amine conversion, followed by carbamate protection of the amino group, nitration with nitric acid (100 %) and trifluoroacetic anhydride and was completed by deprotection with aqueous ammonia.

The obtained products were characterized by elemental analysis and vibrational spectroscopy (IR). The energetic properties of GNAP were determined using bomb calorimetric measurements and calculated with the EXPLO5 V6.02 computer code, showing better values regarding energy of explosion ($\Delta_E U° = -4813$ kJ kg^{-1}) detonation velocity ($V_{det} = 7165$ m s^{-1}) as well as detonation pressure ($p_{CJ} = 176$ kbar) than the comparative polymers GAP and polyGLYN. The explosion properties were tested by impact sensitivity (IS), friction sensitivity (FS), differential scanning calorimetry (DSC), thermogravimetric analysis (TGA) and electrostatical discharge (ESD) equipment. The results revealed GNAP to be insensitive towards friction and electrostatical discharge, less sensitive towards impact (40 J) and a decomposition temperature (170 °C) in the range of polyGLYN.

3.1 Introduction

Polymers play an important role in modern energetic formulations of any kind. They are mostly used as binders in order to reduce the sensitivity of energetic materials towards heat, impact, friction and to improve the mechanical resistance, by constructing a protective matrix around the mainly solid energetic ingredients.[1]

The use of inert polymers, such as hydroxyl-terminated polybutadiene (HTPB) or terpolymers based on butadiene, acrylonitrile and acrylic acid (polybutadiene acrylonitrile, PBAN) is widely reported.[2] Although these polymers are well suited as binders due to their benefitial properties, they have major issue of being non-energetic. The use of such binders in energetic formulations leads to a loss of the energetic performance of the overall system. Therefore the development of energetic polymers gained more and more interest in the past decades.[1 3 4]

Two examples of energetic polymers, which are already commercially available are the glycidyl azide polymer (GAP) and poly(glycidyl nitrate) (polyGLYN) (**Figure 3.1**).

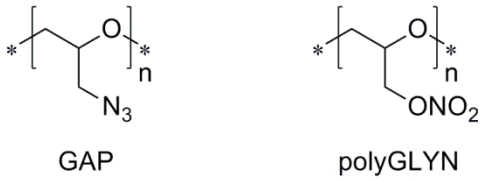

Figure 3.1 Structures of GAP and polyGLYN.

Due to their liquid consistency both compounds need to be cured if used as binders in energetic formulations. This is achieved by adding a curing agent to the binder containing explosive composition. Usually diisocyanato compounds are used to cure the hydroxyl-terminated glycidyl polymers forming an urethane linkage. The reaction of GAP with the curing agent diphenylmethane-4,4'-diisocyanate (MDI) is shown in **Scheme 3.1** as example. [5]

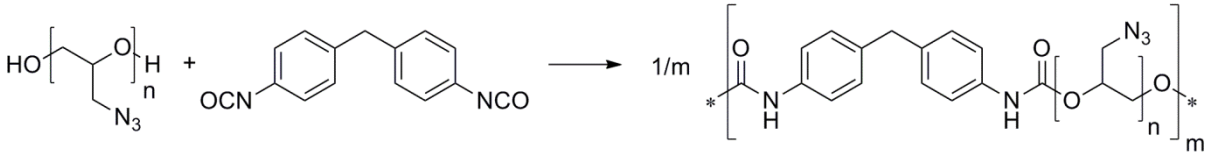

Scheme 3.1 Curing of hydroxyl-terminated GAP using MDI.

This curing step of glycidyl polymer however has the disadvantage of reducing the final energy output of the formulation, as the used isocyanates are non-energetic. Furthermore, curing of these polymers is often accompanied with gas evolution leading to void formation in the composition. Therefore, the objective of this work was to synthesize a solid glycidyl based energetic polymer for binder applications.

3.2 Results and Discussion

3.2.1 Synthesis

It was necessary to convert the azide moieties of GAP into amino groups before proceeding to the desired nitramine by applying the STAUDINGER reaction.[6] To avoid multiple nitration, the amino groups of **1** were protected using ethyl chloroformate. After nitration, the deprotection of **3** was performed with aqueous ammonia. The desired compound **4** was obtained as a yellow, sticky powder. Due to the solid character of GNAP (**4**), no or at least less curing agents should be needed if used in energetic formulations. The synthetic route to obtain GNAP is shown in **Scheme 3.2**.

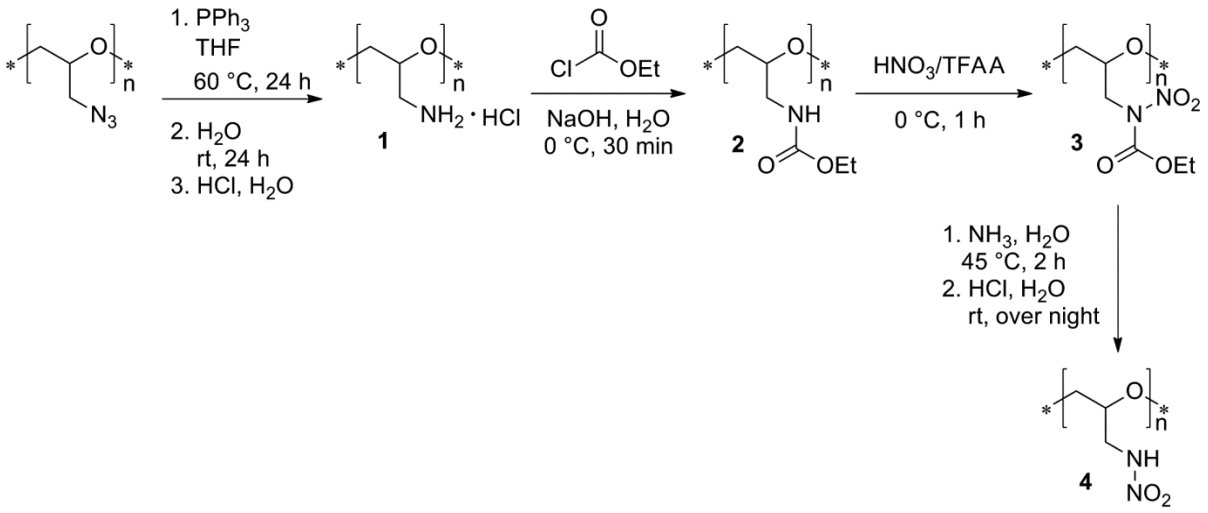

Scheme 3.2 Synthetic route towards glycidyl nitramine polymer (GNAP).

3.2.2 Spectroscopic and Elemental Analysis

The obtained compounds were characterized using IR spectroscopy and elemental analysis. Measured IR spectra of GAP and all synthesized compounds are depicted in **Figure 3.2**.

After the concluded STAUDINGER azide-amine conversion, the values of the measured elemental analysis of **1** fitted well with the calculated contents for one hydrochloride molecule and 0.5 molecules of water per repeating unit of the amino polymer. A comparison of the IR spectra of GAP and **1** reveals significant differences. The characteristic strong vibration of the azide group of GAP at about 2100 cm^{-1} (A)[7] is completely vanished in the spectrum of the amino hydrochloride **1**. Instead, the valence and bending vibrations of the ammonium group at 3380 cm^{-1} (B) and 1600 cm^{-1} (C), respectively appear.[7 8]

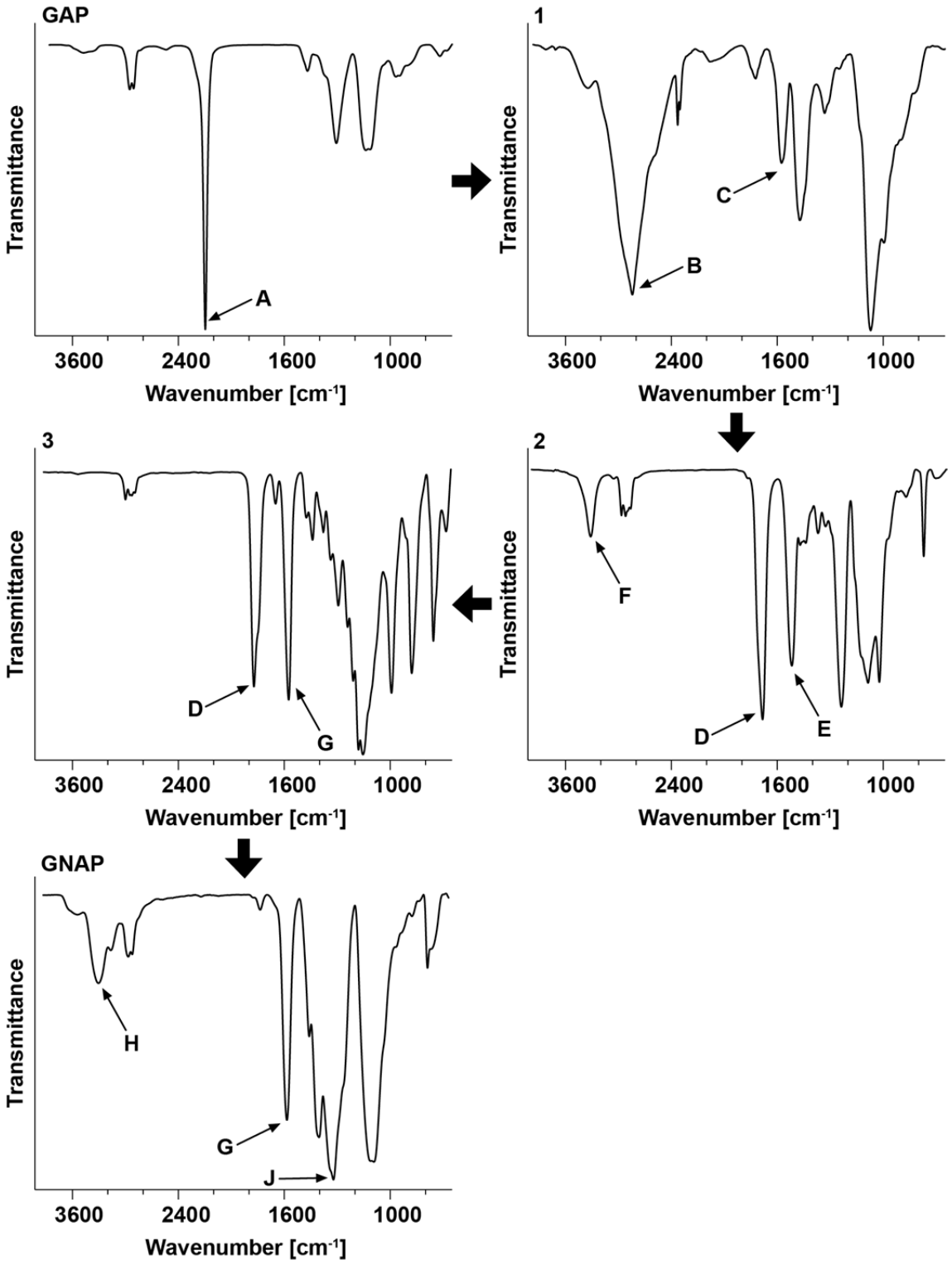

Figure 3.2 Measured IR spectra of GAP, compounds **1-3** and GNAP.

Elemental analysis and measured IR spectra of the carbamate protected amino polymer **2**, as well as for the nitrated carbamate compound **3** proved the formation of both desired products. The IR spectrum of **2** shows the two characteristic carbamate vibrations, the C=O stretching

at 1700 cm^{-1} (D) and the N–H bending vibration (Amide II vibration) at 1520 cm^{-1} (E) with strong intensities. In the vibrational spectrum of **3**, the signals at 3300 cm^{-1} (F) and 1520 cm^{-1} (E) vanish due to the nitration of the protected N–H group. Instead, a strong signal at about 1600 cm^{-1} (G) appears, which can be assigned to the asymmetric vibration of the nitramino group. [7] Besides, the vibration of the carbamate C=O group (D) is moved to higher wavenumbers (1770 cm^{-1}).

After the deprotection of **3** and the following acidification, the elemental analysis of the obtained compound (**4**) revealed a small percentage of remaining carbamate protecting groups in the polymer (1 out of 18 repeating units).

The measured IR spectrum of GNAP shows a lack of the carbamate vibrations and a reappearance of the N–H stretching band at about 3270 cm^{-1} (H) for the primary nitramine.[7] Furthermore the two existing asymmetric and symmetric vibrations (1600 cm^{-1} and 1300 cm^{-1}) of the nitramine group are visible (G, J).[7] This proves the successful synthesis of the glycidyl nitramine polymer (GNAP, **4**).

3.2.3 Thermodynamic and Energetic Properties

Differential scanning calorimetry measurements for the determination of the decomposition temperatures ($T_{dec.}$) of GNAP were performed in closed Al-containers, containing a hole (0.1 mm) for the gas release. GNAP shows a decomposition point at 170 °C (onset of decomposition) (**Figure 3.3**). This value is below the decomposition point of GAP (216 °C)[9] and in the range of polyGLYN (170 °C)[10]. In addition, a TGA was recorded in the temperature range 20-400 °C at a heating rate of 5 °C min^{-1} in an argon atmosphere (**Figure 3.4**). GNAP shows a beginning weight loss around 170 °C, which can be explained by the beginning decomposition of the side chain starting with the nitramine groups. The second step around 220 °C is assignable to the decomposition of the polymeric backbone. Having reached the end temperature of 400 °C an overall (not fully completed) weight loss of 76.7 % was obtained.

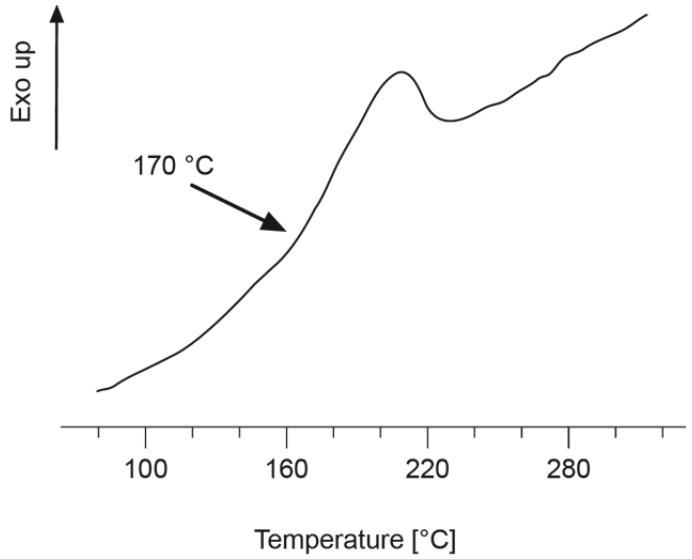

Figure 3.3 DSC plot of GNAP (onset temperatures).

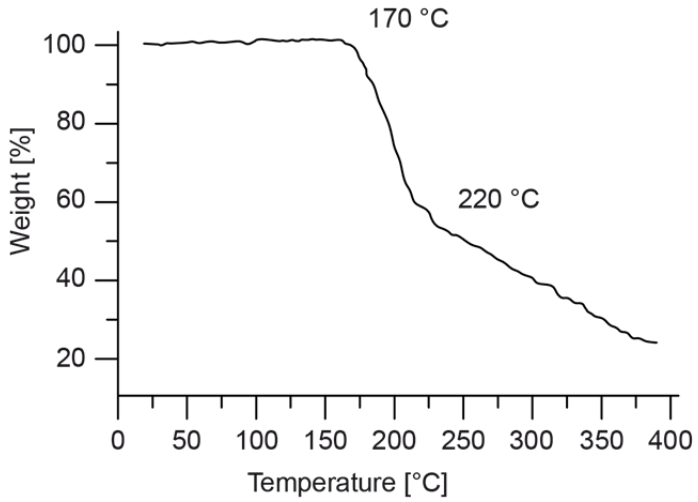

Figure 3.4 TGA plot of GNAP.

The sensitivity data were obtained using a BAM drop hammer and friction tester. [11] These methods revealed that GNAP is insensitive towards friction (>360 N) and less sensitive towards impact (40 J). Compared to GAP (IS: 8 J, FS: > 360 N)[9] and polyGLYN (IS: 10 J, FS: 112 N)[r], GNAP shows higher stability towards impact (40 J) and equal or better stability towards friction (>360 N), which can be regarded as an advantage in terms of safety.

For analyzing the energetic properties of GNAP, the energy of combustion (ΔU_c) was determined *via* bomb calorimetry. The enthalpy of formation could be calculated from the obtained value applying the HESS thermochemical cycle, as reported in literature.[12] The

required heats of formation of H_2O (l) and CO_2(g) with −286 kJ mol^{-1} and −394 kJ mol^{-1} respectively, were obtained from literature.[13] The combustion reaction of GNAP is given in **Scheme 3.3**.

$$C_3H_6N_2O_3 + 3\ O_2 \rightarrow 3\ CO_2\ (g) + 3\ H_2O\ (l) + N_2\ (g)$$

Scheme 3.3 Combustion reaction of GNAP (repeating unit).

All calculations concerning the detonation parameters were carried out using the program package EXPLO5 (version 6.02)[14] and were based on the calculated heats of formation and attributed to the corresponding densities. The obtained data of GNAP is given in **Table 3.1** and compared to the energetic values of GAP and polyGLYN.

Table 3.1 Energetic data of GNAP compared to GAP and polyGLYN.

	GNAP	**GAP[p]**	**polyGLYN[q]**
Formula (repeating unit)	$C_3H_6N_2O_3$	$C_3H_5N_3O$	$C_3H_5NO_4$
Molecular mass [g mol^{-1}]	118.09	99.09	119.08
Impact sensitivity [J][a]	40	8	10[r]
Friction sensitivity [N][b]	>360	>360	112[r]
Ω [%][c]	−81	−121	−60
T_{dec} [°C][d]	170	200	170
ρ [g cm^{-3}][e]	1.5	1.3	1.4
$-\Delta U_{comb}$ [cal g^{-1}][f]	3831	-	-
$-\Delta H_{comb}$ [kJ mol^{-1}][g]	1896	-	-
$\Delta_f H_m°$ [kJ mol^{-1}][h]	−146	142	−323
$\Delta_f U°$ [kJ kg^{-1}][i]	−1261	1545	−2609
EXPLO 5 V6.02 values			
$-\Delta_E U°$ [kJ kg^{-1}][j]	4813	4307	4433
T_E [K][k]	2974	2677	3019
p_{CJ} [kbar][l]	176	129	144
V_{det} [m s^{-1}][m]	7165	6638	6476
Gas vol. [L kg^{-1}][n]	844	822	808
I_s [s][o]	209	207	205

[a] BAM drophammer; [b] BAM friction tester; [c] oxygen balance, [d] temperature of decomposition by DSC (β = 5 °C, onset values); [e] density derived from pycnometer measurement, [f] experimental combustion energy (constant volume); [g] experimental molar enthalpy of combustion, [h] molar enthalpy of formation; [i] energy of formation; [j] energy of explosion; [k] explosion temperature; [l] detonation pressure; [m] detonation velocity; [n] assuming only gaseous products; [o] specific impulse (isobaric combustion, chamber pressure 70 bar, equilibrium expansion); [p] values obtained from the EXPLO5 V6.02 database and ref. [9]; [q] values obtained from refs. [10] and [15]; [r] values determined 2003 by Fraunhofer-Institut für Chemische Technologie, Pfinztal, Germany.

Comparison of the values of $\Delta_E U°$ (an indication of the work performed by the explosive) of GNAP and the references GAP and polyGLYN revealed that GNAP possesses an approximately 10 % higher energy of explosion (GNAP: −4813 kJ kg^{-1}, GAP: −4307 kJ kg^{-1}, polyGLYN: −4433 kJ kg^{-1}). Other important values for the evaluation of the energetic performance are the detonation velocity V_{det} and the detonation pressure p_{CJ}. In case of V_{det}, the value of GNAP (7165 m s^{-1}) exceeds the values of GAP and polyGLYN by 500 m s^{-1} and 700 m s^{-1}, respectively. A comparison of the detonation velocities shows that p_{CJ} of GNAP (176 kbar) is higher by about 50 kbar, in case of GAP and 30 kbar, in case of polyGLYN. Regarding the specific impulse I_s, all the three glycidyl polymers given values are in close range (205-209 s).

Summing up the calculated results of the energetic data, GNAP shows better results in terms of $\Delta_E U°$, V_{det} and p_{CJ} compared to GAP and polyGLYN, which establishes GNAP as an interesting substance for further investigations concerning its suitability as binder in energetic formulations.

3.3 Conclusion

A new glycidyl based energetic polymer was synthesized. With GAP as starting material the desired compound glycidyl nitramine polymer (GNAP) was obtained in a four step synthesis, as a yellow sticky powder. The successful syntheses of the compounds were proven by infrared spectroscopy and elemental analysis. The thermal and physical stabilities of GNAP were determined by DSC measurements and BAM drop hammer and friction tester, respectively. It turned out, that GNAP is insensitive towards friction and equal or less sensitive towards impact than the commercially available energetic polymers GAP and polyGLYN.

The energetic data of GNAP were calculated using the values of the bomb calorimetric measurements and the EXPLO5 version 6.02 computer program. The obtained values reveal a higher energy of explosion, detonation velocity and pressure of GNAP than for the values of the comparative compounds GAP and polyGLYN.

Due to its solid character, no or at least less curing agents are needed when used as a binder. GNAP is therefore of interest as a potential new energetic binder in energetic formulations.

Due to its solid character no or at least less curing agents are needed when used as a binder. GNAP could thus be of interest as a potential new energetic binder in energetic formulations.

3.4 Experimental Part

CAUTION! *All nitramine containing compounds are potentially explosive energetic materials, although no hazards were observed during preparation and handling of these compounds. Nevertheless, this necessitates additional meticulous safety precautions (grounded equipment, Kevlar® gloves, Kevlar® sleeves, face shield, leather coat, and ear plugs).*

Glycidyl amino hydrochloride polymer (1)

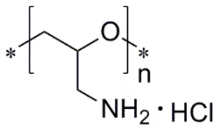

GAP (5.01 g, 50.56 mmol, M_n ~ 2000 g/mol, OH-terminated) was dissolved in 20 mL THF and 2 equivalents PPh_3 (26.52 g, 101.12 mmol) dissolved in 150 mL THF, were added slowly. After stirring for 24 h at 60 °C, the mixture was poured into 200 mL water and stirred for further 24 h at rt. The colorless precipitate was filtered off and the remaining solution was acidified with conc. HCl and washed with dichloromethane (5 x 50 mL). The aqueous phase was evaporated. After drying *in vacuo* 5.43 g (49.55 mmol, 98 %) of **1** were obtained as colorless powder.

Melting point: T_{melt} = 90 °C.
IR (ATR, cm^{-1}): $\tilde{\nu}$ = 3380 (w), 2876 (s), 2362 (m), 2339 (w), 1991 (vw), 1738 (w), 1593 (m), 1593 (w), 1489 (s), 1458 (m), 1421 (w), 1350 (w), 1328 (w), 1091 (vs), 1011 (s), 938 (m), 914 (m), 843 (w).
EA (C_3H_8ClNO): calculated: C 30.39, H 7.65, N 11.81, Cl 29.90 %; found: C 30.03, H 7.44, N 11.65, Cl 31.17 %.

Glycidyl ethyl carbamate polymer (2)

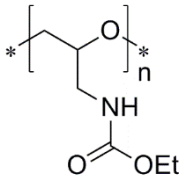

1 (5.83 g, 53.20 mmol) was dissolved in 80 mL (160 mmol) 2 M NaOH and cooled down to 0 °C. Ethyl chloroformate (6.93 g, 63.85 mmol) was added dropwise. The solution was stirred for 30 min at 0 °C. The solvent was decanted and the viscous orange residue was dissolved in 50 mL dichloromethane and washed with brine (2x 30 mL) followed by water (1x 30 mL). The organic phase was dried over $MgSO_4$ and evaporated. After drying under reduced pressure, 4.13 g (28.50 mmol, 54 %) of **2**, as an orange viscous liquid was obtained.

IR (ATR, cm^{-1}): $\tilde{\nu}$ = 3329 (m), 2980 (w), 2934 (w), 2875 (w), 1690 (vs), 1525 (s), 1480 (m), 1445 (m), 1378 (w), 1335 (w), 1245 (vs), 1170 (m), 1093 (s), 1029 (s), 778 (m).
EA ($C_6H_{11}NO_3$): calculated: C 49.65, H 7.64, N 9.65 %; found: C 48.69, H 7.56, N 9.34 %.

Glycidyl ethyl N-nitrocarbamate polymer (3)

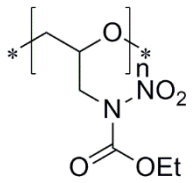

Trifluoroacetic anhydride (TFAA) (83.69 g, 393.7 mmol) was cooled down to 0 °C. Conc. nitric acid (29.77 g, 472.44 mmol) was added dropwise and the mixture was stirred for 10 min. Subsequently, the reaction mixture was added to precooled **2** (3.81 g, 26.25 mmol) and stirred for 1 h at 0 °C. The solution was poured in ice water and stirred overnight. The solvent was decanted and the yellowish residue was dissolved in dichloromethane (50 mL) and washed with brine (2x 20 mL) and water (1x 20 mL). The combined aqueous phases were extracted once with dichloromethane. After drying the combined organic phases over $MgSO_4$, the solvent was evaporated and **3** was dried under reduced pressure to give 4.16 g (21.90 mmol, 83 %) of a yellowish, rubber-like solid.

IR (ATR, cm^{-1}): $\tilde{\nu}$ = 2986 (w), 2914 (vw), 2878 (vw), 1765 (s), 1643 (w), 1568 (s), 1433 (w), 1371 (w), 1288 (m), 1235 (m), 1204 (s), 1174 (vs), 1150 (vs), 986 (s), 873 (s), 750 (s), 679 (w).

EA ($C_6H_{10}N_2O_5$): calculated: C 37.90, H 5.30, N 14.73 %; found: C 37.01, H 5.22, N 14.58 %.

Glycidyl nitramine polymer (GNAP, 4)

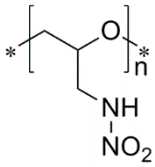

3 (3.97 g, 20.87 mmol) was added to 125 mL conc. aqueous ammonia. The mixture was stirred for 2 h at 45 °C until a clear solution was obtained. After acidifying with conc. HCl the solution was stirred overnight at room temperature. The solvent was decanted and the residue was washed with boiling water (100 mL). The water was decanted and **4** was dried *in vacuo* to yield 64 % (1.58 g, 13.38 mmol) of a yellow, sticky powder.

Density: ρ = 1.5 g cm^{-3}.
DSC (5 °C min^{-1}): T_{dec}: 170 °C.
IR (ATR, cm^{-1}): $\tilde{\nu}$ = 3505 (vw), 3267 (m), 3128 (w), 2930 (w), 2885 (w), 1718 (vw), 1566 (s), 1440 (m), 1384 (s), 1304 (vs), 1093 (vs), 1073 (vs), 858 (vw), 770 (w), 740 (w).
EA ($C_3H_6N_2O_3$ * 0.06 $C_3H_5O_2$): calculated: C 31.19, H 5.18, N 22.87 %; found: C 31.21, H 5.14, N 22.76 %.
Sensitivities: IS: 40 J; **FS**: > 360 N; **ESD**: 1.5 J.

3.5 References

1 H. G. Ang, S. Pisharath, *Energetic Polymers − Binders and Plasticisers for Enhancing Performance*; 1. Edition, Wiley-VCH, Weinheim, **2012**.

2 J. P. Agrawal, *High Energetic Materials: Propellants, Explosives and Pyrotechnics*, 1. Edition, Wiley-VCH, Weinheim, **2009**.

3 a) C. Cossu, M.-C. Heuzey, L.-S. Lussier, C. Dubois, *J. Appl. Polym. Sci.* **2011**, *119*, 3645-3657; b) F. M. Betzler, T. M. Klapötke, S. M. Sproll, *Eur. J. Org. Chem.* **2013**, *2013*, 509-514; c) T. M. Klapötke, S. M. Sproll, *J. Polym. Sci. Pol. Chem.* **2010**, *48*, 122-127; d) A. J. Bellamy, D. S. King, P. Golding, *Propellants, Explos., Pyrotech.*

2004, *29*, 509-514;

[4] A. Provatas, Report *DSTO-TR-0966*, Defence Science and Technology Organisation, Melbourne Victoria, Australia **2000**.

[5] H. R. Blomquist, *US 6802533*, **2004**.

[6] H. Staudinger, J. Meyer, *Helv. Chim. Acta* **1919**, *2*, 635-646.

[7] M. Hesse, H. Meier, B. Zeh, *Spektroskopische Methoden in der organischen Chemie*, 7. Edition, Thieme Verlag, Stuttgart, **2005**.

[8] C. Siguenza, P. Galera, E. Otero-Aenlle, *Spectrochim. Acta* **1980**, *37*, 459-460.

[9] R. Meyer, J. Köhler, A. Homburg, *Explosives*, 6. Edition, Wiley-VCH, Weinheim, **2007**.

[10] A. Provatas, Report DSTO-TR-1171, Defence Science and Technology Organisation, Melbourne Victoria, Australia, **2001**.

[11] http://www.ozm.cz/en/sensitivity-tests/esd-2008a-small-scale-electrostatic-spark-sensiti-vity-test/ (accessed April, 2016).

[12] T. M. Klapötke, M. Stein, J. Stierstorfer, *Z. Anorg. Allg. Chem.* **2008**, *634*, 1711-1723.

[13] a) A. F. Holleman, Wiberg, Nils, E. Wiberg, *Lehrbuch der Anorganischen Chemie*, 101. Edition, de Gruyter, Berlin, **1995**; b) *http://webbook.nist.gov/chemistry* (accessed April, 2016).

[14] a) M. Sućeska, *Propellants, Explos., Pyrotech.* **1991**, *16*, 197−202; b) M. Sućeska, *EXPLO5 V.6.02.*; Zagreb, **2013**.

[15] E. Diaz, *Propellants, Explos., Pyrotech.* **2003**, *28*, 101-106.

ENERGETIC POLYMERS
BASED ON
POLYURETHANES, POLYUREAS
AND
RELATED COMPOUNDS

4. Energetic Polymers Based on Polyurethanes, Polyureas and Related Compounds

Abstract: On the basis of several synthesized diols, in particular 2,2-bis(azidomethyl)propane-1,3-diol (BAMP), 2,2-dinitropropane-1,3-diol (DNPD) or BTEOH, polyurethanes were synthesized in polyaddition reactions using hexamethylene diisocyanate (HMDI), diisocyanato ethane (DIE) or diisocyanato methane (DIM). The obtained polyurethanes were mainly characterized using spectroscopic methods (IR, NMR) and elemental analysis. For the determination of low and high temperature behavior, differential scanning calorimetry (DSC) and thermogravimetric analysis (TGA) were used. Investigations concerning friction and impact sensitivities were carried out using a BAM drop hammer and friction tester. The energetic properties of the polymers were determined using bomb calorimetric measurements and calculated with the EXPLO5 V6.02 computer code. The obtained values were compared to the glycidyl azide polymer (GAP). The compounds turned out to be insensitive towards friction (>360 N) and less sensitive or insensitive towards impact (≥ 40 J). The compounds showed decomposition temperatures between 170 and 350 °C and possessed moderate or low energetic properties, which renders some of the synthesized polymers potential compounds for applications as binders in energetic formulations.

4.1 Introduction

Polyurethanes (PUs) and polyureas (PUAs) can be found in many areas of the daily life, due to their broad versatility. Depending on their ingredients (di- or multifunctional isocyanates and di- or multifunctional alcohols or amines) these compounds can possess many different properties. They are mainly used as foams in various fields, e.g. in mattresses, car seats or in the building industry, but also as varnishes, adhesives or flexible plastics.[1]

Another field in which polyurethanes find application is the military sector. For example, the in the 1950-60's used formulation for the submarine launchable *Polaris A1* missile contained amongst others a polyurethane propellant.[2] Apart from that, the polyurethane formation is mainly used to cure hydroxyl-terminated liquid energetic (pre)polymers, like GAP or poly(NIMMO), after the mixing process with energetic ingredients. As an example, the reaction of GAP with the curing agent diphenylmethane-4,4'-diisocyanate (MDI) is depicted in **Scheme 4.1**.[3 4]

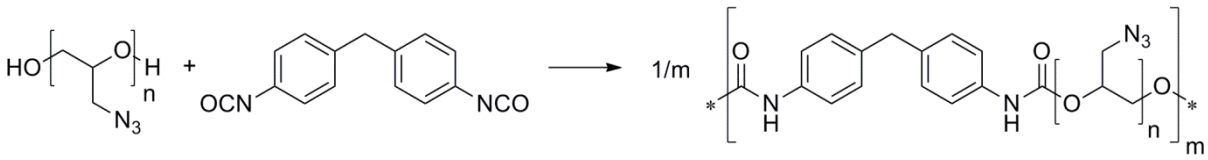

Scheme 4.1 Curing of hydroxyl-terminated GAP *via* the formation of a urethane linkage using MDI.

Due to their overall positive properties, their versatility, chemical and thermal stability [3] and good mechanical properties, as well as increased oxygen balance (PUs) or nitrogen content (PUAs), polyurethanes and -ureas seemed to be promising compounds for the use as energetic binders. Furthermore, carbamate or urea moieties, respectively can form hydrogen bridges to the energetic filler and therefore lead to increased adhesion forces. And, especially for nitramine containing energetic fillers, these carbamate and urea based compounds may be particularly qualified as energetic binder, since these moieties are structurally similar to the amide group, which turned out to form good interactions with nitro groups.[5] Herein we report different synthetic approaches towards new energetic polyurethanes, polyurea and related compounds.

4.2 Results and Discussion

4.2.1 Polyurethanes

4.2.1.1 Precursors

4.2.1.1.1 Precursors with Diisocyanate Function

The polyaddition reactions towards the target polyurethanes were carried out using three different diisocyanates: hexamethylene diisocyanate (HMDI, **1**), diisocyanato ethane (DIE, **5b**) and diisocyanato methane (DIM, **5a**). HMDI was obtained from commercial sources, DIE and DIM were synthesized (slightly modified) according to established procedures.[6] The diisocyanates were prepared pursuant to the CURTIUS rearrangement based on the acyl azides **4a** and **4b**, which were obtained over two steps, starting with the corresponding methyl esters **2a** and **2b** (**Scheme 4.2**).

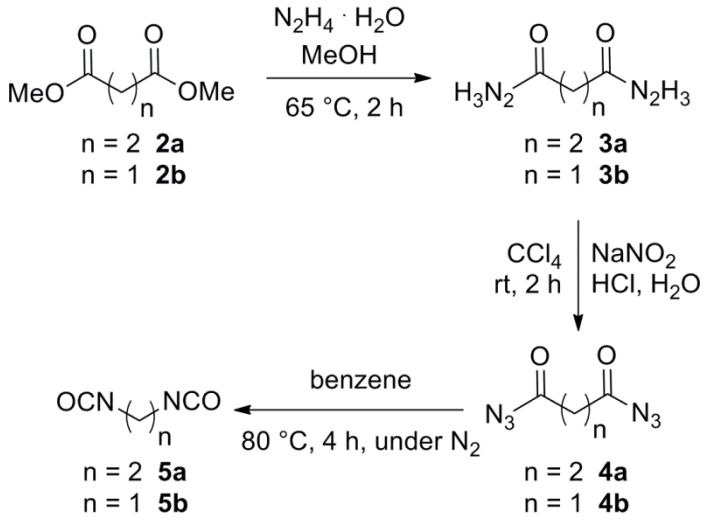

Scheme 4.2 Synthesis of the diisocyanates **5a** and **5b**.

Due to their instability, the acyl azides (**4a** and **4b**) were not further concentrated after purification, but directly converted into the corresponding diisocyanates (**5a** and **5b**). After the completion of the reaction, DIE (**5a**) and DIM (**5b**), with regard to their high reactivity, were also directly used for the polyaddition reaction. The successful formation of the desired diisocyanates (**5a** and **5b**) was confirmed by TLC and IR measurements. Here, the acyl azide

vibration at 2140 cm^{-1} vanished and the isocyanate vibration occurred at 2280 cm^{-1} [7] instead.

4.2.1.1.2 Precursors with Alcohol Function

The diols, prepared in this work were meant to introduce the energetic content into the target polyurethanes. They were either chosen due to their high nitrogen content (azide, triazole, tetrazole) or because of a resulting good oxygen balance (nitro groups). The diols, which were used for the polyurethane syntheses are depicted in **Figure 4.1**.

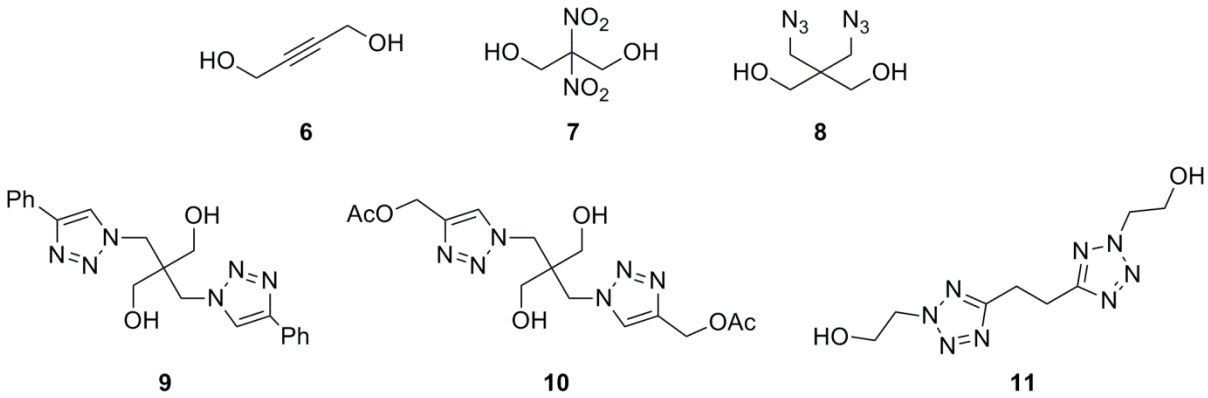

Figure 4.1 Diols applied in the syntheses of polyurethanes.

Syntheses

The acetylene based diol (**6**) was purchased from commercial sources. Diols **7** [8], **8** [9], **9** [10] and **11** [11] were already mentioned in literature and synthesized according to the published procedures. Whereas diol **10** was obtained *via* a copper-catalyzed azide-alkyne cycloaddition using BAMP (**8**) and propargyl acetate (**Scheme 4.3**).

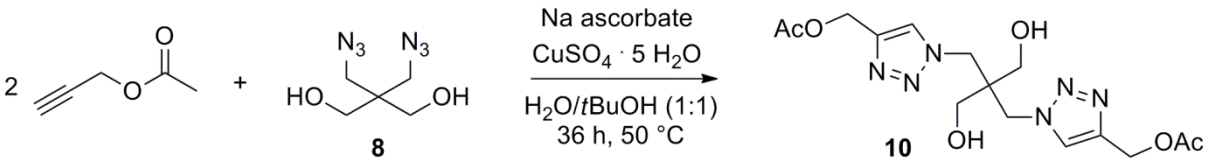

Scheme 4.3 Synthesis of **10** *via* copper-catalyzed azide-alkyne cycloaddition.

The crude product was recrystallized in methanol which gave **10** as colorless crystals in good yield (69 %).

As a further approach, the acetyl protecting group of **10** was removed using alkaline hydrolysis, obtaining a ditriazolo compound, 2,2-bis(hydroxymethyl-1*H*-1,2,3-triazol-1-yl)methyl)propane-1,3-diol (4-ol, **12**) with a tetravalent alcohol function (**Scheme 4.4**).

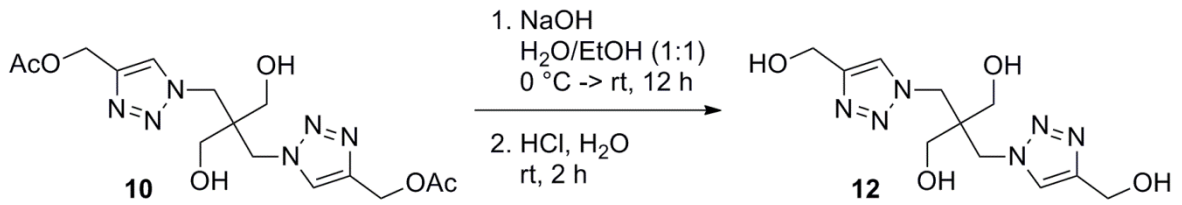

Scheme 4.4 Alkaline hydrolysis of **10** yielding **12** (4-ol) with a fourfold alcohol function.

After purification *via* column chromatography and a following recrystallization, 4-ol (**12**) could be obtained as colorless crystals in low yield (20 %).

Characterization

All synthesized precursors with alcohol function were analyzed using elemental analysis as well as spectroscopic (^{1}H, ^{13}C (for some compounds additionally ^{14}N) NMR and IR) and spectrometric methods. Compounds **7-9** and **11** gave consistent results with the literature values. [8-11]

^{1}H and ^{13}C NMR spectra of **10** and **12** were compared. The signals in the ^{1}H NMR spectra of the unmodified groups in **10** and **12** still occur in the same regions, with 8.11-7.97 ppm for $CH_{triazole}$, 5.12-5.04 ppm for the OH-group of the propane-1,3-diol fragment, 4.39-4.34 ppm for the methylene unit attached to the triazole N and 3.11 ppm for the methylene unit attached to the hydroxyl group in the propane-1,3-diol fragment. Nevertheless, they can clearly be

distinguished from each other, by the disappearance of the signal of the methyl group at 2.03 ppm in the spectrum of **12** and the simultaneous appearance of the signal at 5.22 ppm, which can be assigned to the newly formed OH-groups. Same can be applied for the ^{13}C NMR spectra of **10** and **12**. Whereas the signals of the unmodified molecule fragments show nearly unchanged values, the signals of the acetyl group (with 170.1 (C=O) and 20.6 ppm (CH_3)) of **12** vanish in the spectrum of **10**, which verifies the successful cleavage of the acetyl group. Besides this, the elemental analyses of both compounds verifed very pure products.

Crystal Structures

Crystal structures of **10** and **12** were obtained using single crystal X-ray structure analysis. Single crystals suitable for X-ray diffraction were obtained by recrystallization of the products from MeOH (**10**) or an ethanol/methanol mixture (**12**).

Compound **10** crystallizes in the triclinic space group *P*-1 with two formula units per unit cell (**Figure 4.2**). Calculated density for T = 173 K is 1.389 g cm^{-3}. The bond lengths and angles within the molecular structure of **10** are consistent with comparable values in literature. [12] [13] Although, the molecule *per se* is symmetrically assembled, the crystal structure of **10** does not possess any center of symmetry.

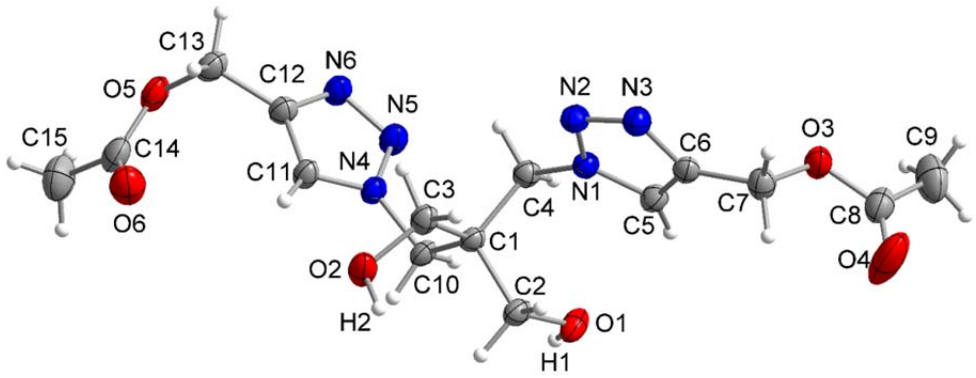

Figure 4.2 Molecular structure of **10**. Thermal ellipsoids are set to 50 % probability. Selected bond distances [Å]: O1−H1 0.904(3), O1−C2 1.419(2), O2−H2 0.871(2), O2−C3 1.412(2), N1−N2 1.342(2), N1−C5 1.354(2), N2−N3 1.321(2), N3−C6 1.361(2), C5−C6 1.365(3), N4−N5 1.350(2), N4−C11 1.347(2), N5−N6 1.322(2), N6−C12 1.363(2), C11−C12 1.366(2); selected bond angles (°): C1−C4−N1 113.2(1), C1−C10−N4 114.0(1), C2−O1−H1 111.6(2), C3−O2−H2 107.8(2); selected torsion angles (°) C1−C2−O1−H1 −73.2(2), C1−C3−O2−H2 84.2(2), C1−C4−N1−N2 −92.1(1), C1−C4−N1−C5 88.1(2), C1−C10−N4−N5 96.9(1), C1−C10−N4−C11 −83.2(2), C4−C3−N4−N3 4.0(2), C1−C4−N1−N2 −92.1(1), C4−N1−C5−H5 1.9(2), C10−N4−C11−H11 2.4(2), O3−C7−C6−N3 58.9(3), O3−C7−C6−C5 −119.7(2), O5−C13−C12−N6 88.9(2), O5−C13−C12−C11 −89.2(2).

In the crystal structure, the molecules are connected by two different intermolecular hydrogen bonds, which are depicted in **Figure 4.3**. The corresponding distances and angles are given in **Table 4.1**. All hydrogen bond lengths lie well within the sum of van der Waals radii (r_w(O) + r_w N) = 3.07 Å) [14] [13] and are short with D···A distances of 2.761(2) Å (O1−H1···N3^{ii}) and 2.856(2) Å (O2−H2···N6^{i}) and are moderately directed with angles of 167.76(2)° and 167.65(3)°, respectively.

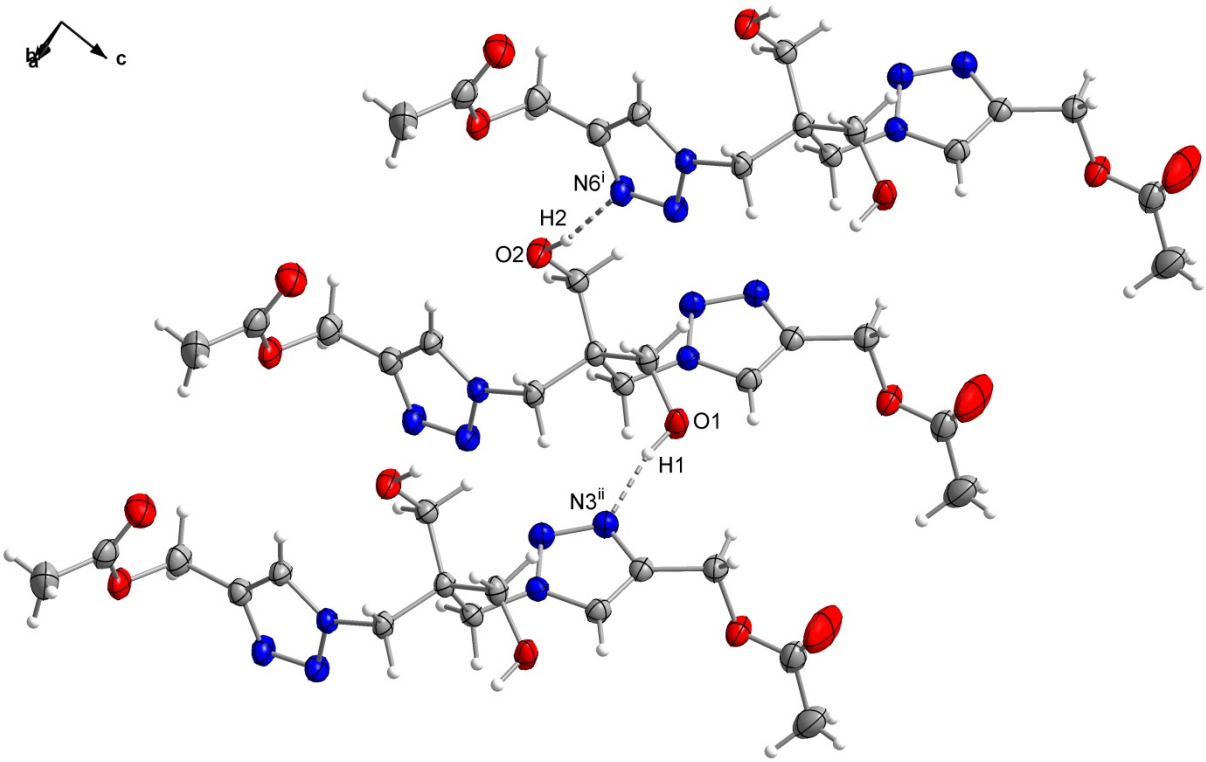

Figure 4.3 Hydrogen bonding scheme in the crystal structure of **10**. Thermal ellipsoids are set to 50 % probability. Symmetry operators: (i) x, −1+y, z; (ii) 1+x, y, z.

Table 4.1 Atom distances [Å] and bond angles (°) of the intermolecular hydrogen bonds in the crystal structure of **10**.

D−H···A	d(D−H) [Å]	d(H···A) [Å]	d(D···A) [Å]	<(D−H···A) [°]
O1−H1···N3^{ii}	0.904(3)	1.871(3)	2.761(2)	167.76(2)
O2−H2···N6^{i}	0.871(2)	2.000(2)	2.856(2)	167.65(3)

Symmetry operators: (i) x, −1+y, z; (ii) 1+x, y, z.

Compound **12** crystallizes in the monoclinic space group $P2_1/n$ with four formula units per unit cell (**Figure 4.4**). Calculated density for T = 173 K is 1.489 g cm^{-3}. One of the CH_2OH moieties of the propane-1,3-diol unit is disordered. For each atom in that group two different positions (C7A−O3A−H3A and C7B−O3B−H3B) within the crystal are possible. Both positions are nearly equally occupied with 50.3 % (O3B) vs 49.7 % (O3A). Here again, despite the theoretical symmetry of the molecule, the crystal structure is asymmetrically assembled.

A closer look at the bond lengths and angles within the molecular structure of the compound reveals no evident differences relative to those of other heterocyclic ring systems. [12] [13]

a)

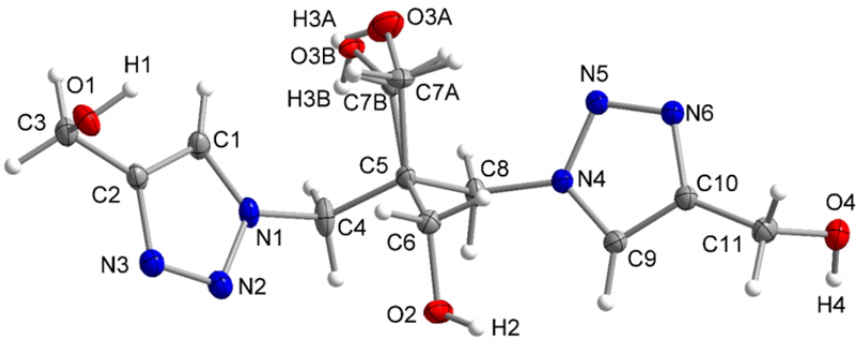

b)

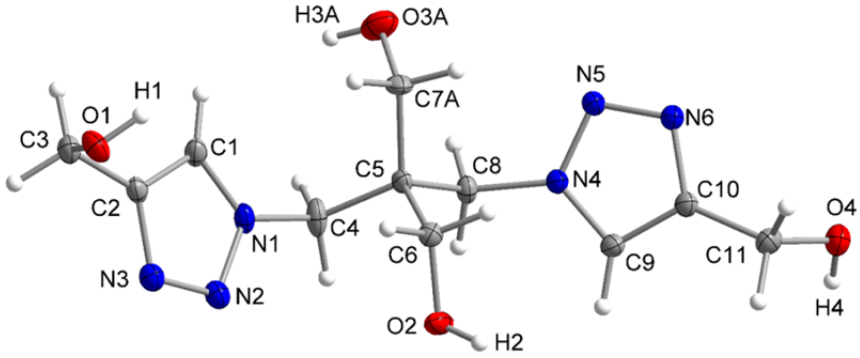

c)

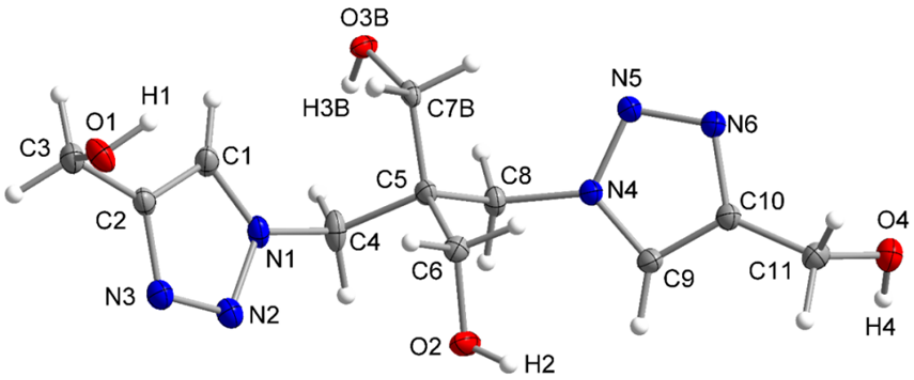

Figure 4.4 Crystal structure of **12** showing **a)** both disordered positions, and the respective separated positions **b)** C7A−O3A−H3A and **c)** C7B−O3B−H3B. Thermal ellipsoids are set to 50 % probability. Selected bond distances [Å]: O1−H1 0.844(2), O1−C3 1.432(2), O2−H2 0.826(2), O2−C6 1.462(2), O3A−H3A 0.839(3), O3A−C7A 1.422(1), O3B−H3B 0.840(3),

O3B−C7B 1.405(1), O4−H4 0.839(4), O4−C11 1.425(2), N1−N2 1.349(2), N1−C5 1.349(2), N2−N3 1.319(2), N3−C2 1.364(2), C1−C2 1.371(2), N4−N5 1.344(2), N4−C9 1.349(2), N5−N6 1.320(2), N6−C10 1.361(2), C9−C10 1.371(2); selected bond angles (°) C3−O1−H1 108.3(2), C6−O2−H2 105.9(1), C6−C5−C7A 102.1(4), C6−C5−C7B 113.8(4), C7A−O3A−H1A 109.5(1), C7A−O3B−H1B 109.5(1), C11−O4−H4 110.7(2), C5−C3A−O3A 109.8(1), C5−C3B−O3B 112.6(1); selected torsion angles (°) C5−C4−N1−N2 −107.7(1), C5−C4−N1−C1 73.7(2), C5−C6−O2−H2 145.7(2), C5−C7A−O3A−H3A 60.0(1), C5−C7B−O3B−H3B 2.3(1), C5−C8−N4−N5 −81.5(1), C5−C8−N4−C9 93.2(2), O1−C3−C2−C1 −102.7(2), O1−C3−C2−N3 75.1(2), O4−C11−C10−C9 102.8(2), O4−C11−C10−N6 −78.8(1), C10−C11−O4−H4 −78.5(2), C2−C3−O1−H1 61.9(2).

The disordered moieties of C7A/B−O3A/B−H3A/B differ, besides different angles of C6-C5-C7A/B with 102.1° and 113.8°, also in the orientation of the OH group with torsion angles of 60.0° vs. 2.3° towards the respective C5−C7 bond. This disorder enables the extra stabilization of the crystal system, since only the H3B atom (of the disordered moiety) participates in the formation of hydrogen bonds. Hence, the structure is stabilized by four different intermolecular hydrogen bonds, which are depicted in **Figure 4.5**. The corresponding distances and angles are given in **Table 4.2**. The hydrogen bonds are either formed between the respective hydroxyl groups or, in one case, between the OH group and the $N6^{i}$ atom of the triazole ring. All hydrogen bond lengths lie well below the sum of van der Waals radii ($r_w(O) + r_w(N) = 3.07$ Å, $r_w(N) + r_w(N) = 3.20$ Å). [14] Two contacts are short with D···A distances of 2.728(1) Å (O1−H1···$N6^{i}$) and 2.671(1) Å (O2−H2···$O1^{ii}$) and are strongly directed with D−H···A angles of 174.44(3)° and 174.90(9)°. The contacts, in which the disordered hydroxyl group is involved are moderately strong with D···A distances of 2.957(1) Å (O3B−H3B···$O4^{iv}$) and 2.957(1) Å (O4−H4···$O3B^{iii}$) and are not strongly directed with D−H···A angles of 149.27(2)° and 138.88(2)°.

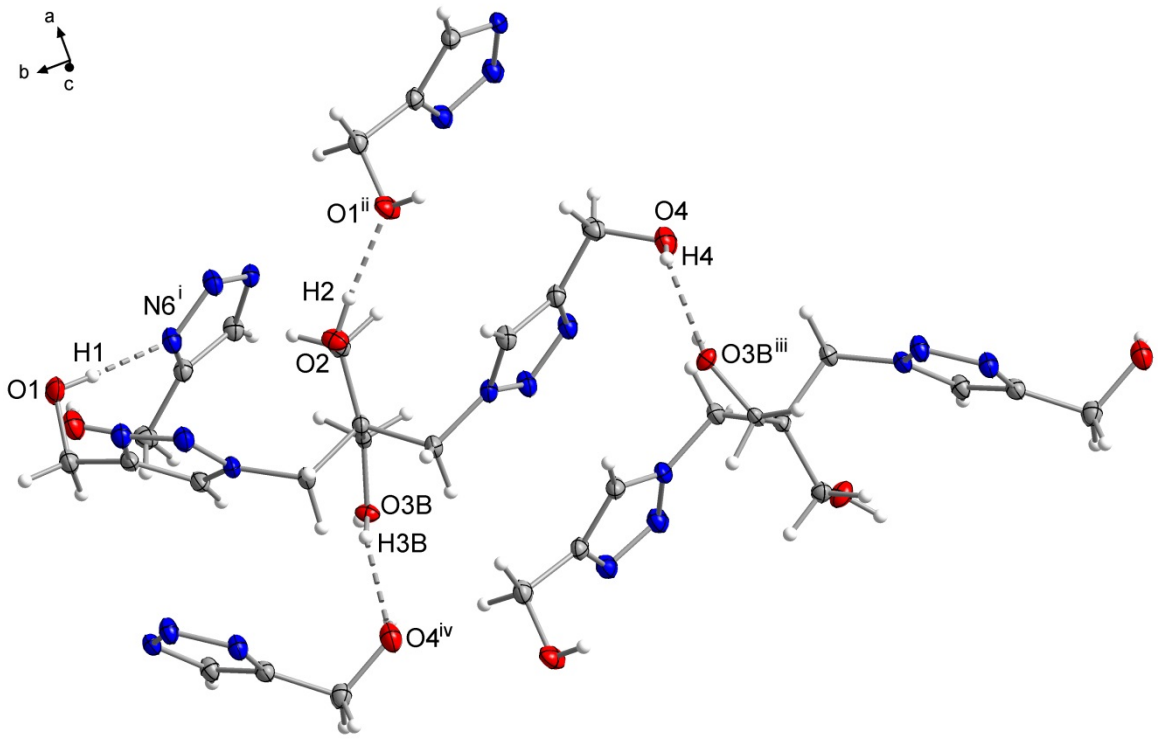

Figure 4.5 Hydrogen bonds of **12** (parts of the involved molecules were omitted for clarity). Thermal ellipsoids are set to 50 % probability. Symmetry operators: (i) −x, −y, −z; (ii) 0.5−x, −0.5+y, 0.5−z; (iii) −0.5−x, −0.5+y, 0.5−z; (iv) −0.5−x, 0.5+y, 0.5+z.

Table 4.2 Atom distances [Å] and bond angles (°) of the intermolecular hydrogen bonds in the crystal structure of **12**.

D−H···A	d(D−H) [Å]	d(H···A) [Å]	d(D···A) [Å]	<(D−H···A) [°]
O1−H1···N6^{i}	0.844(2))	1.940(6)	2.728(1)	174.44(3)
O2−H2···O1^{ii}	0.826(3)	1.848(6)	2.671(1)	174.90(9)
O3B−H3B···O4^{iv}	0.840(3)	2.204(1)	2.957(1)	149.27(2)
O4−H4···O3B^{iii}	0.839(4)	2.273(1)	2.957(1)	138.88(2)

Symmetry operators: (i) −x, −y, −z; (ii) 0.5−x, −0.5+y, 0.5−z; (iii) −0.5−x, −0.5+y, 0.5−z; (iv) −0.5−x, 0.5+y, 0.5+z.

4.2.1.2 Polymerization Reactions

Most polyurethane syntheses were carried out with HDMI as diisocyanato component, due to its commercial availability. Only the diols from the most promising products (regarding yield, purity and energetic properties) were chosen for the reactions with DIE and DIM. Therefore DNPD, BAMP and BTEOH were used for further polymerization reactions, but only the DNPD and BAMP based reactions were successful with DIE and DIM.

4.2.1.2.1 Syntheses

The polyaddition reactions were carried out using dibutyltin dilaurate (DBTDL) as catalyst over two different synthetic routes (**Scheme 4.5**). The obtained products showed a broad spectrum of different consistencies (**Figure 4.6**). The BAMP based polyurethanes **15a** (**Figure 4.6 b**), **15b** and **15c** were yellowish viscous liquids (viscosity increased with the increased number of carbon chains) with excellent to moderate yields of 91 %, 52 % and 42 %. In case of the DNPD based polyurethanes **14a**, **14b** and **14c** the products were either an orange elastic foil (**14a**) (**Figure 4.6 a**) or red ductile solids (**14b**, **14c**) with yields of 96 %, 57 % and 54 %. The polyurethanes with acetylene (**13**) and triazole (**16**, **17**) content were obtained as white powders in good (79 %, **13**) to moderate yields 56 %-45 % (**16** and **17**). The tetrazole based polyurethane **18** was obtained as partly hard elastic colorless solid (**Figure 4.6 c**) in good yield (85 %).

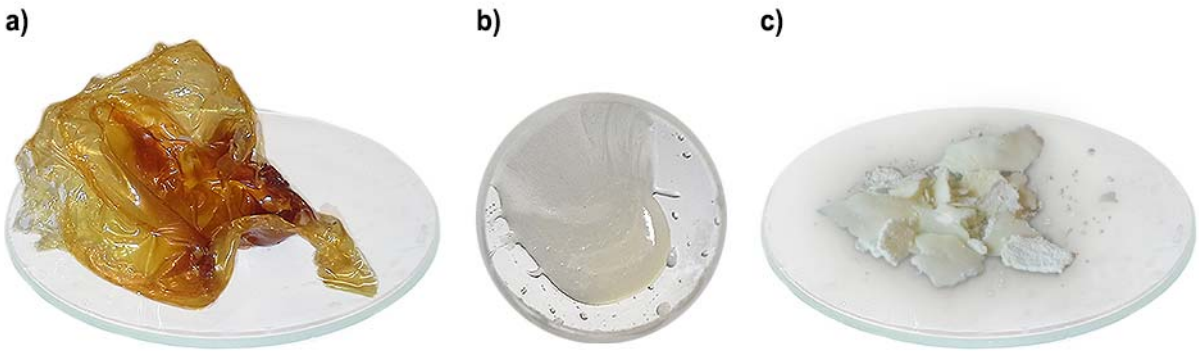

Figure 4.6 Pictures of the different polymer consistencies exemplified by **a)** HMDI-DNPD (**14a**); **b)** HMDI-BAMP (**15a**) and **c)** HMDI-BTEOH (**18**).

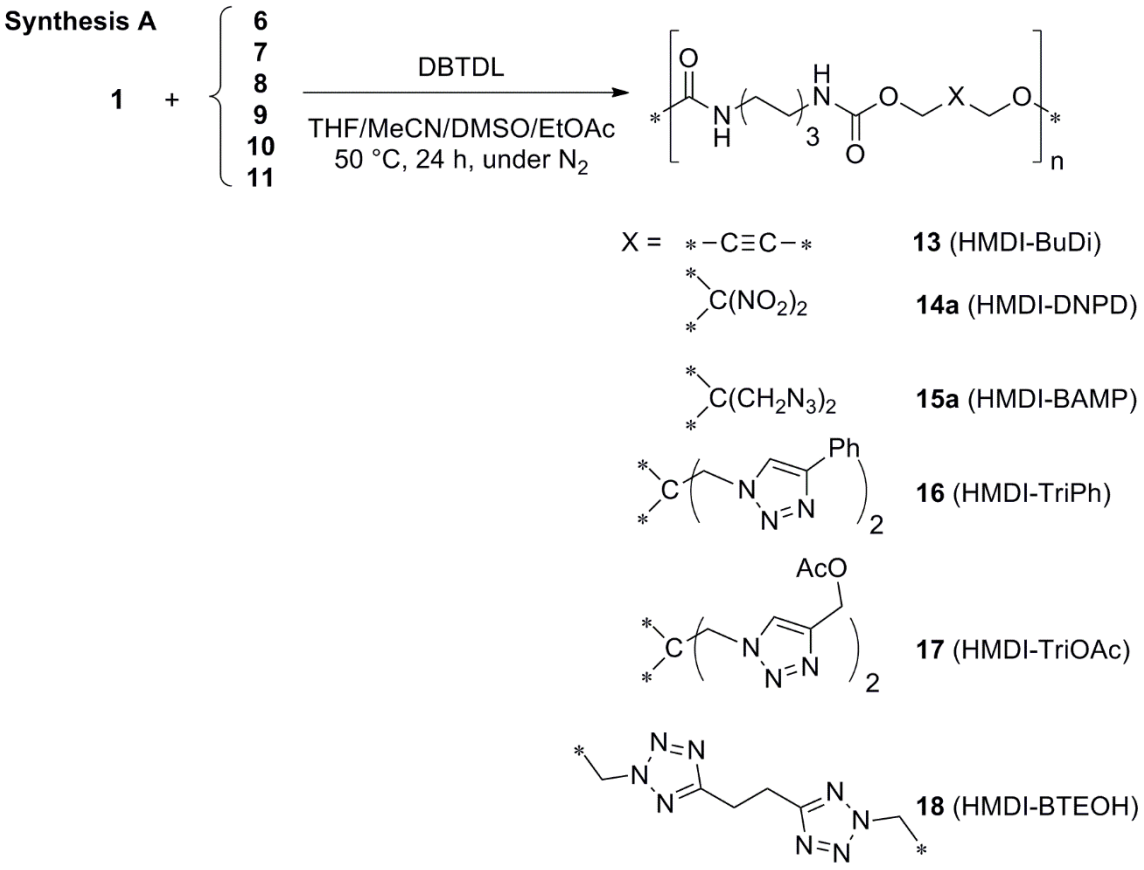

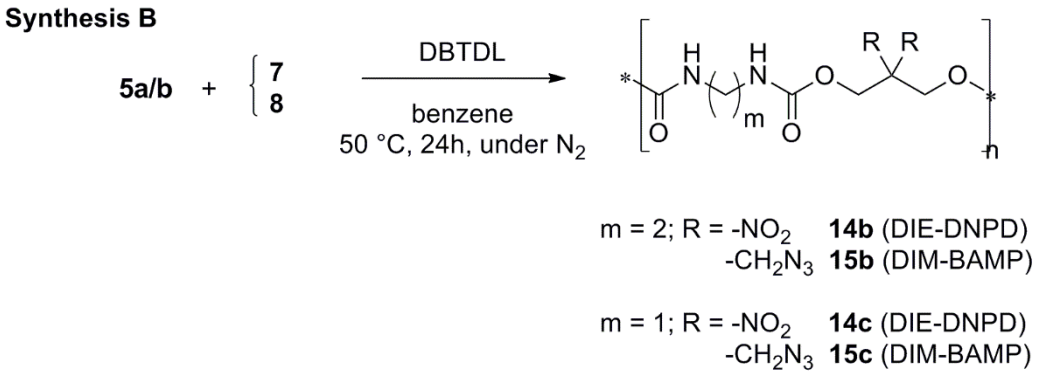

Scheme 4.5 Synthetic routes towards the desired polyurethanes **13-18**.

An attempt has also been made to transform the acetylene polyurethane **13** *via* a 1,3-dipolar cycloaddition into a polyurethane with a backbone implemented triazole (**19**) (**Scheme 4.6**).

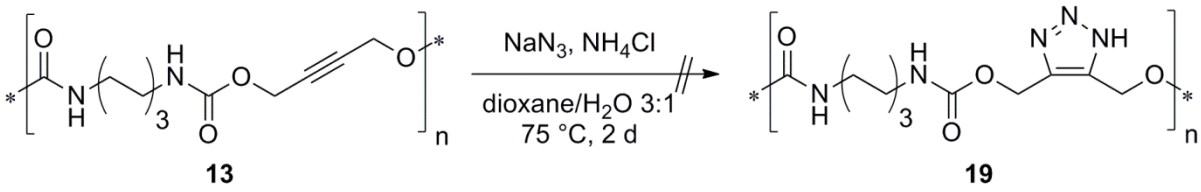

Scheme 4.6 Attempted synthesis of a backbone implemented triazole polyurethane (**19**).

Analysis of the obtained colorless solid revealed only starting material **13**. Reasons for this might either be too mild conditions, which could be resolved by using a stronger Lewis acid like $ZnCl_2$, or the steric hindrance of the polymer, which inhibits the formation of the required conformation for the [3+2] cycloaddition.

4.2.1.2.2 Characterization

NMR measurements were performed in DMSO-*d6*. As example, the recorded ^{1}H and ^{13}C NMR spectra of HMDI-BAMP (**15a**) are depicted in **Figure 4.7**. In the proton NMR spectrum the *trans* and the *cis* conformer of the carbamate N−H group are visible at 7.13 ppm and 6.89 ppm. The signals of the methylene groups of the diol fragment appear at 3.87 ppm (CH_2−O) and 3.40 ppm (CH_2−N_3). The methylene groups of the HMDI corresponding carbon chain show signals at 2.96 ppm (CH_2−NH), 1.31 ppm and 1.23 ppm. The ^{13}C NMR spectrum shows a similar signal pattern as the ^{1}H NMR spectrum. The signals of the carbon atoms corresponding to the diol fragment occur at 62.4 (CH_2−O), 51.3 (CH_2−N_3) and 43.2 (C_q) ppm. The signals appearing at 40.21 ppm (CH_2−NH), 29.3 ppm and 25.9 ppm can be assigned to the carbon atoms of the HMDI chain. At 156.7 ppm the signal of the carboxyl carbon of the carbamate group is visible.

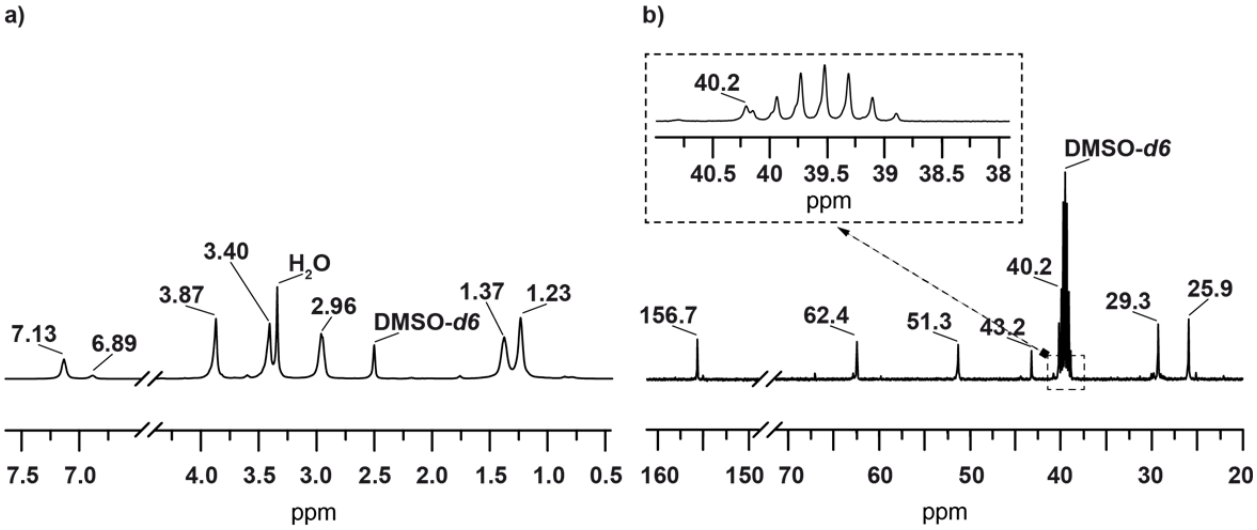

Figure 4.7 **a)** ^{1}H and **b)** ^{13}C NMR spectrum of HMDI-BAMP (**15a**).

The tetrazole based polyurethane **18** could not be dissolved properly in any common deuterated solvent, therefore NMR spectroscopy in solution was not possible. The other compounds (**13**, **14a**,**b**, **15b**, **16**, **17**) show similar values for the specific fragment CH_2−NH−CO−O−CH_2−. In the ^{1}H NMR spectra, the DNPD based compounds **14a** and **14b** show signals around 7.60 ppm for the N−H group and 5.01 ppm for the CH_2−O fragment. Whereas the signals of the other compounds **13**, **15b**, **16** and **17** are shifted to higher field compared to the signals of **14a** and **b** with values at 7.29-7.13 ppm and 4.65 (**13**) or 3.87-3.68 ppm, respectively. The chemical shift of the signal for the CH_2−NH group depends on the respective diisocyanate unit. The compounds based on HMDI (**13**, **14a**, **16**, **17**) show signals around 2.95 ppm, while the signal of the DIE based **14b** and **15b** occurs at 3.02 ppm. In the ^{1}H NMR spectra of **16** and **17**, an extra signal can be found at 5.72 ppm, which can be assigned to the NH-fragment of an urea group. The occurrence of this signal indicates the presence of water in the reaction solvent, which, together with isocyanates, leads to the formation of carbamic acid. Due to its instability, carbamic acid decomposes while eliminating CO_2 to the corresponding amine, which further reacts with the remaining isocyanate to urea compounds.

The ^{13}C NMR spectra of compounds **13**, **14a**,**b**, **15b**, **16** and **17** also confirm the successful formation of the polyurethanes. The signal of the quaternary C atom of the carboxyl group occurs around 154 ppm, the carbon atom of the CH_2−O fragment shows signals around 61 ppm (**14a,b**, **15b**, **16-18**) or 51.3 ppm (**13**). For the CH_2−NH carbon atom the DNPD based **14a** and **14b** show signals around 30 ppm, while the signals for **15b-17** occur around 40 ppm.

The NMR spectra of compounds **14c** and **15c** could not be assigned properly due to a variety of signals, most likely because of a broad dispersion of chain lengths in the obtained product.

The measured IR spectra of all compounds clearly show the characteristic vibrations for monosubstituted carbamates (**Figure 4.8**). At about 3330 cm^{-1} the N−H valence vibration (A) is visible, the valence vibration of the C=O group (amide I) occurs around 1700 cm^{-1} (B), as well as the amide II vibration (N−H bending) and the asymmetric C−O bending vibration at about 1525 cm^{-1} (C) and 1235 cm^{-1} (D), respectively.[7] The asymmetric and symmetric valence vibrations of the NO_2 groups in **14a-c** appear at about 1565 cm^{-1} (overlapping signal with the amide II vibration) and 1320 cm^{-1} (E). [7]

Besides this, the characteristically strong azide vibration is visible at 2100 cm^{-1} (F) in case of the BAMP based **15a-c**. Elemental analysis revealed some remaining inclusions of water and organic solvent in the synthesized polymers. These results, together with the IR and NMR measurements prove the successful synthesis of compounds **14-18**.

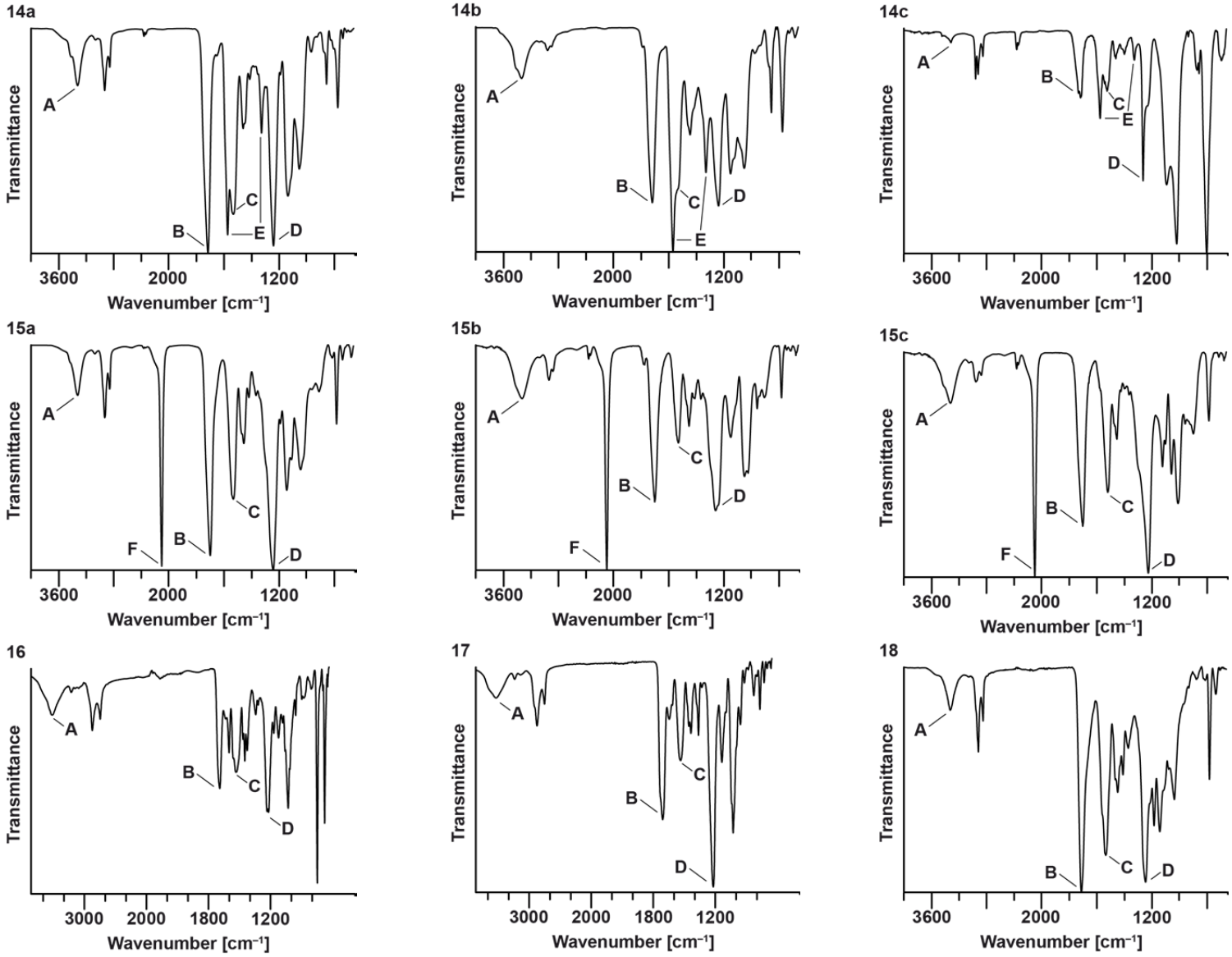

Figure 4.8 IR spectra of **14-18**.

For further characterization, the molecular weights of **14-15** were determined by GPC measurements. As eluent THF containing 0.2 % trifluoroacetic acid was used. The average molecular masses (M_n) are determined to be 3100 g mol^{-1} (**15a**), 850 g mol^{-1} (**14b** and **15b**) and in the range of 600 g mol^{-1} (**14c** and **15c**), corresponding to approximately 10, 3 and 2 molecular formulas in one chain. Although **14a** was soluble in THF, no significant separation could be achieved, most likely due to reprecipitation of the compound on the column. The relatively short chains of the DIE and DIM based urethanes may derive from the fact that the used diols were poorly soluble in the given solvent benzene.

4.2.1.2.3 Thermal Behavior

An important factor for energetic binders is their thermal stability and in case of liquid materials a preferably low glass transition temperature T_g. The determination of the low and high temperature behavior of the polyurethanes was carried out *via* differential scanning calorimetry (DSC). **Figure 4.9** shows the decomposition temperatures of compounds **14a-c**, **15a-c** and **18**.

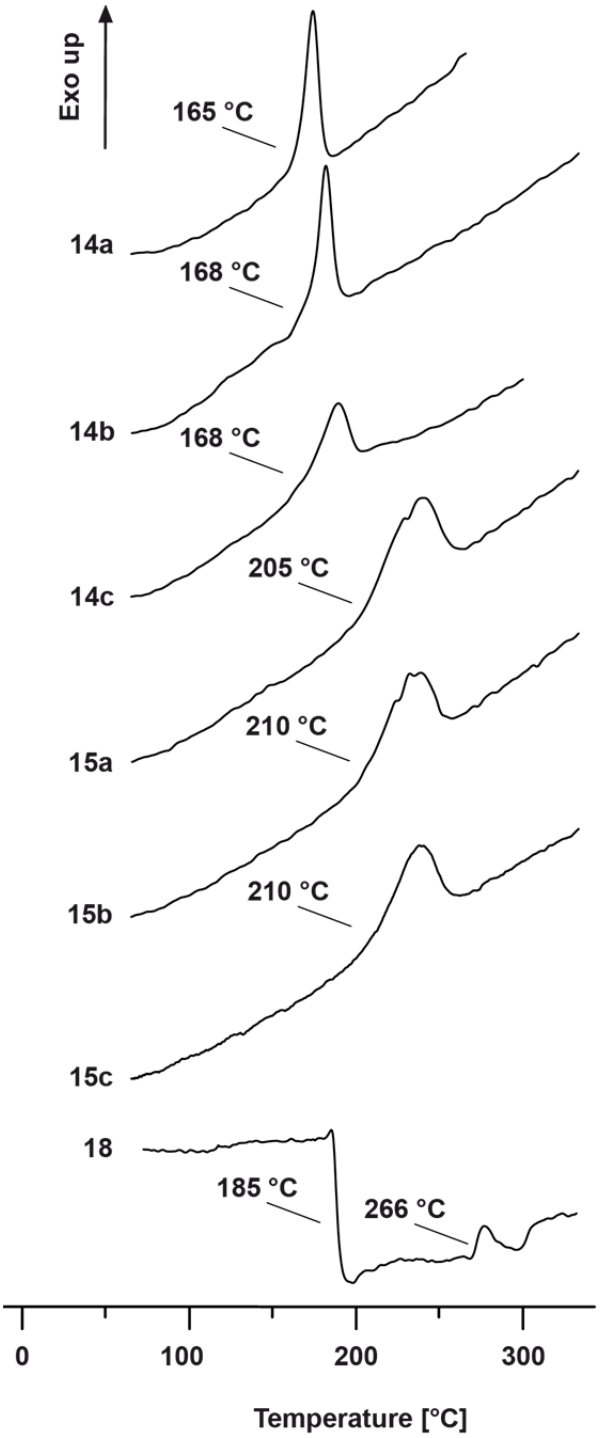

Figure 4.9 DSC plots of decomposition temperatures of **14-18** (onset temperatures).

As expected, the compounds based on the same diol show decomposition temperatures in the same temperature range. DNPD based **14a-c** decompose around 170 °C, which is initiated by the geminal nitro groups. BAMP based **15a-c** are stable up to higher temperatures (around 210 °C), which is in accordance with the thermal stability of aliphatic azides.[15] The triazole

based polyurethane **18** shows a glass transition around 185 °C (which indicates the transition from the hard elastic state into the liquid phase) and a subsequent decomposition point at 266 °C.

The obtained DSC plots of **16** and **17** did not show any significant changes in the curve progression, since either the used amounts of substance (1-2 mg) were insufficient for a detectable phase transformation, or the compounds are stable up to higher temperatures.

Due to their liquid or elastic character additional low temperature DSC measurements were carried out with **15a-c** and **14a** to determine their glass transition temperature (T_g). The obtained plots are depicted in **Figure 4.10**.

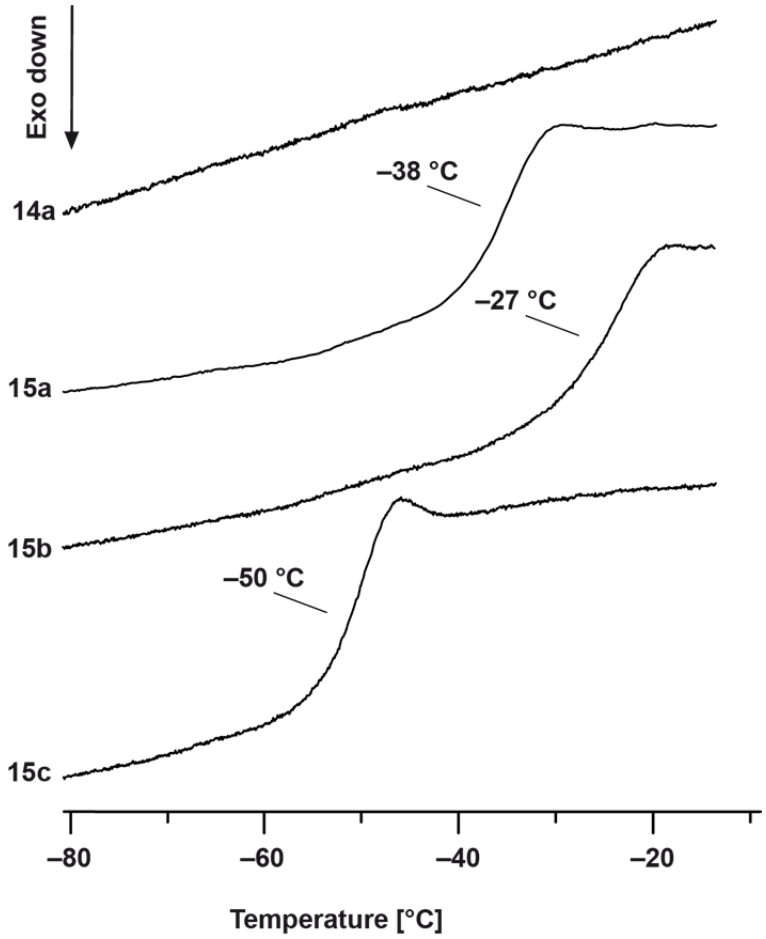

Figure 4.10 DSC plots of glass transition temperatures of **14-15** (T_{gMid}).

The glass transition temperatures of **15a** and **b** with −38 °C and −27 °C are in a good temperature range for application as binder in energetic formulations. Nevertheless, if applied in such matter, a plasticizer additive will be needed to reduce T_g below the requested

minimum working range (usually −55 °C). The low glass transition temperature of **15c** is quite unexpected, since short carbon chains usually result in higher values. This might derive from the non-polymeric character of these compounds (see molecular masses), which usually gives lower glass transition temperatures, compared to polymers with a higher number of repeating units.

Although **14a** shows an elastic character, no glass transition could be observed in the measured temperature range of −120 °C to 10 °C. Either the glass transition point is lower than −120°C or **14a** does not possess any T_g.

To determine the weight loss during the heating process thermogravimetric analysis (TGA) was used for the compounds **14** and **15** (**Figure 4.11**).

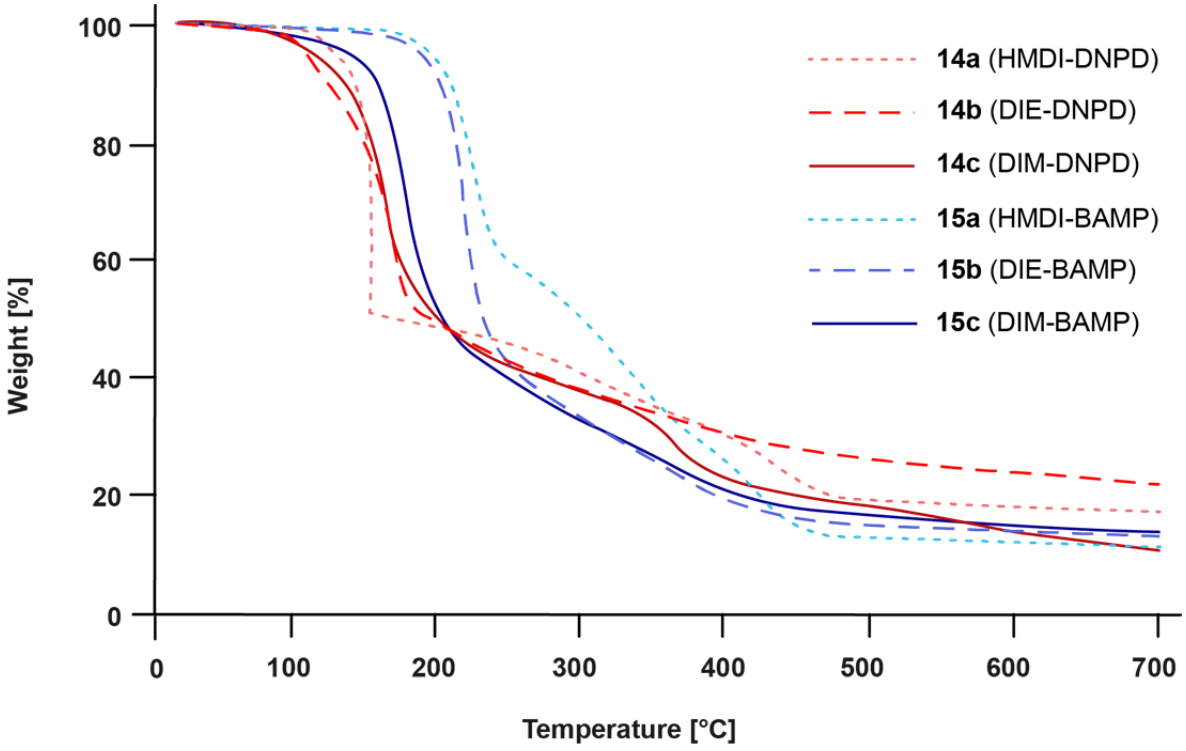

Figure 4.11 TGA plots of compounds **14-15**.

As already observed in the DSC plots (**Figure 4.9**) the compounds based on the same energetic diol show similar behavior. **14b** and **c** show a beginning weight loss at 100 °C, which can be assigned to the loss of H_2O and organic solvent during the heating process. The second step (recognizable by the small dent in the curve at approximately 95 wt%), starting around 170 °C is the beginning decomposition of the polyurethane, starting with the geminal nitro groups. The following steps of weight losses are assignable to the decomposition of the remaining polyurethane backbone, including the carbamate group and the aliphatic chain.

Similar observations can be made for the other four compounds. The decomposition of the compounds is initiated by the decomposition of the energetic functional groups, around 165 °C for **14a** and **c** (after solvent loss, recognizable by the dent in the curve at about 97 wt%) or 200 °C for **15a** and **b** and is followed by a stepwise decomposition of the polymeric backbone. **15c** shows a beginning weight loss at lower temperatures (~150 °C). This can be derived from the low molecular weight fragments, which may volatilize at lower temperatures. At the end temperature of 700 °C the compounds have reached an overall weight loss of 90 % (**15a** and **14c**) to (not fully completed) 80 % (**14b**).

4.2.1.2.4 Energetic Properties

For the determination of inherent energetic potential, compounds **14-18** were investigated. Sensitivity data concerning impact and friction sensitivity were obtained using a BAM drop hammer and friction tester.[16] These methods revealed that compounds **14-18** are insensitive towards friction (>360 N) and less or not sensitive towards impact (≥40 J). Compared to GAP (IS: 8 J, FS: > 360 N)[17] this can be regarded as clear advantage in terms of safety.

For analyzing the energetic properties of **14-18**, the energy of combustion (ΔU_c) was determined *via* bomb calorimetry. The enthalpy of formation could be calculated from the obtained values applying the HESS thermochemical cycle, as reported in literature.[18] The combustion reactions of polyurethanes **14-18** are given in **Scheme 4.7**.

a) $C_{11}H_{18}N_4O_8 + 11.5\ O_2 \rightarrow 11\ CO_2\ (g) + 9\ H_2O\ (l) + 2\ N_2\ (g)$

b) $C_7H_{10}N_4O_8 + 5.5\ O_2 \rightarrow 7\ CO_2\ (g) + 5\ H_2O\ (l) + 2\ N_2\ (g)$

c) $C_6H_8N_4O_8 + 4\ O_2 \rightarrow 6\ CO_2\ (g) + 4\ H_2O\ (l) + 2\ N_2\ (g)$

d) $C_{13}H_{22}N_8O_4 + 16.5\ O_2 \rightarrow 13\ CO_2\ (g) + 11\ H_2O\ (l) + 4\ N_2\ (g)$

e) $C_9H_{14}N_8O_4 + 10.5\ O_2 \rightarrow 9\ CO_2\ (g) + 7\ H_2O\ (l) + 4\ N_2\ (g)$

f) $C_8H_{12}N_8O_4 + 9\ O_2 \rightarrow 8\ CO_2\ (g) + 6\ H_2O\ (l) + 4\ N_2\ (g)$

g) $C_{29}H_{34}N_8O_4 + 35.5\ O_2 \rightarrow 29\ CO_2\ (g) + 17\ H_2O\ (l) + 4\ N_2\ (g)$

h) $C_{23}H_{34}N_8O_4 + 29.5\ O_2 \rightarrow 23\ CO_2\ (g) + 17\ H_2O\ (l) + 4\ N_2\ (g)$

i) $C_{16}H_{26}N_{10}O_4 + 20.5\ O_2 \rightarrow 16\ CO_2\ (g) + 13\ H_2O\ (l) + 5\ N_2\ (g)$

Scheme 4.7 Combustion reaction of **a)** HMDI-DNPD (**14a**); **b)** DIE-DNPD (**14b**); **c)** DIM-DNPD (**14c**); **d)** HMDI-BAMP (**15a**); **e)** DIE-BAMP (**15b**); **f)** DIM-BAMP (**15b**); **g)** HMDI-TriPh (**16**); **h)** HMDI-TriOAc (**17**); **i)** HMDI-BTEOH (**18**) (repeating units).

For a rough comparison of the analytically obtained energetic values, the enthalpy of formation was also calculated *via* quantum-chemical calculations (CBS-4M). As example compound the corresponding monomeric molecule of **14a**, 3-hydroxy-2,2-dinitropropyl(6-formamidohexyl)carbamate, was chosen (**Figure 4.12)**.

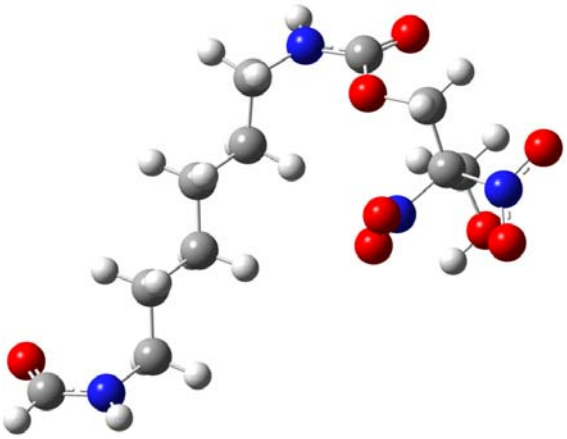

Figure 4.12 Molecular structure of the monomeric molecule 3-hydroxy-2,2-dinitropropyl(6-formamidohexyl)carbamate of **14a**.

Calculations were carried out using the Gaussian G03W (revision B.03) program package.[20] The enthalpies of the gas-phase species M were computed according to the atomization energy method (Equation 4.1) using CBS-4M enthalpies given in **Table 4.3**.[20 21 22]

$$\Delta_f H^\circ_{(g,\,M,\,298)} = H_{(molecule,\,298)} - \Sigma H^\circ_{(atoms,\,298)} + \Sigma \Delta_f H^\circ_{(atoms,\,298)} \qquad (4.1)$$

Table 4.3 CBS-4M electronic enthalpies for atoms C, H, N, O and their literature values for atomic $\Delta H^\circ_f{}^{298}$.

	$-H^{298}_{CBS\text{-}4M}$ [a.u.]	NIST [kJ mol^{-1}]
H	0.500991	218.2
C	37.786156	717.2
N	54.522462	473.1
O	74.991202	249.5

In order to convert the standard enthalpies of formation $\Delta_f H^\circ$(g) for the gas-phase into values for the solid phase, the enthalpy of sublimation $\Delta H_{sub.}$ is required. This value can be estimated using the TROUTON's rule, whereby T_m is the melting point of the solid [23 24]:

$$\Delta H_{sub.}\,[\text{J mol}^{-1}] = 188\ T_m\,[\text{K}]$$

As an approximation, the decomposition temperature of T_{dec} = 165 °C was used as the melting temperature and the enthalpy of sublimation was estimated to be 83 kJ mol^{-1}. The obtained quantum chemical results are summarized in **Table 4.4**.

Table 4.4 Calculation results for the monomeric molecule 3-hydroxy-2,2-dinitropropyl(6-formamidohexyl)carbamate of **14a**.

$-H^{298}$ [a] [a.u].	$-\Delta_f H$ (g, M) [b] [kJ mol^{-1}]	$-\Delta_f H^\circ$(s) [c] [kJ mol^{-1}]
1250.181899	912	1008

[a] CBS-4M electronic enthalpy; [b] gas phase enthalpy of formation; [c] solid state enthalpy of formation.

All calculations concerning the detonation parameters were carried out using the program package EXPLO5 (version 6.02)[25] and were based on the calculated or experimentally obtained heats of formation and attributed to the corresponding densities, determined *via*

pycnometer. The program is based on the steady-state model of equilibrium and uses the Becker-Kistiakowsky-Wilson equation of state (BKW EOS.) for gaseous detonation products and the Murnaghan EOS for both solid and liquid products. It is designed to enable the calculation of detonation parameters at the Chapman-Jouguet point (C-J point). The C-J point was found from the Hugoniot curve of the system by its first derivative.[25] The obtained data of compounds **14-18** are given in **Table 4.5** and compared to the energetic values of GAP.

Table 4.5 Energetic data of compounds **14-**18 compared to GAP.

	14a CBS-4M	**14a**	**14b**	**14c**	**15a**	**15b**	**15c**	**16**	**17**	**18**	**GAP[s]**
Formula	$C_{11}H_{18}N_4O_8$	$C_{11}H_{18}N_4O_8$	$C_7H_{10}N_4O_8$	$C_6H_8N_4O_8$	$C_{13}H_{22}N_8O_4$	$C_9H_{14}N_8O_4$	$C_8H_{12}N_8O_4$	$C_{29}H_{34}N_8O_4$	$C_{23}H_{34}N_8O_4$	$C_{16}H_{26}N_{10}O_4$	$C_3H_5N_3O$
FW (monomer) [g mol^{-1}]	334.28	334.28	278.18	264.15	354.36	298.26	284.23	558.63	550.56	422.44	99.09
IS [J][a]	40	40	40	40	40	40	40	>40	>40	>40	7
FS [N][b]	>360	>360	>360	>360	>360	>360	>360	>360	>360	>360	>360
ESD [J][c]	1.5	1.5	1.5	1.5	-	-	-	-	-	-	-
N [%][d]	16.76	16.76	20.14	21.21	31.62	37.57	39.42	20.06	20.55	33.16	42.41
Ω [%][e]	−111	−111	−63	−49	−145	−113	−101	−203	−194	−155	−121
T_{dec} [°C][f]	165	165	168	168	205	210	220	350	>400	220	216
T_g [°C][g]	-	-	-	-	−38	−25	-	-	-	-	
ρ [g cm^{-3}][h]	1.5	1.5	1.5	1.3	1.3	1.3	1.3	1.5[r]	1.5[r]	1.3	1.3
$-\Delta U_{comb}$ [cal g^{-1}][i]	-	4626	3291	3319	4969	4324	3660	6588	5603	5416	-
$-\Delta H_{comb}$ [kJ mol^{-1}][j]	-	6466	3822	3658	7366	5390	4347	15393	12865	9571	-
$\Delta_f H_m°$ [kJ mol^{-1}][k]	−1008	−435	−362	154	−894	−153	−516	−878	−1045	−441	142
Explo5 V6.02 values											
$-\Delta_E U°$ [kJ kg^{-1}][l]	2901	4545	4805	6244	967	3051	1862	1062	832	2031	4307
T_E [K][m]	2038	2742	3234	4310	1061	2179	1657	1027	928	1549	2677
p_{CJ} [kbar][n]	120	156	176	179	64	98	73	91	98	91	129
V_{det} [m s^{-1}][o]	6222	6873	6986	7038	5065	5885	5182	5930	6233	5869	6638
Gas vol. [L kg^{-1}][p]	777	787	771	838	774	793	777	606	692	763	822
I_s [s][q]	168	199	210	269	122	177	150	115	114	153	207

[a] BAM drop hammer (1 of 6); [b] BAM friction tester (1 of 6); [c] electrostatical discharge , [d] nitrogen content; [e] oxygen content; [f] temperature of decomposition by DSC (onset values); [g] glass transition temperature (T_{gMid}), [h] derived from pycnometer measurements; [i] experimental combustion energy (constant volume); [j] experimental molar enthalpy of combustion, [k] molar enthalpy of formation; [l] energy of explosion, [m] explosion temperature; [n] detonation pressure; [o] detonation velocity ; [p] assuming only gaseous products; [q] specific impulse (isobaric combustion, chamber pressure 70 bar, equilibrium expansion); [r] estimated from structure determination, [s] values obtained from the EXPLO5 V6.02 database and ref. [17].

As expected, due to their lower carbon content, the DIE and DIM based compounds **14b**,**c** and **15b**,**c** show better energetic properties, than their corresponding HMDI based derivatives **14a** and **15a**. Whereas compounds **14a-c** in accordance with their higher oxygen balance Ω, show, in total, better energetic values, than the azide containing **15a-c**. The energetic results based on the calculated enthalpy of formation of **14a** show, over all, little lower detonation values than the experimental obtained values, but are still in the range of GAP. Compared to GAP, **14a-c** show a 6 to 45 % higher energy of explosion $-\Delta_E U°$, which is an indicator for the performed work of an explosive. Other important values for the evaluation of the energetic character of a compound are the detonation velocity V_{det} and detonation pressure p_{CJ}. A comparison of these values shows, that compounds **14a-c** exceed the detonation velocity of GAP by 250-400 m s^{-1}. In case of the detonation pressure, the values of **14a-c** are about 30 to 50 kbar higher. The specific impulse I_s of **14a-c**, an indication for the qualification as propellant, is in the same range like GAP. All in all, the calculations showed moderate energetic properties for the synthesized polyurethanes **14-18**, which establishes most of these compounds as interesting substances for further investigations concerning their suitability as binder in energetic formulations.

4.2.2 Polyureas and Related Compounds

To date only few syntheses of energetic polyureas or related compounds are reported in literature.[26] Most of these syntheses are carried out at harsh conditions, in the melt or at least at very high temperatures (> 100 °C). As example, the polyaddition reaction of HMDI with *N*-[1-(2-hydroxyethyl)-1*H*-tetrazol-5-yl]-*N*-methylhydrazine in the melt is depicted in **Scheme 4.8**.[27]

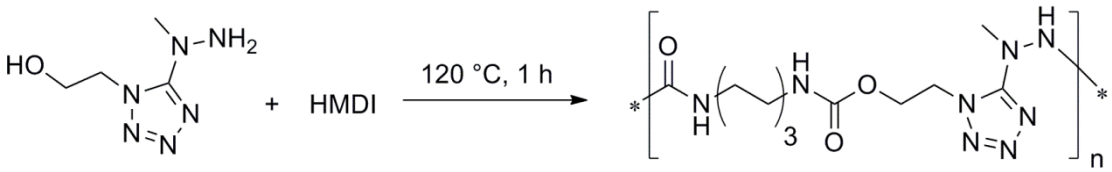

Scheme 4.8 Polyaddition reaction of HMDI and *N*-[1-(2-hydroxyethyl)-1*H*-tetrazol-5-yl]-*N*-methylhydrazine in the melt.

Herein, we report the attempted syntheses of energetic polyureas and related polymers in organic solvent medium at moderate temperatures.

Attempted Polyaddition Reactions

In order to test reaction conditions and process of the polyurea addition, a non-energetic polyurea was prepared from ethylene diamine and HMDI at first (**Scheme 4.9**).

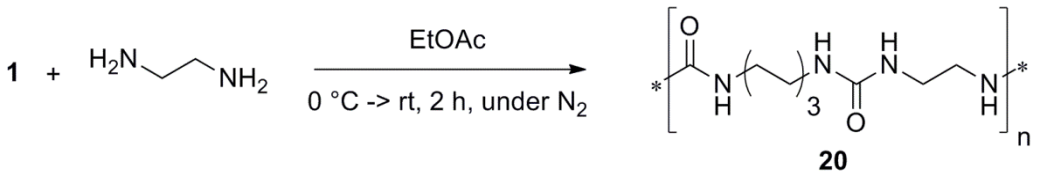

Scheme 4.9 Synthesis of a non-energetic polyurea from HMDI (**1**) and ethylene diamine.

The desired polyurea (**20**) was formed directly on contact between the HMDI solution and the dropwise added ethylene diamine in nitrogen atmosphere at reduced temperature (0 °C) and without any addition of a catalyst.

IR spectra showed the successful formation of the urea group with the N-H stretching vibration at 3326 cm^{-1}, the carbonyl stretching vibration at 1619 cm^{-1} (amide I) and the amide II vibration at 1578 cm^{-1}. Elemental analysis indicated 0.5 remaining molecules of H_2O per repeating unit of **20** (calculated for $C_{10}H_{20}N_4O_2$*0.5 H_2O: C 50.61, H 8.92, N 23.61 %; found: C 50.77, H 8.92, N 23.85 %).

In order to synthesize energetic or at least polyureas with an increased nitrogen content several attempts with different reaction conditions were undertaken using HMDI and different diamino or related compounds (**Scheme 4.10**). The used compounds for the polyaddition reactions are depicted in **Figure 4.13** and were either obtained from commercial sources (**21**, **23**, **24**) or synthesized according to literature procedures (**22**[27], **25**[28]).

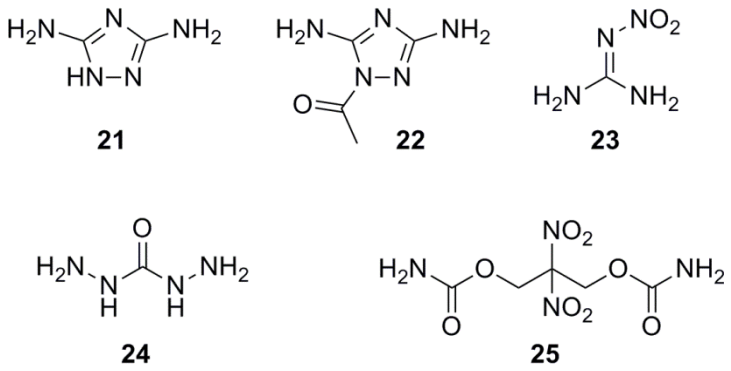

Figure 4.13 Used diamines and related compounds for polyurea syntheses.

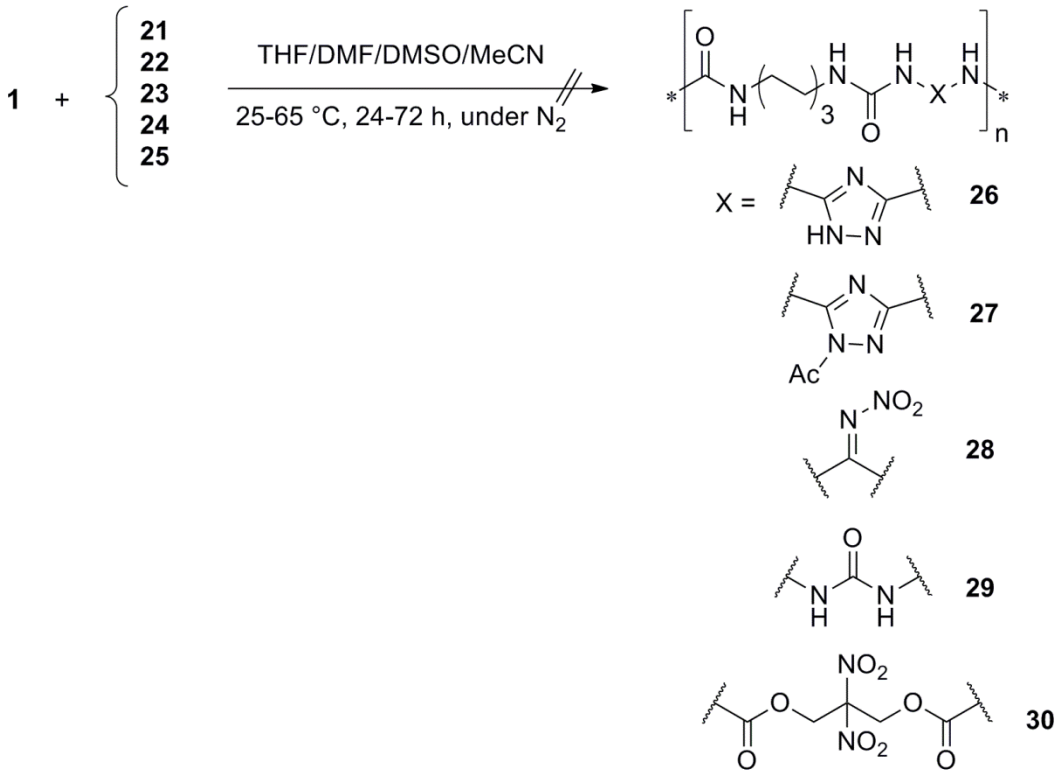

Scheme 4.10 Attempted syntheses towards various nitrogen rich polyurea.

Analyses of the obtained products were carried out using EA, IR, NMR spectroscopy and mass spectrometry.

The reactions of 3,5-diamino-1,2,4-triazole (**21**, DAT) with HMDI in THF over 24 h at 65 °C gave a yellowish solid after the aqueous work up. While the IR spectrum showed the desired signals for the urea group, the amide I and II vibration at 1616 cm^{-1} and 1516 cm^{-1}, another carbonyl stretching vibration was visible at 1710 cm^{-1}. Together with the results of the

elemental analysis, where an increased nitrogen and decreased carbon content was observed (calculated for $C_{10}H_{17}N_7O_2$: C 44.94, H 6.41, N 36.68 %; found: C 41.30, H 6.43, N 40.46 %) and the broad signal range in the ^{1}H NMR spectra, everything points to the fact, that diverse side products were formed, most likely due to the reactive triazole NH group.

To avoid the formation of side products *via* the triazole NH, the acetylated DAT derivative 1-acetyl-3,5-diamino-1,2,4-triazole (ADAT, **22**) was synthesized.[28] Again, no product could be obtained in the polyaddition approach with HMDI after 3 d in THF at 65 °C. During the aqueous work up, large amounts of gas evolved, which indicated the presence of bigger amounts of unreacted HMDI. The unsuccessful synthesis of **27** is most likely because of the inactivity of ADAT (**22**), caused by the acetylation, resulting in an even more electron poor heterocycle and, therefore in a decreased electron density of the attached amine moieties.

Due to its two amino moieties, nitroguanidine (NQ) (**23**) was also chosen for the synthesis of a polyurea (**28**) with HMDI in DMF at 50 °C over three days.

The IR spectra of the obtained yellowish solid showed again the desired urea carbonyl vibration at 1660 cm^{-1} and the amide II vibration at 1510 cm^{-1}, but it lacks vibrations of the nitro group, indicating no integration of the energetic NQ fragment. Elemental analysis, as well, indicated that no formation of **28** had taken place (calculated for $C_9H_{16}N_6O_4$: C 39.70, H 5.92, N 30.87 %; found: C 54.17, H 9.15, N 20.16 %). The found urea but missing nitroimino vibrations in the IR spectrum very strongly suggest the formation of a HMDI-hexamethylene diamine polyurea, which was possibly formed due to present water in the used organic solvent.

The reaction of diaminourea (**24**, DAU) and HMDI was carried out in DMSO for 24 h at 65 °C and gave a colorless precipitate. Whereas, IR measurements were not suitable for the determination of a successful polymer synthesis, due to the presence of the urea group in the starting material, elemental analysis (calculated for $C_9H_{18}N_6O_3$: C 41.85, H 7.02, N 32.54 %; found: C 35.33, H 7.67, 18.17 %) indicated no formation of **29**. This was also confirmed by the measured mass spectrum, which did not give any assignable values. The obtained product was not further investigated.

The reaction towards **30** was carried out using **25** and HMDI in acetonitrile at 65 °C over 24 h.

The obtained colorless solid showed in the IR analyses the carbamate vibrations at 1732 cm^{-1} (amide I), 1565 cm^{-1} (amide II) and 1248 cm^{-1} (C-O stretching) in the IR spectrum but also a strong signal at 1620 cm^{-1}, indicating the presence of the urea group. Furthermore, the

asymmetric and symmetric stretching vibrations of the nitro groups are visible at 1565 cm^{-1} and 1325 cm^{-1}, respectively.

Nevertheless, the elemental analysis showed a quite contaminated product (calculated for $C_{29}H_{34}N_8O_4$: C 37.15, H 4.80, N 19.99 %; found: C 54.90, H 9.04, N 18.71 %). The obtained product could not be purified.

4.3 Conclusion

In this chapter polyaddition reactions towards polyurethanes, polyurea and related polymers were described. The reactions with diamino, dicarbamates or hydrazide moieties did not give any assignable products. Whereas the syntheses towards polyurethanes with various diols were successful and gave products with different consistencies. As diisocyanates hexamethylene diisocyanate (HMDI), diisocyanato ethane (DIE) and diisocyanato methane (DIM) were used. The successful syntheses were mainly proven by elemental analysis, ^{1}H, ^{13}C NMR and infrared spectroscopy. The formed polymers were insensitive towards friction and less or insensitive towards impact. The calculations of the energetic properties, based on bomb calorimetric measurements and the computer program EXPLO5 (version 6.02) showed moderate energetic properties for the compounds. Along with thermal stabilities between 170 and 350 °C and, in case of the liquid polymers, glass transition temperatures as low as −38 °C, the synthesized polyurethanes are promising compounds for applications as new energetic binders in energetic formulations.

4.4 Experimental Part

CAUTION! *All tetrazole, azide or nitro group containing compounds, are potentially explosive energetic materials, although no hazards were observed during preparation and handling of these compounds. Nevertheless, this necessitates additional meticulous safety precautions, while handling these compounds (grounded equipment, Kevlar® gloves, Kevlar® sleeves, face shield, leather coat, ear plugs and safety shield, during reactions).*

4.4.1 General Procedures

General Procedure 1 (GP1), Preparation of the diisocyanates DIE and DIM

The slightly modified reaction was carried out, according to a literature described procedure. [6] Concentrated hydrochloric acid was added dropwise to a solution of the respective hydrazide, sodium nitrite and ice (2 g) in CCl_4 (15-20 mL) at 0 °C, maintaining the temperature below 10 °C. After the addition was completed the mixture was stirred for 2 h and allowed to warm to rt. The completion of the transformation into the acyl azide was observed *via* TLC and IR measurements. The phases were separated and the aqueous phase was extracted, using benzene (3 x 10 mL). The combined organic phases were dried over sodium sulfate and filtrated into a preheated, nitrogen flushed flask. Due to its instability, the acyl azide was not further purified, but directly processed to the corresponding diisocyanate. The solution was therefore heated up in 5 °C steps to 80 °C and stirred for 4 h. The completion of the rearrangement was monitored *via* TLC and IR measurements. The obtained diisocyanate solution was directly used for the polyaddition step.

General Procedure 2 (GP2), Preparation of the HMDI based polyurethanes

A solution of the respective diol in dry organic solvent was degassed for 30 min. HMDI and DBTDL (0.01 mL, 18 µmol) were added in a nitrogen countercurrent and the solution was stirred for 24 h at 50 °C. The reaction mixture was then slowly poured on H_2O (300 mL) and stirred overnight at room temperature. The solvent was decanted and the remaining precipitate was dried *in vacuo*.

General Procedure 3 (GP3), Preparation of the DIE and DIM based polyurethanes

To a freshly prepared solution of the respective diisocyanate in benzene under inert atmosphere, the corresponding diol and DBTDL (0.01 mL, 18 µmol) were added in a nitrogen countercurrent under vigorous stirring. The reaction mixture was stirred at 50 °C for 24 h and then slowly poured on H_2O (200 mL). After stirring overnight the solvent was decanted, the remaining product was washed with hot water and dried *in vacuo*.

4.4.2 Precursors with Diisocyanate Function

Succinyl Hydrazide (3a) [6]

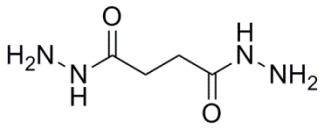

A solution of hydrazine hydrate (6.8 mL, 7.0 g, 140 mmol) and dimethyl succinate (**4**) (3.6 mL, 4.0 g, 27.4 mmol) in methanol (100 mL) was heated to reflux for 2 h. The mixture was then stirred overnight at room temperature. The resulting precipitate was filtered off. The colorless solid was washed using methanol and diethyl ether and dried *in vacuo*, yielding 3.80 g (26.0 mmol, 95 %) of a colorless crystalline solid.

^{1}H NMR (400 MHz, DMSO-d_6, ppm): δ = 8.96 (s, 2H, N*H*), 4.13 (s, 4H, NH_2), 2.24 (s, 4H, CH_2).
^{13}C NMR (101 MHz, DMSO-d_6, ppm): δ = 170.7 (C_q), 28.9 (CH_2).
IR (ATR, cm^{-1}): $\tilde{\nu}$ = 3308 (m), 3288 (s), 3198 (m), 3181 (m), 3043 (w), 1624 (s), 1527 (s), 1459 (m), 1347 (m), 1240 (m), 1181 (m), 1126 (w), 1010 (vs), 947 (m), 749 (m), 659 (m).
EA ($C_4H_{10}N_4O_2$): calculated: C 32.87, H 6.90, N 38.34 %; found: C 32.92, H 6.87, N 38.25 %.

Diisocyanato Ethane (DIE, 5a)

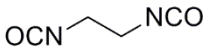

5a was synthesized with HCl_{conc} (1.4 mL, 16.8 mmol) **3a** (1.0 g, 6.8 mmol) and sodium nitrite (1.1 g, 16.0 mmol) in CCl_4 (15 mL) applying **GP1**.

Malonyl Hydrazide (3b) [6 29]

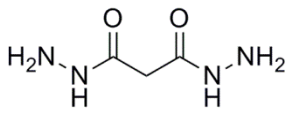

A solution of hydrazine hydrate (9.2 mL, 9.5 g, 189 mmol) and dimethyl malonate (**9**, 8.7 mL, 10 g, 75.6 mmol) in methanol (200 mL) was heated to reflux for 2 h. The mixture was then stirred overnight at room temperature. The resulting precipitate was filtered off. The colorless solid was washed using methanol and diethyl ether and dried *in vacuo*, yielding 9.23 g (69.9 mmol, 92 %) of a colorless crystalline solid.

^{1}H NMR (400 MHz, DMSO-d_6, ppm): δ = 9.05 (s, 2H, N*H*), 4.23 (s, 4H, NH_2), 2.89 (s, 2H, CH_2).
^{13}C NMR (101 MHz, DMSO-d_6, ppm): δ = 166.0 (C_q), 40.1 (CH$_2$).
IR (ATR, cm^{-1}): $\tilde{\nu}$ = 3296 (m), 3264 (m), 3199 (m), 3126 (m), 3032 (m), 2997 (m), 2868 (m), 1663 (s), 1645 (s), 1591 (vs), 1529 (vs), 1416 (m), 1362 (m), 1339 (m), 1247 (m), 1203 (m), 1141 (w), 1051 (vs), 1004 (m), 954 (s), 906 (m), 788 (m), 693 (vs).
EA: ($C_3H_8N_4O_2$): calculated: C 27.27, H 6.10, N 42.41 %; found: C 27.41, H 5.91, N 42.24 %.

Diisocyanato Methane (DIM, 5b)

Compound **5b** was synthesized with HCl_{conc} (1.4 mL, 16.8 mmol) **3b** (1.0 g, 7.6 mmol) and sodium nitrite (1.2 g, 16.8 mmol) in CCl_4 (20 mL) applying **GP1**.

4.4.3 Precursors with Alcohol Function

2,2-Dinitropropane-1,3-diol (DNPD, 7) [8]

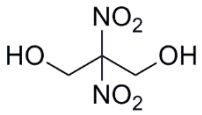

A solution of nitromethane (0.88 mL, 1.00 g, 16.4 mmol) and formaldehyde (2.90 mL, 2.66 g, 31.9 mmol) in H_2O (2.5 mL) was cooled to 0 °C. Afterwards a mixture of sodium hydroxide (0.75 g, 18.8 mmol) in H_2O (2 mL) was added dropwise. The temperature was kept below 40 °C during addition. After stirring at 0 °C for 90 min, sodium nitrite (1.13 g, 16.4 mmol) was added. This mixture was added slowly to a solution of silver nitrate (5.57 g, 32.8 mmol) in H_2O (7.2 mL), while the temperature was kept below 25 °C. After stirring for another 2 h the precipitated silver was filtered off and the product was extracted using diethyl ether (3 x 15 mL). The extract was concentrated *in vacuo* and the resulting solid was purified by recrystallization using dichloromethane, yielding 1.80 g (10.82 mmol, 66 %) of **7** as a colorless crystalline solid.

^{1}H NMR (400 MHz, acetone-d_6, ppm): δ = 5.34 (t, $^3J_{HH}$ = 6.1 Hz, 2H, O*H*), 4.51 (d, $^3J_{HH}$ = 6.1 Hz, 4H, CH_2).
^{13}C NMR (101 MHz, acetone-d_6, ppm): δ = 119.7 (C_q), 61.7 (CH$_2$).
IR (ATR, cm^{-1}): $\tilde{\nu}$ = 3238 (br, s), 2972 (w), 2881 (w), 1562 (vs), 1460 (w), 1445 (w), 1348 (m), 1319 (s), 1258 (m), 1067 (vs), 1035 (vs), 922 (w), 874 (w), 843 (w), 762 (m), 684 (w).
EA ($C_3H_6N_2O_6$): calculated: C 32.87, H 6.90, N 38.34 %; found: C 32.92, H 6.87, N 38.25 %.

2,2-Bis(azidomethyl)propane-1,3-diol (BAMP, 8) [9]

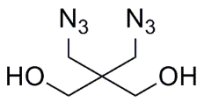

Sodium azide (1.74 g, 28.8 mmol) and 2,2-bis(bromomethyl)propane-1,3-diol (2.8 g, 10.7 mmol) were dissolved in 20 mL DMSO and heated to 100 °C for 48 h. Then H_2O (15 mL) and brine (15 mL) were added. The solution was extracted using ethyl acetate (3 x 20 mL). The combined organic phases were washed with brine (2 x 20 mL) and dried over sodium sulfate. After filtration *n*-heptane (25 mL) was added to the crude liquid and the solvents were removed under reduced pressure. Drying *in vacuo*, yielded 1.85 g (9.94 mmol, 93 %) of **8** as a yellowish liquid.

^{1}H NMR (400 MHz, DMSO-d_6, ppm): δ = 4.74 (t, $^3J_{HH}$ = 5.2 Hz, 2H, O*H*), 3.29 (s, 4H, CH_2−N_3), 3.27 (d, $^3J_{HH}$ = 5.2 Hz, 4H, CH_2−OH).
^{13}C NMR (101 MHz, DMSO-d_6, ppm): δ = 59.8 (*C*H_2−OH), 51.2 (C_q), 45.5 (*C*H_2−N_3).
^{14}N NMR (DMSO-d_6, ppm): δ = −129 (N_β), −170 (N_γ), −310 (N_α).
IR (ATR, cm^{-1}): $\tilde{\nu}$ = 3358 (br m), 2937 (w), 2884 (w), 2092 (vs), 1723 (w), 1661 (m), 1447 (m), 1357 (w), 1272 (s), 1179 (vw), 1128 (vw), 1036 (s), 922 (w), 887 (w).
EA ($C_5H_{10}N_6O_2$): calculated: C 32.26, H 5.41, N 45.14 %; found: C 32.13, H 5.68, N 42.61 %.

2,2-Bis((4-phenyl-1H-1,2,3-triazol-1-yl)methyl)propane-1,3-diol (9)[10]

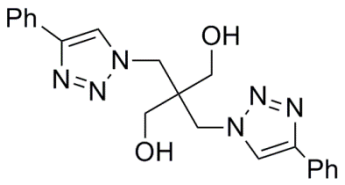

BAMP (0.50 g, 2.69 mmol) was dissolved in 10 mL of a 1:1 solution of water and *t*-BuOH. To this solution, phenylacetylene (0.59 mL, 5.37 mmol) was added, followed by aqueous solutions of sodium ascorbate (53 mg in 1.0 mL water, 10 mol%) and copper(II) sulfate pentahydrate (7 mg in 0.5 mL water, 1 mol%). The reaction mixture was refluxed for 12 h at room temperature. Water (50 mL) was added and the solution was filtrated. The white precipitate was washed with water (2 x 25 mL) and dried *in vacuo* to yield 0.53 g (1.36 mmol, 51 %) of a colorless powder.

^{1}H NMR (400 MHz, DMSO-d_6, ppm): δ = 8.51 (s, 2H, CH_{triazole}), 7.86 (pseudo d, J_{app} = 7.7 Hz, 4H, H_{o}), 7.45 (pseudo t, J_{app} = 7.7 Hz, 4H, H_{m}), 7.34 (pseudo t, J_{app} = 7.7 Hz, 2H, H_{p}), 5.06 (t, $^{3}J_{\text{HH}}$ = 4.5 Hz, 2H, OH), 4.50 (s, 4H, CH_2−N$_{\text{triazole}}$), 3.24 (d, $^{3}J_{\text{HH}}$ = 4.5 Hz, 4H, CH_2−OH).

^{13}C NMR (101 MHz, DMSO-d_6, ppm): δ = 146.0 ($C_{\text{q,triazole}}$), 130.7 (triazole−$C_{\text{q,phenyl}}$), 128.9 (CH$_{\text{triazole}}$), 127.9 (C_{m}), 125.2 (C_{o}), 123.2 (C_{p}), 60.0 (CH$_2$-OH), 49.8 (C_{q}), 45.4 (CH$_2$−N$_{\text{triazole}}$).

IR (ATR, cm^{-1}): $\tilde{\nu}$ = 3182 (w), 3147 (w), 2908 (vw), 2860 (vw), 1736 (vw), 1465 (w), 1445 (w), 1360 (w), 1232 (w), 1190 (w), 1145 (vw), 1100 (w), 1082 (s), 1059 (vs), 1053 (s), 983 (w), 899 (vw), 818 (vw), (vw), 797 (w), 772 (vs), 712 (w), 686 (s).

EA ($C_{21}H_{22}N_6O_2$): calculated: C 64.60, H 5.68, N 21.52 %; found: C 64.50, H 5.46, N 21.19 %.

MS (DEI+): *m/z* (%) = 390.2 [M^{+}] (77), 362.2 (17), 334.2 (40), 333.2 (23), 246.2 (76), 214.2 (43), 156.1 (42), 116.1 (100), 103.1 (69), 91.1 (49), 41.1 (23), 39.1 (14).

2,2-Bis(acetoxymethyl-1H-1,2,3-triazol-1-yl)methyl)propane-1,3-diol (10)

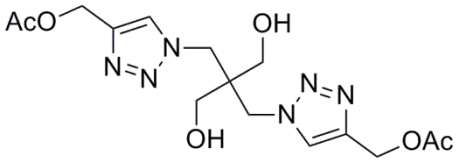

BAMP (3.00 g, 16.12 mmol) was dissolved in 20 mL of a 1:1 solution of water and *t*-BuOH. To this solution, propargyl acetate (3.16 g, 32.14 mmol) was added, followed by aqueous solutions of sodium ascorbate (200 mg in 0.2 mL water) and copper(II)sulfate pentahydrate (26 mg in 0.1 mL water). The reaction mixture was refluxed for 12 h at 50 °C. The solvent was concentrated under reduced pressure to approx. 15 mL. Recrystallization out of methanol followed by filtration and washing with water gave 4.04 g (10.57 mmol, 66 %) of **10** as colorless crystals.

DSC (5 °C min^{-1}): T_{melt} = 144, T_{dec} = 310 °C.

^{1}H NMR (400 MHz, DMSO-d_6, ppm): δ = 8.11 (s, 2H, C$H_{triazole}$), 5.12 (s, 4H, CH_2–OAc), 5.04 (d, $^{3}J_{HH}$ = 4.6 Hz, 2H, O*H*), 4.39 (s, 4H, CH_2–$N_{triazole}$), 3.11 (t, $^{3}J_{HH}$ = 4.6 Hz, 4H, CH_2–OH), 2.03 (s, 6H, CH_3).

^{13}C NMR (101 MHz, DMSO-d_6, ppm): δ = 170.1 (*C*=O), 141.6 ($C_{q,triazole}$), 126.5 (*C*$H_{triazole}$), 59.8 (*C*H_2–OH), 57.0 (*C*H_2–OAc), 49.5 (C_q), 45.3 (*C*H_2–$N_{triazole}$), 20.6 (*C*H_3).

IR (ATR, cm^{-1}): $\tilde{\nu}$ = 3240 (m), 3158 (w), 2933 (w), 2880 (w), 2105 (w), 1748 (m), 1733 (s), 1556 (w), 1470 (w), 1434 (w), 1392 (m), 1364 (w), 1338 (w), 1253 (m), 1222 (vs), 1148 (m), 1130 (m), 1096 (m), 1048 (vs), 997 (m), 967 (w), 956 (w), 895 (w), 845 (w), 831 (w), 804 (m), 770 (w), 718 (w), 684 (w), 674 (w), 664 (w).

EA ($C_{15}H_{22}N_6O_6$): calculated: C 47.12, H 5.80, N 21.98 %; found: C 47.06, H 5.87, N 21.98 %.

MS (DEI+)**:** *m/z* (%) = 382.3 $[M]^+$ (6), 337.2 (17), 295.3 (19), 182.2 (24), 140.2 (34), 84.1 (30.34), 43.1 (100).

2,2-Bis(hydroxymethyl-1H-1,2,3-triazol-1-yl)methyl)propane-1,3-diol (4-ol, 12)

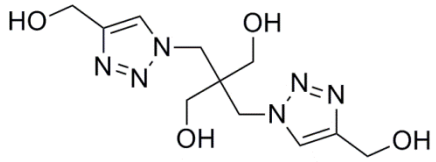

Compound **10** (1.5 g, 3.92mmol) was dissolved in 20 mL of a 1:1 solution of water and ethanol and cooled to 0 °C. An aqueous sodium hydroxide solution (1.25 g, 31.36 mmol, in 5 mL H_2O) was added dropwise, keeping the temperature below 10°C. The solution was stirred at room temperature for 12 h. The solution was then acidified with conc. HCl. The solvent was removed under reduced pressure. The crude residue was then purified *via* column chromatography (stationary phase: silica, mobile phase: *n*-hexane/aceton/methanol (1:1:3). Recrystallization in a methanol/ethanol mixture gave 0.6 g of **12** (3.01 mmol, 51 %) as colorless crystals.

^{1}H NMR (270 MHz, DMSO-d_6, ppm): δ = 7.97 (s, 2H, C$H_{triazole}$), 5.22 (br. s, 2H, O*H*), 5.12 (br. s, 2H, O*H*), 4.53 (s, 4H, $C_{q,triazole}$−CH_2−OH), 4.34 (s, 4H, CH_2−$N_{triazole}$), 3.11 (s, 4H, C_q−CH_2−OH) ppm.

^{13}C NMR (68 MHz, DMSO-d_6, ppm): δ =147.8 ($C_{q,triazole}$), 124.4 (*C*$H_{triazole}$), 59.8 (*C*H_2−OH), 55.0 (*C*H_2−OH), 49.3 (C_q), 45.4 (*C*H_2−$N_{triazole}$) ppm.

EA ($C_{11}H_{18}N_6O_4$): calculated: C 44.29, H 6.08, N 28.52 %; found: C 44.22, H 6.31, N 25.52 %.

MS (DEI+): *m/z* (%) = 255.3 $[M]^+$ (9.9), 195.2 (59.4), 168.2 (61.5), 125.2 (28.4), 81.1 (55.5), 45.1 (100), 31.1 (45.3).

1,2-Bis(hydroxyethyl-5-tetrazolo)ethane (BTEOH, 11) [11]

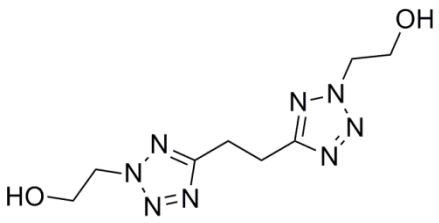

NaOH (1.73 g, 43.2 mmol) was dissolved in water (40 mL). Compound **5** (3.84 g, 23.1 mmol) and chloroethanol (4.10 g, 3.4 mL, 50.9 mmol) were added and the mixture was stirred at 100 °C for 18 h. After concentrating under reduced pressure, hot ethanol (20 mL) was added. After cooling, the formed precipitate was filtered off while the filtrate was washed with cold ethanol and filtered again. After concentrating under reduced pressure and further drying *in vacuo*, 4.42 g (17.4 mmol, 75 %) of **11** were obtained as a colorless viscous liquid.

^{1}H NMR (400 MHz, DMSO-d_6, ppm): δ = 5.12 (m, 2H), 5.04 (m, 2.2H), 4.44 (m, 4.5H); 4.37 (m, 1.7H), 3.87 (m, 4.5H), 3.76 (m, 4.1H), 3.44 (m, 4.5H), 3.38 (m, 10.5H).
^{13}C NMR (101 MHz, DMSO-d_6, ppm): δ = 164.6, 164.4, 155.0, 154.8, 62.8, 62.5, 59.7, 59.1, 55.4, 55.4, 49.4, 49.3, 23.2, 22.6, 20.8, 20.3.
IR (ATR, cm^{-1}): $\tilde{\nu}$ = 3356 (m), 2945 (w), 2884 (w), 1644 (br w), 1524 (m), 1500 (m), 1425 (s), 1361 (m), 1244 (m), 1198 (m), 1129 (m), 1064 (vs), 958 (m), 867 (s).
MS (DEI+) *m/z* (%): 255.3 $[M+H]^+$ (3.5), 195.2 (59.6), 168.2 (100.0), 124.2 (28.5), 81.1 (44.5), 45.1 (57.2), 31.1 (15.84).

4.4.4 HMDI Based Polyurethanes

Poly[hexamethylene(but-2-yne)carbamate] (HMDI-BuDi, 13)

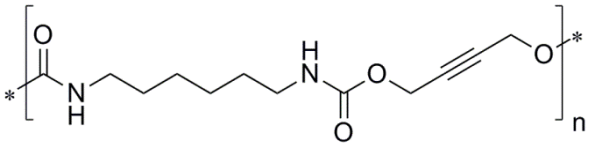

HMDI-BuDi was synthesized from but-2-yne-1,3-diol (2.05 g, 23.8 mmol) in ethyl acetate (50 mL) with 1 eq. of HMDI (3.82 mL, 23.8 mmol) and DBTDL, applying **GP2**. The reaction gave 4.79 g (18.8 mmol, 79 %) of **13** as a colorless powder.

^{1}H NMR (400 MHz, DMSO-d_6, ppm): δ = 7.29 (br. t, 2H, N*H*), 4.65 (br. s, 4H, CH_2−O), 2.95 (br. q, $^{3}J_{HH}$ = 6.5 Hz, 4H, CH_2−NH), 1.36 (br. m, 4H, CH_2−CH_2−NH), 1.22 (br. m, 4H, CH_2−CH_2CH_2).
^{13}C NMR (101 MHz, DMSO-d_6, ppm): δ = 155.3 (*C*=O), 81.5 (−*C*≡), 51.3 (*C*H_2−O), 40.3 (*C*H_2−NH), 29.8 (*C*H_2−CH_2−NH), 25.9 (*C*H_2−CH_2CH_2).
IR (ATR, cm^{-1}): $\tilde{\nu}$ = 3323 (m), 2942 (m), 2864 (w), 2021 (vw), 1685 (vs), 1541 (vs), 1363 (w), 1339 (w), 1259 (m), 1219 (m), 1153 (m), 1050 (w), 996 (m), 775 (w).
EA ($C_{12}H_{18}N_2O_4$): calculated: C 56.68, H 7.13, N 11.02 %; found: C 56.53, H 7.51, N 11.49 %.

Poly[hexamethylene(2,2-dinitropropylene)carbamate] (HMDI-DNPD, 14a)

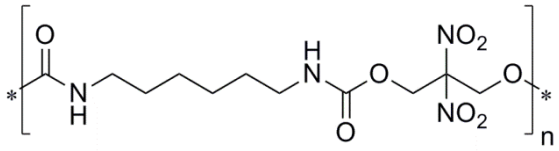

HMDI-DNPD was synthesized from DNPD (1.0 g, 6.0 mmol) in THF (40 mL) with 1 eq. of HMDI (0.97 mL, 6.0 mmol) and DBTDL, applying **GP2**. The reaction gave 1.92 g (5.74 mmol, 96 %) of **14a** as orange, ductile solid.

DSC (5 °C min^{-1}): T_{dec} = 165 °C.

^{1}H NMR (400 MHz, DMSO-d_6, ppm): δ = 7.58 (br. m, 2H, N*H*), 5.00 (br. s, 4H, CH_2−O), 2.95 (br. m, 4H, CH_2−NH), 1.35 (br. m, 4H, CH_2−CH_2−NH), 1.21 (br. m, 4H, CH_2−CH_2CH_2).

^{13}C NMR (101 MHz, DMSO-d_6, ppm): δ = 153.9 (*C*=O), 115.6 (C_q), 60.9 (*C*H_2−O), 30.4 (*C*H_2−N), 29.0 (*C*H_2−CH_2−NH), 25.8 (*C*H_2−CH_2CH_2).

IR (ATR, cm^{-1}): $\tilde{\nu}$ = 3330 (m), 2934 (m), 2860 (w), 1712 (vs), 1570 (vs), 1527 (vs), 1457 (m), 1408 (m), 1322 (m), 1235 (vs), 1130 (s), 1047 (s), 960 (w), 848 (m), 766 (m), 729 (w).

EA ($C_{11}H_{18}N_4O_8$ * 0.25 THF * 0.5 H_2O):calculated: C 39.89, H 5.86, N 15.51 %; found: C 39.81, H 5.92, N 15.55 %.

Poly[hexamethylene(2,2-bis(azidomethyl)propylene)carbamate] (HMDI-BAMP, 15a)

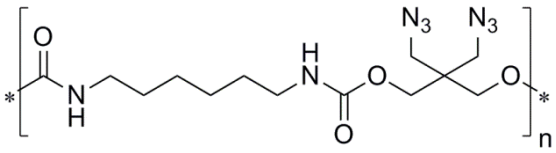

HMDI-BAMP was synthesized from BAMP (1.11 g, 5.95 mmol) in THF (40 mL) with 1 eq. of HMDI (0.96 mL, 5.95 mmol) and DBTDL, applying **GP2**. The reaction gave 1.91 g (5.39 mmol, 91 %) of **15a** as yellowish, highly viscous liquid.

DSC (5 °C min^{-1}): T_{dec} = 205 °C.

^{1}H NMR (400 MHz, DMSO-d_6, ppm): δ = 7.13 (br. s, 1.7H, N*H trans* conformer), 6.89 (br. s, 0.3H, N*H cis* conformer), 3.87 (br. s, 4H, CH_2−O), 3.40 (br. s, 4H, CH_2−N_3) 2.96 (br. s, 4H, CH_2−NH), 1.37 (br. s, 4H, CH_2−CH_2−NH), 1.23 (br. s, 4H, CH_2−CH_2CH_2).

^{13}C NMR (101 MHz, DMSO-d_6, *ppm*): δ = 155.7 (*C*=O), 62.4 (*C*H_2−O), 51.3 (*C*H_2−N_3), 43.2 (C_q), 40.2 (*C*H_2−N), 29.3 (*C*H_2−CH_2−NH), 25.9 (*C*H_2−CH_2CH_2).

IR (ATR, cm^{-1}): $\tilde{\nu}$ = 3324 (w,), 2929 (m), 2857 (w), 2097 (vs), 1694 (vs), 1525 (s), 1449 (m), 1412 (w), 1359 (w), 1235 (vs), 1136 (s), 1035 (s), 900 (w), 805 (w), 772 (m), 729 (w), 666 (w).

EA ($C_{13}H_{22}N_8O_4$ * 0.3 THF * 0.1 H_2O): calculated: C 45.15, H 6.56, N 29.66 %; found: C 45.17, H 6.71, N 29.57 %.

MS (DCI+): *m/z* (%) = 355.4 (9) [monomeric unit + H]$^{+}$, 201.4 (5), 187.3 (41), 86.2 (11), 57.2 (100), 43.2 (17).

Poly[hexamethylene(2,2-bis((4-phenyl-1H-1,2,3-triazol-1-yl)methyl)propylene]carbamate (HMDI-TriPh, 16)

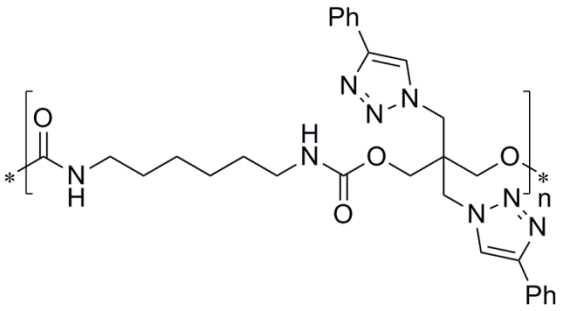

HMDI-TriPh was synthesized from **9** (1.93 g, 4.9 mmol) in a 9:1 mixture of THF/DMSO (50 mL) with 1 eq. of HMDI (0.79 mL, 4.9 mmol) and DBTDL, applying **GP2**. The reaction gave 1.54 g (2.8 mmol, 56 %) of **16** as a colorless powder.

DSC (5 °C min^{-1}): T_{dec} = 350 °C.

^{1}H NMR (400 MHz, DMSO-d_6, ppm): δ = 8.52 (s, 2H, C$H_{triazole}$), 7.83 (br. m, 4H, H_o), 7.45 (br. m, 4H, H_m), 7.33 (br. t, 2H, H_p), 7.19 (br. m, 2H, NH), 4.56 (br. s, 4H, CH_2−$N_{triazole}$), 3.73 (br. s, 1.5H, CH_2−O), 2.94 (br. m, 4.3H, CH_2−NH), 1.28 (br. m, 10.2H CH_2−CH_2−NH).

IR (ATR, cm^{-1}): $\tilde{\nu}$ = 3321 (w), 3136 (w), 2933 (w), 2857 (w), 1704 (m), 1649 (w), 1615 (m), 1547 (m), 1482 (m), 1463 (m), 1440 (m), 1358 (w), 1334 (w), 1249 (s), 1233 (s), 1184 (m), 1138 (m), 1099 (w), 1045 (s), 972 (w), 913 (w), 824 (vw), 764 (vs), 710 (w), 694 (s).

EA ($C_{29}H_{34}N_8O_4$ * 0.5 H_2O): calculated: C 61.36, H 6.21, N 19.74 %; found: C 61.49, H 6.39, N 19.34 %.

MS (DEI+): *m/z* (%) = 559.7 [monomeric unit +H]$^+$ (3), 414.6 (3), 391.5 (100), 246.4 (77), 116.2 (87), 103.2 (48).

Poly[hexamethylene(2,2-bis((acetoxymethyl-1H-1,2,3-triazol-1-yl)methyl)propylene)carbamate] (HMDI-TriOAc, 17)

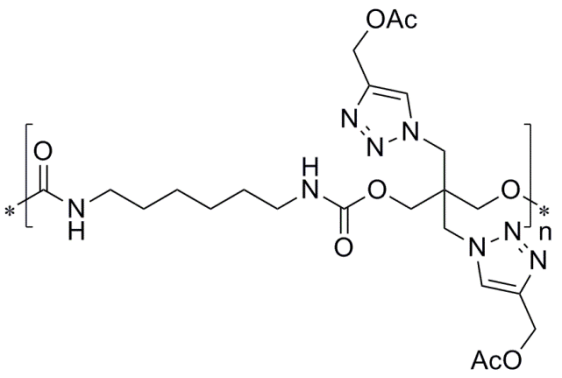

HMDI-TriOAc was synthesized from **10** (2.11 g, 6.0 mmol) in THF (50 mL) with 1 eq. of HMDI (0.96 mL, 6.0 mmol) and DBTDL, applying **GP2**. The reaction gave 1.68 g (3.1 mmol, 51 %) of **17** as a colorless powder.

DSC (5 °C min^{-1}): T_{dec} = >400 °C.

^{1}H NMR (400 MHz, DMSO-d_6, ppm): δ = 8.11 (s, 2H, C$H_{triazole}$), 7.16 (br. m, 1.6H, N*H trans* conformer), 6.87 (br. m, 0.4H, N*H cis* conformer), 5.12 (br. s, 4H, CH_2−OAc), 4.85 (br. m, 4H, CH_2−$N_{triazole}$), 3.68 (br. m, 3.5H, CH_2−O), 2.96 (br. m, 4.4H, CH_2−NH), 1.28 (br. m, 10.8H, CH_2−CH_2−NH).

IR (ATR, cm^{-1}): $\tilde{\nu}$ = 3325 (w), 3146 (w), 2930 (m), 2857 (w), 1713 (s), 1650 (m), 1540 (s), 1461 (m), 1440 (m), 1367 (m), 1224 (vs), 1141 (s), 1032 (s), 961 (m), 923 (w), 831 (w), 773 (m), 732 (w), 703 (w).

EA ($C_{23}H_{34}N_8O_8$ * 0.7 H_2O * 0.5 THF): calculated: C 50.11, H 6.63, N 18.70 %; found: C 50.27, H 6.83, N 18.57 %.

MS (DEI+): *m/z* (%) = 424.5 $[M+H]^+$ (3), 337.4 (10), 212.3 (9), 140.2 (19), 43.1 (100).

Poly[hexamethylene(1,2-bis(hydroxyethyl-5-tetrazolo)ethane)carbamate] (HMDI-BTEOH, 18)

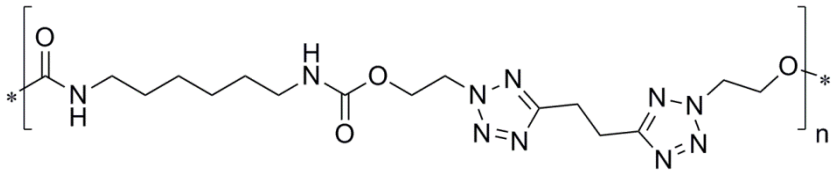

HMDI-BTEOH was synthesized from **11** (1.00 g, 3.9 mmol) in acetonitrile (50 mL) with 1.5 eq. of HMDI (0.95 mL, 5.9 mmol) (to compensate the remaining alcohol in BTEOH) and DBTDL, applying **GP2**. The reaction gave 1.67 g (3.4 mmol, 88 %) of **17** as a colorless powder.

IR (ATR, cm^{-1}): $\tilde{\nu}$ = 3329 (m), 2921 (m), 2851 (w), 1705 (vs), 1532 (vs), 1455 (m), 1367 (w), 1248 (vs), 1238 (vs), 1178 (m), 1098 (s), 1029 (vs), 872 (w), 801 (w), 774 (m), 727 (w), 667 (w).

EA: ($C_{16}H_{26}N_{10}O_4$ * 1 H_2O * 0.7 THF): calculated: C 45.99, H 6.90, N 28.53 %; found: C 45.59, H 6.72, N 26.06 %.

4.4.5 DIE/DIM Based Polyurethanes

Poly[ethylene(2,2-dinitropropylene)carbamate] (DIE-DNPD, 14b)

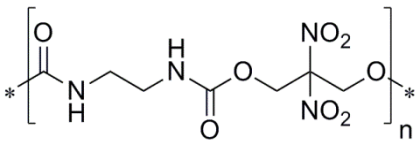

DIE-DNPD was synthesized from a solution of DIE in benzene and DNPD (1.0 g, 6.0 mmol), applying **GP3**. The reaction gave 0.95 g (3.42 mmol, 57 %) of **14b** as reddish, glutinous solid.

DSC (5 °C min^{-1}): T_{dec} = 168 °C.

^{1}H NMR (400 MHz, DMSO-d_6, ppm): δ = 7.62 (br, 2H, N*H*), 5.01 (br, 4H, CH_2−O), 3.02 (br, 4H, CH_2−N).

^{13}C NMR (101 MHz, DMSO-d_6, ppm): δ = 154.1 (*C*=O), 115.4 (C_q), 61.1 (*C*H_2−O), 29.0 (*C*H_2−NH).

IR (ATR, cm^{-1}): $\tilde{\nu}$ = 3333 (w), 2957 (w), 2886 (w), 1714 (vs), 1562 (vs), 1520 (s), 1438 (m), 1322 (m), 1230 (vs), 1143 (s), 1116 (s), 1043 (s), 963 (w), 863 (w), 845 (m), 764 (m), 673 (w).

EA ($C_7H_{10}N_4O_8$ * 0.5 H_2O * 0.3 C_6H_6): calculated: C 34.40, H 4.49, N 17.83 %, found C 34.32, H 4.52, N 18.23 %.

Poly[methylene(2,2-dinitropropylene)carbamate] (DIM-DNPD, 14c)

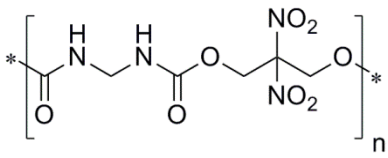

DIM-DNPD was synthesized from a solution of DIM in benzene and DNPD (1.27 g, 6.8 mmol), applying **GP3**. The reaction gave 0.97 g (3.7 mmol, 54 %) of **14c** as reddish solid.

DSC (5 °C min^{-1}): T_{dec} = 168 °C.
IR (ATR, cm^{-1}): $\tilde{\nu}$ = 3318 (w), 2960 (w), 2923 (w), 2853 (w), 2358 (w), 2341 (w), 1729 (w), 1713 (w), 1517 (m), 1538 (w), 1520 (w), 1456 (w), 1394 (w), 1321 (w), 1257 (s), 1085 (s), 1012 (vs), 927 (vw), 863 (w), 849 (w), 792 (vs), 686 (w).
EA ($C_6H_8N_4O_8$ * 1 H_2O * 0.35 C_6H_6): calculated: C 31.43, H 3.94, N 18.12 %; found: C 31.36, H 4.33, N 17.96 %.

Poly[ethylene(2,2-bis(azidomethyl)propylene)carbamate] (DIE-BAMP, 15b)

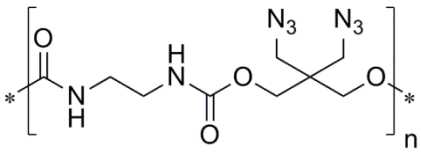

DIE-BAMP was synthesized from a solution of DIE in benzene and BAMP (1.12 g, 6.00 mmol), applying **GP3**. The reaction gave 0.93 g (3.12 mmol, 52 %) of **15b** as yellow, viscous liquid.

DSC (5 °C min^{-1}): T_{dec} = 210 °C.

^{1}H NMR (400 MHz, DMSO-d_6, ppm): δ = 7.19 (br, 2H, N*H*), 3.83 (br, 4H, CH_2−O), 3.29 (br, CH_2−N_3), 3.02 (br, 4H, CH_2−NH).

^{13}C NMR (101 MHz, DMSO-d_6, ppm): δ = 154.9 (*C*=O), 58.6 (*C*H_2−O), 50.0 (*C*H_2−N_3), 43.2 (C_q), 39.3 (*C*H_2−NH).

IR (ATR, cm^{-1}): $\tilde{\nu}$ = 3328 (w), 2938 (w), 2875 (w), 2360 (w), 2094 (vs), 1697 (s), 1524 (m), 1447 (m), 1404 (w), 1359 (w), 1253 (vs), 1142 (s), 1042 (s), 950 (m), 896 (w), 772 (w), 700 (w), 667 (w).

EA ($C_9H_{14}N_8O_4$ * 0.1 H_2O): calculated: C 36.02, H 4.77, N 37.34 %; found: C 35.75, H 4.91, N 37.58 %.

MS (DEI+): *m/z* (%) = 597.7 (0.1) [dimeric unit + H]$^+$, 387.5 (2), 299.4 (2) [monomeric unit + H]$^+$, 273.4 (6), 131.2 (56), 113.2 (39), 86.2 (80), 81.2 (24), 72.2 (19), 69.2 (36), 57.2 (44), 54.2 (47), 43.1 (82), 30.1 (64), 28.1 (100).

Poly[methylene(2,2-bis(azidomethyl)propylene)carbamate] (DIM-DNPD, 15c)

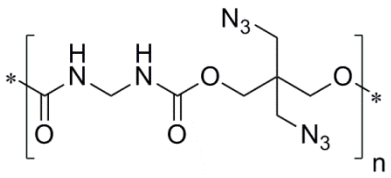

DIE-BAMP was synthesized from a solution of DIE in benzene and BAMP (1.12 g, 6.00 mmol), applying **GP3**. The reaction gave 0.93 g (3.12 mmol, 52 %) of **15b** as yellow, viscous liquid.

DSC (5 °C min^{-1}): T_{dec} = 210 °C.
IR (ATR, cm^{-1}): $\tilde{\nu}$ = 3323 (w), 2956 (w), 2875 (w), 2089 (vs), 1697 (s), 1514 (s), 1448 (m), 1393 (w), 1360 (w), 1219 (vs), 1116 (m), 1094 (w), 1050 (m), 1002 (s), 950 (w), 890 (w), 777 (w), 704 (w), 667 (w).
EA ($C_8H_{12}N_8O_4$ * 1 H_2O * 0.3 C_6H_6): calculated: C 36.14, H 4.89, N 34.41 %; found: C 36.57, H 5.29, N 34.68 %.

4.4.5 Precursors with Diamino Function

1-Acetyl-3,5-diamino-1,2,4-triazole (22)[28]

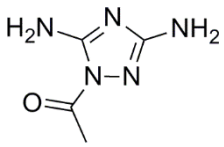

A solution of 3,5-diamino-1,2,4-triazole (**21**, 10 g, 101 mmol) was dissolved in H_2O (40 mL). Afterwards acetic anhydride (12.4 g, 11.5 mL, 121 mmol) was added dropwise at rt. After stirring for 1 h the colorless precipitate was filtered off, washed with water and dried *in vacuo*, yielding 12.83 g (90.91 mmol, 90 %) **22** as colorless powder.

^{1}H NMR (400 MHz, DMSO-d_6, ppm): δ = 7.34 (s, 2H, NH_2), 5.64 (s, 2H, NH_2), 2.34 (s, 3H, CH_3).
^{13}C NMR (101 MHz, DMSO-d_6, ppm): δ = 169.9 (C_q), 161.6 (C_q), 156.5 (C_q), 23.0 (CH_3).
IR (ATR, cm^{-1}): $\tilde{\nu}$ = 3415 (m), 3390 (m), 3294 (m), 3223 (m), 3129 (m), 1709 (s), 1640 (s), 1569 (m), 1450 (m), 1395 (s), 1366 (vs), 1337 (s), 1178 (m), 1134 (m), 1117 (m), 1066 (m), 1044 (m), 973 (m), 839 (w), 758 (w), 700 (w).
EA ($C_4H_7N_5O$): calculated: C 34.04, H 5.00, N 49.62 %; found: C 33.99, H 4.92, N 49.32 %.

4.5 References

1 R. B. Seymour, G. B. Kauffman, *J. Chem. Ed.* **1992**, *69*, 909-910.

2 http://fas.org/nuke/guide/usa/slbm/a-1.htm (accessed April, 2016).

3 M. A. Daniel, Report *DSTO-GD-0492*, Defence Science and Technology Organisation, Edinburgh South Australia,, Australia **2006**.

4 H. R. Blomquist, *U.S. Patent 6,802,533*, **2004**.

5 J. M. Bellerby, C. Kiriratnikom, *Propellants, Explos., Pyrotech.* **1989**, *14*, 82-85.

[6] C. King, *J. Am. Chem. Soc.* **1964**, *86*, 437-440.

[7] M. Hesse, H. Meier, B. Zeh, *Spektroskopische Methoden in der organischen Chemie*, 7. Edition, Thieme Verlag, Stuttgart, **2005**.

[8] a) R. Kaplan, H. Shechter, *J. Am. Chem. Soc.* **1961**, *83*, 3535-3536; b) L. Garver, V. Grakauskas, K. Baum, *J. Org. Chem.* **1985**, *50*, 1699-1702.

[9] D. Diaz, S. Punna, P. Holzer, A. K. McPherson, K. B. Sharpless, V. V. Fokin, M. G. Finn, *J. Polym. Sci. Pol. Chem.* **2004**, *42*, 4392-4403.

[10] T. R. Chan, R. Hilgraf, K. B. Sharpless, V. V. Fokin, *Org. Lett.* **2004**, *6*, 2853-2855.

[11] A Chafin, D. J. Irvin, M. H. Mason, S. L. Mason, *Tetrahedron Lett.* **2008**, *49*, 3823-3826.

[12] F. H. Allen, O. Kennard, D. G. Watson, L. Brammer, A. G. Orpen, R. Taylor, *J. Chem. Soc., Perkin Trans. 2* **1987**, *12*, S1-S9.

[13] J. Gonzáles, V. M. Perez, D. O. Jiménez, G. Lopez-Valdez, D. Corona, E. Cuevas-Yañez, *Tetrahedron Lett.* **2011**, *52*, 3514-3517.

[14] A. F. Holleman, E. Wiberg, N. Wiberg, *Lehrbuch der anorganischen Chemie*, de Gruyter, New York, **2007**.

[15] a) G. L'abbé, *Chem. Rev.* **1969**, 69, 345-363; b) S. Bräse, C. Gil, K. Knepper, V. Zimmermann, *Angew. Chem. Int. Ed.* **2005**, *44*, 5188-5240.

[16] http://www.bam.de (accessed April, 2016).

[17] R. Meyer, J. Köhler, A. Homburg, *Explosives*, 6. Edition, Wiley-VCH, Weinheim, **2007**.

[18] T. M. Klapötke, M. Stein, J. Stierstorfer, *Z. Anorg. Allg. Chem.* **2008**, *634*, 1711-1723.

[19] M. J. Frisch, et al., *Gaussian 03*, *Revisin B04*, Gaussian, Inc., Wallingford, CT, USA, **2004**.

[20] L. A. Curtiss, K. Raghavachari, P. C. Redfern, J. A. Pople, *J. Chem. Phys.* **1997**, *106*,

1063-1079.

[21] E. F. C. Byrd, B. M. Rice, *J. Phys. Chem. A* **2006**, *110*, 1005–1013.

[22] B. M. Rice, S. V. Pai, J. Hare, *Comb. Flame* **1999**,*118*, 445–458.

[23] T. M. Klapötke, *Chemistry of High-Energy Materials*, 3. Edition, De Gruyter, Berlin, **2015**.

[24] M. S. Westwell, M. S. Searle, D. J. Wales, D. H. Williams, *J. Am. Chem. Soc*., 117, 5013, **1995**.

[25] a) M. Sućeska, Calculation of the detonation properties of C-H-N-O explosives, *Propellants, Explos., Pyrotech.* **1991**, *16*, 197–202; b) Sućeska, M. *EXPLO5 V.6.02*. Zagreb (Croatia), **2013**.

[26] a) T. M. Klapötke, S. M. Sproll, *J. Polym. Sci. Pol. Chem.* **2009**, *48*, 122-127; b) K. Banert, T. M. Klapötke, S. M. Sproll, *Eur. J. Org. Chem.* **2009**, *2*, 275-281; c) S. M. Sproll, *Ph.D. Thesis*, Ludwig-Maximilians-Universität München, **2009**.

[27] A. Dippold, T. M. Klapötke, F. A. Martin, *Z. anorg. Allg. Chem.* **2011**, *637*, 1181-1193.

[28] Q. J. Axthammer, B. Krumm, T. M. Klapötke, *J. Org. Chem.* **2015**, *80*, 6329-6335.

[29] P. Spoerri, A. Erickson, *J. Am. Chem. Soc.* **1938**, *60*, 400–402.

ENERGETIC POLYMERS BASED ON EPOXIDES

5. Energetic Polymers Based on Epoxides

Abstract: This chapter deals with the attempts of developing energetic epoxy resins based on tetrazoles. Hence, several approaches are described for obtaining mono- and difunctional epoxy (bis)tetrazoles. In the course of obtaining suitable starting materials for the reactions towards the respective epoxy tetrazoles, 1,2-bis(tetrazole-5-yl)ethanes containing divinyl and bisallyl groups were synthesized. The compounds could be isolated as 2,2'- and 1,2'-*N*-substituted constitutional isomers and were analyzed using ^{1}H, ^{13}C, 2D NMR and IR spectroscopic measurements, as well as elemental analysis and mass spectrometry. Further investigations concerning their thermal and physical stability revealed that the compounds are insensitive towards impact and friction and stable up to 190 °C (divinyl compounds) and 230 °C (bisallyl compounds). Furthermore their detonation properties were calculated with the EXPLO5 V6.02 software using calculated heats of formation (CBS-4M). Approaches of epoxidating the respective double bonds only gave a monoepoxydated compound in one case, which was identified by NMR and HRMS measurements.

5.1 Introduction

Epoxides represent a broad and versatile compound class in the field of polymer syntheses. On the basis of epoxides, polymers (epoxy resins) can be obtained over different synthetic routes. Compounds with one epoxy group can be polymerized *via* a cationic polymerization, using a Lewis acid/alcohol system as initiator resulting in a glycidyl polymer (**Scheme 5.1**). This route is used, for example, for the synthesis of the energetic polymers GAP or polyGLYN.[1]

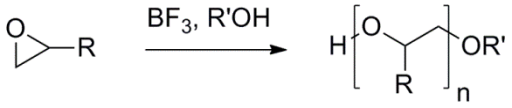

Scheme 5.1 Cationic polymerization towards glycidyl polymers.

Another synthetic route towards epoxy resins is based on, at least, difunctional epoxy compounds, such as bisphenol A epoxy resins, which are obtained in a reaction of bisphenol A diglycidyl ether (**1**, BADGE) and a diol (bisphenol A) (**Scheme 5.2**). Non-energetic binders of that typ are used, for example, in pyrotechnic formulations (Epon 813/Veramides 140 binder system).[2] For that purpose the epoxy prepolymers are additionally cured using multifunctional amines like triethylenetetramine (TETA).

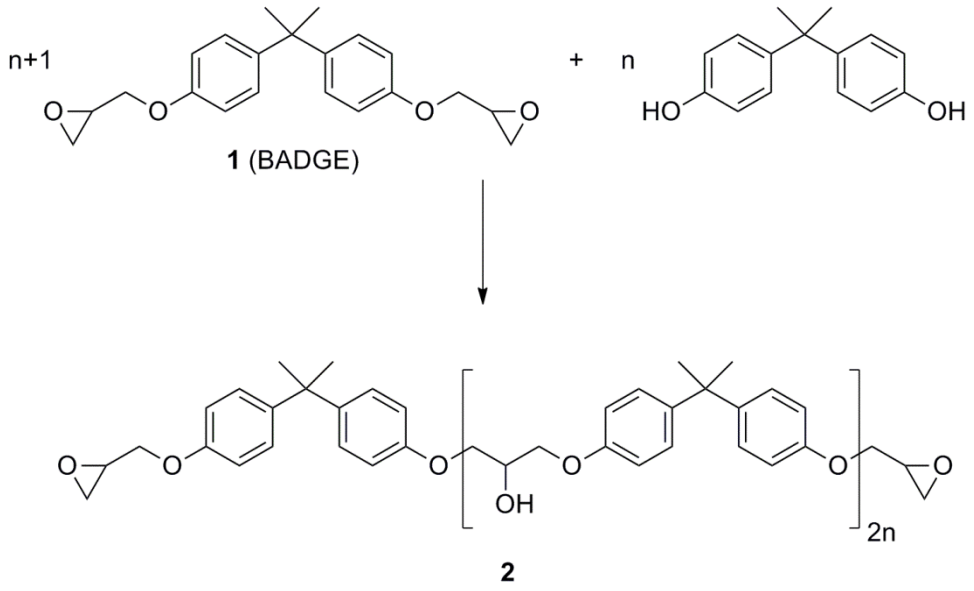

Scheme 5.2 Reaction towards bisphenol A epoxy resin.

There are different ways of preparing epoxides. They either can be synthesized from alkenes using epoxidizing agents (**Scheme 5.3 a**), such as peroxy acids.[3] They also can be obtained after ring opening reactions of alcohols with epichlorohydrin (ECH) in basic milieu, like BADGE (**Scheme 5.3 b**)[4], or in general over other intramolecular nucleophilic substitution reactions with alcohols[5] (**Scheme 5.3 c**).

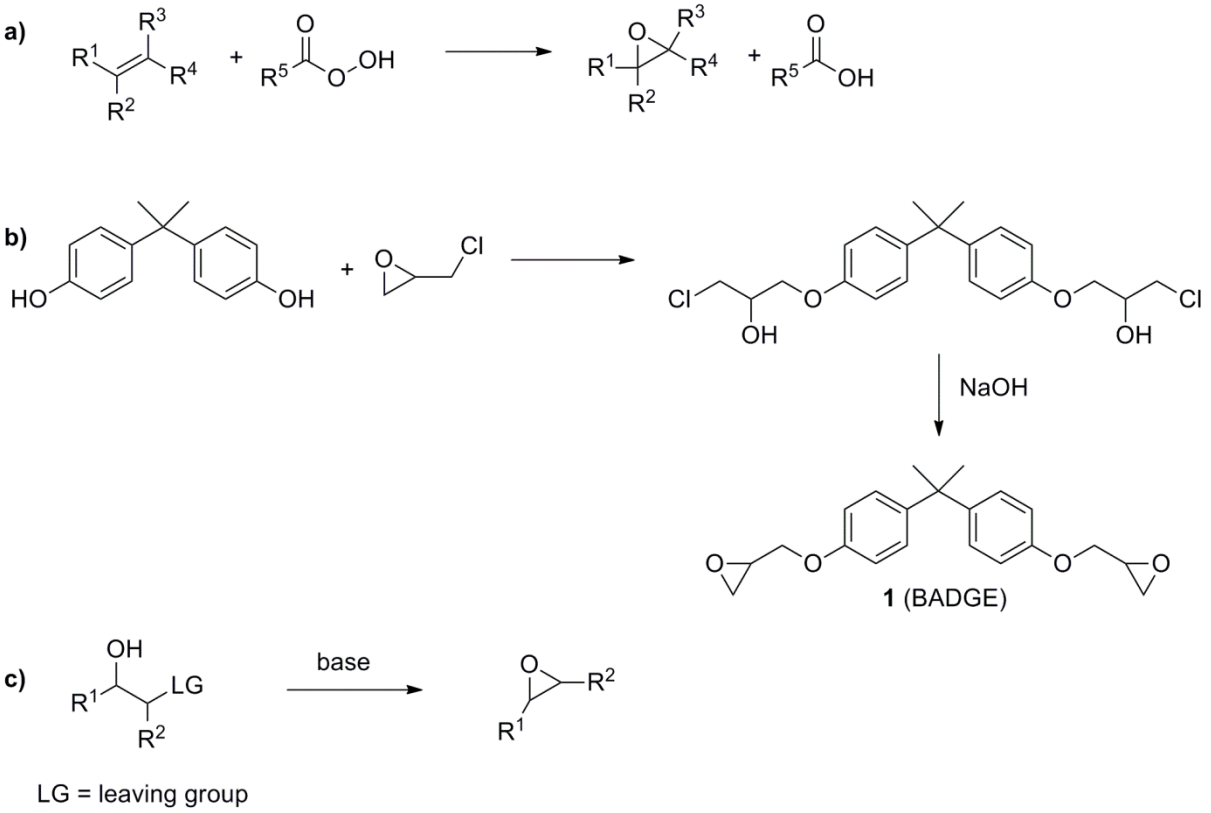

Scheme 5.3 Reactions towards epoxides **a)** over epoxidizing agents, **b)** with alcohols and ECH, **c)** intramolecular substitution reactions.

The goal of the work, described in this chapter was the synthesis of nitrogen-enriched (tetrazole based) epoxy resins for the use as energetic binders. Several attempts were carried out in order to obtain both, mono- and diepoxy tetrazolo compounds for subsequent polymerization steps (see **Scheme 5.1** and **5.2**). The desired target monomers are depicted in **Figure 5.1**.

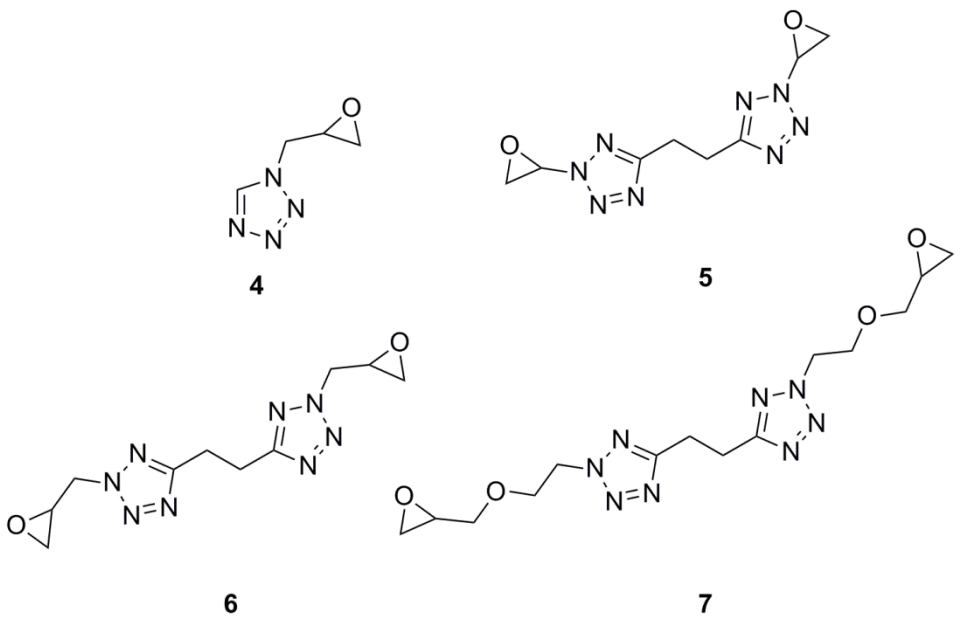

Figure 5.1 Target epoxides for further polymerization reactions towards epoxy resins.

5.2 Monoepoxy Polymers

5.2.1 Syntheses

For the syntheses of the target monoepoxy compound **4** three different precursors were used (**Figure 5.2**).

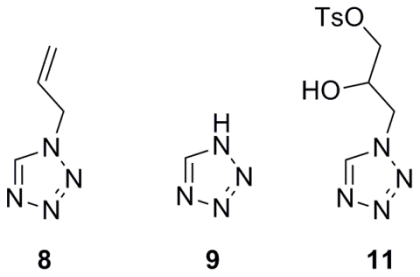

Figure 5.2 Used precursors for the attempted epoxide syntheses of **4**.

Allyltetrazole (**8**) was synthesized according to a literature described procedure and was obtained as a yellow liquid in good yield (82 %).[6] 1*H*-tetrazole (**9**) was obtained from commercial sources.

As new compound, **11** was synthesized in a two-step reaction on the basis of 1*H*-tetrazole (**9**) (**Scheme 5.4**)

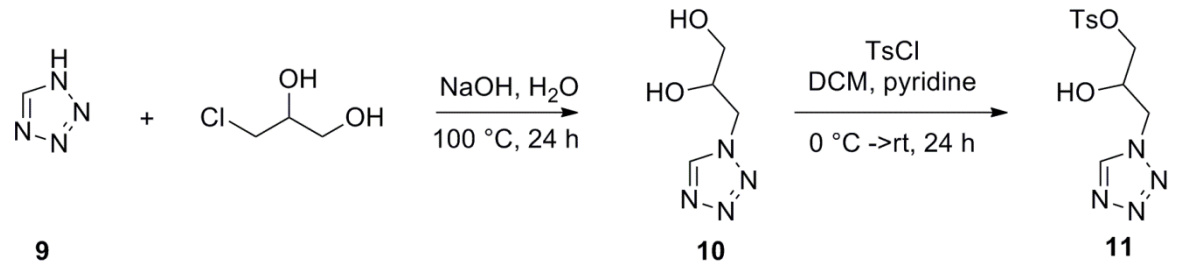

Scheme 5.4 Synthesis of the monotosylated precursor **11** (for **10** and **11** the main isomers are depicted).

3-Tetrazolyl propane-1,2-diol (**10**) was obtained analog to the synthetic procedure described for 2,3-dihydroxypropyl-5-aminotetrazole[7] in a simple substitution reaction of **9** with 3-monochloropropane-1,2-diol (3-MCPD) in very good yield (97 %, including all isomers, which were not separated) as yellowish, viscous oil. It was then treated with tosyl chloride. After purification *via* column chromatography **11** could only be obtained in low yield (31 %, including all isomers, which were not separated), as yellow oil. The small yield can be explained by the high number of possible side reactions.

Starting from **8**, **9** and **11** different synthetic routes towards the desired epoxide 4 were tested (**Scheme 5.5**).

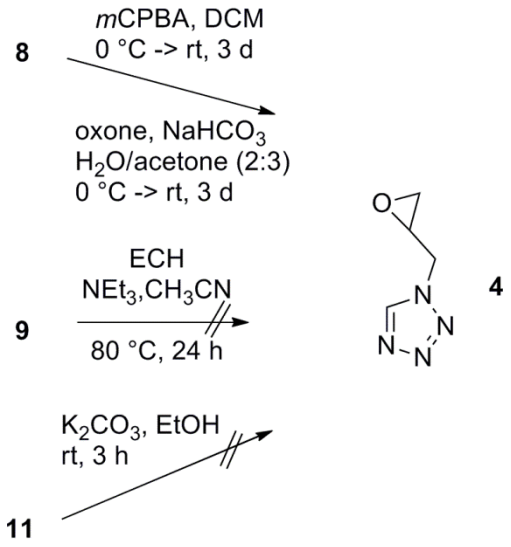

Scheme 5.5 Attempted syntheses towards monoepoxy compound **4**.

Compound **8** was treated with the epoxidizing agents *m*CPBA and the *in situ* formed dimethyldioxirane (DMDO) from acetone and oxone. The reactions were monitored by TLC, but no reaction progress was visible. The mass spectra of aliquots taken from the reaction mixtures confirmed the presence of **4** in the reaction medium of the *m*CPBA approach (calculated $[M+H]^+$: 127.0614, found: 127.0615). However, **4** could not be isolated from the reaction mixture successfully. The reaction approach with DMDO did not give any suitable reaction product, probably because of the low concentration of formed DMDO (around 0.07-0.09 M in the reaction medium)[8].

The reaction of ECH with **9** gave a colorless oil, but neither analytics (MS, NMR) from the crude reaction mixture nor from the obtained oil gave any assignable results. Most likely, a polymeric product was formed during the reaction, which could not be identified.

The attempted cyclization of **11** according to a literature procedure[9] was also not successful, probably because of the low amount of **11** and the broad number of possible side products, the desired product could not be isolated.

5.2.2 Characterizations

Compound **8** was analyzed using NMR, IR and elemental analysis, giving results which were consistent with literature values. [6] Compounds **10** and **11** were mainly characterized by mass spectrometry, IR spectroscopy and elemental analysis, since the resulting products consisted of different constitutional isomers, which complicated the assignment of the obtained values in the NMR spectra.

The successful formation of the target diol **10** was proven by high resolution mass spectrometry (calculated for $[M+H]^+$: 145.0720, found: 145.0721). Elemental analysis was not possible because of the highly viscous consistency of **10**, which hindered the complete removal of water and ethanol. The IR spectrum of **10** showed the broad band of the OH groups around 3300 cm^{-1} in medium intensities. A comparison with the IR spectrum of **11** shows a decreasing intensity of the OH valance vibration and an appearance of signals at 3140 cm^{-1} (valance vibration of Ar−H) and 1355 and 1170 cm^{-1} (sulfonate vibrations), which proved the presence of the tosylate group.[10] Additional mass spectrometry and elemental analysis confirmed the successful synthesis of **11**.

Due to its twofold alcohol function, **10** might be an interesting compound as crosslinking agent or initiator for cationic polymerizations (see **Scheme 5.1**) in the field of energetic binders and formulations.

5.3 Diepoxy Polymers

5.3.1 Syntheses

For the different attempted reactions towards the desired difunctional epoxy tetrazoles **5-7** several starting materials were synthesized (**Figure 5.3**).

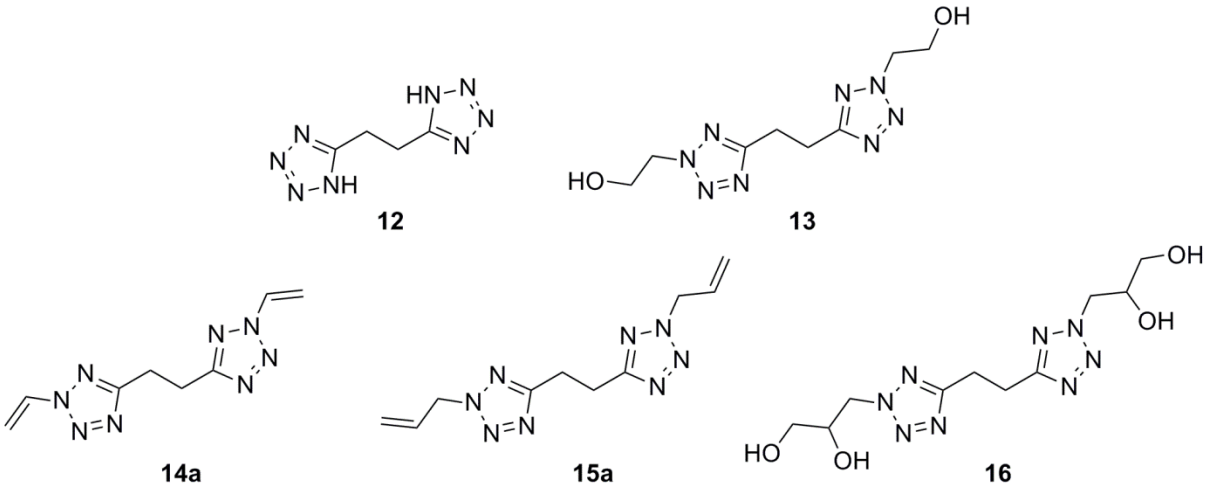

Figure 5.3 Synthesized starting materials for the syntheses of the difunctional epoxy bistetrazoles **5-7** (the main isomers are depicted).

Compounds 1,2-bis(tetrazol-5-yl)ethane (**12**, BTE) and 1,2-bis(hydroxyethyl tetrazol-5-yl)ethane (**13**, BTEOH) were synthesized in close accordance to literature procedures.[11 12] 1,2-Bis(2-vinyl-2*H*-tetrazol-5-yl)ethane (**14a**, 2,2-DvBTE) was prepared in a substitution/elimination reaction using **12** and 1,2-dibromoethane in analogy to described procedures for related divinyl bistetrazoles (**Scheme 5.6**).[13]

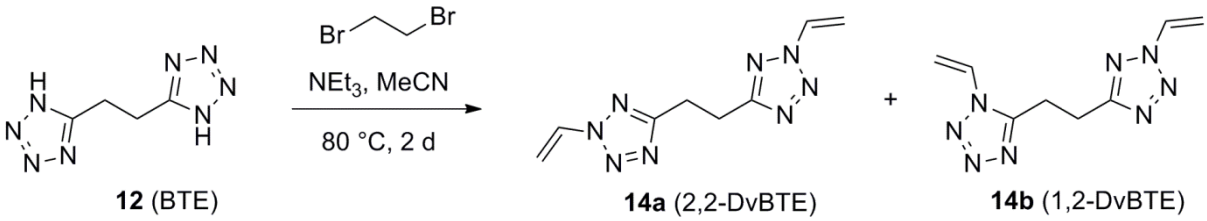

Scheme 5.6 Synthesis of the divinyl derivatives (**14a** and **b**) of BTE.

After the purification *via* column chromatography compound **14a** was obtained as colorless

solid in 31 % yield, which could be recrystallized in an *n*-hexane/EtOAc mixture. As second product the constitutional isomer 1-vinyl-5-(2-(2-vinyl-2*H*-tetrazol-5-yl)ethyl)-1*H*-tetrazole (**14b**, 1,2-DvBTE) could also be purified as colorless solid in low yield (18 %).

The bisallyl derivatives of BTE were obtained in a substitution reaction using allylbromide (**Scheme 5.7**).

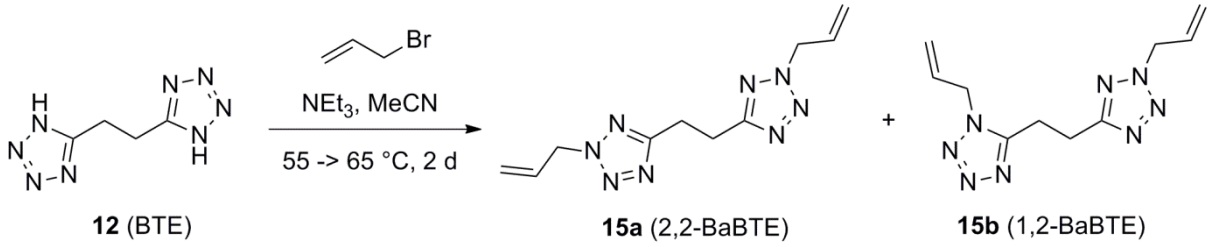

Scheme 5.7 Synthesis of the bisallyl derivatives (**15a** and **b**) of BTE.

After the purification *via* column chromatography, compounds **15a** (1,2-bis(2-allyl-2H-tetrazol-5-yl)ethane, 2,2-BaBTE) and **15b** (1-allyl-5-(2-(2-allyl-2*H*-tetrazol-5-yl)ethyl)-1*H*-tetrazole, 1,2-BaBTE) were obtained as colorless liquids in low yields with 28 and 15 %, respectively.

Compound **16** was obtained as highly viscous oil in a similar reaction step like for **10** (see **Scheme 5.4**) in good yield (92 %, including all isomers, which were not separated). With this compound the transformation to the corresponding ditosylated compound for a twofold intramolecular ring closure was also attempted, but gave no product after the purification step. In order to obtain the difunctional epoxy BTE derivatives **5-7** several reaction conditions and paths were tested. A summary of the attempted reaction routes is given in **Scheme 5.8**.

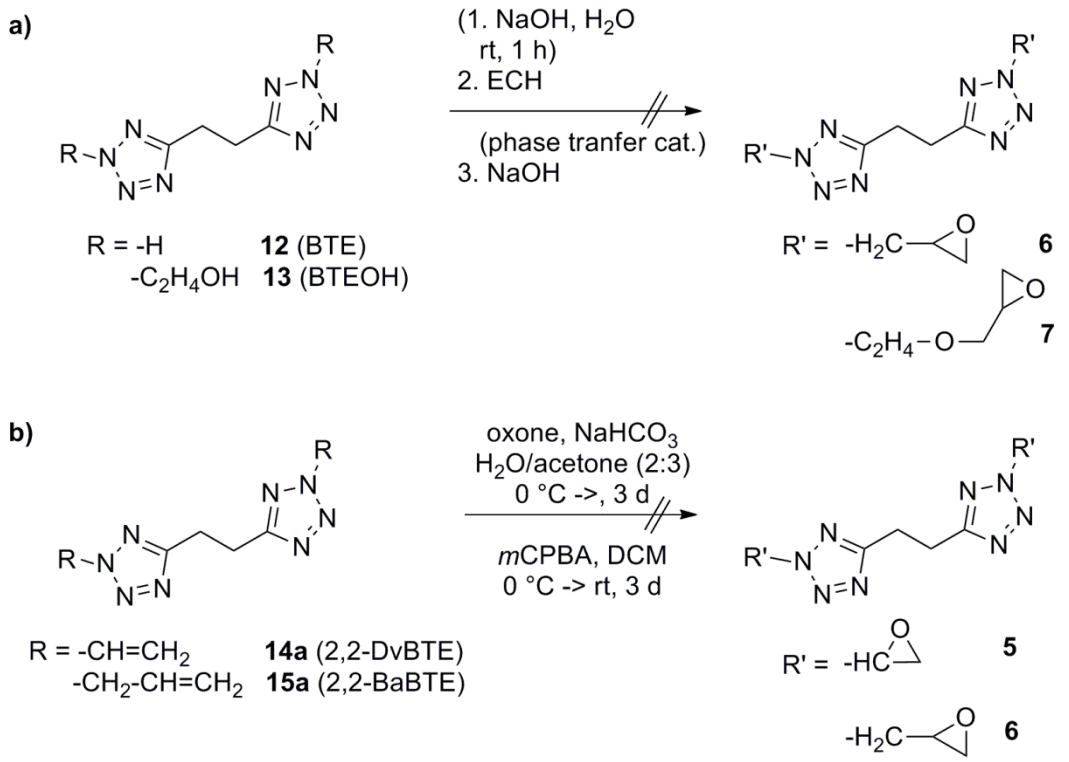

Scheme 5.8 Attempted syntheses of the diepoxidated compounds **5-7** using **a)** epichlorohydrin in various setups and **b)** two different epoxidizing agents (*m*CPBA and DMDO).

Although the various attempts with ECH and **12** or **13** (with varying basic conditions, and used phase transition catalyst) showed reaction progress by color changes of the reaction medium or precipitates after work up, the resulting analytical values (EA, MS, NMR) could not be assigned to any possible reaction product. Most likely, polymeric products were formed, which were not further investigated, tough.

The reactions of **14a** and **15a** with the epoxidizing agents *m*CPBA and DMDO did not yield the difunctionalized epoxy compounds **5** and **6**, but only gave starting material (**14a**) or the monoepoxidated compound **17** as yellowish liquid in moderate yield (62 %) (**Figure 5.4**).

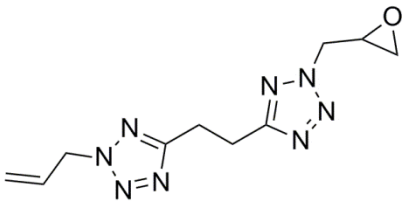

17

Figure 5.4 Obtained monoepoxy compound 2-glycidyl-5-(2-(2-allyl-2*H*-tetrazol-5-yl)ethyl)-2*H*-tetrazole (**17**).

5.3.2 Characterization

The synthesized compounds were characterized using elemental analysis, mass spectrometry, as well as ^{1}H, ^{13}C NMR and IR spectroscopy. The crystal structure of **14a** was obtained using single crystal X-ray diffraction.

BTE (**12**) and BTEOH (**13**) gave consistent results with the literature values.[11 12] Compound **16** was characterized using mainly IR and mass spectrometry.

Because of its fourfold alcohol function **16** might represent an interesting compound as crosslinking agent or initiator for cationic polymerizations (see **Scheme 5.1**) in the field of energetic binders and formulations.

5.3.2.1 Spectroscopic Analyses

As solvent for the NMR measurements DMSO-d_6 was used. For a clear assignment of the exact positions of the carbon and hydrogen atoms in 2,2-BaBTE (**15a**) and 1,2-BaBTE (**15b**) 2D NMR measurements were carried out. The obtained spectra of the HMQC and HMBC 2D NMR measurements are depicted in **Figure 5.8** and **5.9**.

Both isomers can be distinguished sheer alone because of their signal patterns in the 1D ^{1}H and ^{13}C NMR spectra (**Figure 5.5** and **5.6**). In the ^{1}H NMR spectrum of **15a** five different, partly overlapping signals can be observed: at 6.04 ppm (CH of the allyl group), 5.29 ppm (CH_{cis} of the terminal CH_2 of the allyl group), 5.28 ppm (aliphatic CH_2 of the allyl group), 5.20 ppm (CH_{trans} of the terminal CH_2 of the allyl group) and 3.33 ppm (CH_2) in a 2:6:2:4

ratio. The signals show different coupling patterns due to their different interactions with the surrounding hydrogen atoms. The CH of the allyl group appears as a doublet of doublet of triplets analog to its $^{3}J_{HH}$ couplings to the CH_{trans} and CH_{cis} of the terminal CH_2 and to the aliphatic CH_2. The geminal hydrogen atoms of the terminal CH_2 group show also a doublet of doublet of triplets splitting, representing the respective $^{3}J_{HH}$, $^{4}J_{HH}$ (to the aliphatic CH_2) and the $^{2}J_{HH}$ coupling. Both geminal hydrogen atoms can be distinguished because of their differing $^{3}J_{HH}$ coupling constants (17.2 Hz (H_{trans}) and 10.1 Hz (H_{cis})). The aliphatic CH_2 group of the allyl group splits into a doublet of doublet of doublets representing the respective couplings to the CH and the terminal CH_2 hydrogen atoms.

The ^{1}H NMR spectrum of **15b** shows ten different overlapping signals (**Figure 5.5**) with a 2:5:3:4 ratio. The signal at 3.39 ppm represents the two different CH_2 groups attached to the respective C_q of the tetrazole rings and shows a A_2B_2 spin system of higher order. The signal is also overlapped by the signal of residual water, which explains the higher integral value.

A comparison of the ^{13}C NMR spectra of **15a** and **b** (**Figure 5.6**) proves the existence of two different isomers, too. Whereas the spectrum of **15a** shows only five different signals (as indicator for symmetrically substituted tetrazole rings), **15b** must be the asymmetric 1,2'-*N*-substituted isomer, because of its ten different signals.

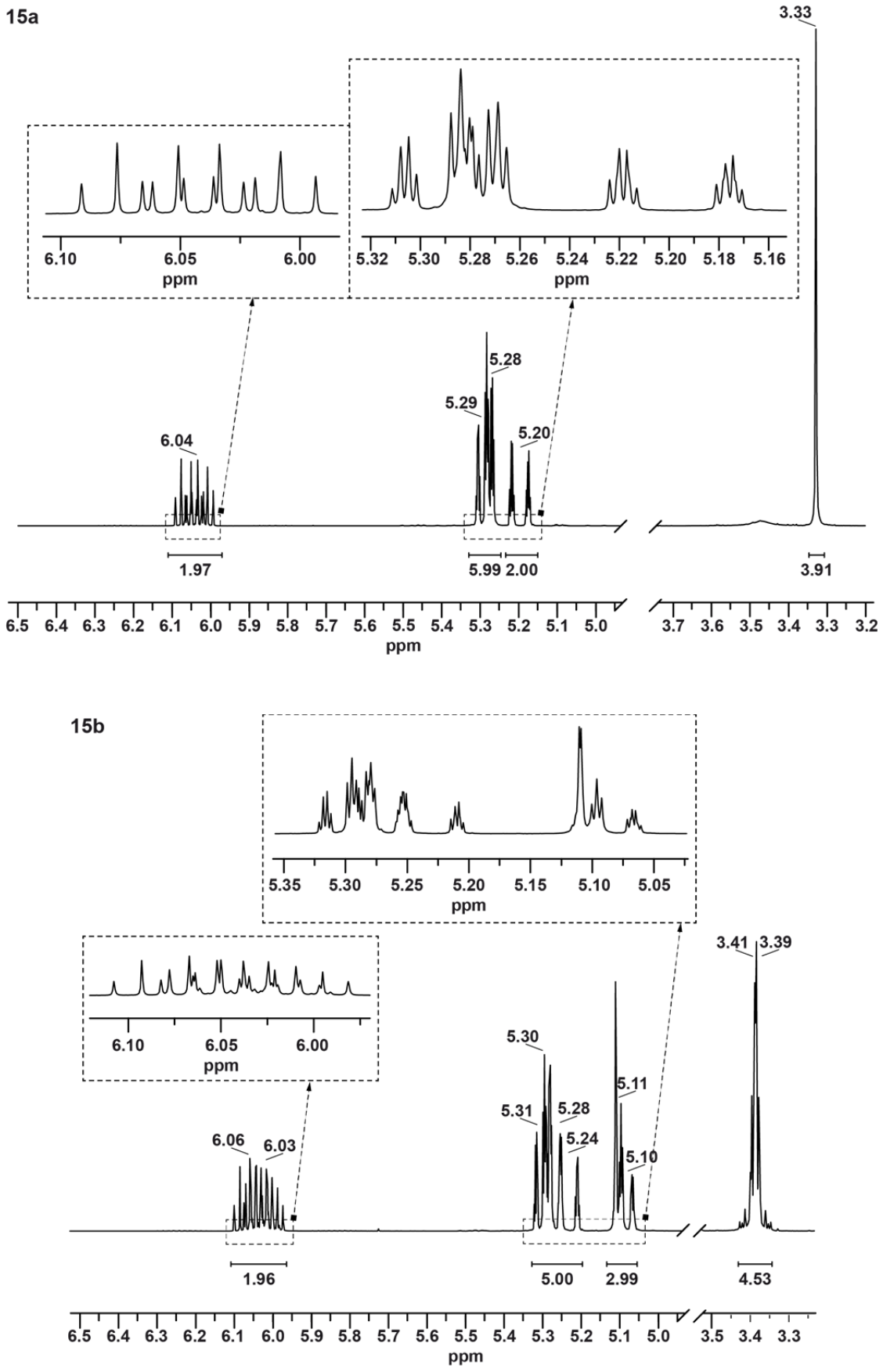

Figure 5.5 ^{1}H NMR spectra of **15a** and **15b**.

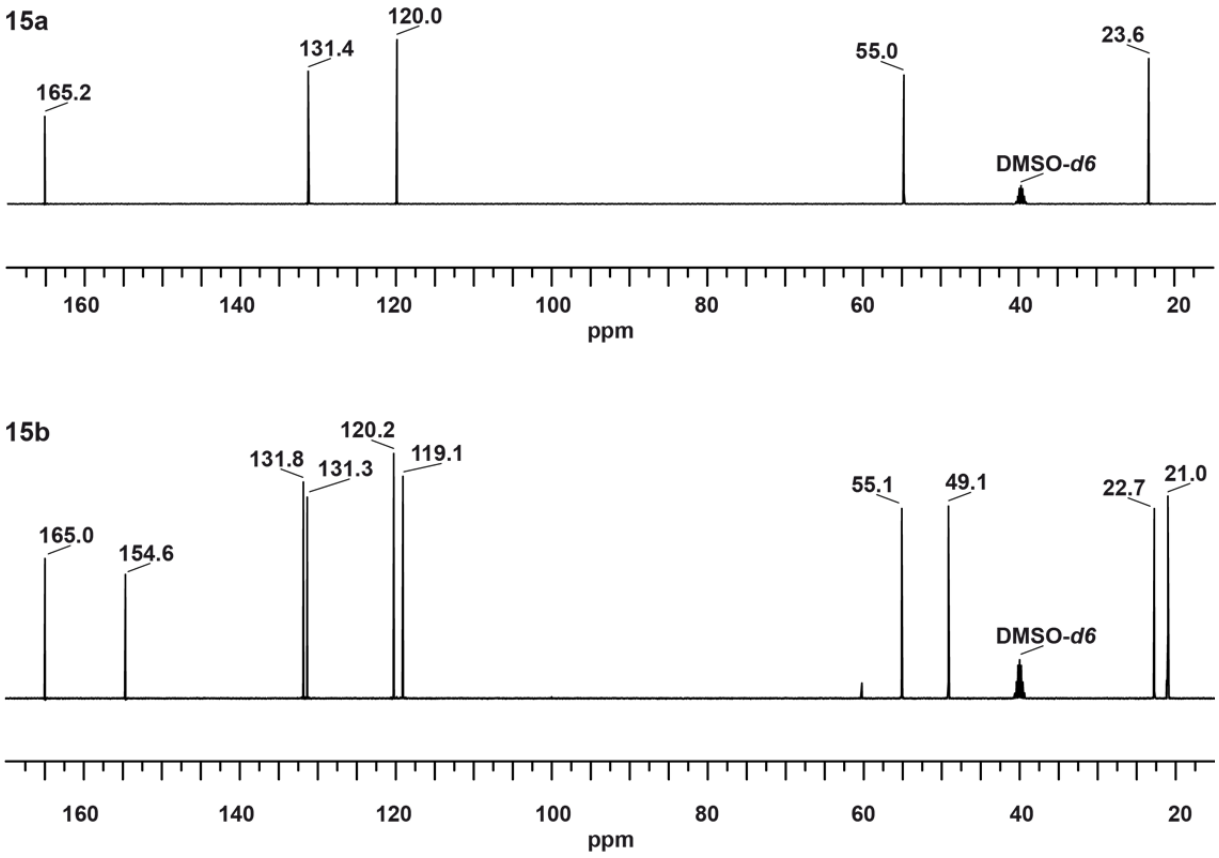

Figure 5.6 ^{13}C NMR spectra of **15a** and **15b**.

In order to determine, which kind of symmetrically *N*-substituted isomer was formed as **15a** (1,1'- or 2,2'-), along with the general assignment of the proton and carbon positions in **15a** and **15b** the HMQC and HMBC 2D NMR measurements were the methods of choice.

Here, the 1- or the 2-*N*-substituted position can be distinguished by the occurring $^{3}J_{CH}$ long-range heteronuclear carbon-proton coupling between the quaternary carbon in the tetrazole ring and the protons of the aliphatic CH_2 allyl group attached to the N1 atom of the tetrazole ring (**Figure 5.7**).

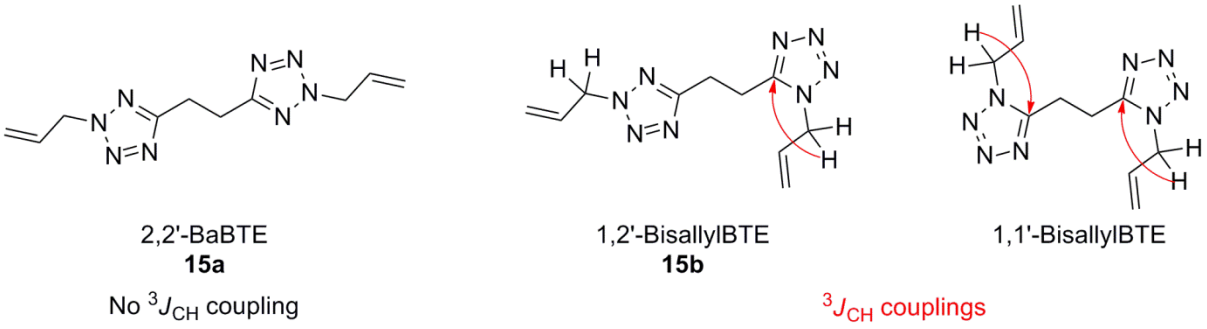

Figure 5.7 $^3J_{CH}$ couplings for the differentiation between the 2- and 1-*N*-substituted allyl positions.

The HMBC experiments (**Figure 5.8**) verified the 2,2'-*N*-substitution pattern for **15a**, since no $^3J_{CH}$ coupling between the H4 hydrogens and the C1 carbon atoms are visible in the 2D NMR spectrum. However, the 2D HMBC spectrum of **15b** shows the presence of the $^3J_{CH}$ coupling between C2 and H8 (illustrated by the red dashed circle), which confirms the asymmetric 1,2'-*N*-substituted structure.

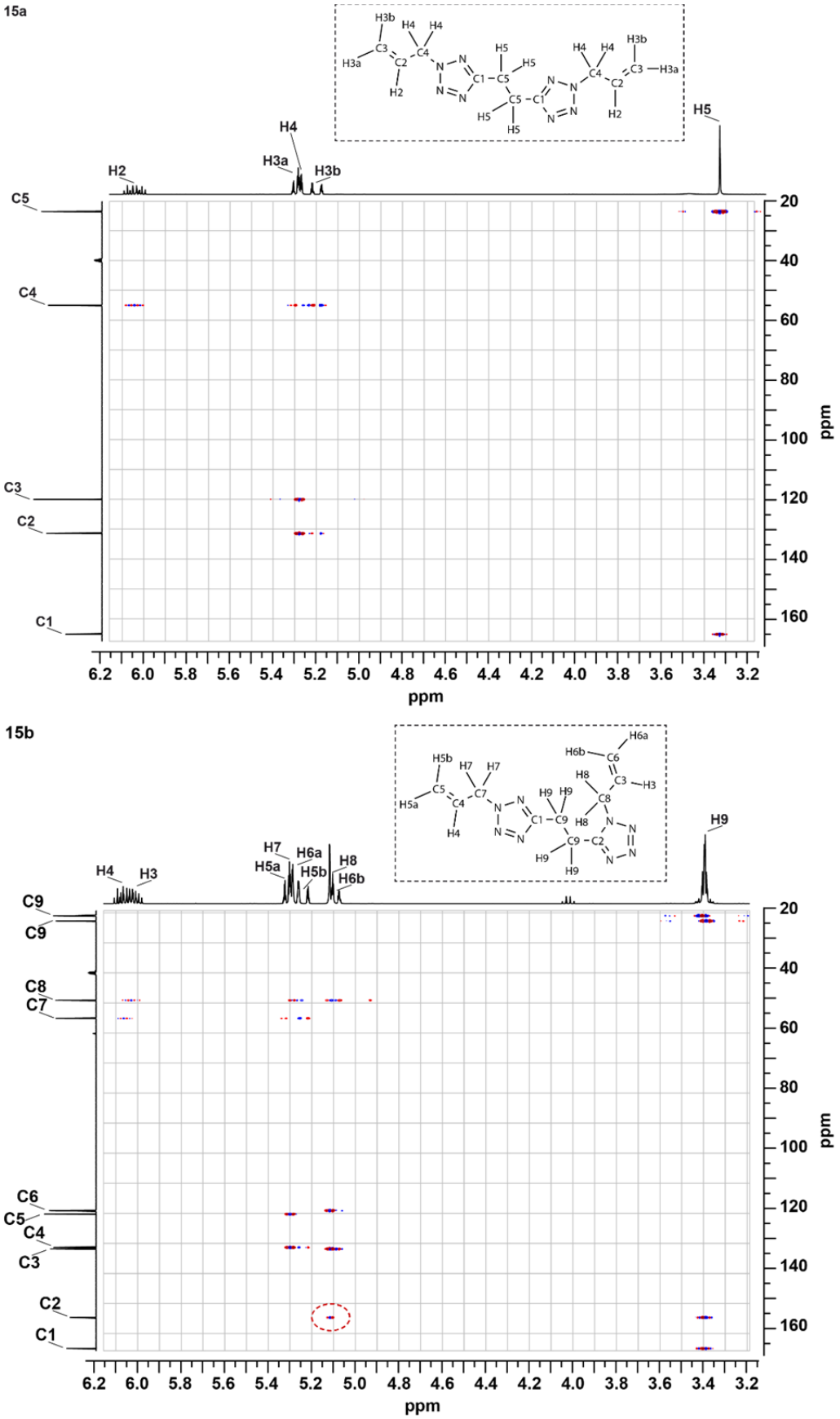

Figure 5.8 HMBC 2D NMR spectra of **15**a and **15b**. (Red dashed circle shows the occurring $^{3}J_{CH}$ coupling for the 1-*N*-substituted isomer).

For the assignment of the remaining carbon and hydrogen positions in **15a** and **15b** the HMQC measurements were beneficial (**Figure 5.9**). The resulting spectra enabled the allocation of the carbon atoms signals C3 and C4 of **15b** to the overlapping signals of their corresponding protons H3 and H4 (see enlargement). Even though C3 and C4 are in close proximity to one another (131.8 and 131.3 ppm).

A precise distinction between the two different C9 carbon atoms and their corresponding H9 protons of **15b** was not possible, tough.

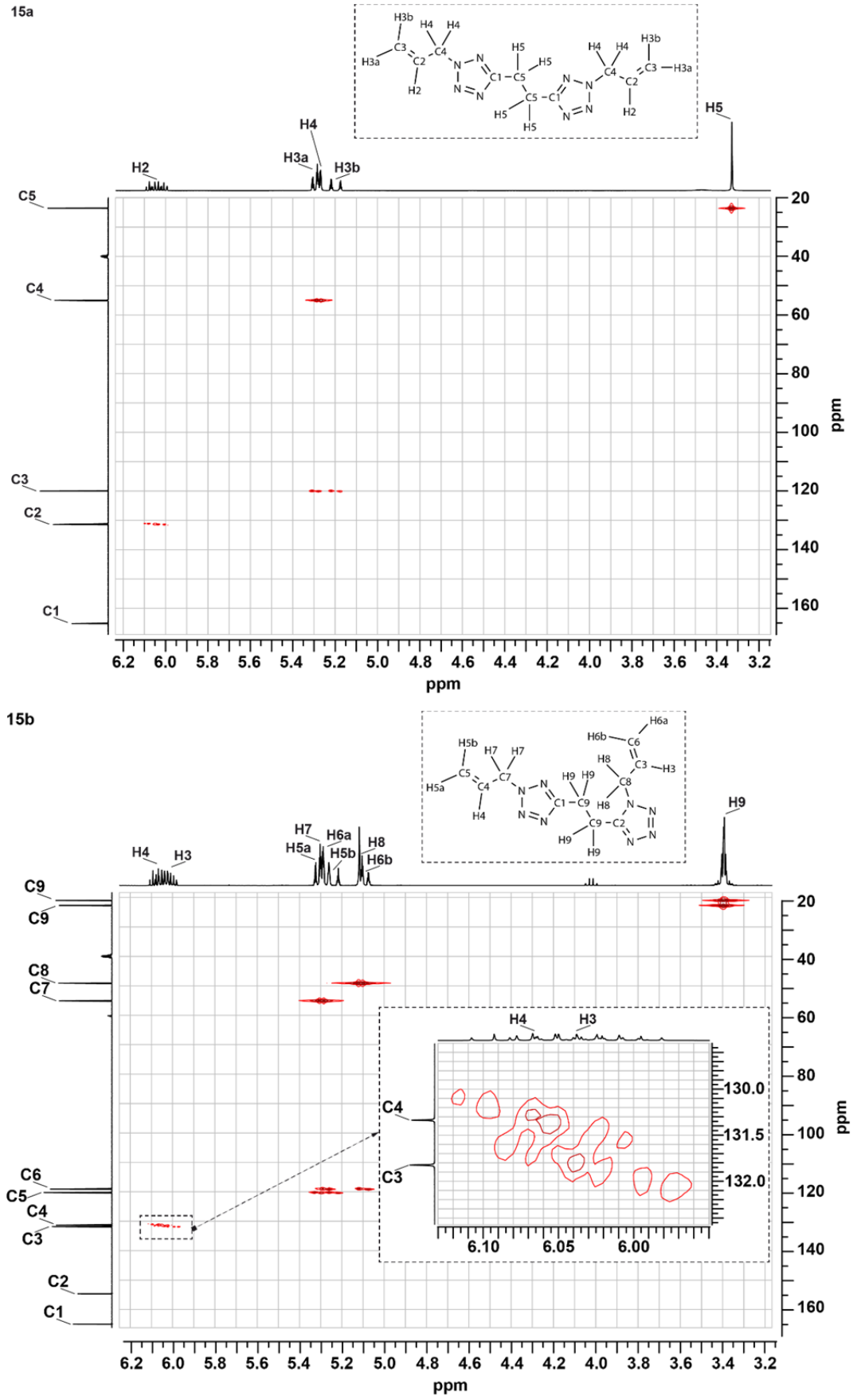

Figure 5.9 HMQC 2D NMR spectra of **15**a and **15b**.

The measured ^{1}H spectrum of **14a** shows four different signals with a 2:2:2:4 ratio (**Figure 5.10**). At 7.79 ppm the CH of the vinyl group is visible as a doublet of doublets, representing the interactions with the geminal hydrogen atoms of the terminal vinyl-CH_2. These two geminal hydrogen atoms of the vinyl group show also doublets of doublets, as coupling patterns. The signal at 6.06 ppm can be assigned to the H_{trans} of the terminal vinyl-CH_2, because of its bigger $^{3}J_{HH}$ coupling constant (15.5 Hz) compared to the $^{3}J_{HH}$ coupling value (8.7 Hz) of the H_{cis} at 5.47 ppm. The protons of the aliphatic CH_2 group occur at 3.41. Similar to the results of the **15b** measurement, the ^{1}H NMR spectrum of **14b** shows eight different, partly overlapping signals with a ratio of 1:1:1:1:2:4, representing the asymmetric 1,2'-*N*-substituted divinyl compound. The new signals of the CH and the CH_{trans} protons of the 1-*N*-substituted vinyl group can clearly be assigned with 7.47 ppm and 5.97 ppm, whereas the signals of the two CH_{cis} protons are overlapping and cannot be allocated properly. The signal around 3.47 ppm represents the two different CH_2 groups attached to the respective C_q of the tetrazole rings and shows a A_2B_2 spin system of higher order.

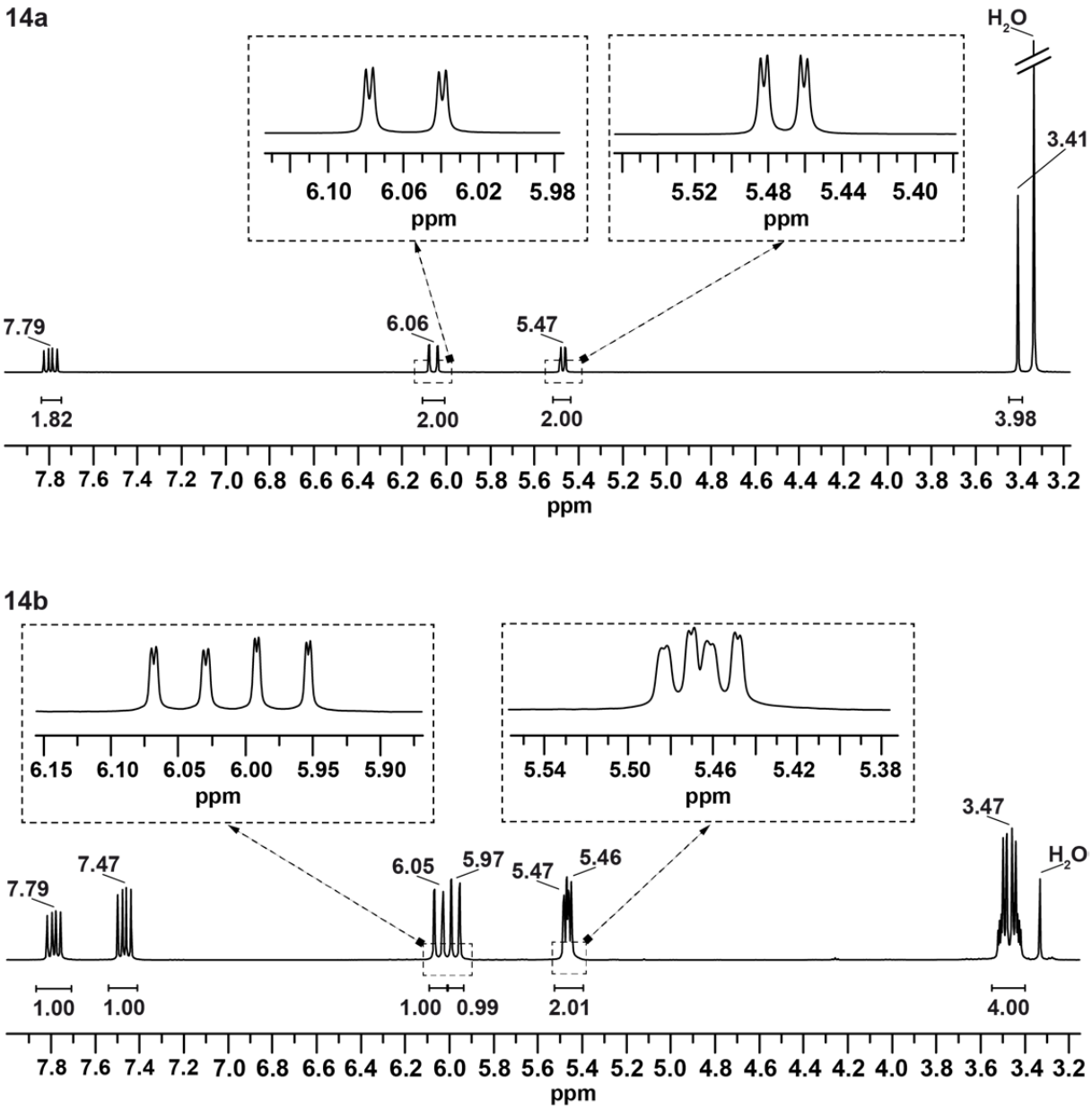

Figure 5.10 ^{1}H NMR spectra **14a** and **14b**.

The obtained results of the 2D NMR measurements of **15a** and **15b** can be applied to the 1D NMR measurements of **14a** and **14b**.

Here again, the comparison of the ^{13}C NMR spectra of **14a** and **b** (**Figure 5.11**) also proves the existence of two different isomers. Whereas the spectrum of **14a** shows only four different signals (as indicator for symmetrically substituted tetrazole rings), **14b** must be the asymmetric 1,2'-*N*-substituted isomer, because of its eight different signals. In analogy to the bisallyl compounds **15a** and **b**, **14a** and **b** show signals at 164.9 ppm ($C_{q,tetrazole}$), 130.1 ppm (CH vinyl), 109.0 ppm (CH_2 vinyl) and around 22.9 ppm (aliphatic CH_2), which represent the

2-*N*-substituted fragment. The additional signals in the ^{13}C NMR spectrum of **14b** at 153.3, 126.5, 109.9 and 20.5 ppm can be assigned in an analogous manner to the 1-*N*-substituted isomer.

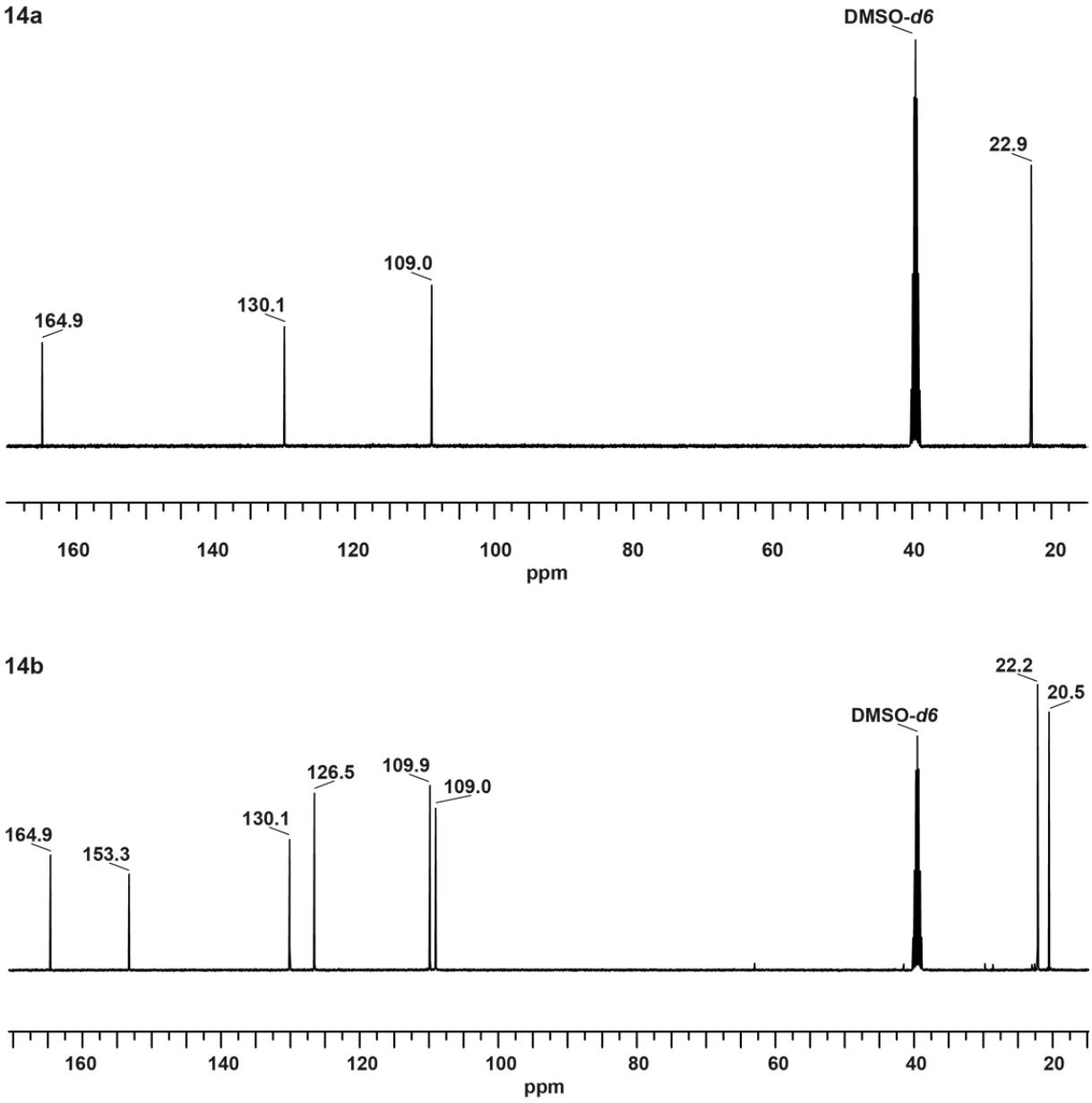

Figure 5.11 ^{13}C NMR spectra **14a** and **14b**.

The obtained ^{1}H (**Figure 5.12**) and ^{13}C NMR (**Figure 5.13**) spectra of compound **17** prove the formation of the monoepoxidated 2,2-BaBTE (**15a**), since the spectra clearly show the signals for the 2-*N*-substituted allyl group with all its coupling patterns and ratios, but also additional signals, which are not consistent with the values for the 1-*N*-substituted fragment.

The extra signals in the ^{1}H NMR spectrum of **17** are referring to the glycidyl group. The signals at 5.03 ppm and 4.62 ppm represent the diastereotopic protons of the CH_2 group attached to the oxirane ring, showing doublets of doublets with a $^{3}J_{HH}$ (3.1 Hz and 6.8 Hz) coupling to the proton of the CH group of the oxirane ring and a $^{2}J_{HH}$ geminal (14.6 Hz) coupling. At 3.44 ppm a dddd is visible, which can be assigned to the proton of the CH group in the oxirane ring, coupling with each of the surrounding diastereotopic protons of the CH_2 groups. The diastereotopic protons of the CH_2 oxirane group occur at 2.86 ppm and 2.67 ppm showing again doublet of doublets with coupling constants of $^{3}J_{HH}$ = 4.2 and 2.5 Hz and $^{2}J_{HH}$ = 5.0 Hz.

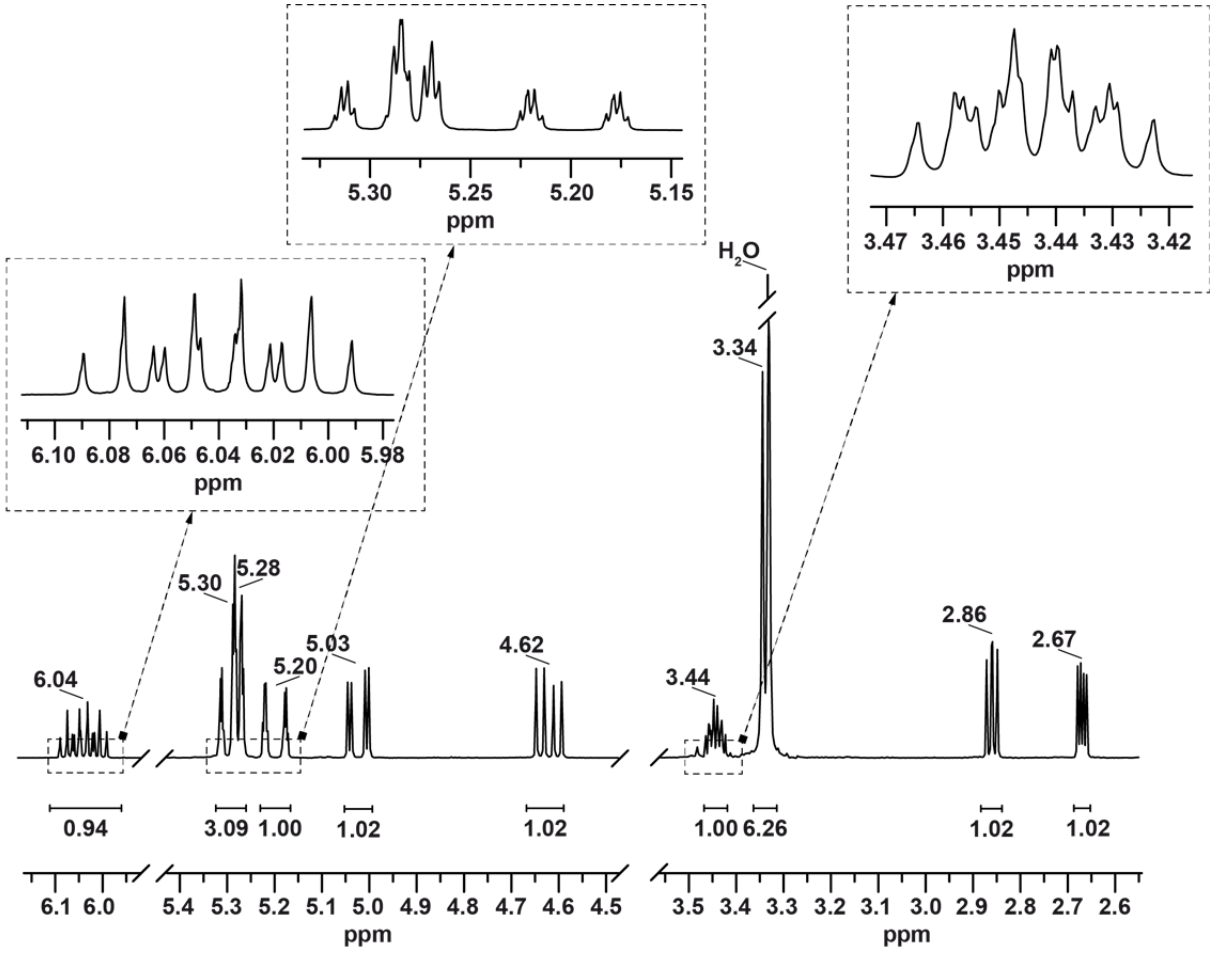

Figure 5.12 ^{1}H NMR spectrum of **17**.

In the ^{13}C NMR spectrum, only a closer look reveals the ten different carbon signals. The signals representing the respective C_q, CH_2-N and CH_2-C_q carbon atoms occur at very similar values with 164.9 vs. 164.8 ppm, 54.6 ppm vs. 54.5 ppm and 23.10 vs. 23.09 ppm (**Figure 5.13**). Besides this, the obvious two new signals (compared to **15a**) at 49.1 (CH) and

44.9 ppm (CH_2) can be assigned to the carbon atoms of the oxirane ring.

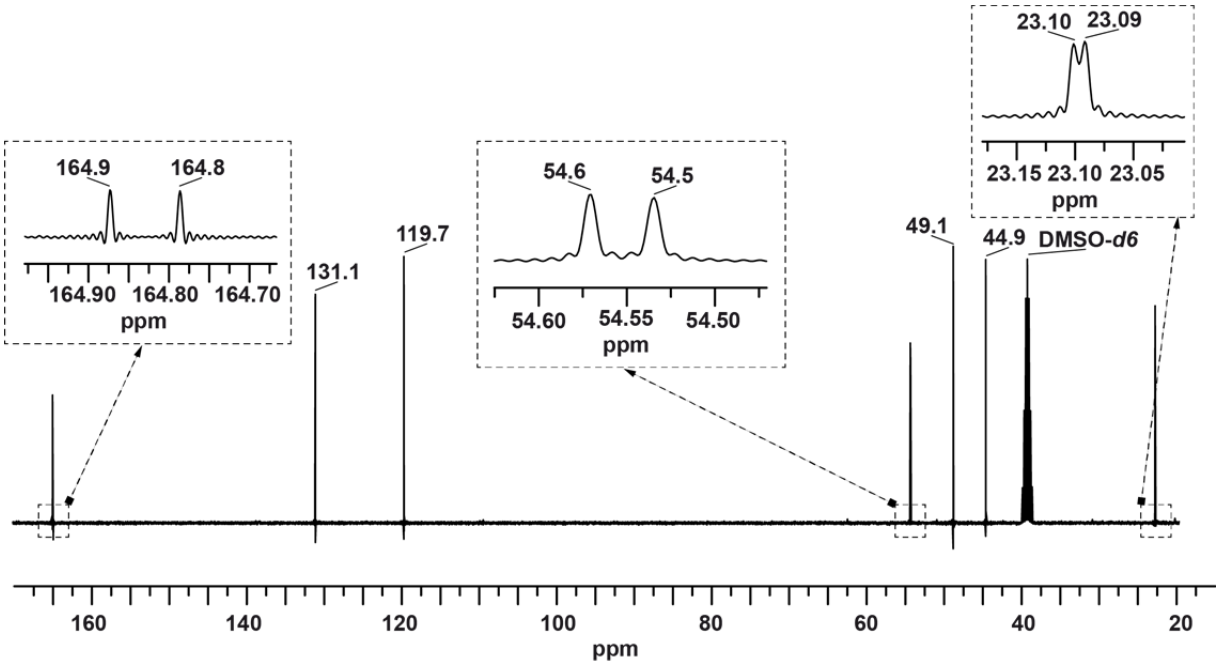

Figure 5.13 ^{13}C NMR spectrum of **17**.

5.3.2.2 Crystal Structure

The crystal structure of **14a** was obtained using single crystal X-ray structure analysis. Single crystals suitable for X-ray diffraction were obtained by recrystallization of the product from an *n*-hexane/ethyl acetate mixture. Compound **14a** crystallizes in the monoclinic space group $P2_1/c$ with two formulas per unit cell. Calculated density for T = 173 K is 1.414 g cm^{-3}. The bond lengths and angles within the crystal structure of **14a** are consistent with comparable values in literature.[14 15] The formula unit of 2,2-DvBTE (**14a**) is shown in **Figure 5.14** along with selected bond lengths, angles and torsion angles. The molecular structure itself shows a slightly twisted assembly with a torsion angle of 110.8° for the C1^{i}-C1-C2-N2 fragment. The vinyl group is nearly in one plane with the tetrazole ring with a torsion angle of the vinyl group towards the tetrazole ring of 4.0°.

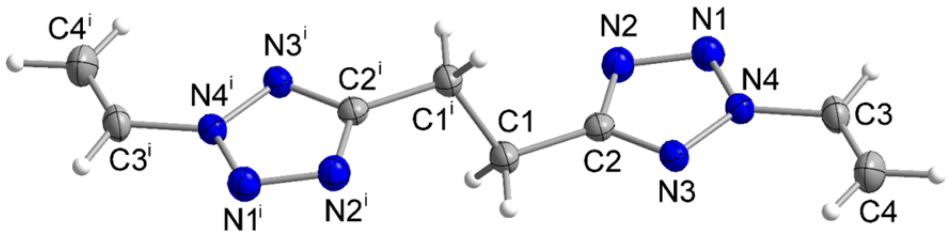

Figure 5.14 Crystal structure of 2,2-DvBTE (**14a**). Thermal ellipsoids are set to 50 % probability. Symmetry operator: (i) −x, 2−y, −z. Selected bond distanced (Å): N1-N2 1.316(1), N1-N4 1.327(1), N2-C2 1.353(1), N3-C2 1.327(1), N3-N4 1.336(1), N4-C3 1.419(1), C1-C2 1.487(2), C3-C4 1.304(2); selected bond angles (°): $C1^{i}$-C1-C2 112.1(1), C4-C3-N4 123.0(1), C4-C3-H3 124.8(1), N4-C3-H3 112.2(1); selected torsion angles (°): $C1^{i}$-C1-C2-N2 110.8, $C1^{i}$-C1-C2-N3 −67.6(1), C4-C3-N4-N1 −175.3(1), C4-C3-N4-N3 4.0(2), H3-C3-N4-N1 5.2(1), H3-C3-N4-N3 −175.6(1).

Due to the lack of suitable donors no hydrogen bonds are observed in the crystal system to stabilize the supramolecular structure. As shown in **Figure 5.15**, the crystal structure of **14a** consists of stacked alternately oriented molecules which form infinite zig-zag rows along the *a*-axis. The layers are stacked above each other.

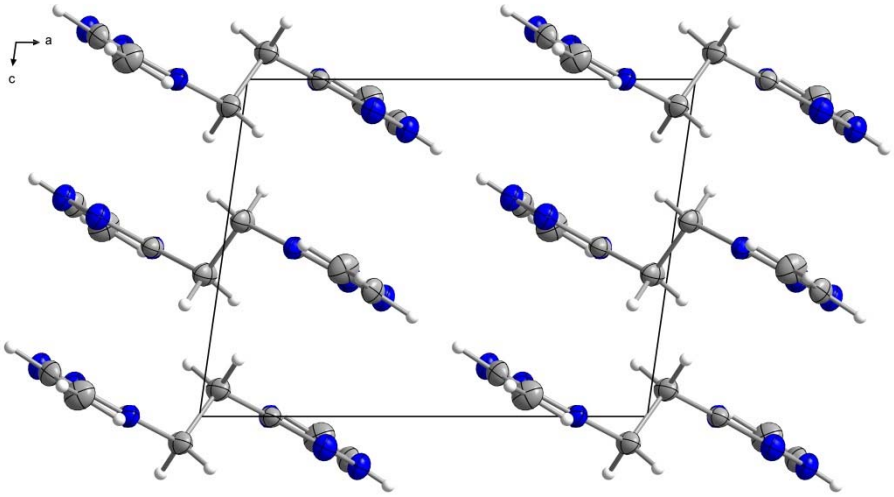

Fgure 5.15 Crystal structure of **14a**. Thermal ellipsoids are set to 50 % probability. View along the *b*-axis.

5.3.2.3 Thermal Stability

The behavior at high temperatures of compounds **14-15** was determined *via* differential scanning calorimetry with a heating rate of 5 °C min^{-1}. The obtained plots are depicted in **Figure 5.16**.

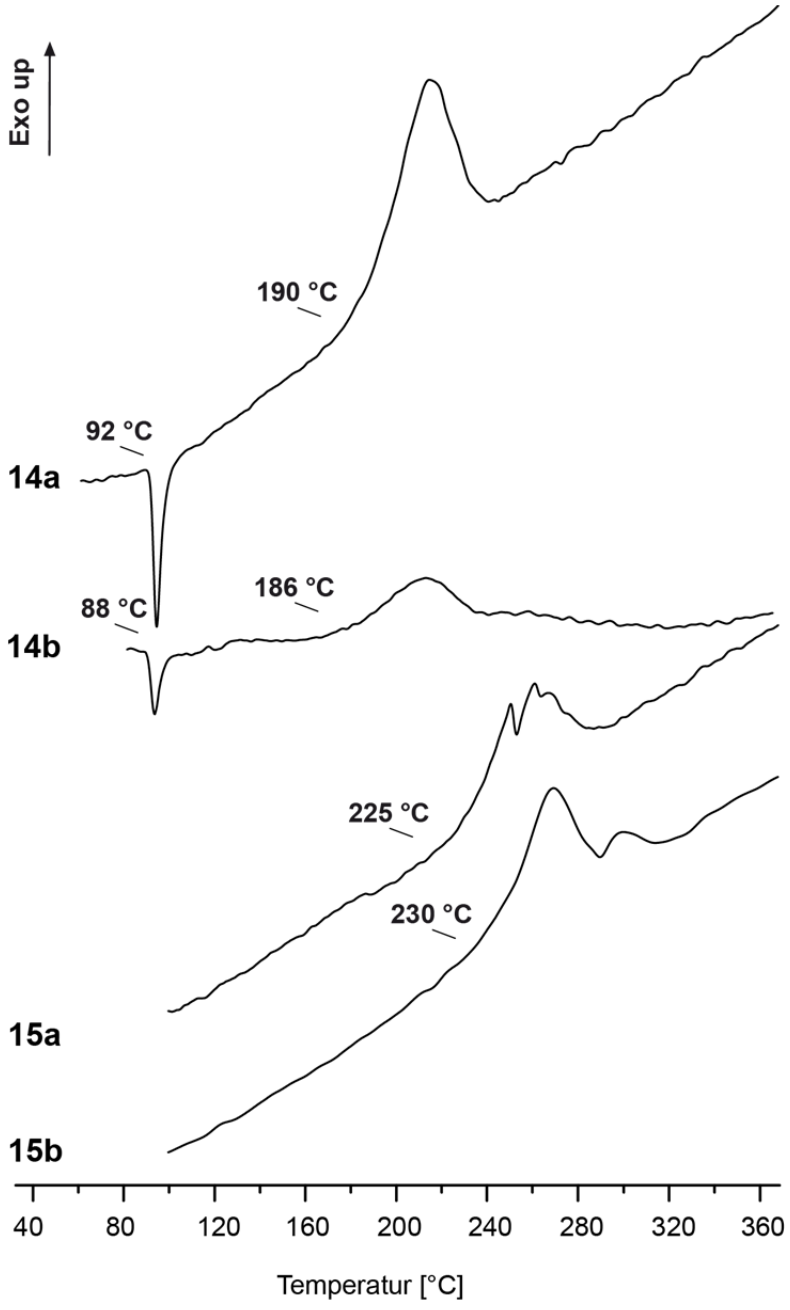

Figure 5.16 DSC plots of decomposition temperatures of **14-15**.

The compounds harboring the same functional groups show similar melting and decomposition temperatures. The vinyl based compounds **14a** and **14b** show melting points around 90 °C and decomposition temperatures around 190 °C. Whereas the liquid allyl based compounds are stable up to higher temperatures with T_{dec} around 230 °C.

5.3.3 Energetic Data

For the determination of inherent energetic potential, sensitivities and energetic properties of **14-15** were investigated. The impact and friction sensitivities of **14-15** were explored by BAM methods.[16] All compounds were tested as insensitive towards impact (>40 J) and friction (>360 N).

For calculating the energetic properties of compounds **14-15** quantum chemical calculations had to be run. Initial structure optimizations were performed for **14b**, **15a** and **b** at the B3LYP/cc-pVDZ level of theory using the Gaussian 09 revision A.02 program package[17]. The enthalpies (H) and free energies (G) were calculated using the CBS-4M method.[18]

Table 5.1 Calculation results.

	$-H^{298}$ [a] / a.u.	$-\Delta_f H$ (g, M) [b] /kJ mol^{-1}	$\Delta_f H_{vap}$ [c]/ ΔH_{sub} [d] /kJ mol^{-1}
14a	747.665119	703.8	68.65
14b	747.6624795	710.8	67.90
15a	826.139667	650.8	44.83
15b	826.134454	667.1	45.28

[a] CBS-4M electronic enthalpy; [b] gas phase enthalpy of formation; [c] enthalpy of vaporization; d enthalpy of sublimation.

Detonation parameters were calculated using the EXPLO5 V6.02 computer code[19] with the CBS-4M generated enthalpies of formation. The calculations were performed using the densities obtained by pycnometric measurements at room temperature or from the crystal structure measurement. The calculated detonation values of **14-15** are given in **Table 5.2.**

Table 5.2 Energetic Data of the divinyl and bisallyl compounds **14a**,**b** and **15a**,**b**.

	14a	**14b**	**15a**	**15b**
Formula	$C_8H_{10}N_8$	$C_8H_{10}N_8$	$C_{10}H_{14}N_8$	$C_{10}H_{14}N_8$
FW [g mol^{-1}]	218.22	218.22	246.27	246.27
IS [J][a]	>40	>40	>40	>40
FS [N][b]	>360	>360	>360	>360
N [%][c]	51.35	51.35	45.50	45.50
T_{dec} [°C][e]	190	186	225	230
ρ [g cm^{-3}][f]	1.4[o]	1.4[p]	1.2	1.2
$\Delta_f H_m°$ [kJ mol^{-1}][g]	635	643	605	622
$\Delta_f U°$ [kJ kg^{-1}][h]	2907	2970	2452	2504
Explo5 V6.02 values				
$-\Delta_E U°$ [kJ kg^{-1}][i]	3681	3743	3398	3448
T_E [K][j]	2317	2341	2131	2150
p_{CJ} [kbar][k]	148	149	99	99
V_{det} [m s^{-1}][l]	7109	7132	6148	6167
Gas vol. [L kg^{-1}][m]	702	703	737	737
I_s [s][n]	197	198	188	189

[a] BAM drop hammer (1 of 6); [b] BAM friction tester (1 of 6); [c] nitrogen content; [d] oxygen content; [e] temperature of decomposition by DSC (onset values), [f] derived from pycnometer measurements; [g] molar enthalpy of formation; [h] energy of formation; [i] energy of explosion; [j] explosion temperature; [k] detonation pressure; [l] detonation velocity ; [m] assuming only gaseous products; [n] specific impulse (isobaric combustion, chamber pressure 70 bar, equilibrium expansion), [o] obtained from x-ray measurements and recalculated for ρ at rt using equation given in ref.[20], [p] estimated from structure determination.

The obtained detonation values show moderate energetic properties for **14-15**. Due to their higher $\Delta_f H_m°$ value and density, as well as lower carbon content, vinyl based **14a** and **14b** show an about 1000 m s^{-1} increased detonation velocity (V_{det}) and an about 50 kbar higher detonation pressure (p_{CJ}), when compared to the respective allyl based isomers **15a** and **15b**. A comparison of the corresponding isomers, in relation to each other, revealed slightly increased detonation values for the unsymmetrically substituted compounds, due to their higher enthalpy of formation.

5.4 Conclusion

In order to obtain starting materials for energetic epoxy resins several approaches towards mono- and difunctional epoxy tetrazoles were carried out. In the course of generating suitable precursors for the epoxidation steps, divinyl and bisallyl derivatives of 1,2-bis(tetrazol-5-yl)ethane were synthesized and characterized. Two different constitutional isomers of each compound could be isolated. The compounds were investigated regarding their thermal behavior as well as their sensitivities and energetic properties. In summary, the epoxidation approaches using *m*CPBA and DMDO were not fully successful, but only gave a monoepoxidated allyl bistetrazole.

5.5 Experimental Part

5.5.1 Compounds for Monoepoxy

1-Allyl-1H-tetrazole (8)[6]

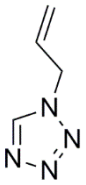

NaN_3 (2.73 g, 41.9 mmol) and allylamine (**7,** 2.00 g, 35.0 mmol) were dissolved in ethyl orthoformate (8.63 mL). Glacial acetic acid (20.58 mL) was added slowly at 0 °C. The solution was then stirred for 3 h at 100 °C. After cooling to rt conc. HCl (3.42 mL, 35.0 mmol) was added dropwise and the solution was stirred overnight. The reaction mixture was filtered and concentrated under reduced pressure. Ethanol (15 mL) was added and the mixture was filtered and concentrated again. To purify the product a column chromatography was performed (EtOAc/*n*-hexane 3:1) yielding 3.15 g (28.61 mmol, 82 %) of compound **8** as a yellow liquid.

^{1}**H NMR** (400 MHz, DMSO-d_6, ppm): δ = 9.40 (s, 1H, C$H_{tetrazole}$), 6.06 (ddt, $^3J_{HH}$ = 17.0, 10.3, 5.9 Hz, 1H, −CH=CH$_2$), 5.31 (ddt, 1H, $^4J_{HH}$ = 1.3 Hz, $^3J_{HH}$ = 10.3 Hz, $^2J_{HH}$ = 1.2 Hz, CH=CHH_{cis}), 5.20 (ddt, $^4J_{HH}$ = 1.6, $^3J_{HH}$ = 17.0 Hz, $^2J_{HH}$ = 1.2 Hz, 4H, CH=CHH_{trans}), 5.20 (ddd, $^4J_{HH}$ = 1.6, 1.3 Hz, $^3J_{HH}$ = 5.9 Hz, 2H, CH_2−N).

^{13}**C NMR** (101 MHz, DMSO-d_6, ppm): δ = 143.9 (CH$_{tetrazole}$), 131.6 (−CH=CH$_2$), 119.5 (CH=CH$_2$), 49.6 (CH$_2$−N).

IR (thin film, ATR, cm^{-1}): $\tilde{\nu}$ = 3133 (w), 2989 (w), 1720 (w), 1647 (w), 1481 (m), 1423 (m), 1340 (w), 1290 (w), 1250 (w), 1167 (s), 1100 (vs), 1022 (w), 991 (m), 966 (m), 939 (s), 874 (m), 767 (m), 720 (m), 659 (s).

EA ($C_4H_6N_4$): calculated: C 43.63, H 5.49, N 50.88 %; found: C 43.51, H 5.43, N 50.91 %.

3-Tetrazolyl propane-1,2-diol (10)

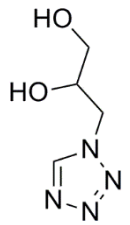

1*H*-Tetrazole (**10**, 0.25 g, 3.6 mmol) and NaOH (0.14 g, 3.6 mmol) were dissolved in H_2O (2 mL), 3-MCPD (0.39 g, 3.6 mmol) was added dropwise and the solution was stirred for 18 h at 100 °C. The solvent was removed under reduced pressure and hot ethanol (20 mL) was added to the remaining solution which was then cooled for 18 h to 7 °C. The precipitate was filtered off, the solvent was removed under reduced pressure and traces of volatiles were removed *in vacuo* yielding 0.50 g (3.47 mmol, 97 %) of compound **13** as yellowish oil.

IR (ATR, cm^{-1}): $\tilde{\nu}$ = 3252 (m), 2986 (m), 2881 (m), 2688 (m), 2495 (m), 1442 (m), 1427 (m), 1398 (m), 1360 (w), 1286 (w), 1230 (w), 1177 (w), 1146 (w), 1106 (m), 1074 (m), 1037 (vs), 942 (w), 878 (w), 836 (w), 793 (w), 738 (m), 699 (m), 664 (w).
HRMS (ESI): *m/z* calculated $[M+H]^+$: 145.0720, found: 145.0721.

1-(1H-Tetrazol-1-yl)-2-hydroxy-3-(4-methylbenzenesulfonate)propane (11)

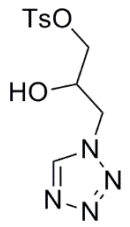

3-Tetrazolyl propane-1,2-diol (**10**) (0.60 g, 4.1 mmol) was dissolved in DCM (10 mL) and pyridine (10 mL). The mixture was cooled to 0 °C and *p*-TsCl (0.91 g, 4.8 mmol) was added in portions. The solution was stirred for 18 h at room temperature, while the reaction process was monitored by TLC (eluent: EtOAc/chloroform 6:4). The solvent was removed under reduced pressure and the residue was purified using column chromatography (eluent: EtOAc/chloroform 6:4) yielding 0.38 g (1.27 mmol, 31 %) of compound **14** as a yellow oil.

IR (thin film, ATR, cm^{-1}): $\tilde{\nu}$ = 3355 (w), 3144 (w), 2958 (w), 2926 (w), 1926 (w), 1730 (w), 1597 (w), 1494 (w), 1442 (w), 1401 (w), 1355 (s), 1308 (w), 1285 (w), 1211 (w), 1189 (m), 1173 (vs), 1131 (w), 1121 (w), 1095 (w), 1027 (w), 1018 (w), 987 (m), 932 (m), 813 (m), 757 (m), 707 (w), 686 (w), 663 (s), 634 (w), 611 (w), 592 (w), 577 (w).
MS (FAB+): *m/z* = 299.4 $[M+H]^+$.
EA ($C_{11}H_{14}N_4O_4S$): calculated: C 44.29, H 4.73, N 18.78, S 10.75 %; found: C 44.58, H 4.97, N 17.71, S 10.43 %.

1-(Oxiran-2-ylmethyl)-1H-tetrazole (4)

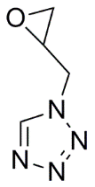

- *via m*CPBA

1-Allyl-1*H*-tetrazole (**8**, 0.30 g, 2.72 mmol) was dissolved in DCM (20 mL) and cooled to 0 °C. *m*CPBA (1.88 g, 10.9 mmol) was added in one portion and the reaction mixture was stirred for 2-72 h at room temperature. The reaction process was monitored by TLC (eluent: *n*-Hex/DCM/EtOAc 5:2:3). The mixture was heated to 40 °C. The compound could not be isolated.

HRMS (ESI+): *m/z* calculated $[M+H]^+$: 127.0614, found: 127.0615.

5.5.2 Difunctionalized Compounds

Bistetrazoloethane (12, BTE)[11]

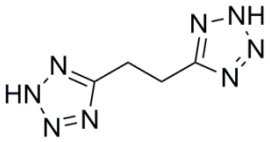

Succinonitrile (8.00 g, 99.9 mmol), zinc(II) chloride (27.34 g, 209.9 mmol) and sodium azide (19.50 g, 299.9 mmol) were suspended in water (100 ml). The mixture was heated to 100 °C under stirring overnight. After cooling to room temperature the precipitate was filtered off and washed with water. The precipitate was suspended in hydrochloric acid (64 ml water with 16 ml conc. HCl) and heated to 85 °C. Then conc. HCl was added dropwise until everything was dissolved. The recrystallization mixture was cooled to 7 °C overnight and filtration followed by washing with water led to the final product **12** yielding 15.7 g (94.50 mmol, 94 %).

^{1}H NMR (400 MHz, acetone-d_6, ppm): δ = 3.38 (s, 4H, CH_2).
^{13}C NMR (101 MHz, DMSO-d_6, ppm): δ = 154.8 (C_q), 20.9 (CH$_2$).
IR (ATR, cm^{-1}): $\tilde{\nu}$ = 3136 (w), 3015 (w), 2874 (w), 2704 (m), 2628 (m), 1582 (m), 1413 (m), 1260 (m), 1221 (m), 1113 (m), 1092 (m), 1058 (s), 1000 (m), 947 (m), 868 (m), 807 (m), 788 (m), 716 (w), 697 (m).
EA ($C_4H_6N_8$): calculated: C 28.92, H 3.64, N 67.44 %; found: C 29.04, H 3.59, N 67.41 %.

1,2-Bis(2-vinyl-2H-tetrazol-5-yl)ethane (14a, 2,2-DvBTE) and 1-vinyl-5-(2-(2-vinyl-2H-tetrazol-5-yl)ethyl)-1H-tetrazole (14b, 1,2-DvBTE)

1,2-Dibromoethane (8.3 ml, 96.30 mmol) was dissolved in acetonitrile (30 ml) and heated to 80 °C. BTE (**12**, 4.000 g, 24.08 mmol) was dissolved in acetonitrile (20 ml) and triethylamine (8.3 ml, 96.30 mmol). This mixture was added into the reaction flask over 5 h using a dropping funnel. Stirring at 80 °C was continued for 2 d. After cooling to ambient temperature, brine (50 ml) was added and the aqueous phase was extracted with ethyl acetate (3 x 100 ml). The combined organic phases were dried over $MgSO_4$ and the volatiles were removed *in vacuo*. The crude product was purified using column chromatography on silica gel (eluent: *n*-hexane/DCM/EtOAc = 5/3/2).

a) 2,2-DvBTE (14a)

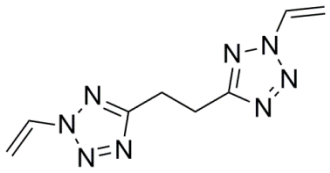

Compound **14a** was obtained as a colorless solid in 31 % yield (1.63 g, 7.46 mmol, R_f = 0.6) and was recrystallized from a *n*-hexane/ethyl acetate mixture.

DSC (5 °C min^{-1}): T_{melt} = 92 °C; T_{dec} = 190 °C.
^{1}H NMR (400 MHz, DMSO-d_6, ppm): δ = 7.79 (dd, $^3J_{HH}$ = 15.5 Hz, 8.7 Hz, 2H, −C*H*=CH_2), 6.06 (dd, $^3J_{HH}$ = 15.5 Hz, $^2J_{HH}$ = 1.5 Hz, 2H, CH=CHH_{trans}), 5.48 (dd, $^3J_{HH}$ = 8.7 Hz, $^2J_{HH}$ = 1.5 Hz, 2H, CH=CHH_{cis}), 3.42 (s, 4H, CH_2−$C_{tetrazole}$).
^{13}C NMR (101 MHz, DMSO-d_6, ppm): δ = 164.9 ($C_{tetrazole}$), 130.1 (−*C*H=CH_2), 109.0 (CH=*C*H_2), 22.9 (*C*H_2−$C_{tetrazole}$).
IR (ATR, cm^{-1}): $\tilde{\nu}$ = 3119 (w), 3108 (w), 3060 (w), 3010 (w), 2988 (w), 2399 (w),1919 (w), 1842 (w), 1738 (w), 1694 (w), 1643 (m), 1509 (s), 1480 (w), 1442 (w), 1408 (w), 1384 (m), 1353 (m), 1290 (w), 1263 (w), 1182 (m), 1130 (w), 1078 (w), 1031 (m), 1006 (s), 961 (s), 914 (s), 776 (w), 757 (s), 740 (s), 730 (s).
EA ($C_8H_{10}N_8$): calculated: C 44.03, H 4.62, N 51.24 %; found: C 44.10, H 4.68, N 51.24 %.
HRMS (ESI+): *m/z* calculated $[M+H]^+$: 219.1101, found: 219.1100.

b) 1,2-DvBTE (14b)

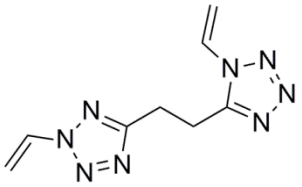

Compound **14b** was obtained as a colorless solid in 18 % yield (0.95 g, 4.33 mmol, R_f = 0.2).

DSC (5 °C min^{-1}): T_{melt} = 88 °C : T_{dec} = 186 °C.

^{1}H NMR (400 MHz, DMSO-d_6, ppm): δ = 7.79 (dd, $^3J_{HH}$ = 15.5 Hz, 8.7 Hz, 2H, N2‘−C*H*=CH$_2$), 7.47 (dd, $^3J_{HH}$ = 15.3 Hz, 8.7 Hz, 1H, N1−C*H*=CH$_2$), 6.05 (dd, $^3J_{HH}$ = 15.5 Hz, $^2J_{HH}$ = 1.1 Hz, 1H, N2‘−CH=CH*H*$_{trans}$), 5.97 (dd, $^3J_{HH}$ = 15.3 Hz, $^2J_{HH}$ = 1.1 Hz, 1H, N1−CH=CH*H*$_{trans}$), 5.47 (dd, $^3J_{HH}$ = 8.7 Hz, $^2J_{HH}$ = 1.1 Hz, 1H, CH=CH*H*$_{cis}$), 5.46 (dd, $^3J_{HH}$ = 8.7 Hz, $^2J_{HH}$ = 1.1 Hz, 1H, CH=CH*H*$_{cis}$), 3.47 (m, 4H, *C*H$_2$−C$_{tetrazole}$).

^{13}C NMR (101 MHz, DMSO-d_6, ppm): δ = 164.9 (*C*$_{q,tetrazole}$−N1‘−N2‘−CH=), 153.3 (*C*$_{q,tetrazole}$−N1−CH=), 130.1 (N2’−*C*H=CH$_2$), 126.5 (N1−*C*H=CH$_2$), 109.9 (N1−CH=*C*H$_2$), 109.0 (N2’−CH=*C*H$_2$), 22.2 (*C*H$_2$−C$_{tetrazole}$), 20.5 (*C*H$_2$−C$_{tetrazole}$).

IR (ATR, cm^{-1}): $\tilde{\nu}$ = 3100 (w), 2988 (w), 1743 (w), 1647 (m), 1501 (m),, 1437 (m), 1410 (m), 1378 (m), 1342 (w), 1291 (w), 1258 (m), 1181 (m), 1127 (m), 1087 (s), 1013 (vs), 950 (s), 919 (m), 792 (m), 726 (w), 700 (w).

EA ($C_8H_{10}N_8$): calculated: C 44.03; H 4.62; N 51.35 %; found: C 44.12, H 4.59, N 51.20 %.

1,2-Bis(2-allyl-2H-tetrazol-5-yl)ethane (15a, 2,2-BaBTE) and 1-allyl-5-(2-(2-allyl-2H-tetrazol-5-yl)ethyl)-1H-tetrazole (15b, 1,2-BaBTE)

Allyl bromide (4.8 ml, 55.38 mmol) was dissolved in acetonitrile (20 ml) and heated to 55 °C. BTE (**12**, 4.000 g, 24.08 mmol) was dissolved in acetonitrile (20 ml) and triethylamine (7.7 ml, 55.38 mmol). This mixture was added into the reaction flask over 5 h using a dropping funnel. Stirring at 65 °C was continued for 2 days. Brine (50 ml) was added and the aqueous phase was extracted with ethyl acetate (3 x 100 ml). The combined organic phases were dried over $MgSO_4$ and the volatiles were removed *in vacuo*. The crude product was purified using column chromatography on silica gel (eluent: *n*-hexane/DCM/EtOAc = 5/3/2).

a) 2,2-BaBTE (15a)

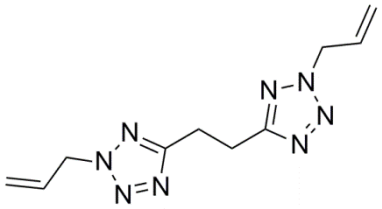

Compound **15a** was obtained as a yellowish liquid in 28 % yield (1.71 mg, 6.94 mmol, R_f = 0.4).

DSC (5 °C min^{-1}): T_{dec} = 225 °C.

^{1}H NMR (400 MHz, DMSO-d_6, ppm): δ = 6.04 (ddt, $^3J_{HH}$ = 17.2, 10.1, 5.9 Hz, 2H, −C*H*=CH$_2$), 5.29 (ddt, $^4J_{HH}$ = 1.3 Hz, $^3J_{HH}$ = 10.1 Hz, $^2J_{HH}$ = 1.2 Hz, 2H, CH=CH*H*$_{cis}$), 5.28 (ddd, $^4J_{HH}$ = 1.6, 1.3 Hz, $^3J_{HH}$ = 5.9 Hz, 4H, C*H*$_2$−N), 5.20 (ddt, $^4J_{HH}$ = 1.6 Hz, $^3J_{HH}$ = 17.2 Hz, $^2J_{HH}$ = 1.2 Hz, 2H, CH=CH*H*$_{trans}$), 3.33 (s, 4H, C*H*$_2$-C$_{q,tetrazole}$).

^{13}C NMR (101 MHz, DMSO-d_6, ppm): δ = 165.2 (*C*$_{q,tetrazole}$), 131.4 (−*C*H=CH$_2$), 120.0 (CH=*C*H$_2$), 55.0 (*C*H$_2$−N), 23.6 (*C*H$_2$-C$_{q,tetrazole}$).

IR (ATR, cm^{-1}): $\tilde{\nu}$ = 3090 (w), 2934 (w), 1730 (m), 1648 (w), 1495 (s), 1424 (m), 1400 (m), 1375 (w), 1336 (m), 1292 (w), 1260 (w), 1203 (m), 1174 (m), 1077 (m), 1028 (m), 989 (s), 936 (s), 921 (s), 795 (s), 710 (w), 673 (w).

EA ($C_{10}H_{14}N_8$): calculated: C 48.77, H 5.73, N 45.50 %; found: C 48.46, H 5.44, N 45.13 %.

HRMS (ESI+): *m/z* calculated $[M+H]^+$: 247.1414, found: 247.1412.

b) 1,2-BaBTE (15b)

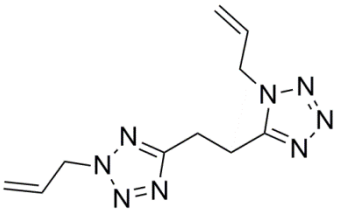

Compound **15b** was obtained as a yellowish liquid in 15 % yield (0.89 g, 3.71 mmol, R_f = 0.2).

DSC (5 °C min^{-1}): T_{dec} = 230 °C.

^{1}H NMR (400 MHz, DMSO-d_6, ppm): δ = 6.06 (m, 1H, N2‘−CH_2−C*H*=CH_2), 6.03 (m, 1H, N1−CH_2−C*H*=CH_2), 5.31 (m, 1H, N2‘−CH_2−CH=CH*H*$_{cis}$), 5.30 (m, 2H, N2‘−C*H*$_2$), 5.28 (m, 1H, N1−CH_2−CH=CH*H*$_{cis}$), 5.24 (m, 1H, N2‘−CH_2−CH=CH*H*$_{trans}$), 5.11. (m, 2H, N1−C*H*$_2$), 5.10 (m, 1H, N1−CH_2−CH=CH*H*$_{trans}$), 3.41 (m, 2H, C*H*$_2$−C$_{q,tetrazole}$), 3.39 (m, 2H, C*H*$_2$−C$_{q,tetrazole}$).

^{13}C NMR (101 MHz, DMSO-d_6, ppm): δ = 165.0 (*C*$_{q,tetrazole}$−N1‘−N2‘−CH_2), 154.6 (*C*$_{q,tetrazole}$−N1−CH_2), 131.8 (N1−CH_2−*C*H=), 131.3 (N2‘−CH_2−*C*H=), 120.2 (N2‘−CH_2−CH=*C*H_2), 119.1 (N1−CH_2−CH=*C*H_2), 55.1 (N2‘−*C*H_2−), 49.1 (N1−*C*H_2−), 22.7 (*C*H_2−C$_{q,tetrazole}$), 21.5 (*C*H_2−C$_{q,tetrazole}$).

IR (ATR, cm^{-1}): $\tilde{\nu}$ = 3089 (w), 2940 (w), 1647 (w), 1522 (m), 1498 (s), 1459 (m), 1420 (s), 1336 (m), 1292 (w), 1249 (m), 1199 (w), 1172 (w), 1177 (w), 1083 (m), 1030 (m), 989 (vs), 924 (vs), 849 (m), 791 (s), 703 (w), 670 (w).

EA ($C_{10}H_{14}N_8$): calculated: C 48.77, H 5.73, N 45.50 %; found: C, 48.75; H, 5.70; N, 44.73 %.

HRMS (ESI+): *m/z* calculated [M+H]$^+$: 247.1414, found: 247.1412.

3,3'-(Ethane-1,2-diylbis(2H-tetrazol-5,2-diyl)) bis(propane-1,2-diol) (16, BTE-4OH)

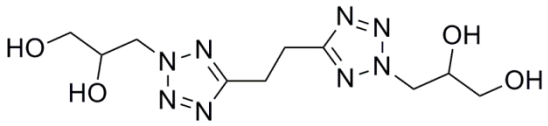

BTE (**12**, 1.00 g, 6.0 mmol) and NaOH (0.48 g, 12.0 mmol) were dissolved in H_2O (20 mL) and 3-MCPD (1.33 g, 12.0 mmol) was added dropwise within one hour. The reaction mixture was stirred for 18 h at 100 °C. After cooling to room temperature, the solution was acidified (pH 6) using aqueous HCl. The solvent was then removed under reduced pressure and hot ethanol (20 mL) was added to the remaining solution which was then cooled for 18 h to 7 °C. The precipitate was filtered off and the solvent was removed under reduced pressure. After drying *in vacuo* 1.80 g (5.72 mmol, 95 %) of **16** were obtained as highly viscous, colorless oil.

IR (thin film, ATR, cm−1): $\tilde{\nu}$ = 3278 (m), 2929 (m), 2878 (m), 1649 (w), 1523 (w), 1498 (w), 1427 (m), 1406 (m), 1365 (w), 1328 (w), 1255 (w), 1203 (w), 1077 (m), 1036 (vs), 927 (w), 873 (w), 788 (w), 746 (w), 698 (w), 629 (w), 561 (w).
HRMS (ESI+): *m/z* calculated $[M+H]^+$: 315.1524, found: 315.1524.
EA ($C_{10}H_{18}N_8O_4$): calculated: C 38.21, H 5.77, N 35.65 %; found: C 33.94, H 6.23, N 27.91 %.

2-Allyl-5-(2-(2-(oxiran-2-yl methyl)-2H-tetrazol-5-yl)ethyl)-2H-tetrazole (17)

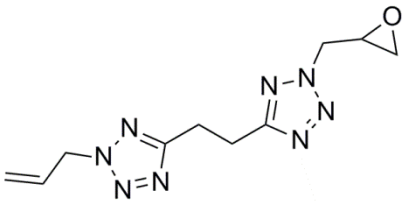

a) With oxone

DiallylBTE (**15a,** 200 mg, 0.813 mmol) was dissolved in acetone (30 ml) and water (18 ml). Sodium bicarbonate (2.047 g, 24.38 mmol) was added and the mixture was cooled to 0 °C. Oxone (1.998 g, 6.501 mmol) was added in small portions while stirring (1 h, 0 °C). The mixture was allowed to warm to room temperature while stirring was continued overnight. The precipitate was filtered off. Brine was added to the filtrate followed by extraction with ethyl acetate (3 x 100 ml). The combined organic phases were dried over $MgSO_4$ and the volatiles were removed *in vacuo*. Column chromatography on silica gel (eluent: *iso*-hexane/DCM/EtOAc = 5/2/3) gave **17** in negligible yield.

^{1}H NMR (400 MHz, DMSO-d_6, ppm): δ = 6.04 (ddt, $^3J_{HH}$ = 17.1, 10.2, 6.0 Hz, 1H, −C*H*=CH$_2$), 5.30 (ddt, $^4J_{HH}$ = 1.2 Hz, $^3J_{HH}$ = 10.2 Hz, $^2J_{HH}$ = 1.3 Hz, 1H, CH=CHH_{cis}), 5.28 (ddd, $^4J_{HH}$ = 1.5, 1.2 Hz, $^3J_{HH}$ = 6.0 Hz, 2H, N−CH_2−CH=), 5.20 (ddt, $^4J_{HH}$ = 1.5 Hz, $^3J_{HH}$ = 17.1 Hz, $^2J_{HH}$ = 1.3 Hz, 1H, CH=CHH_{trans}), 5.03 (dd, $^3J_{HH}$ = 3.1 Hz, $^2J_{HH}$ = 14.6 Hz, 1H, CH*H*'−CH$_{epoxide}$), 4.62 (dd, $^3J_{HH}$ = 6.8 Hz, $^2J_{HH}$ = 14.6 Hz, 1H, C*H*H'−CH$_{epoxide}$), 3.44 (dddd, $^3J_{HH}$ = 6.8, 4.2, 3.1, 2.5 Hz, 1H, −C*H*−O), 3.34 (s, 4H, CH_2−C$_{q,tetrazole}$), 2.86 (dd, $^3J_{HH}$ = 4.2 Hz, $^2J_{HH}$ = 5.0 Hz, 1H, CH*H*'−O), 2.67 (dd, $^3J_{HH}$ = 2.5 Hz, $^2J_{HH}$ = 5.0 Hz, 1H, C*H*H'−O).
^{13}C NMR (101 MHz, DMSO-d_6, ppm): δ = 164.8 ($C_{q,tetrazole}$), 164.7 ($C_{q,tetrazole}$), 131.0 (−*C*H=CH$_2$), 119.7 (CH=*C*H$_2$), 54.6 (*C*H$_2$−N), 54.5 (*C*H$_2$−N),), 49.0 (*C*H−O), 44.9 (*C*H$_2$−O), 23.1 (*C*H$_2$-C$_{q,tetrazole}$), 23.1 (*C*H$_2$-C$_{q,tetrazole}$).
HRMS (ESI+): *m/z* calculated $[M+H]^+$: 263.1363, found: 263.1361.

b) With mCPBA

DiallylBTE (**15a,** 150 mg, 0.609 mmol) was dissolved in dichloromethane (10 ml). The solution was cooled to 0 °C. 3-chloroperbenzoic acid (70 %, 600 mg, 2.438 mmol) was added in one portion and stirring was continued for 2 h. The mixture was then allowed to warm to room temperature and stirring was continued for further 3 d. A 10 % aqueous solution of sodium thiosulfate was added, followed by extraction with ethyl acetate (3 x 100 ml). The combined organic phases were dried over $MgSO_4$ and the volatiles were removed *in vacuo*. Column chromatography on silica gel (eluent: *iso*-hexane/dichloromethane/ethyl acetate = 5/2/3) gave 0.1 g (0.38 mmol, 62 %) of **17** as yellowish oil.

^{1}H NMR (400 MHz, DMSO-d_6, ppm): δ = 6.04 (ddt, $^3J_{HH}$ = 17.1, 10.3, 5.9 Hz, 1H, −C*H*=CH_2), 5.30 (ddt, $^4J_{HH}$ = 1.3 Hz, $^3J_{HH}$ = 10.3 Hz, $^2J_{HH}$ = 1.2 Hz, 1H, CH=CHH_{cis}), 5.27 (ddd, $^4J_{HH}$ = 1.6, 1.3 Hz, $^3J_{HH}$ = 5.9 Hz, 2H, N−CH_2−CH=), 5.20 (ddt, $^4J_{HH}$ = 1.6 Hz, $^3J_{HH}$ = 17.1 Hz, $^2J_{HH}$ = 1.2 Hz, 1H, CH=CHH_{trans}), 5.02 (dd, $^3J_{HH}$ = 3.2 Hz, $^2J_{HH}$ = 14.7 Hz, 1H, CH*H*'−$CH_{epoxide}$), 4.62 (dd, $^3J_{HH}$ = 6.8 Hz, $^2J_{HH}$ = 14.7 Hz, 1H, C*H*H'−$CH_{epoxide}$), 3.44 (dddd, $^3J_{HH}$ = 6.8, 4.1, 3.2, 2.5 Hz, 1H, −C*H*−O), 3.33 (s, 4H, CH_2−$C_{q,tetrazole}$), 2.86 (dd, $^3J_{HH}$ = 4.1 Hz, $^2J_{HH}$ = 5.0 Hz, 1H, CH*H*'−O), 2.67 (dd, $^3J_{HH}$ = 2.5 Hz, $^2J_{HH}$ = 5.0 Hz, 1H, C*H*H'−O).
^{13}C NMR (101 MHz, DMSO-d_6, ppm): δ = 164.8 ($C_{q,tetrazole}$), 164.7 ($C_{q,tetrazole}$), 131.0 (−*C*H=CH_2), 119.7 (CH=*C*H_2), 54.6 (*C*H_2−N), 54.5 (*C*H_2−N),), 49.0 (*C*H−O), 44.9 (*C*H_2−O), 23.1 (*C*H_2-$C_{q,tetrazole}$), 23.1 (*C*H_2-$C_{q,tetrazole}$).
HRMS (ESI+): *m/z* calculated $[M+H]^+$: 263.1363, found: 263.1361.

5.6 References

1 H. G. Ang, S. Pisharath, *Energetic Polymers − Binders and Plasticisers for Enhancing Performance*; 1. Edition, Wiley-VCH, Weinheim, **2012**.

2 a) J. J. Sabatini, A. V. Nagori, G. Chen, P. Chu, R. Damavarapu, T. M. Klapötke, *Chem. Eur. J.* **2012**, *18*, 628-631; b) J. J. Sabatini, J. M. Raab, R. K. Hann, *Chem. Asian J.* **2012**, *7*, 1657-1663; c) J. J. Sabatini, J. M. Raab, R. K. Hann, *Propellants Explos. Pyrotech.* **2012**, *37*, 592-596.

[3] K. P. C. Vollhardt, N. E. Schore, H. Butenschön, *Organische Chemie*, 4. Edition, WILEY-VCH, **2005**.

[4] R. S. Bauer, K. C. B. Dangayach, *US 5098965*, **1992**.

[5] J. J. Baldwin, A. W. Raab, K. Mensler, B. H. Arison, D. E. McClure, *J. Org. Chem.* **1978**, *43*, 4876-4877.

[6] P. N. Gaponik, V. P. Karavai, Y. V. Grigor'ev, *Khimiya Geterotsiklicheskikh Soedinenii* **1985**, *11*, 1521-1524.

[7] K. R. Tarantik, *Ph.D. Thesis*, Ludwig-Maximilians-Universität München, **2010**.

[8] R. W. Murray, M. Singh, *Org. Synth.* **1998**, *9*, 288-293.

[9] R. J. Bergeron, R. Müller, J. Bussenius, J. S. McManis, R. L. Merriman, R. E. Smith, H. Yao, W. R. Weimar, *J. Med. Chem.* **2000**, *43*, 224–235.

[10] M. Hesse, H. Meier, B. Zeh, *Spektroskopische Methoden in der organischen Chemie*, 7. Edition, Thieme Verlag, Stuttgart, **2005**.

[11] Z. P. Demko, K. B. Sharpless, *J. Org. Chem.* **2001**, *66*, 7945-7950.

[12] A Chafin, D. J. Irvin, M. H. Mason, S. L. Mason, *Tetrahedron Lett.* **2008**, *49*, 3823-3826.

[13] P. A. Aleshunin, U. N. Dimitrieva, V. A. Ostrovskii, *Russ. J. Org. Chem.* **2011**, *47*, 1882-1888.

[14] A. F. Holleman, E. Wiberg, N. Wiberg, *Lehrbuch der anorganischen Chemie*, de Gruyter, New York, **2007**.

[15] C. A. K. Diop, M. F. Mahon, K. C. Molloy, L. Ooi, P. R. Raithby, M. M. Venter, S. J. Teat, *Cryst. Eng. Comm.* **2002**, *4*, 462-466.

[16] http://www.bam.de (accessed April, 2016).

[17] M. J. Frisch, G. W. Trucks, H. B. Schlegel, G. E. Scuseria, M. A. Robb, J. R. Cheeseman, V. B. Scalmani, B. Mennucci, G. A. Petersson, H. Nakatsuji, M. Caricato,

X. Li, H. P. Hratchian, A. F. Izmaylov, J. Bloino, G. Zheng, J. L. Sonnenberg, M. Hada, M. Ehara, K. Toyota, R. Fukuda, J. Hasegawa, M. Ishida, T. Nakajima, Y. Honda, O. Kitao, H. Nakai, T. Vreven, J. A. Montgomery, J. E. Peralta, F. Ogliaro, M. Bearpark, J. J. Heyd, E. Brothers, K. N. Kudin, V.-N. Staroverov, R. Kobayashi, J. Normand, K. Raghavachari, A. Rendell, J. C. Burant, S. S. Iyengar, J. Tomasi, M. Cossi, N. Rega, J. M. Millam, M. Klene, J. E. Knox, J. B. Cross, V. Bakken, C. Adamo, J. Jaramillo, R. Gomperts, R. E. Stratmann, O. Yazyev, A. J. Austin, R. Cammi, C. Pomelli, J. W. Ochterski, R. L. Martin, K. Morokuma, V. g Zakrzewski, G. A. Voth, P. Salvador, J. J. Dannenberg, S. Dapprich, A. D. Daniels, Ö. Farkas, J. B. Foresman, J. V. Ortiz, J., J. Cioslowski, D. J. Fox,. *Gaussian 09*. Rev. A.03 ed.; Gaussian, Inc.: Wallingford CT, **2009**.

18 a) J. W. Ochterski, G. A. Petersson, J. A. Montgomery Jr., A complete basis set model chemistry. V. Extensions to six or more heavy atoms, *J. Chem. Phys.* **1996**, *104*, 2598; b) J. A. Montgomery Jr., M. J. Frisch, J. W. Ochterski, G. A. Petersson, A complete basis set model chemistry. VII. Use of the minimum population localization method, *J. Chem. Phys.* **2000**, *112*, 6532.

19 a) M. Sućeska, Calculation of the detonation properties of C-H-N-O explosives, *Propellants, Explos., Pyrotech.* **1991**, *16*, 197–202; b) Sućeska, M. *EXPLO5 V.6.02*. Zagreb (Croatia), **2013**.

20 D. Izsák, T. M. Klapötke, F. H. Lutter, C. Pflüger, *Eur. J. Chem*. **2016**, *in press*.

ENERGETIC PLASTICIZERS

6. Energetic Plasticizers

Abstract: Different carboxylic acid derivatives of 2,2-dinitropropane-1,3-diol (DNPD), 2,2-bis(azidomethyl)propane-1,3-diol (BAMP) and 1,2-bis(hydroxyethyl tetrazol-5-yl)ethane (BTEOH) were synthesized in this study in order to investigate their suitability as energetic plasticizers. The syntheses were carried out using the acyl chlorides of acetic, propionic and butyric acid. The obtained products were characterized by elemental analysis, nuclear magnetic resonance (^{1}H, ^{13}C, ^{14}N NMR) and vibrational spectroscopy (IR). The energetic properties of the synthesized compounds were calculated on the basis of the computed heats of formation at the CBS-4M level of theory using the EXPLO5 version 6.02 computer code. Investigations of physical stabilities were carried out using BAM drop hammer and friction tester. Low and high temperature behavior was determined by differential scanning calorimetry (DSC). The energetic and physical properties of the synthesized compounds were compared to the literature known energetic plasticizers *N*-butyl nitratoethylnitramine (BuNENA) and diethylene glycol bis(azidoacetate) ester (DEGBAA). For analyzing the plasticizing abilities, mixtures of glycidyl azide polymer (GAP) and poly(3-nitratomethyl-3-methyloxetan) (polyNIMMO) were prepared with two propionyl based compounds in different ratios and investigated with respect to their glass transition temperatures and viscosity. Both compounds showed plasticizing effects in the range of BuNENA.

6.1 Introduction

The use of plasticizers in modern explosive and propellant formulations is essential due to the improvement of performance parameters as well as safety and mechanical conditions. When added, plasticizers should mainly influence thermal stability, glass transition temperature and processing of such formulations in a positive way.[1]

Established non-energetic plasticizers are, for example organic phthalates, like dioctyl phthalate (DOP) and esters of adipic acid, like dioctyl adipate (DOA) which have the disadvantage of reducing the energy output of an explosive formulation, when used as plasticizing additive.[2,3]

A broad spectrum of energetic plasticizers for propelling systems and smokeless powders provide organic compounds containing nitro groups[4], nitrate esters[4], or nitratoethyl nitramines (NENAs)[5]. Another interesting substance class within this field are compounds with a geminal dinitromethylene unit. To date only a few investigations concerning 2,2-dinitropropane-1,3-diyl compounds and their suitability as energetic plasticizers are known.[6,7,8]

Another substance class, which gained more attention in the field of energetic plasticizers, are organic azido compounds.[9,10,11] Besides their good energetic properties, like high heats of formation and minimum smoke generation, azido plasticizers generally show good mixing compatibility with established energetic binders, like GAP, polyNIMMO.[9,10]

A further substance class which provides favourable properties, are compounds based on tetrazoles. In fact, tetrazoles are investigated for application in every subfield of energetic materials, primary explosives[12], secondary explosives[13], propellants[14] as well as pyrotechnics[15], due to their high nitrogen content (up to >80 %), good thermal stability and their energetic character.

Main demands for the optimal energetic plasticizer are a good or at least moderate energetic content, low glass transition temperature, low viscosity, absence of volatility, high oxygen balance and high stability towards thermal and physical stimuli.[1]

Herein we report the synthesis and characterization of esters with varying carbon chain lengths on the basis of the three above mentioned energetic substance classes. On the one hand, the geminal dinitromethylene class on the basis of the 2,2-dinitropropane-1,3-diyl unit. Only few of these compounds are known in today's literature in the research field of energetic plasticizers. Furthermore, they are interesting due to their increased oxygen content. On the other hand, the 2,2-bis(azidomethyl)propane-1,3-diyl unit, which should bring along all the

already mentioned advantages of organic azides for energetic plasticizers. As representative for the third substance class, the tetrazoles, compounds containing a 1,2-bis(tetrazolo)ethane fragment were chosen.

As references for the synthesized compounds *N*-butyl-2-nitratoethylnitramine (BuNENA), in case of the dinitro compounds, and diethylene glycol bis(azidoacetate) ester (DEGBAA)[10], in case of the azido compounds, were chosen (**Figure 6.1**).

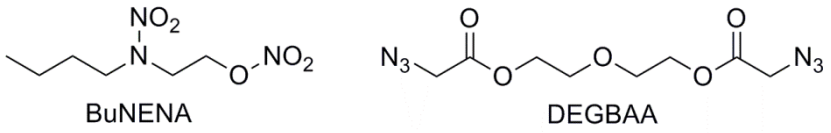

Figure 6.1. Molecular structures of BuNENA and DEGBAA.

6.2 Results and Discussion

6.2.1 Synthesis

On the basis of 2,2-bis(azidomethyl)propane-1,3-diol (BAMP, **1**), 2,2-dinitropropane-1,3-diol (DNPD, **2**) and 1,2-bis(hydroxyethyl tetrazole-5-yl)ethane (BTEOH, **3**), which are depicted in **Figure 6.2**, seven different carboxyl derivatives were synthesized. BAMP[16], DNPD[17] and BTHEOH[18] were synthesized according to literature known procedures. The following reaction with acyl chlorides of different carbon chain lengths in their corresponding carboxylic anhydrides (as solvent) at room temperature gave the desired esters **1-7** (**Scheme 7.1**).

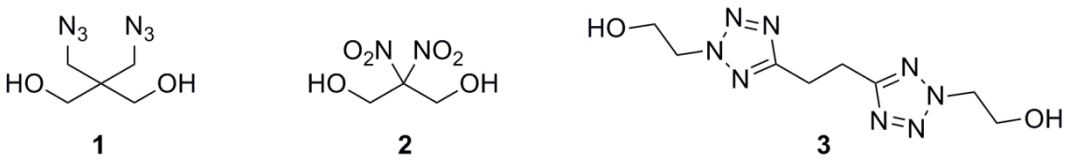

Figure 6.2 Used diols for the ester syntheses.

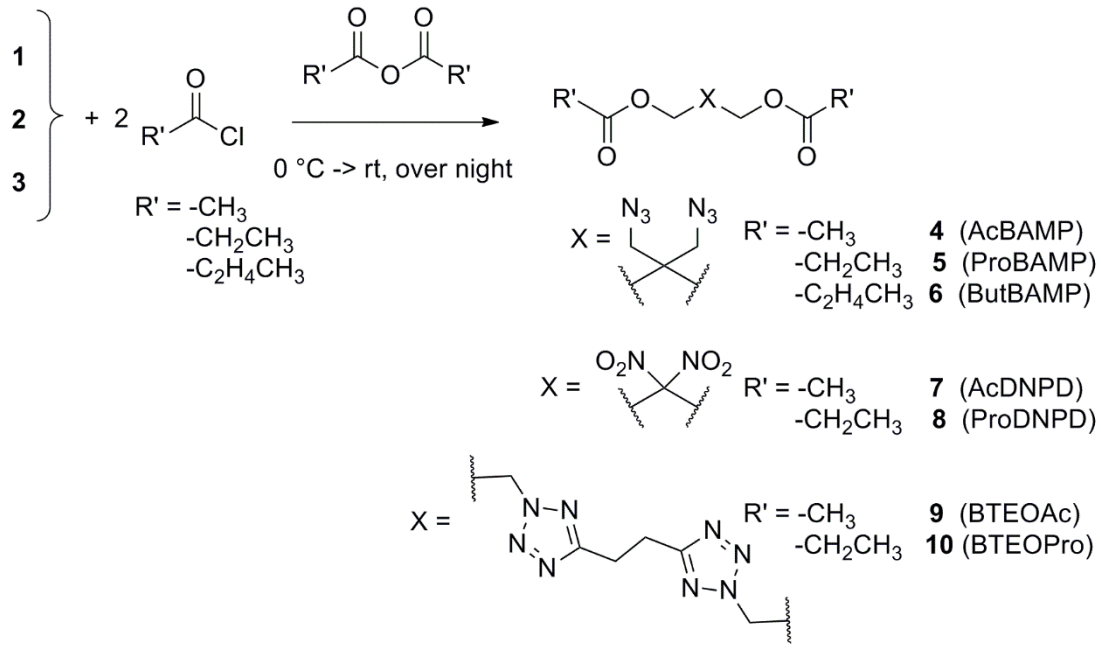

Scheme 6.1. Synthesis of the BAMP, DNPD and BTEOH based esters **4-10** using different acyl chlorides.

Compounds **4** and **7** have already been mentioned in literature, but neither in that context nor according to that method.[19 20] The synthesized products were colorless to yellowish liquids (**4-8**) or waxy solids (**9**, **10**). Compounds **4**, **5**, **7** and **8** were obtained in good yields (82-76 %). Compounds **6**, **9** and **10** could only be obtained in low yields with 23-14 %.

6.2.2 Spectroscopic Analysis

The synthesized compounds **4-10** were analyzed using ^{1}H, ^{13}C and ^{14}N NMR spectroscopy in DMSO-*d6*. The ^{1}H NMR spectra of the compounds show the expected chemical shifts and coupling patterns (**Figures 6.3-6.5**). The protons of the methylene groups belonging to the respective diol fragment (−CH_2−R, with R = -O, -N_3, -$N_{tetrazole}$ or -$C_{tetrazole}$) are not affected by the carbon chain elongation of R'. They show constant values for the corresponding diol derivatives, with 5.13 ppm (CH_2−O) for **7** and **8** (**Figure 6.4**), 3.98 and 3.48 ppm (CH_2−O and CH_2−N_3) for **4-6** (**Figure 6.3**) or 4.88, 4.46 and 3.30 ppm (−CH_2−O, -CH_2−$N_{tetrazole}$, CH_2−$C_{tetrazole}$) for **9** and **10** (**Figure 6.5**).

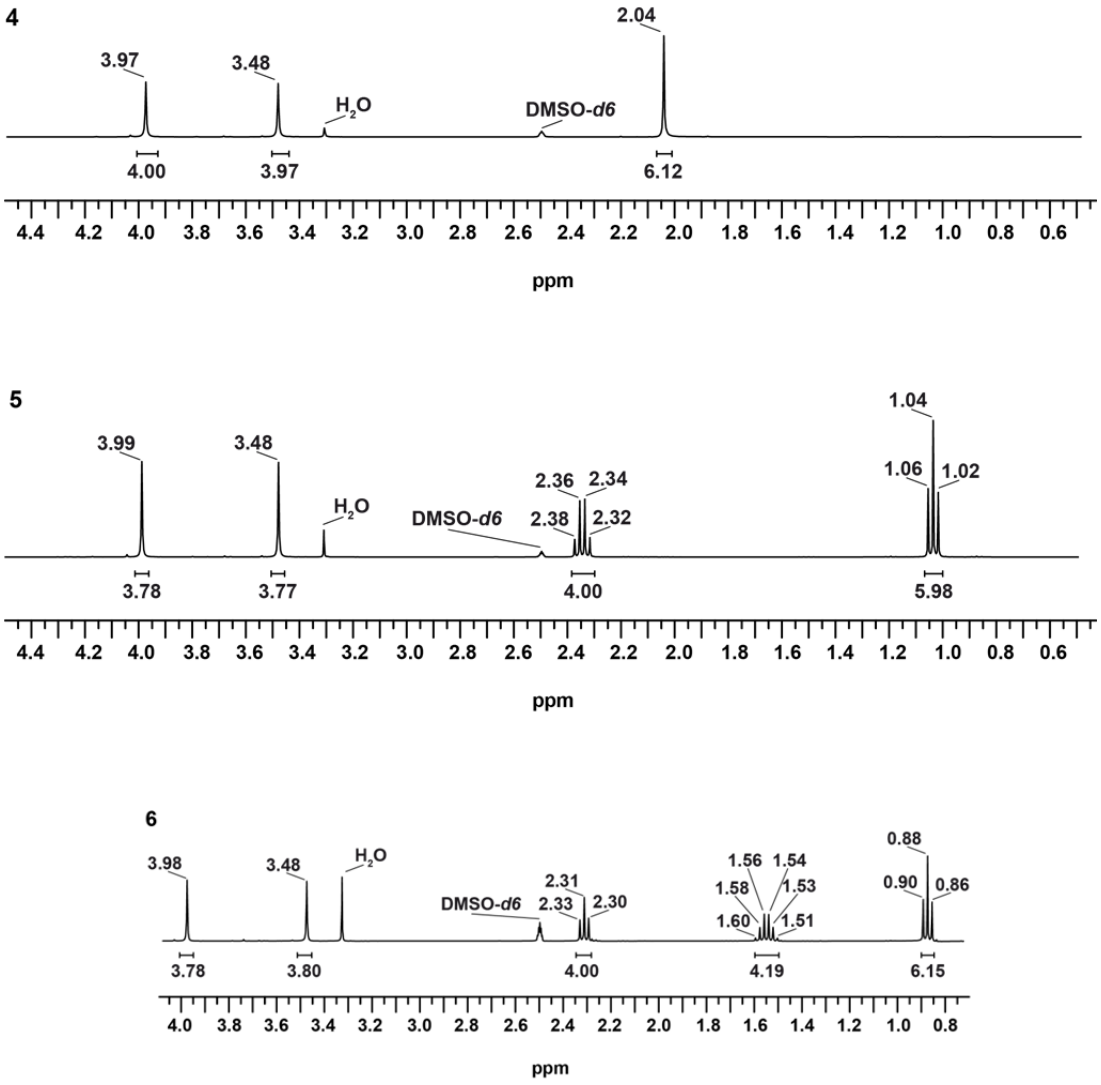

Figure 6.3 ^{1}H NMR spectra of the BAMP based esters AcBAMP (**4**), ProBAMP (**5**) and ButBAMP (**6**).

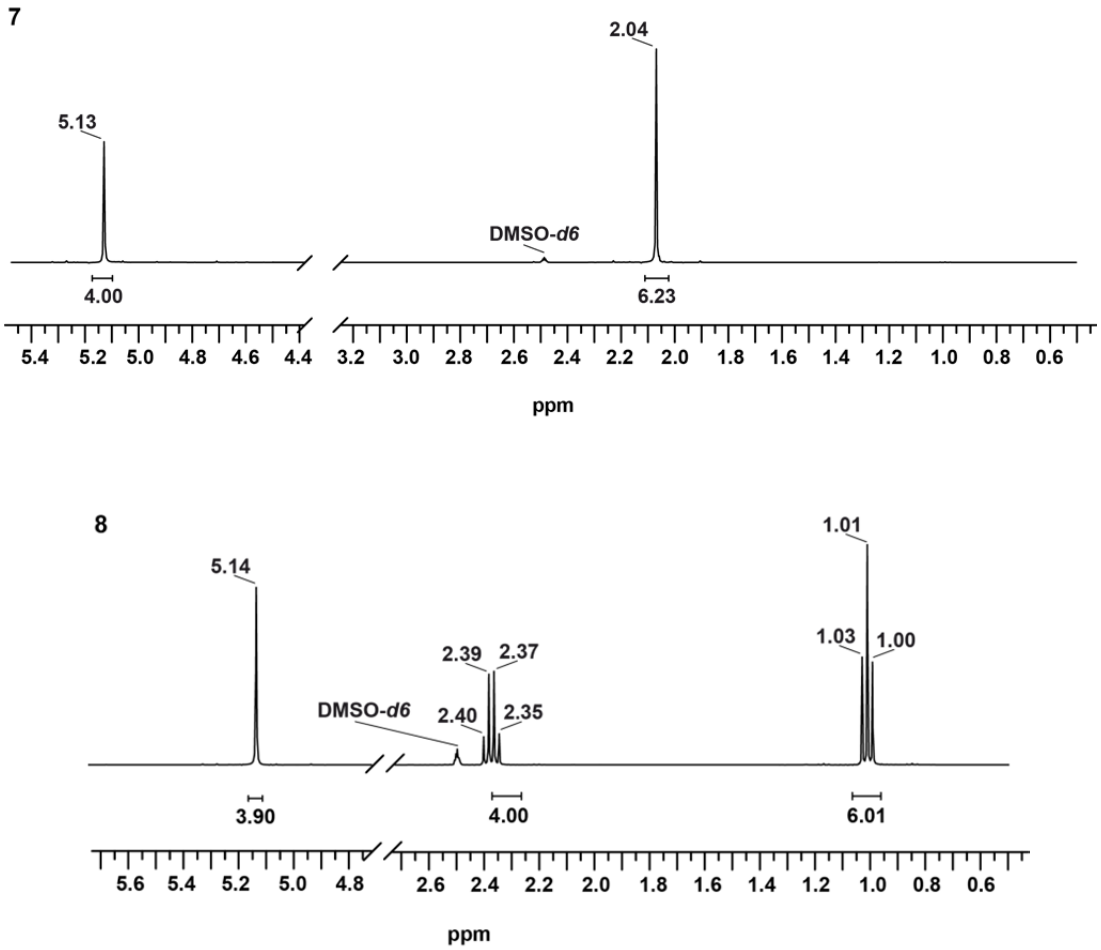

Figure 6.4 ^{1}H NMR spectra of the DNPD based esters AcDNPD (**7**) and ProDNPD (**8**).

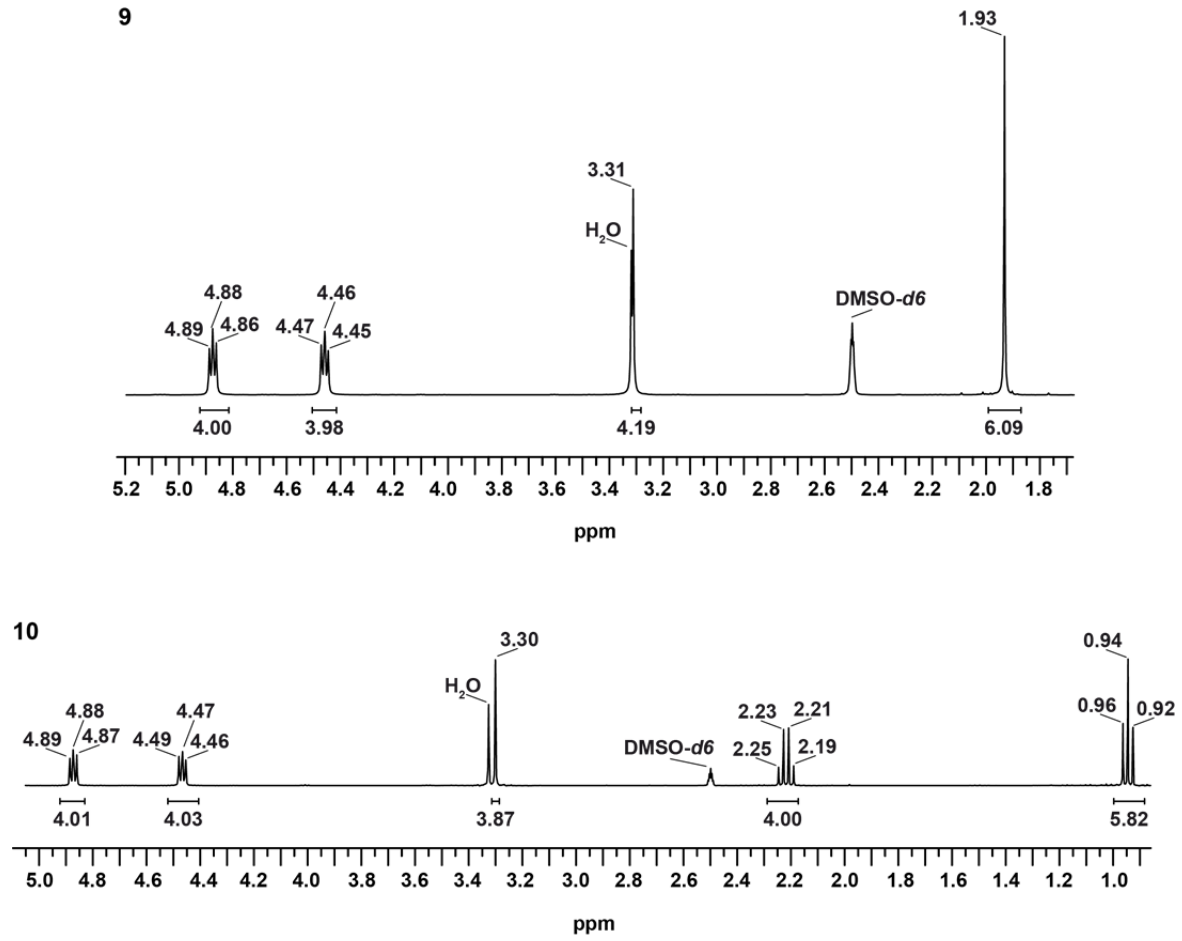

Figure 6.5 ^{1}H NMR spectra of the BTEOH based esters BTEOAc (**9**) and BTEOPro (**10**).

The ^{13}C NMR spectra of **4-10** confirm the assumed structure from the ^{1}H NMR results. The chain elongation of R' is proven by the occurrence of the expected signals for the corresponding aliphatic groups. The chemical shifts of the signals of the carbon atoms of the respective diol fragment remain constant (**Figure 6.6-6.8**). The signals of the carboxyl carbons occur in the range of 173.2−168.9 ppm, the inner quaternary carbon atoms show signals at 164.8 ppm (**9** and **10**) (**Figure 6.8**), 115.1 ppm (**7** and **8**) (**Figure 6.7**) and 42.7 ppm (**4-6**) (**Figure 6.6**). The signal for the respective CH_2−O fragment occurs in the range of 62.5-60.6 ppm for all compounds. The signals for the other methylene carbons can be found either at 51.2 ppm (CH_2−N_3, **4-6**) or at 51.5 and 23.1 ppm (CH_2−$N_{tetrazole}$ and CH_2−$C_{tetrazole}$, **9** and **10**).

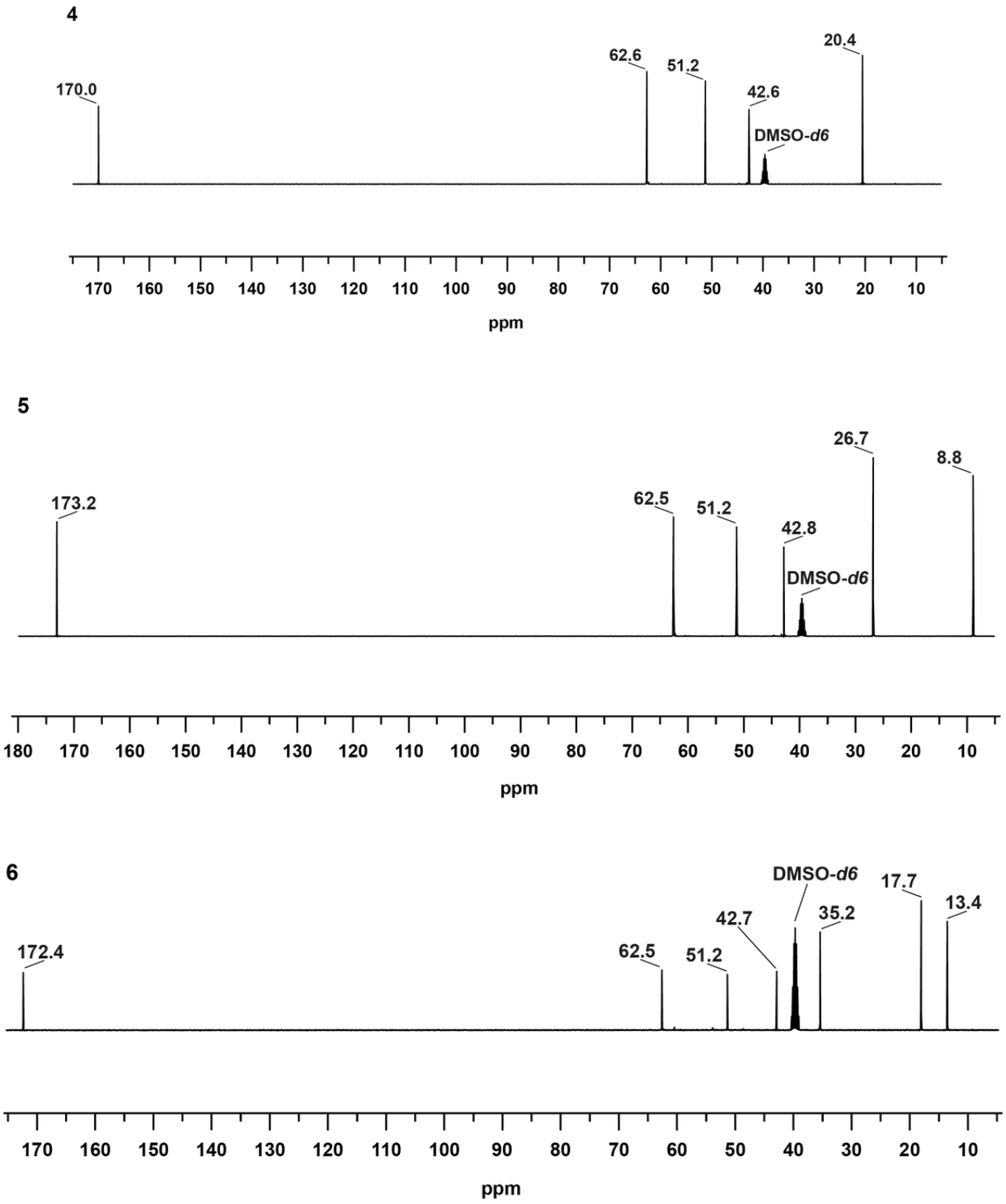

Figure 6.6 ^{13}C NMR spectra of the BAMP based esters AcBAMP (**4**), ProBAMP (**5**) and ButBAMP (**6**).

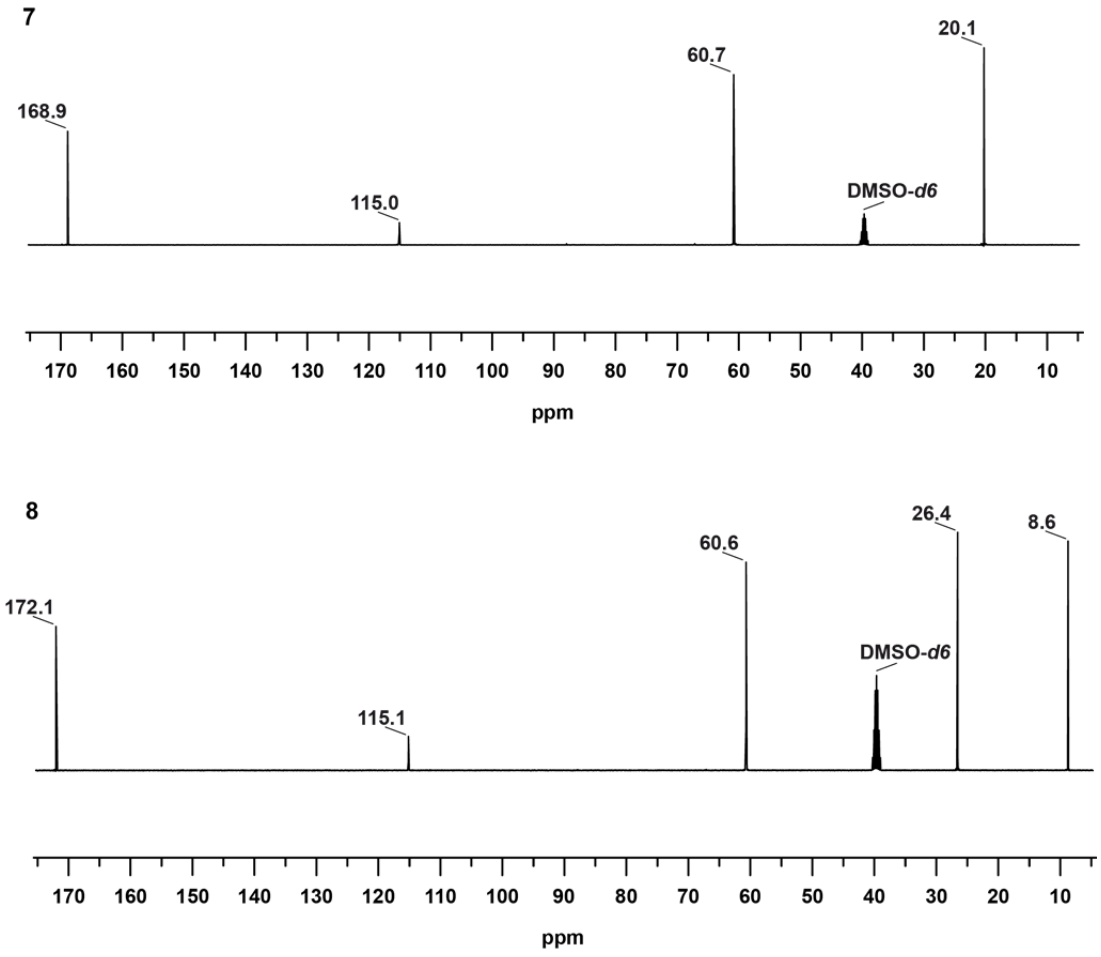

Figure 6.7 ^{13}C NMR spectra of the DNPD based esters AcDNPD (**7**) and ProDNPD (**8**).

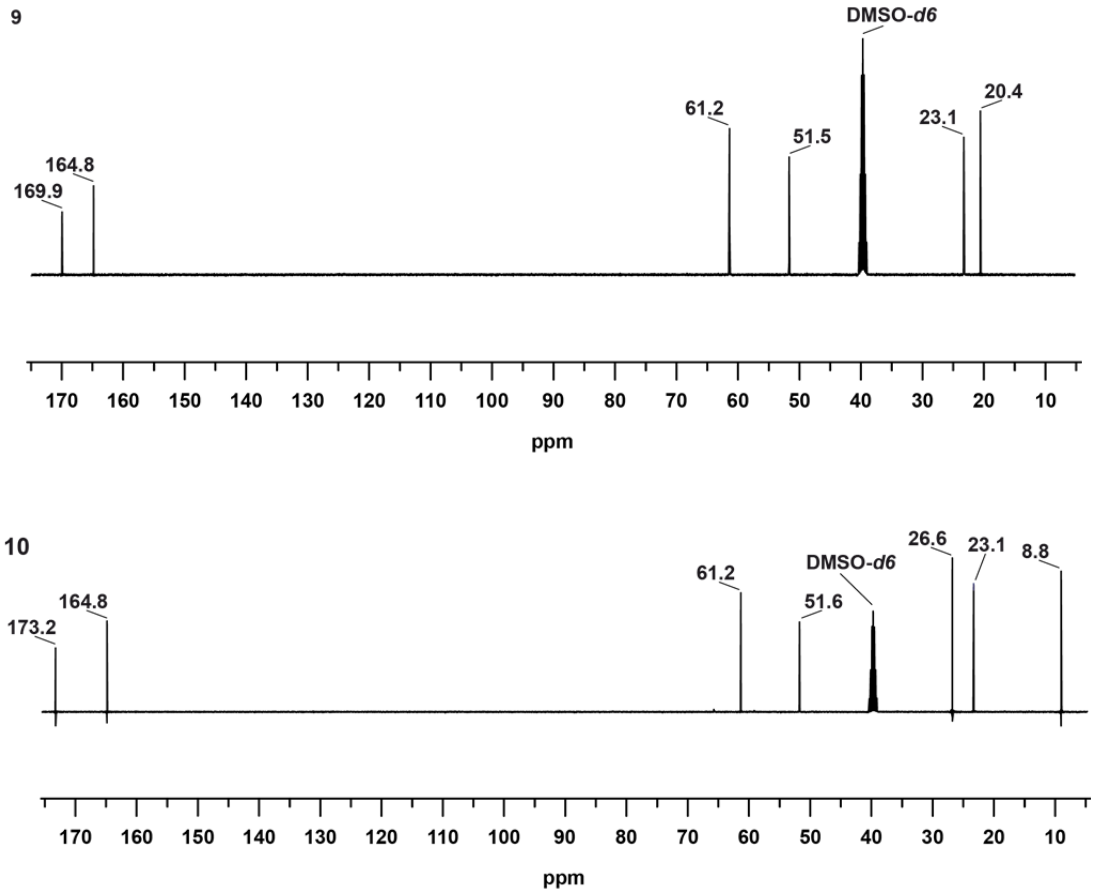

Figure 6.8 ^{13}C NMR spectra of the BTEOH based esters BTEOAc (**9**) and BTEOPro (**10**).

The ^{1}H and ^{13}C NMR spectra of the BTEOH based compounds **9** and **10** explain the low yields of these compounds, because obviously only the 2,2'-*N*-substituted isomers were obtained after the purification step (cf. ^{1}H and ^{13}C NMR spectra of 1,2'- and 2,2'-*N*-bistetrazolo isomers in **Chapter 5.3.2.1**).

The ^{14}N NMR spectra of **4-6** show the expected signals for the azido function.[21] A sharp signal for the N_β (−133−134 ppm), a broader signal for the N_γ (−175−180 ppm) and a very broad signal for N_α (−301−342 ppm) are visible, too.

The signal of the ^{14}N NMR spectra of **7** and **8** appears at −16 ppm, which can be assigned to the NO_2 groups.[21]

For further characterization vibrational (IR) spectra were recorded. A comparison of the measured spectra makes obvious that with increasing carbon chain length the signal intensity of the CH_2 valence vibration is also increasing (**A**) (**Figure 6.9**).[22] The existence of the carboxyl groups is proven in all cases by the signals appearing at 1760−1730 cm^{-1} (C=O, **B**) and 1215−1150 cm^{-1} (C-O, **C**).[22] Furthermore, the presence of the energetic functional groups is also proven by the signals either at 2100 cm^{-1} (**D**), representing the azido groups of **4-6**[23] or

at 1570 cm^{-1} (**E**), representing the asymmetric valence vibration of the nitro groups of **7** and **8**[22].

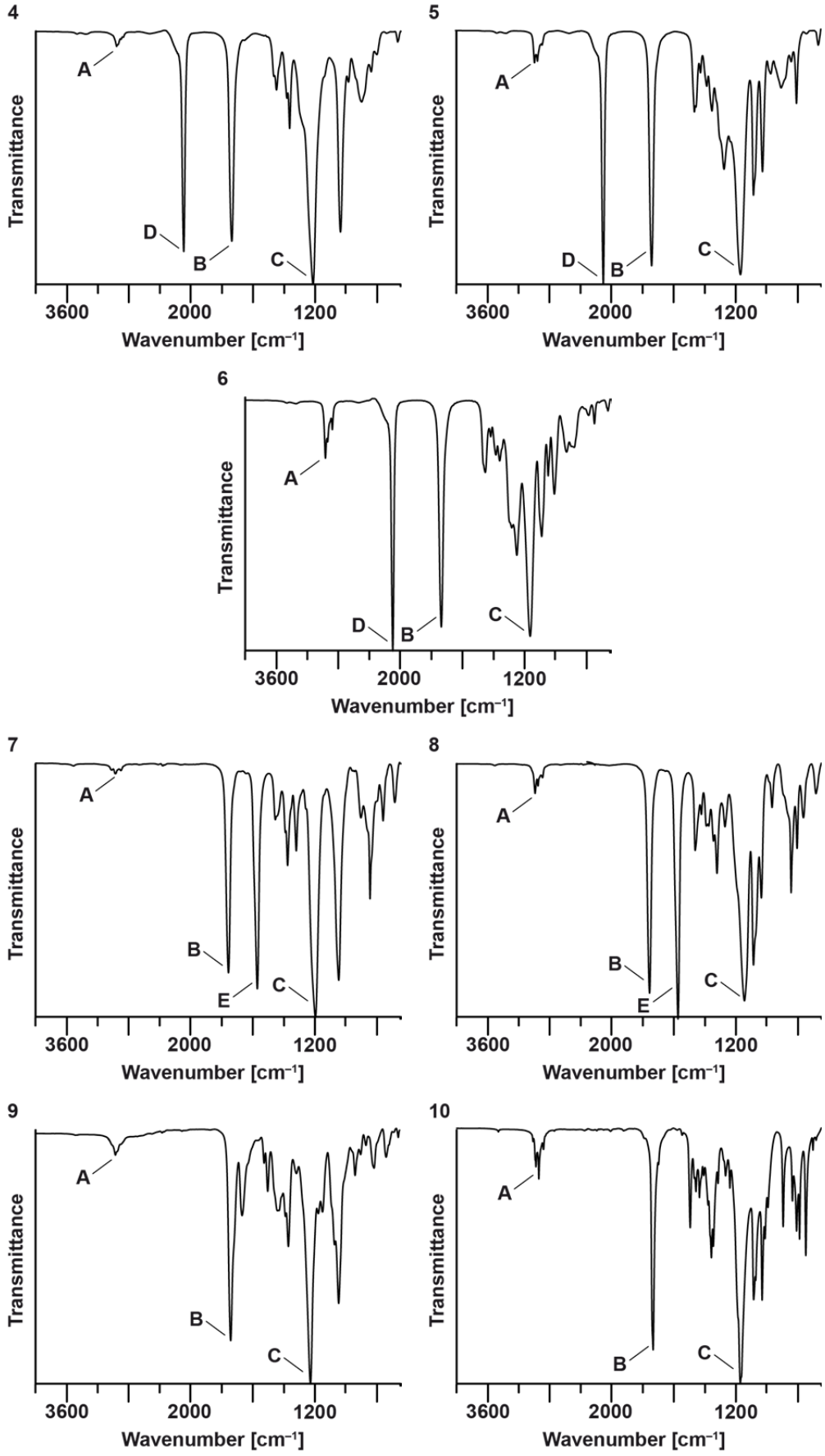

Figure 6.9 IR spectra of AcBAMP (**4**), ProBAMP (**5**), ButBAMP (**6**), AcDNPD (**7**), ProDNPD (**8**), BTEOAc (**9**) and BTEOPro (**10**).

6.2.3 Thermodynamic Properties

6.2.3.1 Thermal Stability

The behavior at high temperatures was determined *via* differential scanning calorimetry with a heating rate of 5 °C min^{-1}. The obtained plots are depicted in **Figure 6.10**. Due to their volatility, compounds **4-6** had to be measured in closed Al-pans, otherwise no results were obtained. As can be seen, the obtained plots of the DNPD based compounds **7** and **8** show a sharp drop of the DSC curve around the decomposition point, which indicates the opening of the Al-pan, because of a too high inner pressure. This necessitated a remeasurement of the decomposition temperatures of compounds **7** and **8** in high pressure Au-pans (F20). The obtained plots of the high pressure DSC measurements are depicted in **Figure 6.11**.

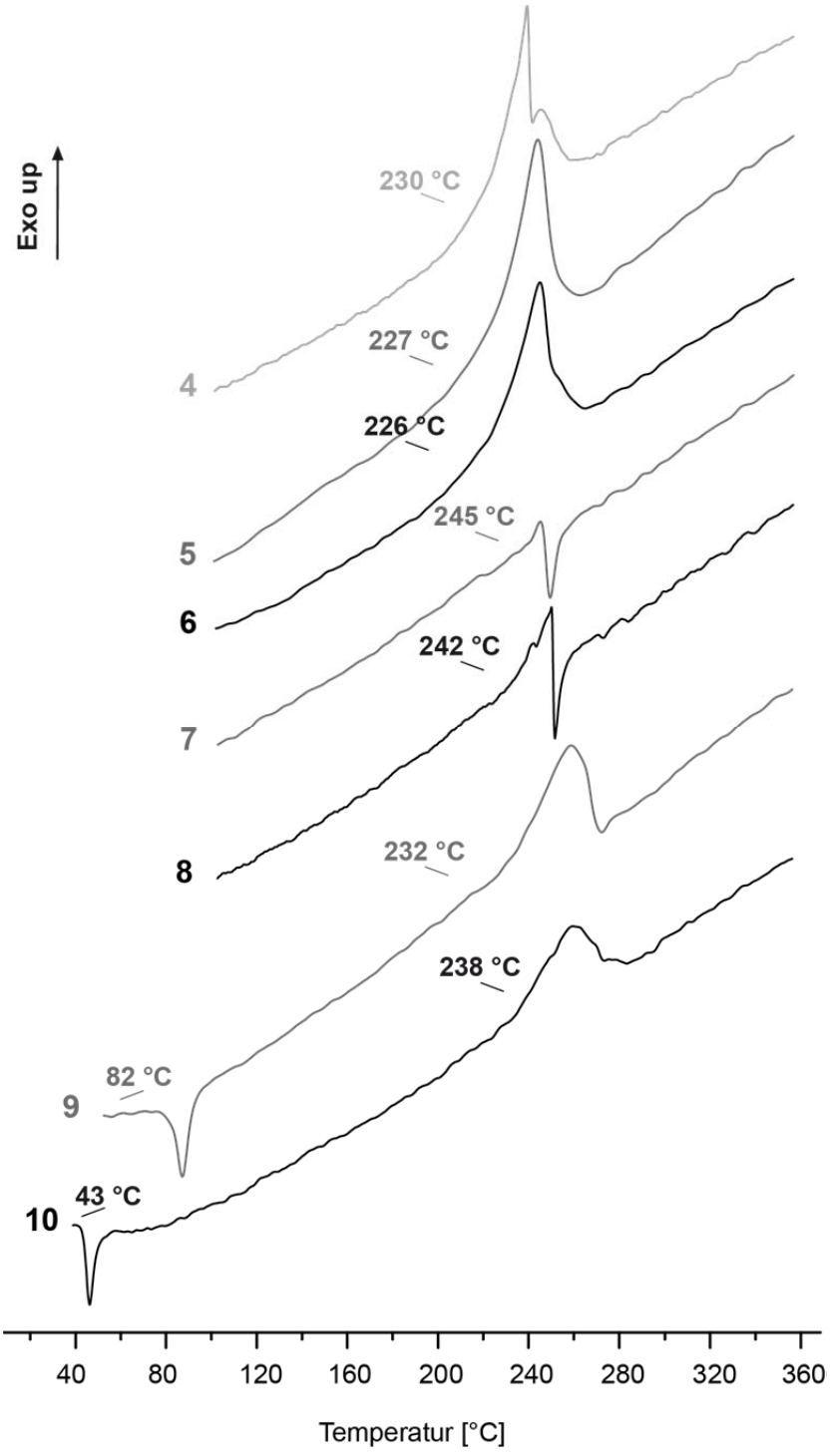

Figure 6.10 DSC plots of decompositon temperatures of **4-10**.

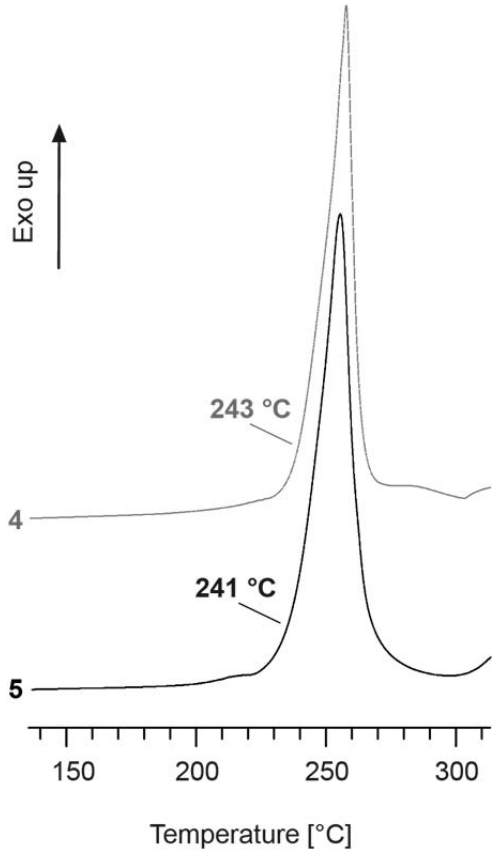

Figure 6.11 Obtained plots of the high pressure DSC measurements of **7** and **8**.

All compounds possess good thermal stabilities at which the DNPD based esters are stable up to higher temperatures, with values around 240 °C (**Figure 6.11**). The azido based compounds **4-6** show decomposition temperatures in the range of 230 °C. Whereas the decomposition temperatures of the tetrazole based compounds **9** and **10** diverge about 10 °C from each other, with 232 °C and 240 °C. They also show melting points at 43 °C and 82 °C. Due to the broad gap between T_{melt} and T_{dec} with 150-200 °C, **9** and **10** may be of interest for further melt-castable applications.

In order to investigate the volatility behavior of the liquid compounds **4-8** thermogravimetric analysis (TGA) were carried out with ProBAMP (**5**) and ProDNPD (**8**) as example compounds (**Figure 6.12**). As reference TGA was also measured with BuNENA. The obtained curves illustrate, why no results were obtained durring the DSC measurements with perforated Al-pans. The compounds turned out to be volatile at lower temperatures.

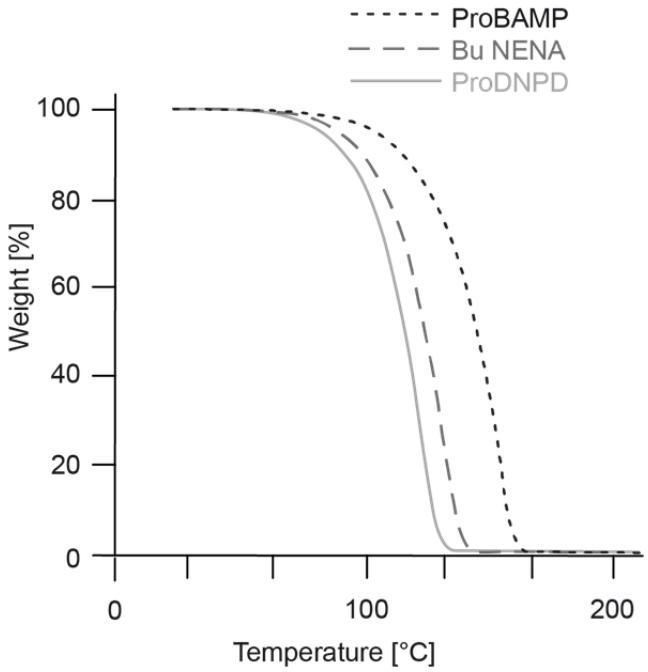

Figure 6.12 TGA plots of **2** and **5** compared to BuNENA.

ProDNPD (**8**) shows a beginning weight loss around 70 °C, which is about 10 °C lower than the value of BuNENA (around 80 °C), whereas ProBAMP (**5**) starts to volatilize at an about 30 °C higher temperature (~ 100 °C). The complete weight loss of all compounds is accomplished around 130 °C (ProDNPD), 140 °C (BuNENA) and 160 °C (ProBAMP).

6.2.3.2 Low Temperature Behavior

The glass transition temperatures of **4-8** were determined *via* differential scanning calorimetry (DSC) in a temperature range from −120 °C to +10 °C with a heating rate of 5 °C min^{-1}. Compounds **4-8** show excellent values, with glass transition temperatures of −70 °C and below (**Figure 6.13**). As expected, the glass transition temperature drops with the elongation of the carbon chain.

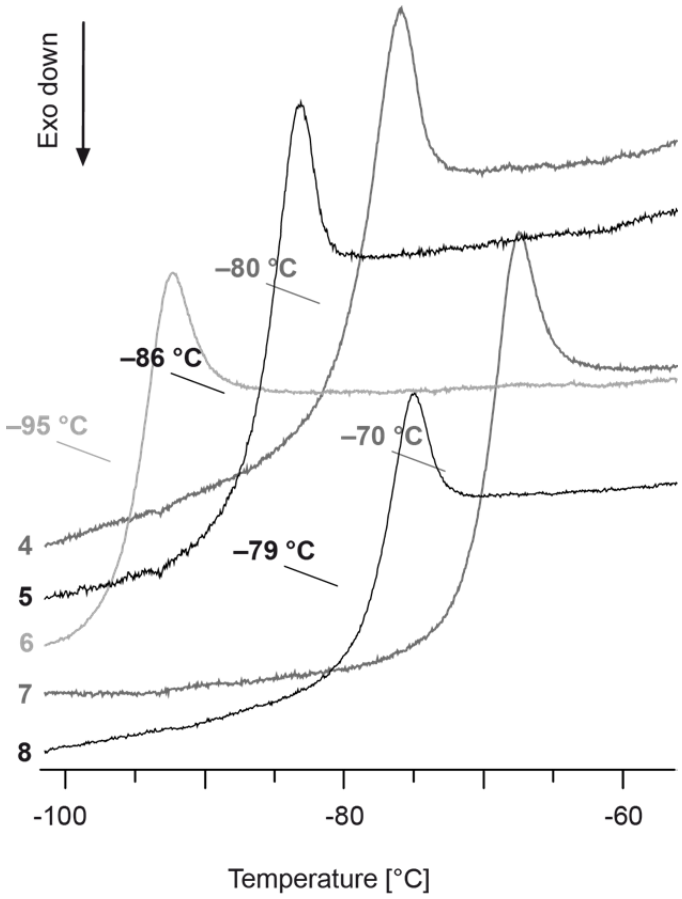

Figure 6.13 DSC plots of glass transition temperatures of **4-8**.

The DNPD based esters possess good glass transition temperatures with values of −70 °C (AcDNPD, **7**) and −79 °C (ProDNPD, **8**). Whereas the BAMP based derivatives show even lower values for T_g, starting with −78 °C (AcBAMP, **4**), over −86 °C (ProBAMP, **5**), down to −94 °C in case of ButBAMP (**36**).

6.2.4 Sensitivities and Energetic Properties

The impact and friction sensitivities were explored by BAM methods.[24] All compounds were tested as insensitive towards impact (>40 J) and friction (>360 N).

For calculating the energetic properties of compounds **4-10** quantum chemical calculations had to be run. Initial structure optimizations were performed at the B3LYP/cc-pVDZ level of theory using the Gaussian 09 revision A.02 program package[25]. Heats of formation of compounds **4-10** were calculated with the atomization method (Equation 6.1) using CBS-4M enthalpies (at room temperature) given in **Table 6.1**.[26 27]

$$\Delta_f H^\circ_{(g,\,M,\,298)} = H_{(molecule,\,298)} - \Sigma H^\circ_{(atoms,\,298)} + \Sigma \Delta_f H^\circ_{(atoms,\,298)} \qquad (\mathbf{6.1})$$

Table 6.1. CBS-4M electronic enthalpies for atoms C, H, N, O and their literature values for atomic $\Delta H^\circ_f{}^{298}$.

	$-H^{298}_{CBS\text{-}4M}$ / a.u.	NIST[28] / kJ mol^{-1}
H	0.500991	218.2
C	37.786156	717.2
N	54.522462	473.1
O	74.991202	249.5

The enthalpies (H) were calculated using the complete basis set (CBS) method of Petersson and coworkers in order to obtain very accurate energies. The CBS models use the known asymptotic convergence of pair natural orbital expressions to extrapolate from calculations using a finite basis set to the estimated complete basis set limit. CBS-4 begins with a HF/3-21G(d) structures optimization, the zero point energy is computed at the same level. It then uses a large basis set SCF calculation as a base energy, and a MP2/6-31+G calculation with a CBS extrapolation to correct the energy through second order. A MP4(SDQ)/6-31+ (d,p) calculation is used to approximate higher order contributions. In this study we applied the modified CBS-4M method (M referring to the use of Minimal Population localization) which is a reparametrized version of the original CBS-4 method and also includes some additional empirical corrections.[26]

In order to be able to convert the standard enthalpies of formation $\Delta_f H^\circ$(g) for the gas-phase

into values for the condensed and solid phase, the enthalpy of vaporization $\Delta H_{vap.}$ (for liquids) and $\Delta H_{sub.}$ (for solids) is required additionally. These values can be estimated using the TROUTON's rule.[29] With the calculated enthalpy of vaporization the gas-phase enthalpy of formation can be converted into the corresponding condensed-phase enthalpy of formation. **Table 6.2** shows the results of the calculations.

Table 6.2. Calculation results.

	$-H^{298}$ [a] / a.u.	$-\Delta_f H$ (g, M) [b] /kJ mol^{-1}	$\Delta_f H_{vap/sub}$ [c] /kJ mol^{-1}
4	979.342825	196.8	45.28
5	1057.817702	250.8	45.01
6	1136.292346	304.1	44.92
7	982.662516	825.8	46.45
8	1061.138526	882.7	46.27
9	1205.290540	273.7	66.96
10	1283.765986	329.1	59.44

[a] CBS-4M electronic enthalpy; [b] gas phase enthalpy of formation; [c] enthalpy of vaporization.

Detonation parameters were calculated using the EXPLO5 V6.02 computer code[30] with the CBS-4M calculated enthalpies of formation. The program is based on the steady-state model of equilibrium and uses the Becker-Kistiakowsky-Wilson equation of state (BKW EOS.) for gaseous detonation products and the Murnaghan EOS for both solid and liquid products. It is designed to enable the calculation of detonation parameters at the Chapman-Jouguet point (C-J point). The C-J point was found from the Hugoniot curve of the system by its first derivative.[30] The calculations were performed using the densities obtained by pycnometric measurements at room temperature.

The calculated detonation values, energetic properties and decomposition as well as glass transition points of compounds **4-10** are given in **Table 6.3** and were compared to the literature known plasticizers DEGBAA (for azido plasticizer) and BuNENA (for *gem*-nitro plasticizer), respectively.

Compared to DEGBAA all three BAMP based esters show overall better physical and energetic properties. They possess a higher detonation pressure p_{CJ} (79 kbar (**4**), 72 kbar (**5**), 62 kbar (**6**) *versus* 46 kbar (DEGBAA)) and velocity V_{det} (5420 m s^{-1} (**4**), 5292 m s^{-1} (**5**), 5048 m s^{-1} (**6**) *versus* 4363 m s^{-1} (DEGBAA)). Furthermore they are less sensitive towards

friction and impact, are stable up to higher temperatures and have a significantly lower glass transition temperature. All these values emphasize **4-6** as potentiel compounds for the use as energetic azido plasticizers.

The DNPD based esters show lower values regarding V_{det} (5683 m s^{-1} (**7**), 5111 m s^{-1} (**8**) *versus* 6275 m s^{-1} (BuNENA)) and specific impulse I_s (181 s (**7**), 177 s (**8**) *versus* 216 s (BuNENA)) compared to BuNENA. However, since **7** and **8** are less sensitive towards friction (FS (BuNENA) 108 N) and more stable up to much higher temperatures, they possess a clear advantage in terms of safety. Compared to the BAMP based compounds their detonation values lie within the same range, which marks them as suitable energetic plasticizers as well.

The bistetrazolo compounds **9** and **10** show the highest detonation velocities of the synthesized compounds, with 6750 m s^{-1} and 6326 m s^{-1}, a detonation pressure in the range of BuNENA, with 111 kbar (**10**) or above with 133 kbar (**9**) but the lowest specific impulse, with values around 160 s.

Besides this, all compounds show lower explosion temperatures T_E compared to the reference compounds. This can be seen as an advantage, when used as plasticizing additives in formulations for propelling charges, since it diminishes the erosion of the gun barrel.

Table 6.3. Sensitivities and detonation parameters of **4-10** compared to DEGBAA and BuNENA.

	4	**5**	**6**	**DEGBAA[p]**	**7**	**8**	**BuNENA[q]**	**9**	**10**
Formula	$C_9H_{14}N_6O_4$	$C_{11}H_{18}N_6O_4$	$C_{13}H_{22}N_6O_4$	$C_8H_{12}N_6O_4$	$C_7H_{10}N_2O_8$	$C_9H_{14}N_2O_8$	$C_6H_{13}N_3O_5$	$C_{12}H_{18}N_8O_4$	$C_{14}H_{22}N_8O_4$
FW [g mol^{-1}]	270.25	298.30	326.17	256.22	250.04	278.22	207.18	338.32	366.38
IS [J][a]	>40	>40	>40	>10	>40	>40	40[r]	>40	>40
FS [N][b]	>360	>360	>360	160	>360	>360	108[r]	>360	>360
N [%][c]	31.10	28.17	25.75	32.80	11.20	10.07	20.28	33.12	30.58
Ω [%][d]	−124	−145	−162	−112	−70	−98	−104	−137	−153
T_{dec} [°C][e]	230	227	226	215	241	243	165	232	240
T_g [°C][f]	−80	−86	−95	−63	−70	−78	−84[s]	-	-
ρ [g cm^{-3}][g]	1.21	1.16	1.09	1.00	1.33	1.22	1.21	1.51[t]	1.40[t]
$-\Delta_f H_m°$ [kJ mol^{-1}][h]	242	296	349	329	872	926	167	340	389
$-\Delta_f U°$ [kJ kg^{-1}][i]	785	876	948	1178	3387	3222	680	895	947
Explo5 V6.02 values									
$-\Delta_E U°$ [kJ kg^{-1}][j]	3018	2795	22615	2639	3420	3267	5044	2381	2259
T_E [K][k]	2123	1930	1795	2038	2528	2317	2961	1738	1649
p_{CJ} [kbar][l]	79	72	62	46	100	75	117	133	111
V_{det} [m s^{-1}][m]	5420	5292	5048	4363	5683	5111	6275	6750	6326
Gas vol. [L kg^{-1}][n]	793	799	807	806	772	786	914	740	749
I_s [s][o]	175	171	167	169	181	177	216	161	159

[a] BAM drop hammer (1 of 6); [b] BAM friction tester (1 of 6); [c] nitrogen content; [d] oxygen content; [e] temperature of decomposition by DSC (onset values); [f] glass transition temperature (T_{gMid}), [g] derived from pycnometer measurements; [h] molar enthalpy of formation; [i] energy of formation; [j] energy of explosion; [k] explosion temperature; [l] detonation pressure; [m] detonation velocity ; [n] assuming only gaseous products; [o] specific impulse (isobaric combustion, chamber pressure 70 bar, equilibrium expansion); [p] values obtained from reference[10], [q] values obtained from reference [1]; [r] values obtained from reference[31]; [s] value obtained from reference[6], [t] estimated from structure determination.

6.2.5 Applications

In order to study the plasticizing effects, propionyl based ProBAMP (**5**) and ProDNPD (**8**) were chosen as example compounds. The esters **5** and **8** were mixed in ratios of 25, 35 and 50 wt-% with the uncured energetic polymers glycidyl azide polymer (GAP) and poly(3-nitratomethyl-3-methyloxetan) (polyNIMMO). For a better comparison of the plasticizing effect, mixtures of GAP and polyNIMMO in the same ratio were also prepared with BuNENA. To determine their plasticizing influence, values of T_g of the neat polymers were compared to the values of the mixtures (**Table 6.4**).

Table 6.4 Glass transition temperatures of neat **5**, **8**, GAP and polyNIMMO and their corresponding mixtures (ratios).

Substance	T_g (neat) [°C]	T_g (0.25) [°C]	T_g (0.35) [°C]	T_g (0.5) [°C]
GAP	−49	-	-	-
ProBAMP (**5**)	−86	−60	−64	−71
ProDNPD(**8**)	−78	−59	−61	−65
BuNENA	−84 [a]	−63	−67	−72
PolyNIMMO	−32	-	-	-
ProBAMP (**5**)	−86	−53	−55	−69
ProDNPD(**8**)	−78	−54	−55	−66
BuNENA	−84 [a]	−63	−64	−75

[a] Value obtained from reference[6].

In case of the polyNIMMO mixtures, both compounds decrease the glass transition temperature by a similar value. Whereas, in case of GAP, **5** shows better decreasing effects on T_g than **8**. The mixtures of **5** decrease the glass transition temperature by values in the range of the corresponding BuNENA mixtures.

Furthermore, the ability of **5** and **8** to lower the viscosity of polyNIMMO and GAP was investigated considering the respective 50/50 mixtures at 20 °C and 50 °C (**Table 6.5**). The viscosity of the mixtures was independent from the shear rate.

Table 6.5. Viscosity of 50/50 mixtures of polyNIMMO and GAP with **5** and **8** at 20 and 50 °C.

Polymer	Plasticizer	Viscosity [a] [mPa s]	
		20 °C	50 °C
GAP	-	5,550	628
	ProBAMP (**5**)	269	62
	ProDNPD (**8**)	289	62
	BuNENA	281	60
PolyNIMMO	-	270,000	11,900
	ProBAMP (**5**)	915	163
	ProDNPD (**8**)	627	116
	BuNENA	662	126

[a] Values obtained at a shear rate of 10 s^{-1}.

In case of the GAP mixtures, the performances of both compounds (**5** and **8**) in lowering the viscosity are very similar to the effectiveness of BuNENA, which is considered to be very efficient in this respect. For the polyNIMMO mixtures, ProDNPD (**8**) and BuNENA have comparable effects in lowering the viscosity. They are both more efficient than ProBAMP (**5**) in that case.

6.3 Conclusion

In this chapter, the one-step syntheses and characterizations of seven different carboxylic esters on the basis of 2,2-bis(azidomethyl)propane-1,3-diol, 2,2-dinitropropane-1,3-diol and 1,2-bis(hydroxyethyl tetrazole-5-yl)ethane using acetyl, propionyl and butyryl chloride were described. The obtained products were liquids or waxy solids. The successful synthesis of the compounds was proven by ^{1}H, ^{13}C and ^{14}N NMR, vibrational spectroscopy (IR) and EA.
Furthermore, the compounds were investigated regarding their sensitivities towards impact and friction, as well as their thermal stabilities and low temperature behavior and volatility. The compounds turned out to be insensitive towards friction and impact. The liquid compounds possess relatively high decomposition temperatures with approximately 230 °C and 240 °C and very low glass transition temperatures between −70 °C and −95 °C, but are volatile at temperatures around 70-100 °C. The waxy, solid compounds based on

bistetrazoloethane show a broad gap of around 200 °C between their melting and decomposition temperature (~240 °C), which makes them interesting compounds for melt-castable applications. Determination of the detonation parameters of the synthesized compounds was performed by the EXPLO5 (Version 6.02) computer code using calculated enthalpies of formation (CBS-4M) and densities determined *via* pycnometric measurements The compounds show moderate detonation values in the region of V_{det} = 6750-5048 m s^{-1} and p_{CJ} = 62-133 kbar.

For estimating the plasticizing effect, the influence on the glass transition temperature and viscosity of polyNIMMO and GAP was investigated by measuring mixtures of those with the propionyl based liquid esters in different ratios. Both compounds reduce the glass transition temperature of the polymers roughly by the same value. Furthermore both compounds were also efficient in lowering the viscosity of polyNIMMO and GAP. All these properties mark the synthesized esters as promising energetic plasticizers for the use in energetic formulations.

6.4 Experimental Part

6.4.1 General Procedure (GP1)

The respective diol (3-5 mmol) was dissolved in the acid anhydride (15-25 mL) and cooled to 0 °C. The corresponding acyl chloride (4 equivalents) was added dropwise and the mixture was allowed to warm to room temperature while stirring overnight. The reaction mixture was cooled to 0 °C, a saturated aqueous solution of $NaHCO_3$ (50-70 mL) was added in portions and stirred for 1 h. The solution was then extracted with EtOAc (3 x 30 mL) and the combined organic phases were washed again with saturated aqueous $NaHCO_3$ (3 x 30 mL) and water (1 x 30 mL). The organic phase was then dried over $MgSO_4$ and the volatiles were removed *in vacuo*. For **2**, **3** and **5-7** the crude product was further purified by column chromatography.

6.4.2 2,2-Bis(azidomethyl)propane-1,3-diol Based Esters

2,2-Bis(azidomethyl)propane-1,3-diyl diacetate (AcBAMP, 4)

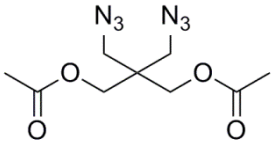

AcBAMP was synthesized from BAMP (1.0 g, 5.37 mmol) and acetyl chloride (1.53 mL, 21.50 mmol) in acetic anhydride (20 mL) applying **GP1**. The reaction gave 1.19 g (4.41 mmol, 82 %) of **4** as colorless liquid.

Density: ρ = 1.21 g cm^{-3}.
DSC (5 °C min^{-1}): T_{dec} = 230 °C.
^{1}H NMR (400 MHz, DMSO-*d6*, ppm): δ = 3.97 (s, 4H, CH_2−O), 3.48 (s, 4H, CH_2−N_3), 2.05 (s, 6H, CH_3).
^{13}C NMR (DMSO-d_6, ppm): δ = 170.0 (*C*=O), 62.6 (*C*H_2−O), 51.2 (*C*H_2−N_3), 42.6 (C_q), 20.4 (*C*H_3).
^{14}N NMR (DMSO-d_6, ppm): δ = −134 (N_β), −175 (N_γ), −342 (N_α).
IR (ATR, cm^{-1}): $\tilde{\nu}$ = 2962 (w), 2097 (s), 1739 (s), 1452 (w), 1385 (w), 1367 (m), 1217 (s), 1040 (s), 988 (w), 904 (m), 842 (w).
EA ($C_9H_{14}N_6O_4$, 270.25 g mol^{-1}): calculated: C 40.00, H 5.22, N 31.10 %; found: C 40.27, H 4.93, N 31.06 %.
Sensitivities: IS: 40 J; **FS**: > 360 N.

2,2-Bis(azidomethyl)propane-1,3-diyl dipropionate (ProBAMP, 5)

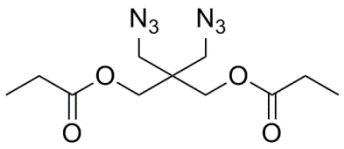

ProBAMP was synthesized from BAMP (1.0 g, 5.37 mmol) and propionyl chloride (1.88 mL, 21.48 mmol) in propionic anhydride (15 mL) applying **GP1**. After purification (*n*-hexane:ethyl acetate = 8:2), 1.25 g (4,21 mmol, 78 %) of **5** were obtained as colorless liquid

Density: ρ = 1.16 g cm^{-3}.

DSC (5 °C min^{-1}): T_{dec} = 227 °C.

^{1}H NMR (400 MHz, DMSO-d_6, ppm): δ = 3.99 (s, 4H, CH_2−O) 3.48 (s, 4H, CH_2−N$_3$), 2.35 (q, $^{3}J_{HH}$ = 7.5 Hz, 4H, CH_2−CH$_3$), 1.04 (t, $^{3}J_{HH}$ = 7.5 Hz, 6H, CH_3).

^{13}C NMR (DMSO-d_6, ppm): δ = 173.2 (*C*=O), 62.5 (*C*H$_2$-O), 51.2 (*C*H$_2$-N$_3$), 42.8 (C_q), 26.7 (*C*H$_2$), 8.8 (*C*H$_3$).

^{14}N NMR (DMSO-d_6, ppm): δ = −133 (N_β), −178 (N_γ), −301 (N_α).

IR (ATR, cm^{-1}): $\tilde{\nu}$ = 2983 (w), 2945 (w), 2095 (s), 1738 (s), 1463 (m), 1424 (w), 1384 (w), 1350 (m), 1272 (m), 1167 (s), 1083 (s), 1025 (s), 972 (w), 905 (w), 806 (m).

EA ($C_{11}H_{18}N_6O_4$, 298.30 g mol^{-1}): calculated: C 44.29, H 6.08, N 28.17 %; found: C 44.16, H 6.01, N 28.46 %.

Sensitivities: IS: 40 J; **FS**: > 360 N.

2,2-Bis(azidomethyl)propane-1,3-diyl dibutyrate (ButBAMP, 6)

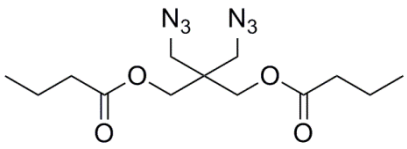

ButBAMP was synthesized from BAMP (1.0 g, 5.37 mmol) and butyryl chloride (2.22 mL, 21.48 mmol) in butyric anhydride (25 mL) applying **GP1**. After purification (*n*-hexane:ethyl acetate = 8:2), 0.25 g (0.77 mmol, 14 %) of **6** were obtained as colorless liquid.

Density: ρ = 1.09 g cm^{-3}.

DSC (5 °C min^{-1}): T_{dec} = 226 °C.

^{1}H NMR (400 MHz, DMSO-d_6, ppm): δ = 3.98 (s, 4H, CH_2−O), 3.48 (s, 4H, CH_2−N$_3$), 2.31 (t, $^{3}J_{HH}$ = 7.3 Hz, 4H, CH_2−CH$_2$), 1.55 (sextet, $^{3}J_{HH}$ = 7.3 Hz, 4H, CH_2−CH$_3$), 0.88 (t, $^{3}J_{HH}$ = 7.3 Hz, 6H, CH_3).

^{13}C NMR (DMSO-d_6, ppm): δ = 172.4 (*C*=O), 62.5 (*C*H$_2$−O), 51.2 (*C*H$_2$−N$_3$), 42.7 (C_q), 35.2 (*C*H$_2$) 17.8 (*C*H$_2$), 13.4 (*C*H$_3$).

^{14}N NMR (DMSO-d_6, ppm): δ = −133 (N_β), −180 (N_γ), −302 (N_α).

IR (ATR, cm^{-1}): $\tilde{\nu}$ = 2966 (m), 2938 (w), 2877 (w), 2095 (s), 1737 (s), 1454 (m), 1418 (w), 1386 (w), 1361 (w), 1284 (m), 1251 (s), 1165 (s), 1090 (m), 1049 (m), 1009 (w), 930 (w), 881 (w), 751 (w).

EA ($C_{13}H_{22}N_6O_4$, 326.25 g mol^{-1}): calculated: C 47.84, H 6.79, N 25.75 %; found: C 47.99, H 6.80, N 25.50 %.

Sensitivities: IS: 40 J; **FS**: > 360 N.

6.4.3 2,2-Dinitropropane-1,3-diol Based Esters

2,2-Dinitropropane-1,3-diol diacetate (AcDNPD, 7)

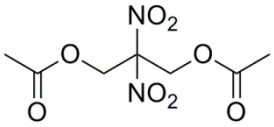

AcDNPD was synthesized from DNPD (0.5 g, 3.01 mmol) and acetyl chloride (0.86 mL, 12.04 mmol) in acetic anhydride (10 mL) applying **GP1**. The reaction gave 0.62 g (2.48 mmol, 82 %) of **7** as colorless liquid.

Density: ρ = 1.33 g cm^{-3}.

DSC (5 °C min^{-1}): T_{dec} = 241 °C.

^{1}H NMR (400 MHz, DMSO-d_6, ppm): δ = 5.13 (s, 4H, CH_2−O), 2.08 (s, 6H, CH_3).

^{13}C NMR (DMSO-d_6, ppm): δ = 168.9 (*C*=O), 115.0 (C_q), 60.7 (*C*H$_2$−O), 20.1 (*C*H$_3$).

^{14}N NMR (DMSO-d_6, ppm): δ = −16 (*N*O$_2$).

IR (ATR, cm^{-1}): $\tilde{\nu}$ = 2970 (w), 1758 (s), 1572 (s), 1456 (w), 1392 (w), 1377 (m), 1321 (m), 1198 (s), 1047 (s), 905 (w), 846 (m), 762 (w), 686 (w).

EA ($C_7H_{10}N_2O_8$, 250.16 g mol^{-1}): calculated: C 33.61, H 4.03, N 11.20 %; found: C 33.59, H 3.98, N 11.69 %.

Sensitivities: IS: 40 J; **FS**: > 360 N.

2,2-Dinitropropane-1,3-diol dipropionate (ProDNPD, 8)

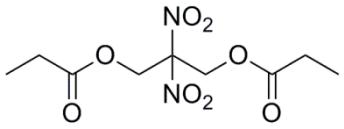

ProDNPD was synthesized from DNPD (0.5 g, 3.01 mmol) and propionyl chloride (1.05 mL, 12.04 mmol) in propionic anhydride (10 mL) applying **GP1**. After purification (*n*-hexane:acetone = 7:3), 0.64 g (2.29 mmol, 76 %) of **8** were obtained as colorless liquid.

Density: ρ = 1.22 g cm^{-3}.
DSC (5 °C min^{-1}): T_{dec} = 242 °C.
^{1}H NMR (400 MHz, DMSO-d_6, ppm): δ = 5.14 (s, 4H, CH_2−O), 2.38 (q, $^{3}J_{HH}$ = 7.5 Hz, 4H, CH_2−CH$_3$), 1.01 (t, $^{3}J_{HH}$ = 7.5 Hz, 6H, CH_3).
^{13}C NMR (DMSO-d_6, ppm): δ = 172.1 (*C*=O), 115.2 (C_q), 60.6 (*C*H$_2$−O), 26.4 (*C*H$_2$), 8.6 (*C*H$_3$).
^{14}N NMR (DMSO-d_6, ppm): δ = −16 (NO$_2$).
IR (ATR, cm^{-1}): $\tilde{\nu}$ = 2988 (w), 2948 (w), 2890 (w), 1756 (s), 1570 (s), 1462 (m), 1422 (w), 1391 (w), 1375 (w), 1344 (w), 1321 (m), 1270 (w), 1145 (s), 1086 (s), 1035 (m), 967 (w), 844 (m), 806 (m), 765 (w), 684 (w).
EA ($C_9H_{14}N_2O_8$, 278.22 g mol^{-1}): calculated: C 38.85, H 5.07, N 10.07 %; found: C 39.07, H 5.05, N 10.08 %.
Sensitivities: IS: 40 J; **FS**: > 360 N.

6.4.4 1,2-Bis(hydroxyethyl tetrazol-5-yl)ethane Based Esters

1,2-Bis(hydroxyethyl tetrazol-5-yl)ethane diacetate (BTEOAc, 9)

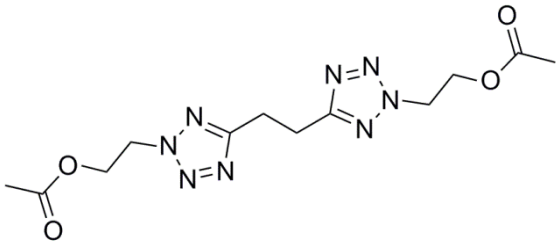

BTEOAc was synthesized from BTEOH (1.0 g, 3.93 mmol) and acetyl chloride (1.12 mL, 15.73 mmol) in acetic anhydride (20 mL) applying **GP1**. After purification (*n*-hexane:ethyl acetate = 3:7), 0.31 g (0.92 mmol, 23 %) of **9** were obtained as waxy solid.

DSC (5 K min^{-1}): T_{melt} = 82 °C; T_{dec} = 232 °C.

^{1}H NMR (DMSO-d_6, ppm): δ = 4.88 (t, $^{3}J_{HH}$ = 5.3 Hz, 4H, CH_2-CH_2−O), 4.46 (t, $^{3}J_{HH}$ = 5.3 Hz, 4H, CH_2-O), 3.31 (s, 4H, CH_2-$C_{tetrazole}$), 1.93 (s, 6H, CH_3).

^{13}C NMR (DMSO-d_6, ppm): δ = 169.9 (*C*=O), 164.8 ($C_{q,tetrzole}$), 61.2 (CH_2−O), 51.5 (CH_2−$N_{tetrazole}$), 23.1 (CH_2−$C_{tetrazole}$), 20.4 (CH_3).

IR (ATR, cm^{-1}): $\tilde{\nu}$ = 2971 (w), 2360 (w), 2337 (w), 2063 (w), 1877 (w), 1733 (s), 1696 (w), 1658 (w), 1501 (m), 1460 (w), 1440 (m), 1426 (m), 1386 (m), 1368 (m), 1324 (w), 1225 (s), 1194 (s), 1164 (m), 1073 (s), 1043 (s), 1029 (s), 1004 (m), 939 (s), 828 (m), 802 (m), 786 (m), 748 (s), 696 (w), 661 (w).

EA ($C_{12}H_{18}N_8O_4$, 338.32 g mol^{-1}): calculated: C 42.60, H 5.36, N 33.12 %; found: C 42.94, H 5.39, N 32.58 %.

HRMS (ESI+): *m/z* calculated $[M+H]^+$: 339.1524, found: 339.1525.

1,2-Bis(hydroxyethyl tetrazol-5-yl)ethane dipropionate (BTEOPro, 10)

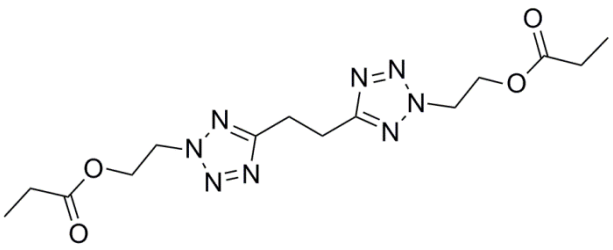

BTEOPro was synthesized from BTEOH (1.0 g, 3.93 mmol) and propionyl chloride (1.37 mL, 15.73 mmol) in propionic anhydride (15 mL) applying **GP1**. After purification (*n*-hexane:ethyl acetate:DCM = 1.3:1.3:1), 0.25 g (0.69 mmol, 18 %) of **9** were obtained as waxy solid.

DSC (5 K min^{-1}): T_{melt} = 43 °C; T_{dec} = 240 °C.

^{1}H NMR (DMSO-d_6, ppm): δ = 4.88 (t, $^{3}J_{HH}$ = 5.5 Hz, 4H, CH_2-CH_2-O), 4.47 (t, $^{3}J_{HH}$ = 5.5 Hz, 4H, CH_2-O), 3.30 (s, 4H, CH_2-$C_{tetrazole}$), 2.22 (q, $^{3}J_{HH}$ = 7.5 Hz, 4H, CH_2-CH_3), 0.94 (t, $^{3}J_{HH}$ = 7.5 Hz, 6H, CH_3).

^{13}C NMR (DMSO-d_6, ppm): δ = 173.2 (C=O), 164.8 ($C_{q,tetrzole}$), 61.2 (CH_2−O), 51.6 (CH_2−$N_{tetrazole}$), 26.6 (CH_2−CH_3), 23.1 (CH_2−$C_{tetrazole}$), 8.8 (CH_3).

IR (ATR, cm^{-1}): $\tilde{\nu}$ = 3017 (w), 2978 (w), 2941 (w), 2881 (w), 1734 (s), 1699 (w), 1547 (w), 1495 (m), 1458 (m), 1436 (m), 1408 (w), 1380 (m), 1359 (m), 1346 (m), 1316 (w), 1268 (w), 1240 (m), 1167 (s), 1087 (s), 1074 (s), 1032 (s), 1013 (m), 994 (m), 897 (m), 837 (m), 810 (m), 791 (m), 750 (m), 704 (w), 684 (w).

EA ($C_{14}H_{22}N_8O_4$, 366.38 g mol^{-1}): calculated: C 45.90, H 6.05, N 30.58 %; found: C 45.73, H 6.06, N 29.74 %.

HRMS (ESI+): *m/z* calculated $[M+H]^+$: 367.1837, found: 367.1834.

6.5 References

[1] H. G. Ang, S. Pisharath *Energetic Polymers – Binders and Plasticizers for Enhancing Performance*, WILEY-VCH, Weinheim, **2012**.

[2] J. P. Agrawal, *High Energy Materials*, WILEY-VCH, Weinheim **2010**.

[3] R. S. Damse, A. Singh, *Def ence Sci. J.* **2008**, *58*, 86-93.

[4] A. Provatas, Report *DSTO-TR-0966*, Defence Science and Technology Organisation, Melbourne Victoria, Australia **2000**.

[5] H. Licht, H. Ritter, B. Wanders, "NENA-Sprengstoffe", *27th Annual Conference of ICT*, Karlsruhe, Germany, June 25-28, **1996**.

[6] N. Wingborg, C. Eldsäter, *Propellants, Explos., Pyrotech.* **2002**, *27*, 314-319.

[7] T. K. Highsmith, D. W. Doll, L. F. Cannizzo, *US 6,425,966*, **2002**.

[8] S. Ek, C. Eldsäter, P. Goede, E. Holmgren, R. Tryman, N. Latypov, Y. G. Y. Raymond, L. Y. Wang, Synthesis and Characterisation of 2,2-Dinitro-1,3-propanediol-based Plasticisers, *New Trends Res. Energ. Mater., Proc. 8th Semin.*, Pardubice, Czech Republic, April 10-12, **2005**.

[9] D. Kumari, H. Singh, M. Patil, W. Thiel, C. S. Pant, S. Banerjee, , *Thermochim. Acta* **2013**, *562*, 96-104.

[10] D. Drees, D. Löffel, A. Messmer, K. Schmid, P*ropellants, Explos., Pyrotech.* **1999**, *24*, 159-162.

[11] C. S. Pant, R. M. Wagh, J. K. Nair, G. M. Gore, M. Thekkekara, S. Venugopalan, *Propellants, Explos., Pyrotech.* **2007**, *32*, 461-467.

[12] a) D. Fischer, T. M. Klapötke, J. Stierstorfer, *Angew. Chem. Int. Ed.* **2014**, *53*, 8172-8175; b) S. Huber, D. Izsák, K. Karaghiosoff, T. M. Klapötke, S. Reuter, *Propellants, Explos,. Pyrotech.* **2014**, *39*, 793–801; c) J. W. Fronabarger, M. D. Williams, W. B. Sanborn, J. G. Bragg, D. A. Parrish, M. Bichay, *Propellants, Explos., Pyrotech.* **2011**,

36, 541-550.

[13] N. Fischer, D. Fischer, T. M. Klapötke, D. G. Piercey, J. Stierstorfer, *J. Mater. Chem.* **2012**, *22*, 20418-20422.

[14] a) N. Fischer, D. Izsák, T. M. Klapötke, S. Rappenglück, J. Stierstorfer, *Chem. Eur. J.* **2012**, *18*, 4051–4062; b) H. Bendler, H. Gawlick, G. Marondel, W. Siegelin, *US 3468730A*, **1968**.

[15] a) G. Steinhauser, K. Tarantik, T. M. Klapötke, *J. Pyrotech*. **2008**, *27*, 3; b) A. Hammerl, G. Holl, T.M. Klapötke, P. Mayer, H. Nöth, H. Piotrowski, M. Warchhold, *Eur. J. Inorg. Chem*. **2002**, *4*, 834; c) T.M. Klapötke, J. Stierstorfer, K. R. Tarantik, I. D. Thoma, *Z. Anorg. Allg. Chem*. **2008**, *634*, 2777; d) E.-C. Koch, *J. Pyrotech*. **2001**, *13*, 1.

[16] D. Diaz, S. Punna, P. Holzer, A. K. McPherson, K. B. Sharpless, V. V. Fokin, M. G. Finn, *J. Polym. Sci. Pol. Chem.* **2004**, *42*, 4392-4403.

[17] a) R. Kaplan, H. Shechter, *J. Am. Chem. Soc.* **1961**, *83*, 3535-3536; b) L. Garver, V. Grakauskas, K. Baum, *J. Org. Chem.* **1985**, *50*, 1699-1702.

[18] A Chafin, D. J. Irvin, M. H. Mason, S. L. Mason, *Tetrahedron Lett.* **2008**, *49*, 3823-3826.

[19] V. O. Rodionov, V. V. Fokin, M. G. Finn, *Angew. Chem. Int. Ed.* **2005**, *44*, 2210-2215.

[20] H. Feuer, G. B. Bachman, J. P. Kispersky, *J. Am. Chem. Soc.* **1951**, *73*, 1360.

[21] M. Witanowski, L. Stefaniak, G. A. Webb, *Nitrogen NMR Spectroscopy*, Academic Press, London, **1993**.

[22] M. Hesse, H. Meier, B. Zeh, *Spektroskopische Methoden in der organischen Chemie*, 7. Edition, Thieme Verlag, Stuttgart, **2005**.

[23] E. Lieber, C. N. Ramachandra Rao, T. S. Chao, C. W. W. Hoffman, *Anal. Chem.* **1957**, *29*, 916-918.

[24] http://www.bam.de (accessed April, 2016).

[25] M. J. Frisch, G. W. Trucks, H. B. Schlegel, G. E. Scuseria, M. A. Robb, J. R. Cheeseman, V. B. Scalmani, B. Mennucci, G. A. Petersson, H. Nakatsuji, M. Caricato, X. Li, H. P. Hratchian, A. F. Izmaylov, J. Bloino, G. Zheng, J. L. Sonnenberg, M. Hada, M. Ehara, K. Toyota, R. Fukuda, J. Hasegawa, M. Ishida, T. Nakajima, Y. Honda, O. Kitao, H. Nakai, T. Vreven, J. A. Montgomery, J. E. Peralta, F. Ogliaro, M. Bearpark, J. J. Heyd, E. Brothers, K. N. Kudin, V.-N. Staroverov, R. Kobayashi, J. Normand, K. Raghavachari, A. Rendell, J. C. Burant, S. S. Iyengar, J. Tomasi, M. Cossi, N. Rega, J. M. Millam, M. Klene, J. E. Knox, J. B. Cross, V. Bakken, C. Adamo, J. Jaramillo, R. Gomperts, R. E. Stratmann, O. Yazyev, A. J. Austin, R. Cammi, C. Pomelli, J. W. Ochterski, R. L. Martin, K. Morokuma, V. g Zakrzewski, G. A. Voth, P. Salvador, J. J. Dannenberg, S. Dapprich, A. D. Daniels, Ö. Farkas, J. B. Foresman, J. V. Ortiz, J., J. Cioslowski, D. J. Fox,. *Gaussian 09*. Rev. A.03 ed.; Gaussian, Inc.: Wallingford CT, **2009**.

[26] a) J. W. Ochterski, G. A. Petersson, J. A. Montgomery Jr., A complete basis set model chemistry. V. Extensions to six or more heavy atoms, *J. Chem. Phys.* **1996**, *104*, 2598; b) J. A. Montgomery Jr., M. J. Frisch, J. W. Ochterski, G. A. Petersson, A complete basis set model chemistry. VII. Use of the minimum population localization method, *J. Chem. Phys.* **2000**, *112*, 6532.

[27] a) L. A. Curtiss, K. Raghavachari, P. C. Redfern, J. A. Pople, Assessment of Gaussian-2 and density functional theories for the computation of enthalpies of formation, *J. Chem. Phys.* **1997**, *106*, 1063; b) E. F. C. Byrd, B. M. Rice, Improved Prediction of Heats of Formation of Energetic Materials Using Quantum Chemical Methods, *J. Phys. Chem*. A **2006**, *110*, 1005−1013; c) B. M. Rice, S. V. Pai, J. Hare, Predicting Heats of Formation of Energetic Materials Using Quantum Chemical Calculations, *Comb. Flame* **1999**, *118*, 445−458.

[28] P. J. Lindstrom, W. G. Mallard (Editors), NIST Standard Reference Database Number 69, http://webbook.nist.gov/chemistry/ (accessed April, 2016).

[29] F. Trouton, *Philos. Mag.* **1884**, *18*, 54-57.

[30] a) M. Sućeska, Calculation of the detonation properties of C-H-N-O explosives,

Propellants, Explos., Pyrotech. **1991**, *16*, 197–202; b) Sućeska, M. *EXPLO5 V.6.02*. Zagreb (Croatia), **2013**.

[31] D. Izsák, *Masterthesis*, Ludwig-Maximilians-Universität München, **2011**.

SUMMARY

7. Summary

The general goal of this thesis was the synthesis and characterization of new energetic polymers and plasticizers based on organic azides, nitro groups and tetrazoles. Additionally, some other compounds containing triazoles and nitramino groups were investigated.
The most intensively investigated topic was the synthesis and characterization of energetic polyurethanes (PUs). Here, several energetic diols were used for the polyaddition reactions of diisocyanates, varying in carbon chain length. The most promising compounds among the synthesized polyurethanes were based on 1,2-dinitropropane-1,3-diol (DNPD) and 1,2-bis(azidomethyl)propane-1,3-diol (BAMP) and the diisocyanates hexamethylene diisocyanate (HMDI) or diisocyanate ethane (DIE). (**Scheme 7.1**).

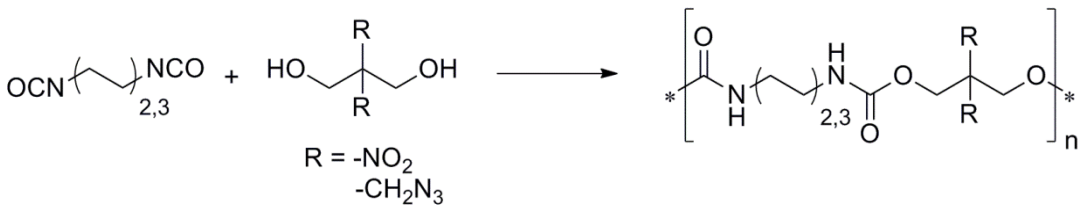

Scheme 7.1 Synthesis of the polyurethanes.

Depending on their diol component, the obtained polymers had a honey-like liquid (BAMP) or an elastic to ductile solid (DNPD) character, which is favorable for the application as a binder. All compounds are insensitive towards friction and less sensitive towards impact. The decomposition temperatures of the polymers were again depending on the diol component and showed values around 170 °C (DNPD) or 210 °C (BAMP). The energetic performance of the substances are good, in the cases of the DNPD based PUs in the range or even better than the one of GAP (glycidyl azide polymer), one of the most promising energetic polymers. Whereas, the BAMP based PUs possess lower temperatures of explosion, compared to GAP. This can be seen as an advantage, if they are used as a binder in propelling charges, since the explosion temperature is directly responsible for the erosion of the gun barrel. Another positive feature of the synthesized polyurethanes is the presence of the carbamate moieties. If applied as binders in energetic formulations, the compounds are able to form hydrogen bridges to the energetic filler, which will lead to increased adhesion forces.

During the synthesis process towards the desired diols for the polyaddition reactions, 2,2-bis(hydroxymethyl-1*H*-1,2,3-triazol-1-yl)methyl)propane-1,3-diol (4-ol) was prepared (**Figure 7.1**). The compound was obtained in a two-step reaction *via* a copper-catalyzed azide-alkyne cycloaddition with BAMP. Due to its tetravalent alcohol function the compound might represent a useful cross-linking agent for polymerization reactions.

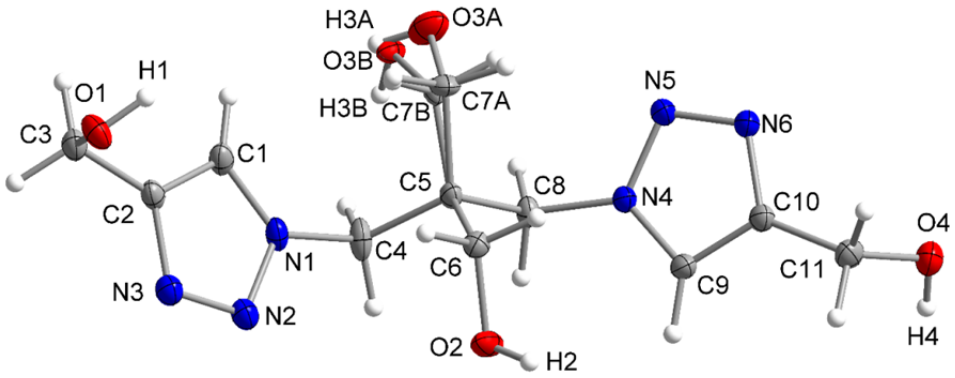

Figure 7.1 Molecular structure of 4-ol.

Another successfully synthesized energetic polymer was based on the glycidyl backbone and introduced the nitramino group as new energetic functional group in context with that kind of polymer. The synthesis was carried out in four steps, applying GAP as the starting material (**Scheme 7.2**).

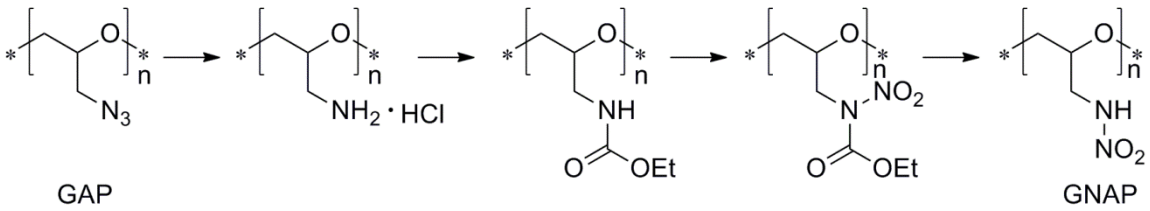

Scheme 7.2 Synthesis of GNAP.

All in all, the synthesized glycidyl nitramine polymer (GNAP) showed better energetic properties than the other glycidyl based energetic polymers, GAP and poly(glycidyl nitrate) (polyGLYN). Additionally, GNAP shows a better stability towards firction (> 360 N) and impact (40 J) compared to the other above mentioned energetic glycidyl polymers, which is a great advantage in terms of safety. Furthermore, GNAP possesses a sticky, solid character,

which makes the use of curing agents (required for the viscous GAP and polyGLYN) unnecessary.

In the course of synthesizing energetic epoxy resins based on mono- and difunctionalized epoxy tetrazoles, two different constitutional isomers of divinyl (1,2-bis(2-vinyl-2H-tetrazol-5-yl)ethane (2,2-DvBTE) (**Figure 7.2**), 1-vinyl-5-(2-(2-vinyl-2H-tetrazol-5-yl)ethyl)-1H-tetrazole (1,2-DvBTE)) and bisallyl (1,2-bis(2-allyl-2H-tetrazol-5-yl)ethane (2,2-BaBTE), 1-allyl-5-(2-(2-allyl-2H-tetrazol-5-yl)ethyl)-1H-tetrazole (1,2-BaBTE)) derivatives of 1,2-bis(tetrazol-5-yl)ethane (BTE) could be isolated and characterized (**Scheme 7.3**). The compounds are insensitive toward impact and friction and possess moderate energetic properties. Moreover, they excel with their relatively high thermal stability, with values around 190 ° to 230 °C, and their high nitrogen content with 46 % and 51 %. Due to their twofold double bonds the substances are very well suited for further processing concerning polymerization or functionalization reactions. Unfortunately, the attempts in synthesizing the mono- and difunctional epoxy compounds maximally yielded traces of the desired compounds or the monoepoxidated molecule, in case of 2,2-BaBTE. Hence, no polymerization steps towards nitrogen-rich epoxy resins were carried out.

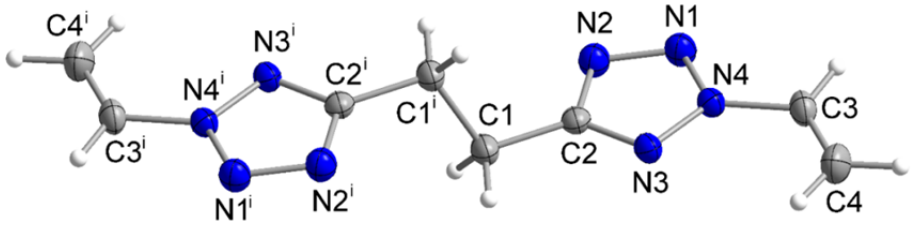

Figure 7.2 Molecular structure of the 2,2'-*N*-substituted isomer of the divinyl derivative of 1,2-bis(tetrazol-5-yl)ethane (2,2-DvBTE).

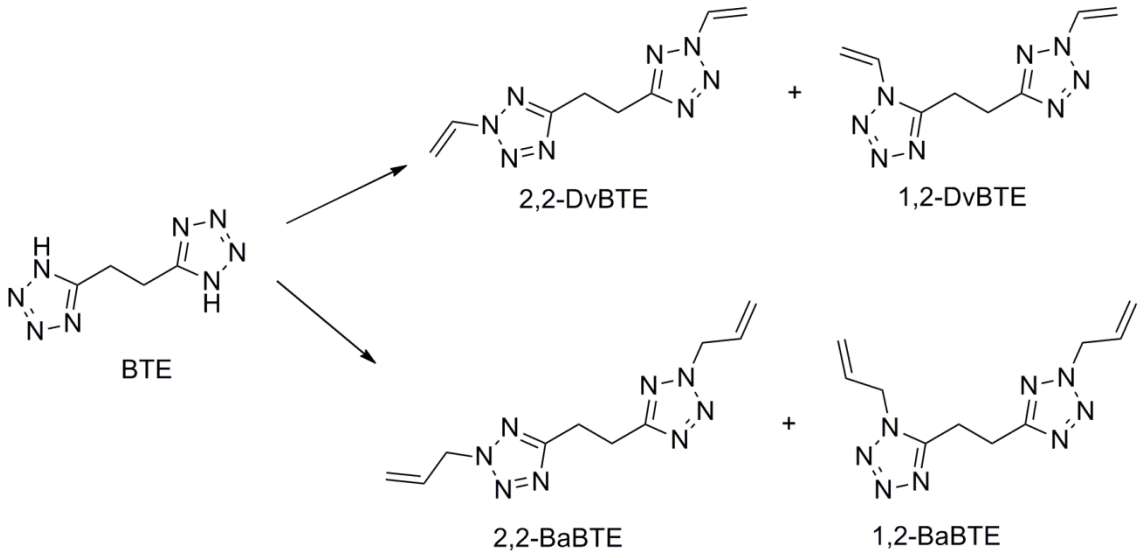

Scheme 7.3 Synthesis of the divinyl and bisallyl derivatives of BTE.

The last topic focused on the investigation of energetic plasticizers based on BAMP, DNPD and 1,2-bis(hydroxyethyl tetrazol-5-yl)ethane (BTEOH). The synthesized compounds were altered in their carbon chain length (**Scheme 7.4**)

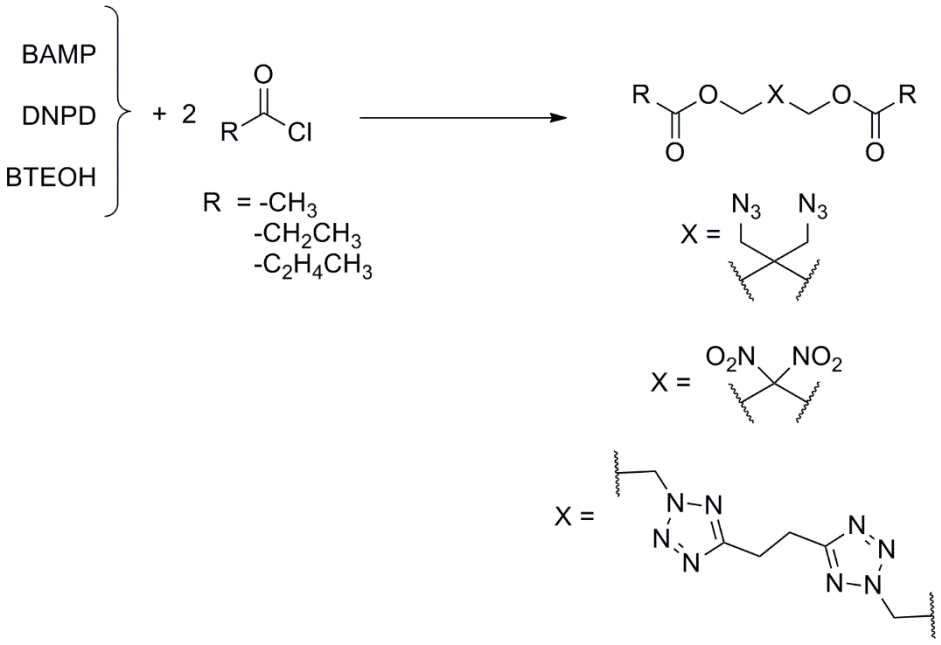

Scheme 7.4 Synthesis of energetic plasticizers.

The esters based on BAMP and DNPD turned out to be promising compounds for plasticizing

applications due to their liquid character. Measurements regarding their glass transition temperature revealed very good values within −70 to −95 °C, which correlate with the range of the known energetic plasticizer *N*-butyl nitratoethylnitramine (BuNENA) around −84 °C. The energetic properties of the plasticizers compete well or even exceed the values of their respective reference, diethylene glycol bis(azidoacetate) ester (DEGBAA, in case of BAMP based compounds) or BuNENA (in case of the DNPD based compounds). Furhermore, they outperform these compounds in terms of safety, since they are insensitive towards friction and impact and possess high decomposition temperatures (230-240 °C).

Plasticizing tests regarding the ability of decreasing glass transition temperature and viscositiy of example mixtures with GAP and polyNIMMO, both used compounds (BAMP and DNPD based propionyl esters) revealed very promising plasticizing properties, comparable to the values of BuNENA.

MATERIALS AND METHODS

8. Materials and Methods

8.1 Chemicals

All used chemical reagents and solvents of analytical grade were obtained either from the companies Sigma-Aldrich, Acros Organics, ABCR or comparable suppliers without any further purification. Hydroxyl-terminated GAP (M_n = 2000 g mol^{-1}) was obtained from BAYERN-CHEMIE mbH.
If necessary, purification of the compounds by column chromatography was performed using Merck silica gel 60 (Ø 40-60 µm). The particularly used solvent is given in the experimental section.

8.2 General Methods

Bomb Calorimetry

Determinations of the bomb calorimetric values were carried out using an isoperibol oxygen bomb calorimeter of the type *Parr 1356*, later *Parr 6200*, equipped with a static bomb.
The calibration of the calorimeter was accomplished by means of the combustion of benzoic acid in oxygen atmosphere at 30 bar.
For the analysis of GNAP, 100 mg to 150 mg substance were mixed with 950 mg to 1100 mg of benzoic acid. The mixture was converted into a pellet which was used for the measurement. All other compounds were analyzed by covering 0.1 g of the substance with 0.5 to 0.6 g paraffin oil.

Crystal Structures

An *Oxford Xcalibur3* diffractometer equipped with a *Spellman* generator (voltage 50 kV, current 40 mA) and a Kappa CCD area detector was employed for data collection using Mo-*K*α radiation (λ = 0.71073 Å). The data collection was realized by using *CrysAlisPro* software.[1] The structures were solved by direct methods using *SIR97*,[2] or *SHELXS-97*[3], refined with *SHELXL-97*[3], finally checked using the *PLATON* software[4] and integrated in the

WinGX software suite.[5] All non-hydrogen atoms were refined anisotropically. Diamond plots are showing thermal ellipsoids with 50 % probability level for the non-hydrogen atoms. The finalized CIF files were checked with *checkCIF*[6] and deposited at the *Cambridge Crystallographic Data Centre*.[7]

Differential Analysis

DSC measurements for decomposition temperature determination were carried out at a heating rate of 5 °C min^{-1} in covered Al-containers with a hole (1 µm) on the top for gas release with a nitrogen flow of 5 mL min^{-1} on a *Linseis PT 10*. As reference sample a closed aluminum container was used. The device was calibrated by standard pure Indium and Zinc at a heating rate of 5 °C min^{-1}. High pressure measurements were carried out at the *Fraunhofer-Institut für Chemische Technologie ICT*, Pfinztal, Germany using *F20* Au-pans on a *TA Q2000* instrument, in a nitrogen atmosphere with a heating rate of 5 °C min^{-1}.
Low temperature DSC measurements were carried out with a *Netzsch 204 Phoenix* or a *TA Q2000* instrument in closed Al-containers, using a heating rate of 10 °C min^{-1}.

Elemental Analysis

Determinations of the carbon, hydrogen and nitrogen content were carried out by combustion analysis using an *Elementar Vario EL* or *Vario Micro Analyzer*. The determined nitrogen values are often lower than the calculated ones, which is common for nitrogen-rich compounds and cannot be avoided.

Electro Static Discharge Sensitivity

Sensitivities towards electrical discharge were determined using the Electric Spark Tester *ESD 2010 EN*.[8]

Impact and Friction Sensitivity

The impact and friction sensitivity was determined using a BAM drophammer and a BAM friction tester.[9] [10] The sensitivities of the compounds are indicated according to the UN

Recommendations on the Transport of Dangerous Goods (+): impact: insensitive > 40 J, less sensitive ≥ 35 J, sensitive ≥ 4 J, very sensitive ≤ 4 J; friction: insensitive > 360 N, less sensitive = 360 N, sensitive < 360 N and > 80 N, very sensitive ≤ 80 N, extreme sensitive ≤ 10 N.

Infrared Spectroscopy

Infrared spectra were recorded from 600 to 4000 cm^{-1} at room temperature on a *Perkin Elmer Spectrum BX FT*-IR System.
The samples were measured neat (ATR, *Smith Detection DuraSampl IR II Diamond ATR*). The absorption bands were reported in wave numbers (cm^{-1}). The intensities are reported in parentheses, distinguishing between, weak (w), medium (m), strong (s) and very strong (vs).

Mass spectrometry

Mass spectra were recorded on a *JEOL MS station JMS 700* instrument, with different ionization methods (DEI, DCI, FAB), which are specified in the experimental section. High resolution measurements were recorded on a *Finnigan MAT 95* instrument.

Melting Points

Melting points were either determined using the DSC data or *via* a *Büchi Melting point B-540*.

Molecular Weights

The molecular weights were measured at the *Fraunhofer-Institut für Chemische Technologie ICT*, Pfinztal, Germany, using an *Agilent Series 1100 HPLC* System with a flow rate of 1.0 mL min^{-1} and an injection volume of 100 µL of the polymer sample dissolved in THF (2 mg mL^{-1}). THF containing 0.2 % trifluoroacidic acid was used as solvent and eluent. As detector an *Agilent Series 1100* refractive index detector was used. The analysis was done using the *PSS WinGPCUniChrom* software. As column a *SDV* column set was used, comprising precolumn *PSS SDV* 5 µ, *PSS SDV* 5 µ 50 Å, *PSS SDV* 5 µ 100 Å, *PSS SDV* 5 µ 1000 Å, *PSS SDV* 5 µ 10^5 Å, with 8.0 mm inner diameter and 300 mm length. The calibration

was done using a narrowly distributed polystyrene standard from Fa. *PSS*, Mainz, within the molar mass range 1.210.000 g mol^{-1} to 162 g mol^{-1}.

Nuclear Magnetic Resonance Spectroscopy

All NMR spectra were recorded at ambient temperature with a *JEOL 270*, *400*, *ECX 400e*, *Bruker 400* or *Bruker 400 TR* instrument. The chemical shifts are reported with respect to the external standard Me_4Si (^1H, ^{13}C), $MeNO_2$ (^{14}N).

Pycnometric Measurements

Pycnometric measurements were carried out with a *Quantachrome Ultrapyc 1200e* helium pycnometer.

Thermogravimetric Analysis

Thermogravimetric analyses (TGA) were either measured in a platinum pan (100 µL) in a nitrogen atmosphere on a *TA TGA Q5000* instrument, using a heating rate of 5 °C min^{-1}, or on a *Setaram 92-2400 TG-DTA 1600* in an argon atmosphere, using a heating rate of 5 °C min^{-1} in a corundum crucible (80 µL).

Viscosity Measurements

Viscostity measurements were carried out on a *MCR 501* (*Anton Paar*) rheometer at 20 °C and 50 °C.

8.3 Calculations

Calculations of the Enthalpy of Formation

The enthalpies (H) and free energies (G) were calculated using the complete basis set (CBS) method of Petersson and coworkers in order to obtain very accurate energies. The modified CBS-4M method (M referring to the use of Minimal Population localization) was applied in any case.[11] If no crystal structure data was available for calculation, initial structure optimizations were performed at the B3LYP/cc-pVDZ level of theory using the Gaussian 09 revision A.02 program package[12]. Further information regarding calculation details and obtained values can be found in the respective passages in the text.

Energetic Calculations

All calculations concerning detonation parameters were carried out using the EXPLO5 (Version 6.02) software.[13] Detailed information regarding theoretical details and used values can be found in the text.

8.4 References

1 a) CRYSALISPRO, Version 1.171.35.11 (release 16.05.2011 CrysAlis171.net), Agilent Technologies, **2011**; b) L. J. Farrugia, *J. Appl. Crystallogr.* **1999**, *32*, 837-838.

2 a) A. Altomare, G. Cascarano, C. Giacovazzo, A. Guagliardi, A. G. G. Moliterni, M. C. Burla, G. Polidori, M. Camalli, R. Spagna, *SIR97*, **1997**; b) A. Altomare, M. C. Burla, M. Camalli, G. L. Cascarano, C. Giacovazzo, A. Guagliardi, A. G. G. Moliterni, G. Polidori, R. Spagna, *J. Appl. Crystallogr.* **1999**, *32*, 115-119.

3 G. M. Sheldrick, *Acta Cryst*. **2008**, *A64*, 112-122.

4 A. L. Spek, PLATON, A Multipurpose Crystallographic Tool, Utrecht University, The Netherlands, **1999**.

[5] L. J. Farrugia, *J. Appl. Cryst.* **1999**, *32*, 837-838.

[6] http://journals.iucr.org/services/cif/checkcif.html (accessed April, 2016).

[7] http://www.ccdc.cam.ac.uk (accessed April, 2016).

[8] a) NATO Standardisation Agreement (STANAG) on Explosives, Electrostatic Discharge Sensitivity Tests, No. 4490, 1st ed., Feb. 19th, **2001**; b) D. Skinner, D. Olson, A. Block-Bolten, *Propellants Explos. Pyrotech.* **1998**, *23*, 34–42; c) S. Zeman, V. Pelikán, J. Majzlk, *Cent. Eur. J. Energ. Mater.* **2006**, *3*, 45–51; d) http://www.ozm.cz/en/sensitivity-tests/esd-2008a-small-scaleelectrostatic-spark-sensitivity-test/ (accessed April, 2016).

[9] a) Bundesanstalt für Materialforschung (BAM), http://www.bam.de (accessed: 26.04.2016); laying down the test methods pursuant to Regulation (EC) No. 1907/2006 of the European Parliament and of the Council on the Evaluation, Authorisation and Restriction of Chemicals (REACH), ABl. L 142, **2008**; b) NATO Standardisation Agreement (STANAG) on Explosives, Impact Tests, No. 4489, 1st ed., Sept. 17th, **1999**; c) WIWEB-Standardarbeitsanweisung 4–5.1.02, Ermittlung der Explosionsgefährlichkeit, hier: der Schlagempfindlichkeit mit dem Fallhammer, Nov. 8th, **2002**; d) NATO Standardisation Agreement (STANAG) on Explosives, Friction Tests, No. 4487, 1st ed., Aug. 22nd, **2002**; e) WIWEB-Standardarbeitsanweisung 4–5.1.03, Ermittlung der Explosionsgefährlichkeit, hier: der Reibempfindlichkeit mit dem Reibeapparat, November 8th, **2002**; f) T. M. Klapötke, B. Krumm, N. Mayr, F. X. Steemann, G. Steinhauser, *Safety Science* **2010**, *48*, 28–34.

[10] Test methods according to the UN Manual of Tests and Criteria, Recommendations on the Transport of Dangerous Goods, United Nations Publication, New York, Geneva, 4th revised ed., **2003**.

[11] a) J. W. Ochterski, G. A. Petersson, J. A. Montgomery Jr., A complete basis set model chemistry. V. Extensions to six or more heavy atoms, *J. Chem. Phys.* **1996**, *104*, 2598; b) J. A. Montgomery Jr., M. J. Frisch, J. W. Ochterski, G. A. Petersson, A complete basis set model chemistry. VII. Use of the minimum population localization method, *J. Chem. Phys.* **2000**, *112*, 6532.

[12] M. J. Frisch, G. W. Trucks, H. B. Schlegel, G. E. Scuseria, M. A. Robb, J. R. Cheeseman, V. B. Scalmani, B. Mennucci, G. A. Petersson, H. Nakatsuji, M. Caricato, X. Li, H. P. Hratchian, A. F. Izmaylov, J. Bloino, G. Zheng, J. L. Sonnenberg, M. Hada, M. Ehara, K. Toyota, R. Fukuda, J. Hasegawa, M. Ishida, T. Nakajima, Y. Honda, O. Kitao, H. Nakai, T. Vreven, J. A. Montgomery, J. E. Peralta, F. Ogliaro, M. Bearpark, J. J. Heyd, E. Brothers, K. N. Kudin, V.-N. Staroverov, R. Kobayashi, J. Normand, K. Raghavachari, A. Rendell, J. C. Burant, S. S. Iyengar, J. Tomasi, M. Cossi, N. Rega, J. M. Millam, M. Klene, J. E. Knox, J. B. Cross, V. Bakken, C. Adamo, J. Jaramillo, R. Gomperts, R. E. Stratmann, O. Yazyev, A. J. Austin, R. Cammi, C. Pomelli, J. W. Ochterski, R. L. Martin, K. Morokuma, V. G. Zakrzewski, G. A. Voth, P. Salvador, J. J. Dannenberg, S. Dapprich, A. D. Daniels, Ö. Farkas, J. B. Foresman, J. V. Ortiz, J., J. Cioslowski, D. J. Fox,. *Gaussian 09*. Rev. A.03 ed.; Gaussian, Inc.: Wallingford CT, **2009**.

[13] a) M. Sućeska, Calculation of the detonation properties of C-H-N-O explosives, *Propellants, Explos., Pyrotech.* **1991**, *16*, 197-202; b) Sućeska, M. *EXPLO5 V.6.02*. Zagreb (Croatia), **2013**.

APPENDIX

9. Appendix

9.1 Abbreviations and Formula Symbols

Abbreviations

AcBAMP	2,2-bis(azidomethyl)propane-1,3-diyl diacetate
AcDNPD	2,2-dinitropropane-1,3-diyl diacetate
ADAT	1-acetyl-3,5-diamino-1,2,4-triazole
ANFO	ammonium nitrate fuel
a.u.	atomic units
BAMP	2,2-bis(azidomethyl)propane-1,3-diol
BAM	Bundesanstalt für Materialforschung und –prüfung
BTE	1,2-bis(terazol-5-yl)ethane
BTEOH	1,2-bis(hydroxyethyl terazol-5-yl)ethane
BTEOAc	1,2-bis(hydroxyethyl tetrazol-5-yl)ethane diacetate
BTEOPro	1,2-bis(hydroxyethyl tetrazol-5-yl)ethane dipropionate
br	broad (IR and NMR)
BuNENA	*N*-butyl-2-nitratoethylnitramine
ButBAMP	2,2-bis(azidomethyl)propane-1,3-diyl dibutyrate
d	doublet (NMR)
DAT	3,5-diamino-1,2,4-triazole
DBX-1	copper(I) 5-nitrotetrazolate
DCI	direct chemical ionization
DEGBAA	diethylene glycol bis(azidoacetate)
DEGDN	diethylene glycol dinitrate
DEI	direct electron ionization
DIE	diisocyanato ethane
DIE-BAMP	poly[ethylene(2,2-bis(azidomethyl)propylene)carbamate]
DIE-DNPD	poly[ethylene(2,2-dinitropropylene)carbamate]
DIM	diisocyanato methane
DIM-BAMP	poly[methylene(2,2-bis(azidomethyl)propylene)carbamate]

DIM-DNPD	poly[methylene(2,2-dinitropropylene)carbamate]
DMF	dimethylformamide
DMSO	dimethylsulfoxide
DNPD	2,2-dinitropropane-1,3-diol
DOA	dioctyl adipate
DOP	dioctyl phtalate
DSC	differential scanning calorimetry
EA	elemental analysis
ECH	epichlorohydrin
EGBAA	ethylene glycol bis(azidoacetate)
ESD	electrostatic discharge
FAB	fast atom bombardment
FS	friction sensitivity
FW	formula weight
GAP	glycidyl azide polymer
GNAP	glycidyl nitramine polymer
HMDI	hexamethylene diisocyanate
HMDI-BAMP	poly[ethylene(2,2-bis(azidomethyl)propylene)carbamate]
HMDI-DNPD	poly[hexamethylene(2,2-dinitropropylene)carbamate]
HMX	high melting explosive (1,3,5,7-tetranitro-1,3,5,7-tetrazocane)
HNS	hexanitrostilbene
HR	high resolution
HTPB	hydroxyl-terminated polybutadiene
IR	infrared spectroscopy
IS	impact sensitivity
K_2DNABT	potassium 1,1’-dinitramino-5,5’-bistetrazolate
LOVA	low-vulnerability amminition
[M]+	molecule peak (MS)
M	molar (mol L^{-1})
m	medium (IR), multiplet (NMR)
MDI	dipehylmethane-4,4’-diisocyanate
MS	mass spectrometry
NC	nitrocellulose

NG	nitroglycerine
NMR	nuclear magnetic resonance
PBAN	polybutadiene acrylonitrile
PBX	polymer-bonded explosive
PETKAA	pentaerythritol tetrakis (acidoacetate)
PNP	polynitropolyphenylene
polyAMMO	poly(3-azidomethyl-3-methyl oxetane)
polyBAMO	poly[3,3-(bisazidomethyl)oxetane]
polyGYLN	poly(glycidyl nitrate)
polyNIMMO	poly(3-nitratomethyl-3-methyl oxetane)
ppm	parts per million
PU	polyurethane
PUA	polyurea
PVN	polyvinyl nitrate
PVT	polyvinyl tetrazole
RDX	royal demolitions explosive (1,3,5-trinitro-1,3,5-triazinane)
rt	room temperature
s	strong (IR), singlet (NMR)
t	triplet (NMR)
TGA	thermogravimetric analysis
THF	tetrahydrofuran
TKX-50	dihydroxylammonium 5,5’-bistetrazol-1,1’-diolate
TMETN	trimethylol ethane trinitrate
TNT	trinitrotoluene
UN	United Nations
vs	very strong (IR)
w	weak (IR)

Formula Symbols

<	angle
δ	isotropic chemical shift
d	atom distance
I_s	specific impulse
${}^{n}J_{HH/CH}$	homo-/heteronuclear coupling constant over *n* nuclei
M	molar mass
M_n	number average molar mass
m/z	mass per charge
~N_2	in N_2 atmosphere
N	nitrogen content
$\tilde{\nu}$	wave number
Ω	oxygen balance
p_{CJ}	detonation pressure
ρ	density
T_{dec}	decomposition temperature
T_E	explosion temperature
T_g	glass transition temperature
T_{melt}	melting temperature
$\Delta_c U$	energy of combustion
$\Delta_E U$	energy of explosion
V_{det}	detonation velocity
wt%	weight percent

9.2 Crystallographic Data

Table 9.1 Crystallographic data for 2,2-bis(acetoxymethyl-1H-1,2,3-triazol-1-yl)methyl)-propane-1,3-diol (**10**).

	10
Measurement #	hx001
Chemical formula	$C_{15}H_{22}N_6O_6$
Molecular weight [g mol^{-1}]	382.39
Color, habit	colorless block
Size [mm]	0.25x0.20x0.15
Crystal system	triclinic
Space group	*P*-1
a [Å]	7.5226(4)
b [Å]	7.9108(4)
c [Å]	15.6300(9)
α [°]	89.247(4)
β [°]	84.447(5)
γ [°]	80.936(5)
V [Å^3]	914.21(9)
Z	2
ρ_{calc} [g cm^{-3}]	1.389
μ [mm^{-1}]	0.109
Irradiation [Å]	MoK_α 0.71073
F(000)	404
Θ-area [°]	4.20-26.00
T [K]	173
Dataset h	$-9 \leq h \leq 9$
Dataset k	$-9 \leq k \leq 9$
Dataset l	$-19 \leq l \leq 19$
Reflecions coll.	9271
Independent refl.	3582
Observed refl.	2746
Parameters	332
R (int)	0.0333
GOOF	1.041
R_1, wR_2 ($I>\sigma I_0$)	0.0435, 0.1044
R_1, wR_2 (all data)	0.0605, 0.1155
Weighting scheme[a]	0.0506, 0.2026
Remaining density [e Å^{-3}]	-0.323, 0.480
Device type	Oxford XCalibur3
Adsorption corr.	multi-scan

[a] $wR_2 = [\Sigma[w(F_0^2-F_c^2)^2]/ \Sigma [w(F_0)^2]]^{1/2}$ where $w=[\sigma_c^2(F_0^2)+(xP)^2+yP]$ and $P=(F_0^2+2F_c^2)/3$

Table 9.2 Crystallographic data for 2,2-bis(hydroxymethyl-1H-1,2,3-triazol-1-yl)-methyl)propane-1,3-diol (4-ol, **12**).

	12
Measurement #	ix505
Chemical formula	$C_{11}H_{18}N_6O_4$
Molecular weight [g mol^{-1}]	298.30
Color, habit	colorless block
Size [mm]	0.40x0.40x0.40
Crystal system	monoclinic
Space group	$P2_1/c$
a [Å]	8.897(5)
b [Å]	14.993(7)
c [Å]	10.507(6)
α [°]	90.00
β [°]	108.260(6)
γ [°]	90.00
V [Å^3]	1331.0(11)
Z	4
ρ_{calc} [g cm^{-3}]	1.489
μ [mm^{-1}]	0.116
Irradiation [Å]	MoK_α 0.71073
F(000)	632
Θ-area [°]	4.26-30.03
T [K]	173
Dataset h	$-12 \leq h \leq 12$
Dataset k	$-21 \leq k \leq 11$
Dataset l	$-14 \leq l \leq 14$
Reflecions coll.	9104
Independent refl.	3866
Observed refl.	2992
Parameters	223
R (int)	0.0248
GOOF	1.025
R_1, wR_2 ($I>\sigma I_0$)	0.0448, 0.1141
R_1, wR_2 (all data)	0.0612, 0.1264
Weighting scheme[a]	0.0602, 0.5354
Remaining density [e Å^{-3}]	-0.471, 0.699
Device type	Oxford XCalibur3
Adsorption corr.	multi-scan

[a] $wR_2 = [\Sigma[w(F_0^2-F_c^2)^2]/ \Sigma [w(F_0)^2]]^{1/2}$ where $w=[\sigma_c^2(F_0^2)+(xP)^2+yP]$ and $P=(F_0^2+2F_c^2)/$

Table 9.3 Crystallographic data for 2,2-bis(hydroxymethyl-1H-1,2,3-triazol-1-yl)-methyl)propane-1,3-diol (2,2-DvBTE, **14a**).

	14a
Measurement #	jx412
Chemical formula	$C_8H_{10}N_8$
Molecular weight [g mol^{-1}]	218.22
Color, habit	colorless block
Size [mm]	0.07x0.31x0.51
Crystal system	monoclinic
Space group	$P2_1/c$
a [Å]	9.137(4)
b [Å]	8.166(4)
c [Å]	6.941(4)
α [°]	90.00
β [°]	98.164(5)
γ [°]	90.00
V [Å^3]	512.61(4)
Z	2
ρ_{calc} [g cm^{-3}]	1.414
μ [mm^{-1}]	0.100
Irradiation [Å]	MoK_α 0.71073
F(000)	228
Θ-area [°]	4.27-26.35
T [K]	173
Dataset h	$-7 \leq h \leq 11$
Dataset k	$-10 \leq k \leq 10$
Dataset l	$-8 \leq l \leq 8$
Reflecions coll.	3803
Independent refl.	1049
Observed refl.	930
Parameters	94
R (int)	0.022
GOOF	1.085
R_1, wR_2 ($I>\sigma I_0$)	0.0302, 0.0698
R_1, wR_2 (all data)	0.0351, 0.0739
Weighting scheme[a]	0.0292, 0.1084
Remaining density [e Å^{-3}]	-0.148, 0.191
Device type	Oxford XCalibur3
Adsorption corr.	multi-scan

[a] $wR_2 = [\Sigma[w(F_0^2-F_c^2)^2]/ \Sigma [w(F_0)^2]]^{1/2}$ where $w=[\sigma_c^2(F_0^2)+(xP)^2+yP]$ and $P=(F_0^2+2F_c^2)/3$

9.3 List of Publications

9.3.1 Articles

1. V. Hartdegen, T. M. Klapötke, S. M. Sproll, Tetrazole-5-carboxylic Acid Based Salts of Earth Alkali and Transition Metal Cations, *Inorg. Chem.*, **2009**, *48*, 9549-9556.

2. V. Hartdegen, T. M. Klapötke, S. M. Sproll, Synthesis and Characterization of a Three-dimensional Coordiation Polymer Based on Copper(II) Nitrate and a Tridentate Tetrazole Ligand, *Z. Naturforsch., B: Chem. Sci.* **2009**, *64b*, 1535-1541.

3. F. M. Betzler, V. A. Hartdegen, T. M. Klapötke, S. M. Sproll, A New Energetic Binder: Glycidyl Nitramine Polymer, *Cent. Eur. J. Energ. Mater.*, **2016**, *in press*.

4. A. B. Bellan, S. Hafner, V. A. Hartdegen, T. M. Klapötke, Polyurethanes Based on 2,2-Dinitropropane-1,3-diol and 2,2-Bis(azidomethyl)propane-1,3-diol as Potential Energetic Binders, *J. Appl. Polym. Sci.* **2016**, *in press.*

5. S. Hafner, V. A. Hartdegen, M. S. Hofmayer, T. M. Klapötke, Potential Energetic Plasticizers on the Basis of 2,2-Dinitropropane-1,3-diol and 2,2-Bis(azidomethyl)propane-1,3-diol, *Propellants, Pyrotech., Explos.* **2016**, *accepted.*

6. V. A. Hartdegen, M. S. Hofmayer, T. M. Klapötke, Synthesis and Characterization of Allyl and Vinyl Based Bistetrazoloethanes as Polymeric Precursors, *Z. Naturforsch., B: Chem. Sci.* **2016**, *submitted.*

9.3.2 Poster Presentations

1. V. Hartdegen, T. M. Klapötke, S. Sproll, New Energetic Materials Based on 2*H*-tetrazole-5-carboxylic Acid, *New Trends in Research of Energetic Materials, 12th, Pardubice, Czech Republic*, **2009**.

2. A. Bellan, V. Hartdegen, T. M. Klapötke, Synthesis and Characterization of a New Energetic Polyurethane, *New Trends in Research of Energetic Materials, 12th, Pardubice, Czech Republic*, **2013**.